Functional characterization of *SR30* splicing and upstream signaling of light-regulated AS during seedling photomorphogenesis

Dissertation

der Mathematisch-Naturwissenschaftlichen Fakultät
der Eberhard Karls Universität Tübingen
zur Erlangung des Grades eines
Doktors der Naturwissenschaften
(Dr. rer. nat.)

vorgelegt von
M. Sc. Theresa Wießner-Kroh
aus Herzberg/Elster

Tübingen
2021

Gedruckt mit Genehmigung der Mathematisch-Naturwissenschaftlichen Fakultät der Eberhard Karls Universität Tübingen.

Tag der mündlichen Qualifikation:	23.07.2021
Dekan:	Prof. Dr. Thilo Stehle
1. Berichterstatter:	Prof. Dr. Andreas Wachter
2. Berichterstatter:	Prof. Dr. Klaus Harter

Table of contents

I. Abbreviations

	Abbreviation	Meaning
A	ABA	Abscisic acid
	ABI4	ABA-insensitive 4
	AFC2	Arabidopsis FUS3-complementing gene 2
	amiR	Artificial microRNA
	AMPK	AMP-activated protein kinase
	AS	Alternative splicing
	ASF	Alternative splice factor, also called SF2 or SRSF1
B	bHLH	Basic helix-loop-helix TF
	bZIP	Basic leucine zipper TF
C	CAB	Chlorophyll A/B binding protein
	COP1	Constitutively photomorphogenic 1
	CRY	Cryptochrome
D	DIN	Dark-inducible (such as DIN1 or DIN6)
	DCMU	3-(3,4-Dichlorophenyl)-1,1-dimethylurea
	DBMIB	Dibromothymoquinone
	Dscam	Down syndrome cell adhesion molecule
E	EBF1/2	EIN3 binding F-box factor1/2
	EIN3	Ethylene insensitive 3
	EJC	Exon junction complex
	ETFQO	Electron-transfer flavoprotein:ubiquinone oxidoreductase
F	FLM	Flowering locus M
G	GRP	Glycine-rich binding protein
H	hnRNP	Heterogeneous nuclear ribonucleoprotein
	HEN1	Hua enhancer 1
	HY5	Elongated hypocotyl 5
	HYH	HY5 homolog
M	MAPK	Mitogen-activated protein kinase
	miRNA	microRNA
	mTOR	Mammalian TOR
	MYBD	MYB-like transcription factor D
N	NMD	Nonsense-mediated decay
P	PHY	Phytochrome

	PIF	Phytochrome-interacting factor
	PPD2	Peapod 2
	PPL1	PSBP-like protein 1
	pre-mRNA	Precursor messenger RNA
	PTB	Polypyrimidine tract binding protein
	PTC	Premature termination codon
Q	qRT-PCR	Quantitative real-time PCR
R	RAPTOR	Regulatory associated protein of TOR
	RPS6	Ribosomal protein S6
	RRC1	Reduced red light response in *cry1 cry2* background
	RRM	RNA recognition motif
	RS	Arginine-/serine-rich protein or domain
	RT-PCR	PCR on cDNA (in combination with reverse transcription of RNA)
	RuBisCo	Ribulose-1,5-bisphosphate carboxylase/oxydase
S	SF2	Splice factor 2, also called ASF or SRSF1
	SFPK	Splice factor protein kinase
	SFPS	Splicing factor for phytochrome signaling
	SIRK1	Sucrose induced receptor kinase1
	SMG	Suppressor of morphological defects in genitalia
	SnAK	SnRK1 activating kinase
	SNF1	Sucrose non-fermenting 1
	SnRK1	SNF1-related kinase 1
	snRNP	Small nuclear ribonucleoprotein particles
	SPA	Suppressor of PHYA
	SR protein	Serine-/arginine-rich protein
	SRSF1	Serine-/arginine-rich splicing factor 1, outdated term SF2/ASF
T	T6P	Trehalose-6-phosphate
	TF	Transcription factor
	TOR	Target of rapamycin
	TPS	T6P synthase
	TRIN1	TOR inhibitor AZD8055-insensitive mutant 1
U	U2AF	U2 auxillary factor
	UFP	Up frameshift protein
	UPR	Unfolded protein response
	UTR	Untranslated region
X	XRN	Exoribonuclease

1. Abstract

Light is of utmost importance for the plant life cycle since it serves as energy source and trigger for plant development. Dark-grown seedlings exhibit closed and pale cotyledons, an apical hook, enlarged hypocotyls and short roots. The photomorphogenic growth is initiated upon first illumination, and the seedling opens up the cotyledons, chloroplasts differentiate to start photosynthesis, hypocotyl elongation is reduced and the root system extends. This developmental transition is characterized and driven by massive reprogramming of gene expression including light-induced changes of alternative splicing (AS) patterns for several hundred events. Remarkably, the majority of dark-expressed splice variants carry nonsense-mediated decay (NMD)-eliciting features. For many light-regulated AS events, illumination provokes the switch to likely productive variants as shown for *REDUCED RED LIGHT RESPONSE IN CRY1 CRY2 BACKGROUND* (*RRC1*) with profound effects on hypocotyl growth. However, the presence of NMD-triggering features does not necessarily result in accelerated RNA decay. The dark-promoted splice variant of *SERINE-ARGININE-RICH PROTEIN 30* (*SR30*), *SR30.2*, appears to be NMD-insensitive although it has a long and intron-containing 3' untranslated region. We could demonstrate that nuclear retention prevents *SR30.2* from being translated, making it NMD immune. Light exposure initiates splicing to *SR30.1* by using a downstream 3' splice site. *SR30.1* is exported to the cytosol and associates with ribosomes for being translated. Moreover, strong expression of *SR30.2* resulted in the accumulation of the minor and NMD-sensitive splicing variant *SR30.3*. We provided evidence that *SR30.3* originates from *SR30.2* by a sequential splicing step using the remaining 3' splice site in *SR30.2*. This example highlights complex and light-dependent regulation of *SR30* expression via subcellular compartmentation of its splicing variants. However, little is known about the regulation upstream of light-regulated AS. Physiological experiments with photoreceptor mutants, exogenous application of different sugars and inhibitors targeting photosynthesis or kinase signaling suggested an important role of energy signaling in light-responsive AS. Interestingly, targets of the central energy sensor SNF1-RELATED KINASE1 (SnRK1) correlated in their expression with light-induced AS shifts. Therefore, we generated inducible *amiR-SnRK1* lines for further investigation. Repression of *SnRK1* resulted in light-grown plants in accelerated senescence, whereas etiolated *amiR-SnRK1* seedlings displayed shortened hypocotyls. Remarkably, a subset of analyzed AS events were shifted to the light-driven splice variant upon *amiR-SnRK1* induction in dark-grown seedlings. However, some AS events did not respond pointing to a different regulation. Surprisingly, inhibition of the SnRK1 antagonist TARGET OF RAPAMYCIN (TOR) resulted in comparable phenotypes and AS responses as seen upon SnRK1 repression. We conclude from our findings that energy signaling regulates light-dependent gene expression also via the mechanism of AS.

Zusammenfassung

Licht ist für den pflanzlichen Lebenszyklus von größter Bedeutung als Energiequelle und essentieller Taktgeber für die Entwicklung der Pflanze. Nach der Keimung weisen im Dunkeln gewachsene Keimlinge geschlossene, fahle Keimblätter, einen apikalen Haken, lange Hypokotyle und kurze Wurzeln auf. Lichtexposition leitet die Photomorphogenese ein, wodurch die Keimlinge ihre Keimblätter öffnen, Photosynthese betreibende Chloroplasten ausbilden, das Hypokotyllängenwachstum verringern und ihr Wurzelsystem expandieren. Dieser Entwicklungsprozess wird von einer lichtinduzierten, transkriptomweiten Umprogrammierung inklusive substantieller Veränderung des alternativen Spleißens (AS) für mehrere hundert Gene begleitet. Die Mehrheit aller dunkelexprimierten Spleißvarianten weist erstaunlicherweise Sequenzmerkmale auf, welche Nonsens-vermittelter mRNA Abbau (engl.: nonsense-mediated mRNA decay, NMD) auslösen, wohingegen Lichtexposition zur Bildung der wahrscheinlich proteinkodierenden Spleißvariante führt. Für den Spleißregulator *REDUCED RED LIGHT RESPONSE IN CRY1 CRY2 BACKGROUND* (*RRC1*) konnten wir zeigen, dass eine lichtinitiierte Spleißmusterverschiebung zur funktionellen mRNA-Variante einen signifikanten Effekt auf das Hypokotyllängenwachstum hat. Allerdings, gibt es auch Transkripte mit NMD-Merkmalen, die dem gezielten RNA-Abbau durch NMD entgehen. Die im Dunkeln favorisierte Spleißvariante von SERINE-*ARGININE-RICH PROTEIN 30* (*SR30*), *SR30.2*, scheint NMD-immun zu sein, trotz eindeutiger NMD-Merkmale. Wir konnten zeigen, dass *SR30.2* im Zellkern zurückgehalten wird und in viel geringerem Ausmaß als *SR30.1* mit Ribosomen assoziiert ist. Da Translation eine Voraussetzung für NMD ist, erscheint *SR30.2* NMD-resistent. Lichtexposition verschiebt das Spleißmuster zu *SR30.1* und fördert die SR30 Proteinexpression. Interessanterweise führt die Überexpression von *SR30.2* zur Akkumulation der schwach exprimierten und NMD-sensitiven Spleißvariante *SR30.3*. Unter Verwendung der verbleibenden 3'-Spleißstelle in *SR30.2*, kann *SR30.3* durch einen sequentiellen Spleißschritt gebildet werden. Diese Ergebnisse verdeutlichen einen komplexen Regulationsmechanismus für die Genexpression von *SR30* durch AS-vermittelte subzelluläre Kompartimentierung der Spleißvarianten. Im Gegensatz zu einzelnen gut charakterisierten AS-Ereignissen, ist nur wenig über die Regulation von lichtabhängigen Spleißmustern bekannt. Exogene Zugabe von verschiedenen Zuckern oder Inhibitoren, die die Photosynthese oder die Kinase-Signalübertragung hemmen, suggerierten, dass zentrale Energiesensoren einen Einfluss auf lichtempfindliche Spleißmuster haben. Interessanterweise korrelierte die Geneexpression von *DARK INDUCIBLE* (*DIN*) *1* und *6*, Zielgene des zentralen Energiesensors SNF1-RELATED KINASE1 (SnRK1), mit den lichtvermittelte AS-Ereignissen. Daher haben wir induzierbare *amiR-SnRK1*-Mutanten zur weiteren Untersuchung generiert. Die Unterdrückung der SnRK1 Signaltransduktion führte zu beschleunigter Seneszenz bei lichtgewachsenen Pflanzen,

während etiolierte *amiR-SnRK1*-Keimlinge verkürzte Hypokotyle zeigten. Bemerkenswert ist, dass die Unterdrückung des SnRK1-Signalweges eine Verschiebung zur lichtabhängigen Spleißvariante für eine Teilmenge der analysierten AS-Ereignisse bewirkte. Einige AS-Ereignisse zeigten jedoch keine Reaktion auf die SnRK1-Inhibition und verweisen auf einen anderen Regulationsmechanismus. Die Analyse des SnRK1-Antagonisten TARGET OF RAPAMYCIN (TOR) ergab, dass eine Herunterregulierung der *TOR* Expression zu vergleichbaren Phänotypen und AS-Antworten wie für die SnRK1-Mutanten führte. Wir schließen aus unseren Erkenntnissen, dass AS durch den Energiestatus der Pflanze reguliert wird und damit zur lichtabhängige Genexpression während der Photomorphogenese beträgt.

II. List of publications and manuscripts

II.1. Published paper

2016

Hartmann, L., Drewe-Boß, P., Wießner, T., Wagner, G., Geue, S., Lee, H.-C., Obermüller, D. M., Kahles, A., Behr, J., Sinz, F. H., Rätsch, G., and Wachter, A. Alternative Splicing Substantially Diversifies the Transcriptome during Early Photomorphogenesis and Correlates with the Energy Availability in Arabidopsis. *The Plant Cell*, 28(11):2715–34, nov 2016.

2018

Hartmann, L., Wießner, T., and Wachter, A. Subcellular Compartmentation of Alternatively Spliced Transcripts Defines SERINE/ARGININE-RICH PROTEIN30 Expression. *Plant Physiology*, 176(4):2886–903, apr 2018.

II.2. Unpublished manuscripts

Saile, J., Wießner-Kroh, T., and Wachter A. Energy Sensor Signalling Affects Early Seedling Development and Correlates with Alternative Splicing

III. Personal contribution

The data presented and discussed here have been either published in Hartmann *et al*. (2016, 2018) or are part of a manuscript (Saile *et al.*, unpublished) (see section II). The research was designed by Andreas Wachter, Lisa Hartmann, Jennifer Saile and myself. RNA sequencing data (which the project is based on) were generated and analyzed by Lisa Hartmann and Andreas Wachter in cooperation with Phillip Drewe-Boß and Gunnar Rätsch (Hartmann *et al*. 2016, Fig. 1, SFig. 1-3). Analyzed AS events were identified by Lisa Hartmann and Andreas Wachter (Hartmann *et al.* 2016, Fig. 2, SFig. 4; Hartmann *et al.* 2018, SFig. 5). A major proportion of the results presented here was done by myself with the technical assistance from Gabriele Wagner, Natalie Faiss and Claudia König. This includes infiltrations, growing of plant material and physiological experiments, RNA extraction, RT-PCR, determination of the relative splice ratio via Bioanalyzer, qRT-PCR, immunoprecipitations, nuclear enrichment, protein extraction, protein detection via western blots, except otherwise stated. Details are described below.

As co-author of Hartmann *et al*. (2016), I provided data for the Fig. 4, 5, 6 and 7, and Suppl. Fig. 5A, 7, 8, 11 to 15. I selected and characterized *rrc1-2* lines complemented with either *genomic RRC1*, or cDNA for *RRC1.1* or *RRC1.2* which are driven by an endogenous promoter including the determination of expression levels of *RRC1* mRNA isoforms and hypocotyl length data (SFig. 7). Constructs and seeds were generated by Lisa Hartmann. I characterized the *snrk1-1.3* mutant regarding its T-DNA insertion site, *SnRK1.1* transcript and SnRK1.1 protein levels (SFig. 13). Annotation of the T-DNA insertion site was done with contributions of Andreas Wachter. The physiological experiments in Fig. 4 (one biological replicate), 5, 6B and 7, and SFig. 11 and 15 were performed and analyzed by myself. I analyzed transcript levels of *DIN*s (Fig. 6C, SFig. 15B), *HXK1* and *CAB1* (SFig. 12). Further, RT-PCR and Bioanalyzer analysis (Fig. 6A) and levels of *RRC1* splice variants (SFig 5A) were generated by me using RNA samples prepared by Lisa Hartmann.

For Hartmann *et al.* (2018), Lisa Hartmann and I contributed equally to the publication. Lisa Hartmann generated and purified the SR30 antibody, and cloned all *SR30*-related constructs. Moreover, she provided the data for *SR30* mRNA isoform expression pattern in wild type under different light qualities and in NMD mutants (Fig. 1, 2A), the SR30 protein detection via immunoblot detection (Fig. 3D-G, SFig. 4B) or confocal microscopy (Fig. 4, SFig. 4A), *SR30* autoregulation via a luciferase reporter assay (Fig. 5) and analyzed *SR30* expression in different T-DNA mutants compared to wild type (SFig. 3). I measured the transcript stability of *SR30* splice variants based on RNA samples provided by Hsin-Chieh Lee (Fig. 2B) and performed the subcellular fractionation of Arabidopsis seedlings and Nicotiana leaves

expressing an SR30 reporter to detect the *SR30* splice variants in the nucleus or cytoplasm (Fig. 2C-G). Further, I co-immunoprecipitated ribosomal protein L18 together with the bound RNA to analyze the transcript abundance of the single *SR30* mRNA isoform at the ribosome (Fig. 3A-C) and I determined the expression level of *SR30* splice variants in RNA degradation-impaired mutants (SFig. 2). The characterization of *SR30.3* expression in dependance on light and in *SR30.1* or *SR30.2* overexpressing plants was performed by myself (Fig. 6).

The unpublished manuscript concerning the involvement of energy sensors SnRK1 and TOR in AS regulation is a shared project by me and Jennifer Saile. For this study, I generated all *amiR-SnRK1* lines including construct design (SFig. 1), cloning, plant transformation, selection, and analysis of transcript and protein levels (Fig. 2, SFig. 8A), except for protein detection in SFig. 8B and C done by Jennifer Saile. Hypocotyl lengths were determined by me (Fig. 1B, SFig. 4A, 9A), Dominik Obermüller (SFig. 2E) and Jennifer Saile (SFig. 4B). I did all physiological experiments of *amiR-SnRK1* lines (Fig. 3, SFig. 6, 7) and provided AS data for SFig 6, whereas Jennifer Saile analyzed AS pattern for Fig. 3 and SFig. 7 using my RNA samples. I observed different phenotypes of *amiR-SnRK1* lines such as chlorosis of light-grown seedlings and accelerated senescence. Based on this, Jennifer Saile did the complete phenotyping experiment and quantified the mortality rate with support of Katarina Erbstein (SFig. 2A-C,D). Additionally, Jennifer Saile measured the chlorophyll content of *amiR-SnRK1* seedlings grown under different light intensities (Fig. 1C, D, SFig. 5). Further, Jennifer Saile provided the data for SFig. 9B-D.

Hartmann *et al.* (2016) was written by Andreas Wachter and Lisa Hartmann with contributions of me. Hartmann *et al*. (2018) was written by Andreas Wachter with contributions of Lisa Hartmann and me. All figures and statistics for both publications were provided by Lisa Hartmann except for SFig 6A in Hartmann *et al.* (2018) that was prepared by myself. The manuscript text of Saile *et al*. (unpublished) was written by myself with contributions of Jennifer Saile and Andreas Wachter. Jennifer Saile and me were equally involved in figure design for the manuscript. Jennifer Saile provided the statistical analysis. All results can be found in the relevant publications or the unpublished manuscript (see section II). The discussion of my dissertation is based on all three studies however focusses on the experiments specified above.

2. Introduction

2.1. Alternative splicing – molecular mechanism to regulate gene expression

The majority of eukaryotic genes consist of several expressed regions, exons, which are interrupted by intragenic segments, introns (Berget *et al.* 1977, Chow *et al.* 1977, Padgett *et al.* 1984, Ruskin *et al.* 1984). Upon transcription, the non-coding sequences of the precursor messenger RNA (pre-mRNA) are removed by a cut-ligation reaction, called splicing. This highly dynamic process is executed by the spliceosome, a large RNA-protein complex encompassing five small nuclear ribonucleoprotein particles (snRNPs: U1, U2, U4/U6, U5) and a large number of auxiliary proteins. Small nuclear uridine-rich RNAs within each snRNPs function as the splicing reaction catalysator (Lerner and Steitz 1979, Lerner *et al.* 1980, Rogers and Wall 1980, Hinterberger *et al.* 1983) and classify the spliceosome as ribozyme. Conserved *cis* elements of the pre-mRNA, including the 5' splice site, 3' splice site and the branch point, define the exon-intron structure (Fig. 1a). The spliceosomal components assemble stepwise at these core splicing signals in cycling reaction to perform the splicing step and the non-coding sequence is removed as a unit (Reddy 2007, Wahl *et al.* 2009, Will and Luhrmann 2011, Staiger and Brown 2013, Lee and Rio 2015, Shi 2017, Wilkinson *et al.* 2019). Interestingly, a splicing process involving multiple, consecutive splicing steps was discovered to extract large introns in Drosophila and human (Duff *et al.* 2015, Sibley *et al.* 2015). First, it was shown for the ULTRABITHORAX gene of *Drosophila melanogaster* which contains one 74 kb long intron, which is spliced out in four steps and was described as recursive splicing. The large intron contains several 3' splice sites. Removal of the first intronic part creates a zero-nucleotide exon and a new 5' splice site is reconstituted. Thus, the next splicing step is able to pursue (Hatton *et al.* 1998, Duff *et al.* 2015). Accordingly, human transcripts important in neuronal development have been reported to undergo recursive splicing, too, whereby a recursive splicing exon (RS-exon) is formed instead of a zero-nucleotide exon, which subsequently competes with the new 5' splice site during the next splicing step. Notably, recursive splicing could be connected to RNA degradation via nonsense-mediated decay (NMD) triggered by incomplete splicing of the large intron (Sibley *et al.* 2015) or by introduction of RS exons carrying premature termination codon (PTC) in human brain tissues (Cook-Andersen and Wilkinson 2015). With this, recursive splicing can act as regulatory switch by differential splice site selection (Sibley *et al.* 2015).

In higher eucaryotes, several transcript isoforms can originate from one pre-mRNA by alternative splicing (AS). Current estimates assume that around 25%, 43%, 61%, up to 70% and more than 95% of multiexonic genes encode more than one mRNA variant in nematodes

(*Caenorhabditis elegans*, Ramani *et al.* 2011), fruit flies (*Drosophila melanogaster*, Khodor *et al.* 2011), Arabidopsis (*Arabidopsis thaliana*, Marquez *et al.* 2012), crop plants (Zhang *et al.* 2010, Thatcher *et al.* 2014, Sun and Xiao 2015, Iñiguez *et al.* 2017) and human (*Homo sapiens sapiens*, Pan *et al.* 2008, Barbosa-Morais *et al.* 2012, Merkin *et al.* 2012), respectively. The major proportion of intron-containing genes encode 2 to 3 or up to 7 transcripts in Arabidopsis (Marquez *et al.* 2012) or in human (Pan *et al.* 2008, Tung *et al.* 2020), respectively. Using an alternative splice site usually results in either intron retention, cassette exon inclusion or skipping next to mutually exclusive exons, and alternative 5' or 3' site selection (Fig. 1b; Nilsen and Graveley 2010, Marquez *et al.* 2012, Braunschweig *et al.* 2013, Reddy *et al.* 2013), however, more complex or less abundant AS types appear as well. A transcriptome-wide analysis of Arabidopsis plants discovered retained introns in expressed mRNA regions carrying exonic as well as intronic features. These special AS events were defined as cryptic introns or exitrons, respectively (Marquez *et al.* 2012, 2015). One of most extreme example of complex AS pattern has been reported for Drosophila *Dscam* gene (encoding Down syndrome cell adhesion molecule) important for its immune system and axon guidance (Park and Graveley 2007). It consists of 115 exons, which are removed in different combinations. Hence up to 38016 different splice variants could be potentially derived from this locus resulting in great collection of protein isoforms (Graveley 2005).

The splice site selection is dependent on several aspects such as specific RNA-protein interactions. Splicing regulator are able to recognize defined *cis* elements within the pre-mRNA. Binding to these sequences results in either enhancing or silencing the usage of a splice site (Fig. 1a, Witten and Ule 2011). Furthermore, the AS pattern are shaped by chromatin structure and transcription dynamics. Histone marks such as methylation or acetylation alter the chromatin structure within the nucleosomes, and hence splice site accessibility is changed (Braunschweig *et al.* 2013). Moreover, transcription efficiency of RNA polymerase II and the formation of RNA secondary structures controls splice site recognition and splicing regulator recruitment to the nascent transcript during transcriptional elongation phase (Wachter 2010, Wachter and Hartmann 2014, Saldi *et al.* 2016, Godoy Herz *et al.* 2019).

While the splicing process is highly conserved in higher eucaryotes, several species-specific differences exist indicating common as well as organism-specific regulatory mechanisms. For instance, exon skipping is the most prevalent splice type in humans, whereas intron retention is favored in plants (Sugnet *et al.* 2004, Marquez *et al.* 2012). However, these frequencies do not necessarily reflect the functional relevance of the different AS types. For example intron retention events participate in regulating mammalian neurogenesis (Yap *et al.* 2012) and exon skipping was reported as prominent AS type for splicing regulators in rice (*Oryza sativa*), grape (*Vitis vinifera*) and soybean (*Glycine max*) (Richardson *et al.* 2011).

Since multiple transcripts are derived from one gene locus via AS, it substantially increases the transcriptional diversity. Thereby alternative transcripts can be affected in its stability (Kalyna *et al.* 2012, Drechsel *et al.* 2013), localization (Le Hir *et al.* 2001, Hachet and Ephrussi 2004, Horne-Badovinac and Bilder 2008) or leads to protein with various functions (Zhang and Mount 2009). Thus, it is not surprising that AS was connected to broad array of biological functions. In human, AS is involved in regulation of essential cellular processes such as cell proliferation, programmed cell death/apoptosis and autophagy (Kelemen *et al.* 2013). Consequently, many diseases are caused by genetic variations within splicing regulatory elements or genes encoding for splicing regulators that attract the pharmaceutical industry to research on therapeutic options (Lee and Rio 2015, Nikas *et al.* 2019). Biological relevance of AS were also demonstrated in plants (Staiger and Brown 2013, Yang *et al.* 2014, Laloum *et al.* 2018). Plant development, physiological processes and responses to biotic and abiotic stress are controlled by AS. Recent study revealed that up to 20 % of multiexonic genes exhibit distinct AS pattern during seed germination of barley. These AS events are mainly related to protein synthesis, energy and carbon metabolism as well as RNA metabolism splicing (Zhang *et al.* 2016). Changes in ambient light conditions trigger transcriptome-wide effect on AS level in young seedlings of Arabidopsis (Shikata *et al.* 2014, Mancini *et al.* 2016) and moss protonema (Wu *et al.* 2014).

Despite the increasing understanding regarding the influence of AS on developmental processes and physiological responses, the functional impact of the most single AS events remains unclear. Compared to thousands of identified AS events, just a few have been functionally characterized and successfully linked to important biological functions in higher eukaryotes. In Drosophila, *OSKAR* mRNA isoform is recruited to the posterior pole of the oocyte cytoplasm upon removal of the first intron located at the 3'UTR, which is important for proper germline and abdomen formation (Le Hir *et al.* 2001, Hachet and Ephrussi 2004). Accordingly, components of the exon-exon junction complex, Y14 and MAGO were found to co-localize with *OSKAR* (Le Hir *et al.* 2001). An exon skipping event within the *STARDUST* mRNA causes an uniformly distribution of this isoform while exon retention leads to transcript accumulation at the apical cell side affecting the epithelial development of Drosophila (Horne-Badovinac and Bilder 2008). The sex determination of fruit flies is dependent on splicing site choice between two competitive 3' splice sites in *TRANSFORMER* pre-mRNA (Fu *et al.* 2007, Telonis-Scott *et al.* 2009, Kelemen *et al.* 2013). In Arabidopsis, the locus of the splicing related protein SERINE-ARGININE RICH (SR)-like 45 (SR45, Golovkin and Reddy 1999) generates two mRNA variants being similarly expressed in Arabidopsis plants. However, *sr45-1* overexpressing either *SR45.1* or *SR45.2* show different rescue phenotypes suggesting tissue-specific function in plant development (Zhang and Mount 2009). Thermosensitive AS pattern of central clock components such as LATE ELONGATED HYPOCOTYL suggest that AS

contributes to control of circadian rhythm in response to external changes (James *et al.* 2012). Interestingly, a substantial proportion of AS events identified during developmental transitions did not show an altered expression on total transcript level suggesting AS provides an independent means to regulate gene expression besides transcriptional control (Aghamirzaie *et al.* 2013, Thatcher *et al.* 2014, Sun and Xiao 2015, Srinivasan *et al.* 2016).

2.2. Nonsense-mediated decay

NMD is a complex RNA surveillance mechanism with impact on gene expression in eukaryotes (Isken and Maquat 2007, Lykke-Andersen and Jensen 2015, Shaul 2015, Dai *et al.* 2016). Peltz and colleagues (1993) invented the term to describe that introducing a PTC into the transcript can trigger RNA decay and thus, it functions in RNA quality control. Genome-wide studies demonstrated that NMD is more than the pure degradation of aberrant transcripts. It rather plays an essential role in post-transcriptional gene regulation by controlled turnover of mRNA isoforms (Lareau *et al.* 2007a, Karousis *et al.* 2016). Selection of an alternative splice site can introduce NMD-eliciting features such as PTCs into the transcript sequence. AS coupled to NMD (AS-NMD) has already been well studied with regard to adaptation of gene expression in the animal system (Lareau *et al.* 2007a, Ni *et al.* 2007). In addition, some studies reported AS-NMD *in planta*, too (Staiger *et al.* 2003, Schoning *et al.* 2008, Palusa and Reddy 2010, Wachter *et al.* 2012a), pointing towards a common mechanism within multicellular organisms. Many genes are regulated by AS-NMD (Lewis *et al.* 2003, Kalyna *et al.* 2012, Drechsel *et al.* 2013). Results of a high-resolution RT-PCR panel implied that around 13 to 18% of all intron-containing genes were subjected to AS-NMD in Arabidopsis (Kalyna *et al.* 2012), which could be confirmed by RNA sequencing data (Drechsel *et al.* 2013). Besides PTCs, further transcript features triggering NMD were discovered, comprising upstream open reading frames in the 5’ untranslated region (UTR) and long as well as intron-containing 3’ UTRs (Fig. 1c; Kalyna *et al.* 2012, Schweingruber *et al.* 2013, Peccarelli and Kebaara 2014). These sequence features are recognized by the NMD core components such as UP FRAMESHIFT (UPF) proteins UPF1 (also known as LBA1 in plants), UPF2 and UPF3 as well as the non-universal SUPPRESSOR OF MORPHOLOGICAL DEFECTS IN GENITALIA (SMG) proteins (Isken and Maquat 2007, Nicholson *et al.* 2010). To elicit NMD, the mature mRNA must be exported from the nucleus to the cytosol. Important to mention at this point that the mature mRNA carries protein complexes at each exon-exon junction (so called exon-exon junction complexes, EJC), which memorize every splicing step. During translation the active ribosome stops at the termination codon and UPF1 and SMG1 are recruited. In case of PTC, the EJC is located in close proximity (~25 nt) downstream of the termination codon so that UFP2 and UPF3, which are bound to the EJC, are able to interact

with the ribosome via the other NMD components. Thus, the mRNA degradation pathway is initiated (Isken and Maquat 2007, Nicholson *et al.* 2010, Lykke-Andersen and Jensen 2015). This process is highly similar in mammals and plants except for some species-specific aspects such as the RNA degradation following the NMD initiation. While endonucleolytic cleavage occurs in animals, plant RNA is cut in a exonucleolytic fashion (Shaul 2015).

NMD was found to be important for developmental processes in animals and plants. In fact, it was described that neurite branching of mammalian neuronal stem cells is significantly reduced by UPF3 mutation as well as chemical NMD inhibition (Alrahbeni *et al.* 2015). Accordingly, NMD core components are essential for proper embryogenesis (Hwang and Maquat 2011, Li *et al.* 2015c) such as SMG1-lacking mice are impaired in their brain and heart development (McIlwain *et al.* 2010). Moreover, many defects in NMD pathway result in programmed cell death. For instance, the unfolded protein response (UPR), which contributes to the protein homeostasis within the cell, is regulated by NMD. The downregulation of IRE1α, a key component of UPR, by NMD interrupts the chronic activation of UPR and hence stress-induced apoptosis is prevented (Karam *et al.* 2015). In plants, NMD was linked to physiological stress responses (Rayson *et al.* 2012, Drechsel *et al.* 2013, Gloggnitzer *et al.* 2014) and development (Hartmann *et al.* 2016, Sureshkumar *et al.* 2016). There are indications that NMD is regulated by external stimuli. While biotic stress such as bacterial infection inhibits NMD to promote plant defense response, which is in line with the autoimmunity phenotype of NMD mutants (Rayson *et al.* 2012, Gloggnitzer *et al.* 2014), NMD targets are stabilized upon salt treatment (Drechsel *et al.* 2013). Contrary to this, light seems to exclude NMD-features by differential splicing and thus promotes protein biosynthesis during the early photomorphogenesis (Hartmann *et al.* 2016).

Transcripts of NMD core components are subjected to feedback loops. In Arabidopsis, the *UPF1* and *UPF3* transcripts harbor long 3'UTRs. For latter, it was demonstrated that mutated *UPF3,* which will not be recognized by the NMD machinery, increases the protein level and subsequently the NMD efficiency indicating NMD downregulates its own capacity to a basal level by targeting its core components (Shaul 2015). Remarkably, some transcripts carrying NMD features are not degraded in animals and plants. These transcripts must have another fate or even a specific function within the cell (Eberle *et al.* 2008, Nicholson *et al.* 2010, Kalyna *et al.* 2012). Accordingly, NMD is proposed to fulfil an important regulatory role during physiological processes next to its RNA surveillance function. In conclusion, AS coupled to NMD represents an effective molecular mechanism modifying the transcriptome and thus physiological processes in an environment-dependent manner.

2.3. Splicing regulators

Splicing regulators comprise two large protein families, the HETEROGENEOUS NUCLEAR RIBONUCLEOPROTEINs (hnRNPs) and the SR proteins. The two protein families can function antagonistically during the splicing process and thereby alter the splice site selection (Wang and Burge 2008, Reddy *et al.* 2012b, Howard and Sanford 2015). Prominent representatives of the hnRNPs are the POLYPYRIMIDINE TRACT BINDING PROTEINS (PTBs) and the plant-specific GLICINE-RICH RNA BINDING PROTEINs (GRPs). During the splicing process, PTBs preferentially bind to a certain cytosine/uracil-rich motif, also known as polypyrimidine tract, upstream of the 3' splice site. Hence, an adjacent splice site can be suppressed with consequences on polyadenylation and mRNA stability (Le Sommer *et al.* 2005, Stauffer *et al.* 2010).

The SR protein family comprises a large number of family members in higher eukaryotes, which all share common structural features (Fig. 1d). Per definition, SR proteins harbor one or two RNA recognition motifs (RRM) situated upstream of an arginine-serine-rich domain (RS domain). The latter consists of at least 50 amino acids of which more than 40% are arginines (R) or serines (S) arranged as SR or RS dipeptides (Manley and Krainer 2010). The RS domain is responsible for protein-protein interactions as well as splicing function (Graveley and Maniatis 1998, Reddy and Shad Ali 2011). SR SPLICING FACTOR1 (SRSF1) (also known as SF2/ASF) was the first SR protein found in human (Ge and Manley 1990, Krainer *et al.* 1990). In total, human has twelve SR proteins (SRSF1 to 12) (Manley and Krainer 2010, Richardson *et al.* 2011). The splice regulators recognize splicing enhancer sequences. Hence, U1 snRNP and U2 auxiliary factor (U2AF) are recruited to the 5' and 3' splice sites that initiates the formation of the pre-spliceosomal complex E at the pre-mRNA (Staknis and Reed 1994, Zahler and Roth 1995). However, Kanopka and colleagues (1996) provided evidence that SR proteins can also promote intron retention by binding to intronic repressor element next to the branchpoint, and thus preventing recruitment of spliceosomal components. Moreover, SR proteins were found be involved in many more processes of the RNA metabolism including nuclear speckle formation, mRNA export, 3' end processing and translational regulation, next to transcription-coupled splicing (Shepard and Hertel 2009, Twyffels *et al.* 2011, Jeong 2017). In 1996, SF2/ASF homologs were successfully identified in plants, including the SR30 protein. They had similar biochemical features as mammalian SR proteins and were able to complement splicing in deficient human cell extract, indicating a functional conservation of SRs within metazoans (Lopato *et al.* 1996a). Interestingly, three plant-specific subfamilies, the RS, RS2Z and SCL subfamily characterized by specific structural peculiarities were found in plants including Arabidopsis (Fig. 1d; Lopato *et al.* 1996b, Golovkin and Reddy 1999, Lopato *et al.* 2002), rice (Iida and Go 2006, Isshiki *et al.* 2006) maize (Gupta *et al.* 2005) and moss (Iida

and Go 2006). The RS subfamily harbors two RNA-recognition motives and a C-terminal RS domain with elevated arginine content while the SCL and RS2Z proteins encompass an extended N-terminus or two zinc knuckle motives, respectively (Lopato *et al.* 1996b, Lopato *et al.* 1999a, Barta *et al.* 2010). This classification is supported by comparative analysis between 27 eukaryotes, including single-cell organisms, animals and plants. According to this study, flowering plants contain approximately the double number of SR members compared to vertebrates, which presumably originate from genome duplications and implicate important plant specific functions (Richardson *et al.* 2011).

SR proteins are directly involved in splicing decision, therefore these proteins undergo a strict regulation on several levels to ensure a precise AS outcome during developmental processes, in different tissues and in response to abiotic stresses (Palusa *et al.* 2007). The splicing regulators target its own pre-mRNA and immature transcripts of its subfamily members to auto- and cross-regulate themselves. Around 80% of the SR pre-mRNAs undergo AS in Arabidopsis and can generate about 95 different mRNA isoforms (Palusa *et al.* 2007). Many of these alternative transcripts carry NMD target features (Palusa and Reddy 2010), suggesting the production of non-functional mRNA isoforms and hence rapid RNA turnover. Contrary, posttranslational modifications such as phosphorylation (Roth *et al.* 1991), methylation (Siebel and Guthrie 1996, Sinha *et al.* 2010) and acetylation (Choudhary *et al.* 2009, Edmond *et al.* 2011) can alter SR protein stability, function or localization. The SR-like protein SR45 provides two major spicing variants differing in a short insertion. Since both sequences are in frame, they were supposed to result in functional proteins (Zhang and Mount 2009). Pleiotropic phenotypes appeared in *sr45-1* suggesting a role in plant development (Ali *et al.* 2007). By either introducing *SR45.1* or *SR45.2*, the petal or the root phenotype could be rescued, respectively, although both transcripts are equally expressed in wild type tissue implicating a further regulatory layer (Zhang and Mount 2009). SR45.1 encompass an eight amino acid insertion with two additional phosphorylation sites compared to SR45.2. Phosphosite-substitution mutants proofed that both phosphorylation sites are essential for the individual capacity of SR45.1 und SR45.2 to rescue single developmental defects of *sr45-1*, and implies a functional impact of SR-phosphoregulation (Zhang and Mount 2009). Accordingly, SCL30 is constitutively targeted by SR protein-specific kinase 4 (SRPK4) whereas mitogen activated kinases (MAPKs) only phosphorylate SCL30 in response to oxidative stress (de la Fuente van Bentem *et al.* 2008). Besides phosphorylation (Roth *et al.* 1991), SR and SR-like proteins are also post-translationally methylated (Siebel and Guthrie 1996, Sinha *et al.* 2010) or acetylated (Choudhary *et al.* 2009, Edmond *et al.* 2011). This post-transcriptional modification can alter the subcellular localization of the splicing regulators e.g. shown for SR45 in Arabidopsis (Ali *et al.* 2003) or SRSF1 in mammals (Gui *et al.* 1994, Colwill *et al.* 1996).

A.

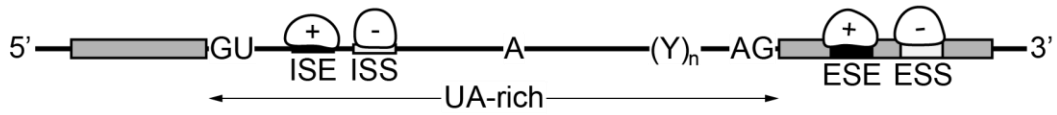

B.

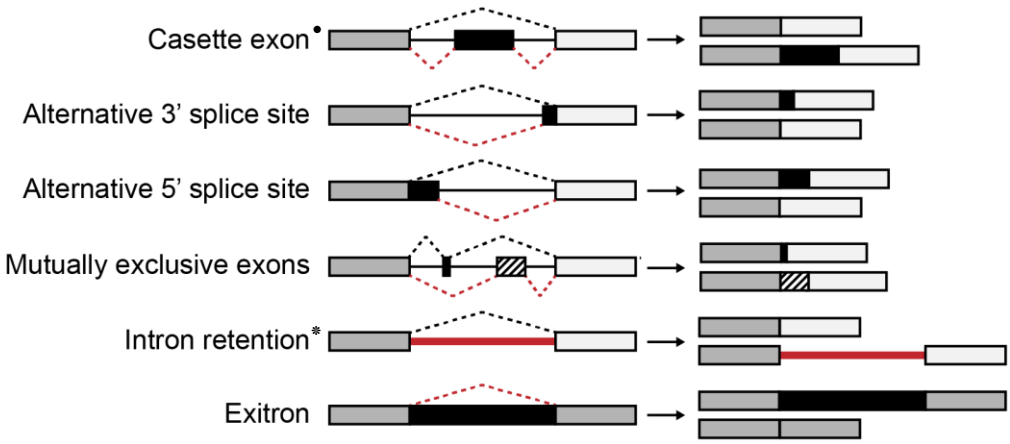

C.

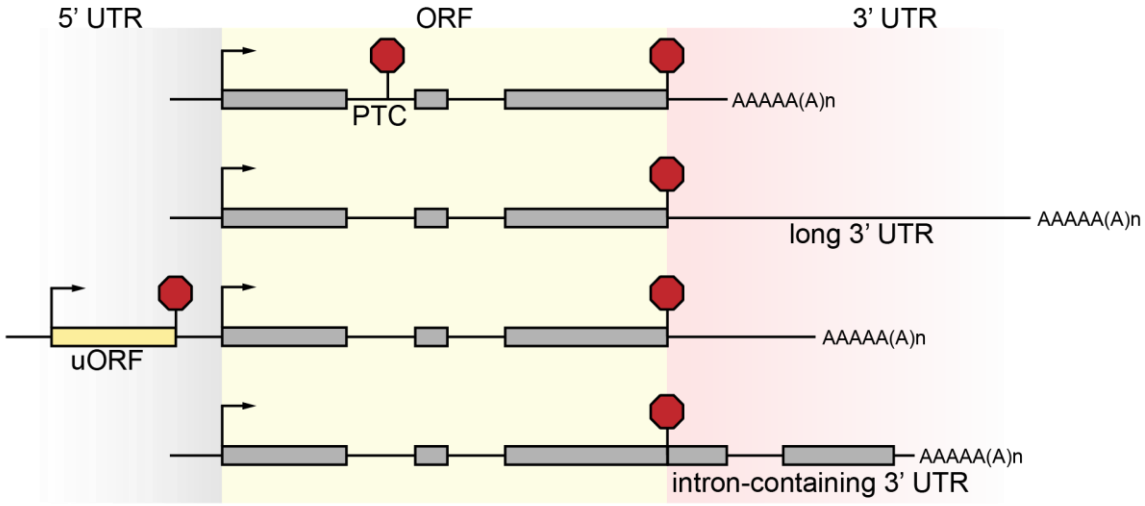

D.

common SR proteins in plants and animals

		members in Arabidopsis	human homologue
SR	RRM RRM SR	SR30, SR34, SR34a, SR34b	SRSF1 (ASF/SF2)
RSZ	RRM Zn RS	RSZ21, RSZ22, RSZ22a	SRSF7 (9G8)
SC	RRM SR	SC35	SRSF2 (SC35)

plant-specific SR proteins

SCL	RRM SR	SCL28, ACL30, SCL30a, SCL33	
RS2Z	RRM Zn Zn SR SP	RS2Z32, RS2Z33	
RS	RRM RRM RS	RS31, RS31a, RS40, RS41	

SR-like proteins

RRM SR RRM	SR45	RNPS1

Figure 1: AS is tightly regulated by complex RNA-protein interactions and significantly enhances the transcriptome diversity. A. The splice site decision is influenced by several essential *cis* elements of the transcript and *trans*-acting factors. Conserved core splicing signals including 5' splice site (GU), 3' splice site (AG), branch point (A) and pyrimidine tract ($(Y)_n$) define exon (box) and intron (line) identity and are recognized by spliceosomal components. Intronic and exonic splice enhancer (ISE/ESE) as well as silencer (ISS/ESS) belong to the auxiliary *cis* elements, and are targeted by *trans*-acting splicing regulators that positively (+) or negatively (-) affect the splicing process. **B.** Basic AS types with binary splice site choice are shown. Gene structure is display as in A. Constitutive and alternative splice junctions are indicated by black or red dashed lines, respectively. Further, retained intron is shown as solid red line. Most prominent AS events differ in plants* and human•. **C.** AS can affect transcript stability by NMD-eliciting features such as premature stop codon (PTC), long or intron-containing 3' untranslated regions (UTR), and upstream open reading frames (uORF) in the 5' UTR. Arrows and octagons represent start and stop codons **D.** Classification of SR and SR-like proteins in *A. thaliana* and their human homologues. All SR proteins have in common one or two RNA-recognitions motives (RRM) followed by one domain enriched in serine-arginine-dinucleotides (SR, RS). Some SR protein additionally contain zinc knuckles (Zn), N-terminal extensions (dark grey box) or serine-proline-rich domains (SP). The different figure parts are based on Syed *et al.* (2012), Reddy *et al.* (2007), Peccarelli and Kebaara (2014) and Barta *et al.* (2010), respectively.

Phosphorylation of the SR proteins resulted in reversible formation of nuclear speckles (Gui *et al.* 1994, Colwill *et al.* 1996, Ali *et al.* 2003). Further SR proteins were detected in such nuclear structures; e.g. SR30, SR33, SR34 (Fang *et al.* 2004) and RS31 (Docquier *et al.* 2004). Nuclear speckles are highly dynamic subcompartments and thought to be RNA processing bodies in line with the SR function. Time-lapse experiments demonstrated that SRs fused to fluorescent proteins assemble, rearrange and shuttle between speckles (Ali *et al.* 2003, Docquier *et al.* 2004). Remarkably, these above-mentioned speckle movements could be blocked by adding transcription or phosphatase inhibitor, respectively, thereby connecting the SR proteins to transcriptional activity as well (Fang *et al.* 2004).

2.4. Regulation of light signaling during early plant development

The life cycle of vascular plant starts with seed germination triggered by different environmental signals including light exposure, temperature, water availability or cold stress (Borthwick *et al.* 1952, Toole *et al.* 1955, Roth-Bejerano *et al.* 1966, Mancinelli *et al.* 1967, Kendrick and Frankland 1969, Taylorson and Hendricks 1972, Kendrick and Heeringa 1986, Bradford 1990, Erwin 1991, Heschel *et al.* 2007). In absence of light, skotomorphogenic growth of the seedling is promoted, which is also known as etiolation. Dark-grown dicot seedlings characteristically exhibit short roots, closed and pale cotyledons connected to an apical hook protecting the shoot apical meristem, and an enhanced hypocotyl elongation rate (Terzaghi and Cashmore 1995, Whitelam *et al.* 1998, Jiao *et al.* 2007). Under natural growth conditions,

these features promote emergence from the soil and exposure to light. Similarly, the mesocotyl of monocots growth expeditiously and carries a furled primary leaf (Markelz *et al.* 2003, Takano *et al.* 2005). Light perception initiates the photomorphogenesis of the seedling to set up all requirements for photosynthesis and thus photoautotrophic life style. The seedling starts to de-etiolate, the leaves open and expand, and chlorophyll is produced while hypocotyl thickening is stimulated (Jiao *et al.* 2007).

Integration of the ambient light conditions is essential for plant survival since light determines the plant development and serves as energy source (Jiao *et al.* 2005, Jiao *et al.* 2007, Kami *et al.* 2010, Galvao and Fankhauser 2015, Kaiserli *et al.* 2015). Besides photomorphogenesis, it controls many other processes, e.g. shade avoidance, phototropism, chloroplast movement, stomatal opening and flowering (Jiao *et al.* 2007). To recognize the surrounding light conditions, plants have evolved different photoreceptor types. Their wavelength specificities are mediated by different chromophores bound to the photoreceptors (Briggs and Olney 2001). Red and far-red light is mainly perceived by phytochromes (PHYs). In Arabidopsis, there are five members of this family, PHYA to PHYE (Sharrock and Quail 1989, Clack *et al.* 1994). Cryptochromes (CRY1, CRY2), phototropins, and ZEITLUPEs are crucial for blue and UV-A light perception, whereas the UV RESISTANCE LOCUS 8 receptor perceives UV-B light (Whitelam 1995, Fankhauser and Chory 1997, Briggs and Huala 1999, Somers *et al.* 2000, Kliebenstein *et al.* 2002). Until now, there is no evidence for photoreceptors detecting green light, however, there are speculations that green light might affect plant development as well (Folta and Maruhnich 2007, Kami *et al.* 2010). PHYs and CRYs are employed during the early seedling development (Galvao and Fankhauser 2015). PHYs represent light-activated photoswitches. In absence of light, PHYs appear in their inactive Pr form inside the cytosol. Red light perception initiates a conformational change to the biologically active Pfr form, which is translocated to the nucleus to promote protein interactions (Sakamoto and Nagatani 1996, Kircher *et al.* 1999) and light-responsive gene expression (Martinez-Garcia *et al.* 2000, Tepperman *et al.* 2001). Conversely, far-red light illumination or darkness trigger either the quick or slow reversion, respectively, to the inactive Pr form (Rockwell *et al.* 2006). In contrast to PHYs, CRY1 shuttles into the cytoplasm upon blue light irradiation and CRY2 is exclusively found within the nucleus (Kleiner *et al.* 1999, Lin and Shalitin 2003). Upon light perception, the photoreceptors stimulate a downstream-acting and complex transcriptional network (Jiao *et al.* 2007, Galvao and Fankhauser 2015). Accordingly, the process of de-etiolation is initiated by light-triggered gene regulation of positively acting transcription factors (TFs) and by repression of negative regulators. The ubiquitin E3 ligase CONSTITUTIVELY PHOTOMORPHOGENIC1 (COP1) is an important repressor of photomorphogenesis in dark-grown seedlings and acts together with SUPPRESSOR OF PHYA (SPA) proteins in a nuclear complex (Wu and Spalding 2007). COP1 ubiquitinates light-

promoting TFs (Kim *et al.* 2017c) such as LONG AFTER RED LIGHT 1 (Seo *et al.* 2003) and ELONGATED HYPOCOTYL 5 (HY5, Osterlund *et al.* 2000a) which are subsequently targeted by the proteasomal degradation. Upon light exposure, COP1 is excluded from the nucleus and thus photomorphogenesis can be initiated by the stabilization of light-promoting TFs. Additionally, Pfr and CRYs are able to inhibit the COP1/SPA complex in the nucleus, thereby further enhancing the light response. However, its specific mode of action is poorly understood so far (Jiao *et al.* 2007, Kami *et al.* 2010, Galvao and Fankhauser 2015). The first direct link between photoreceptors and transcriptional regulation was demonstrated by the identification of the basic helix-loop-helix (bHLH) TFs PHYTOCHROME INTERACTING FACTORs (PIFs) (Castillon *et al.* 2007, Jiao *et al.* 2007, Leivar *et al.* 2009). Arabidopsis genome encodes eight family members (Pham *et al.* 2018). Similar to COP1, PIFs primary promote skotomorphogenesis (Leivar *et al.* 2008). Their phosphorylation by Pfr initiates proteasomal degradation that positively contributes to the photomorphogenesis. Remarkably, PIFs re-accumulated in subsequent dark phases indicating a light-dependent regulatory role in day-night-cycles (Jiao *et al.* 2007). The quadruple mutant *pifQ* (*pif1 pif3 pif4 pif5*) shows a constitutive photomorphogenic phenotype in absence of light comparable to *cop1* (Leivar *et al.* 2008) suggesting PIFs share functional overlap. However, some PIFs fulfil distinct physiological functions, including seed germination (Oh *et al.* 2004, Oh *et al.* 2006), chlorophyll biosynthesis (Huq *et al.* 2004, Monte *et al.* 2004), hypocotyl elongation (Oh *et al.* 2004), leaf senescence (Sakuraba *et al.* 2014) and shade avoidance (Lorrain *et al.* 2008). Remarkably in contrast to the other PIFs, PIF2 and PIF6 represent positive regulators of photomorphogenesis (Pham *et al.* 2018). Light triggers heterodimerization of PIF2 and LONG HYPOCOTYL IN FAR-RED1. The complex binds to PIF1, 3, 4 and 5 to prevent PIF-mediated gene expression (Luo *et al.* 2014).

Differential gene expression during light-mediated developmental transitions also includes the action of non-coding RNAs. HY5 and PHYB were found to bind to light-responsive elements in promoter regions of microRNAs (miRNAs) (Sanchez-Retuerta *et al.* 2018). In fact, miR171, which is involved in the control of chlorophyll biosynthesis, was found to be differentially expressed in *phyB* compared to wild type in rice (Sun *et al.* 2015b). Accordingly, light exposure induces miR171 expression, which in turn downregulates SCARECROWs, and thus derepresses the expression of the chlorophyll biosynthesis key enzyme PCHLIDE OXIDOREDUCTASE (Wang *et al.* 2010, Ma *et al.* 2014). Further support for miRNAs acting during photomorphogenesis revealed a small RNA sequencing study in soybean. Global expression pattern changed upon far-red light illumination in various seedling tissues (Li *et al.* 2014, Sanchez-Retuerta *et al.* 2018). Additionally, mutation in AGO1, an essential component of the RNA-induced silencing complex, correlated with a reduced light response during the de-etiolation. These data suggest miRNAs to target negative regulators involved in opening of

apical hook and cotyledons. Another layer of miRNA regulation represents the induction of miRNA processing proteins by light, e.g. HUA ENHANCER 1 (HEN1), a methyltransferase that stabilizes the miRNAs in the last step of their biogenesis (Sanchez-Retuerta *et al.* 2018). HY5 and its homolog HYH initiate the upregulation of HEN1. Thus, HY5-targeting miR157 is enriched and induces a negative feedback of HY5 via RNA silencing (Tsai *et al.* 2014). Further complexity in the regulatory network results from light-mediated AS control of miRNA-related proteins such as DICER-LIKE 1 and HEN1 (Hernando *et al.* 2017) as well as gene repositioning within the nucleus (Feng *et al.* 2014, Perrella and Kaiserli 2016).

Several studies investigated the impact of light on transcriptome-wide gene expression (Jiao *et al.* 2007, Kami *et al.* 2010, Galvao and Fankhauser 2015). Microarray (Ma *et al.* 2001, Schaffer *et al.* 2001, Tepperman *et al.* 2001, Jiao *et al.* 2005) and RNA sequencing analysis (Shikata *et al.* 2014, Hartmann *et al.* 2016, Mancini *et al.* 2016) demonstrated a widespread reprogramming of the transcriptome in response to changing light conditions. Remarkably, estimations for *Arabidopsis thaliana* and rice predict at least 20 % of the genome to be differentially expressed when comparing etiolated with light-grown seedlings (Jiao *et al.* 2005). Interestingly, transcripts of light signaling-related proteins were shown to be targeted by AS. qRT-PCR analysis revealed that two distinct transcripts originate from the HYH locus in Arabidopsis. The shorter mRNA isoform encodes an alternative HYH protein, which was less susceptible to proteasomal degradation since the COP1-binding domain was spliced out (Sibout *et al.* 2006). COP1 is differentially spliced into *COP1β* in mature seeds and cotyledons. Overexpression of *COP1β* leads to suppression of skotomorphogenic growth in dark-grown seedlings and suggested a dominant negative regulation of *COP1β* on COP1 function (Zhou *et al.* 1998). These single splicing events outlined the first link between light signaling and AS. Moreover, several studies started to analyze whether light affects AS pattern *in planta*. First evidence for light-regulated AS were proved for the ASCORBATE PEROXIDASE (Mano *et al.* 1997) and HYDROXYPYRUVATE REDUCTASE (Mano *et al.* 1999, 2000) in pumpkin (Cucurbita sp.) and triggered a protein isoform-specific subcellular localization. Remarkably, high light irradiation changed the expression pattern of *SR45* and *SR30* mRNA isoforms over time indicating involvement of AS, too (Tanabe *et al.* 2007). Microarray data and RT-PCR panel further verified the AS regulation by different light conditions in Arabidopsis and rice suggesting altered AS pattern might contribute to the global light-responsive gene expression (Simpson *et al.* 2008, Jung *et al.* 2009). The invention and establishment of high-throughput RNA sequencing techniques enabled comprehensive investigation of differential gene expression including AS pattern in a transcriptome-wide manner. Exposure of different light qualities to etiolated Arabidopsis seedlings (Shikata *et al.* 2014, Hartmann *et al.* 2016) and dark-grown moss protonema (*Physcomitrella patens*, Wu *et al.* 2014) resulted in tremendous transcriptional reprogramming after illumination due to differential gene expression and AS.

Moreover, light-grown plants exhibited altered AS pattern as demonstrated by using extended night conditions (Petrillo *et al.* 2014) or light pulses within the dark phase of a diurnal rhythm (Petrillo *et al.* 2014, Mancini *et al.* 2016). However, the comparison of gene expression pattern with AS events showed that both processes seem to be regulated independently since there was a small overlap of common targets and the proportion can be assumed even less considering NMD (Kalyna *et al.* 2012, Drechsel *et al.* 2013). Similar results concerning differential splicing and gene expression pattern were obtained by analyzing temperature-dependent splicing (Pajoro *et al.* 2017).

2.5. Photosynthesis and sugar metabolism

Next to its signaling function, light serves as energy source since the plant is able to convert electromagnetic radiation and inorganic compounds into energy-rich organic biomolecules via photosynthesis (Jiao *et al.* 2007, Kaiserli *et al.* 2015, Johnson 2016). First experiments on photosynthesis date back to the late 18th century. Thereby it was discovered that plants are able to produce inflammable gas and Jan Ingen-Houz demonstrated that light is required for this process (Gest 1988, 2000). By now photosynthesis has been well-studied in terms of chemical reactions and proteins involved in this biological process (Pego *et al.* 2000). The photosynthesis can be described as a two-step-process including light reaction and calvin cycle to reduce carbon dioxide to carbohydrates. The Calvin cycle results in the generation of glyceraldehyde-3-phosphate, which serves as the precursor for more complex carbohydrates including glucose, sucrose and the highly complex storage compound starch (Rolland *et al.* 2006, Voet, Voet and Pratt 2010).

However, the regulation and fine-tuning of photosynthesis with regard to the environmental changes is still subjected to active research. Most of the proteins employed by photosynthesis are encoded in the nuclear genome. Therefore, a tight bilateral communication between chloroplast and nucleus is required (Rodermel 2001, Chan *et al.* 2016). Accordingly, the chloroplast is able to regulate the expression for a subset of nuclear-encoded genes in response to changes in the environment via the retrograde signaling (Nott *et al.* 2006, Chan *et al.* 2016). Doing so, retrograde signaling coordinates multiple signaling pathways including chlorophyll biosynthesis, the redox state monitoring of the photosynthetic electron transport, the expression of plastidal proteins and hormone signaling to control chloroplast function (Nott *et al.* 2006). Additionally, the maturation of chloroplasts during the de-etiolation is also coordinated by the plastid-to-nucleus-communication (Ruckle *et al.* 2007, Ruckle and Larkin 2009, Chan *et al.* 2016).

Photosynthesis is highly dependent on various external signals including light intensity (Schumann *et al.* 2017, Feng *et al.* 2019, Yang *et al.* 2020), CO_2 concentration (Stitt 1991, Van

Oosten *et al.* 1994, 1995), nitrogen resources (Fredeen *et al.* 1991) and temperatures (Bagnall *et al.* 1988). Cellular response to the different environmental factors need to be well-coordinated in order to increase the photosynthetic efficiency, and to prevent photodamage. Previous studies suggested that photoassimilates could have regulatory functions on photosynthesis (Paul and Foyer 2001). Sugars ubiquitously occur within the plant, and their synthesis directly correlates with the photosynthesis rate, which are further supportive aspects (Lee and Daie 1997, Hausler *et al.* 2014, Figueroa and Lunn 2016, Oszvald *et al.* 2018). Accordingly, evidence was provided that photosynthesis end products are able to alter gene expression such as for plastidal proteins (Pego *et al.* 2000) leading to negative feedback control. In general, sugar depletion induces photosynthesis-related genes and increases the photosynthetic capacity, whereas saturated intracellular sugar level represses transcription of these genes (Pego *et al.* 2000), as demonstrated for the photosynthesis key components RIBULOSE-1,5-BISPHOSPHATE CARBOXYLASE/OXYDASE (RuBisCO), PLASTOCYANIN (Krapp *et al.* 1993, Dijkwel *et al.* 1996), DARK-INDUCIBLE (DIN) proteins, and CHLOROPHYLL A/B BINDING PROTEINs (CABs, Fujiki *et al.* 2000, Fujiki *et al.* 2001).

The disaccharides sucrose and trehalose are assumed to play key roles in sugar signaling because of their biochemical properties enabling these sugar molecules to shuttle within the plant (Arnold 1968, Eastmond *et al.* 2002, Rolland *et al.* 2006). Sucrose is one of the major photosynthesis end products and mainly acts as transport molecule. Evidence has been provided that not sucrose itself, but rather its hydrolytic cleavage products have signaling function (Rolland *et al.* 2006, Stein and Granot 2019). It can be metabolized in photosynthetically active tissues (source) or it is transported via the phloem to organs with a demand for carbohydrate import (sink). Moreover, excessive sucrose produced in presence of light turns on starch synthesis within the chloroplast, whereby sucrose is transiently stored in form of macromolecules. In sink tissues, intracellular sucrose is either cleaved into monosaccharides or accumulates in the vacuole for later usage (Rolland *et al.* 2006). Natural diurnal fluctuation and environmental variation can result in sugar starvation triggering catabolism including sucrose hydrolysis and starch breakdown (Kolbe *et al.* 2005, Smith *et al.* 2005, Rolland *et al.* 2006). In contrast to sucrose, trehalose is a low-abundant carbohydrate, being in the micromolar range in Arabidopsis (Lunn *et al.* 2006). Constitutive expression of bacterial trehalose-6-phosphate (T6P) synthase (TPS) or T6P phosphatase caused opposite phenotypical changes considering leaf development and flowering time in Arabidopsis (Schluepmann *et al.* 2003). Moreover, the knock-out mutant of endogenous *tps1* displays a developmental arrest in the torpedo stage during seed maturation, resulting in unviable seeds. The lethality can be overcome by introducing TPS expressed under an inducible or embryo-specific promoter (van Dijken *et al.* 2004, Gomez *et al.* 2010). These studies demonstrated the essential functions of trehalose in plant development. Further investigations revealed that T6P

level were boosted in starved seedlings upon exogenous sucrose supply, and thus turning on the starch synthesis. In addition, the study could demonstrate a close correlation between endogenous T6P and sucrose concentrations in rosette leaves during the day-night-cycle (Lunn *et al.* 2006). Therefore, a trehalose-sucrose-nexus was postulated comprising T6P as signaling molecule and as negative feedback regulator for sucrose metabolism to optimize plant growth (Yadav *et al.* 2014).

Interestingly, exogenous application of high sugar levels interferes with proper photomorphogenesis during early seedling development (Rolland *et al.* 2006), supporting a tight link between light-dependent plant development and sugar signaling. Accordingly, plant growth and many physiological processes arrest under starvation conditions. Upon starvation, the basic metabolism is maintained while energy-consuming processes (e.g. protein biosynthesis) (Blasing *et al.* 2005) and nutrient recycling (e.g. proteolysis, autophagy, senescence) (Hanaoka *et al.* 2002) are repressed or activated, respectively. The identification and characterization of several sugar-signaling-related mutants expanded our understanding of the regulatory networks and additionally revealed connections to phytohormones, including ethylene and abscisic acid (ABA) (Rolland *et al.* 2006).

2.6. Central energy sensors

The maintenance of energy homeostasis is essential for plant survival. Varying levels of nutrients and carbon compounds are integrated by central energy sensors that are highly conserved among eukaryotes. SUCROSE NONFERMENTING RELATED KINASE1 (SnRK1) is promoted under energy limiting conditions to ensure plant survival (Smeekens *et al.* 2010). Baena-Gonzalez and colleagues (2007) identified several *DIN* genes as SnRK1 targets and demonstrated the activation of the SnRK1 signaling pathway by extended darkness. Moreover, this study provided evidence that the kinase is an important developmental regulator during normal vegetative and reproductive growth. Nevertheless, if SnRK1 might be involved in seedling development, too, remains elusive. SnRK1 acts as heterotrimeric protein kinase complex. Its catalytic domain (α-subunit, encoded by SnRK1.1 or SnRK1.2) was shown to execute the signaling function independent of the other subunits, and is highly similar to yeast SUCROSE NON-FERMENTING 1 (SNF1) and mammalian AMP-ACTIVATED PROTEIN KINASE (AMPK). Nevertheless, the β- and plant-specific βγ-subunit are necessary for protein-protein-interaction and localization of the complex (Emanuelle *et al.* 2015, Ramon *et al.* 2019), pinpointing to an essential regulatory function. Upon SnRK1 activation in response to starvation, a highly diverse network of numerous TFs and many phosphorylation targets transduce the SnRK1 signal within the cell (Davies *et al.* 1995, Baena-Gonzalez *et al.* 2007, Smeekens *et al.* 2010, Shen *et al.* 2014, Ye *et al.* 2015, Cho *et al.* 2016, Chan *et al.* 2017,

Bruns *et al.* 2019). For example, dark-induced senescence activates the basic leucine zipper 63 (bZIP63) TF in a SnRK1-dependent manner. SnRK1-mediated phosphorylation leads to dimerization of bZIP63 with other bZIP TFs to induce specific, starvation-related gene expression patterns such as *DIN6* (Baena-Gonzalez *et al.* 2007, Mair *et al.* 2015). Furthermore, gene expression of *α-AMYLASE2* is upregulated in a SnRK1-dependent manner to break down starch for energy production (Laurie *et al.* 2003).

Mis-regulation of SnRK1 drastically alters the plant growth and physiology. Increased SnRK1 expression levels interfere with ABA signaling leading to delayed germination (Radchuk *et al.* 2006, Tsai and Gazzarrini 2012). At later developmental stages, overexpression of SnRK1 stimulates starvation tolerance and plant fitness while it suppresses senescence (Baena-Gonzalez *et al.* 2007). Interestingly, single knock-out mutants of SnRK1 did not show obvious phenotypes, probably due to the partially functional redundancy of SnRK1.1 and SnRK1.2. Conversely, knock-out of both SnRK1 α-subunits in Arabidopsis is embryo-lethal, while induced repression resulted in retarded growth, repressed transition between developmental stages resulting in infertility or accelerated senescence depending on the induction time point (Baena-Gonzalez *et al.* 2007, Nukarinen *et al.* 2016). Accordingly, studies analyzing SnRK1 function in other species revealed overall growth, pollen development, germination rate and cotyledon opening are positively regulated by SnRK1 in moss (Thelander *et al.* 2004), barley (Hordeum vulgare, Zhang *et al.* 2001), rice (Lu *et al.* 2007) and pea (Pisum sativum, Radchuk *et al.* 2010), respectively.

Plants have evolved a highly complex regulatory network to control SnRK1 in response to diverse external signals that need to be integrated. Among others, the kinase activity is promoted by phosphorylation of a conserved Thr in the α-subunit T-loop (Shen and Hanley-Bowdoin 2006, Shen *et al.* 2009, Glab *et al.* 2017). Further, the protein stability is affected by SR45-mediated proteasomal degradation (Carvalho *et al.* 2016), and hexose-6-phosphates, especially T6P, inhibit SnRK1 signaling (Zhang *et al.* 2009, Delatte *et al.* 2011). However, the mechanisms behind this interplay of post-translational modifications, protein processing and the metabolic state inside the cell are still an open research field.

Recently, SnRK1 signaling was connected to TARGET OF RAPAMYCIN (TOR), another central energy sensor that is classified as phosphatidylinositol 3-kinase-related lipid kinase (PIKK, Heitman *et al.* 1991). The research history of TOR started with the isolation of the antifungal and immune suppressive compound rapamycin (Sehgal *et al.* 1975). The drug was originally isolated from the soil bacteria *Streptomyces hygroscopicus* located at Easter Island Rapa Nui. During a yeast mutant screen, two genes (*TOR1* and *TOR2*) could be identified that confer rapamycin toxicity (Heitman *et al.* 1991). Later on, single TOR homologs have been found in mammals (mTOR; Sabatini *et al.* 1994) and plants (TOR; Menand *et al.* 2002). The

kinase is evolutionary conserved and acts such as SnRK1 in a heterotrimeric protein complex. In plants, this heterotrimeric complex includes the accessory proteins REGULATORY ASSOCIATED PROTEIN OF TOR (RAPTOR) and SMALL LETHAL WITH SEC13 PROTEIN 8 (Dobrenel *et al.* 2016). TOR exhibits an opposite regulation compared to SnRK1. Under nutrient-rich conditions, TOR signaling is activated to promote growth via induced mRNA translation, modulation of the cell cycle, and positive regulation of metabolic processes such as lipid synthesis and the pentose phosphate pathway (Sheen 2014). Interestingly, both TOR and SnRK1 are essential regulators of autophagy. SnRK1 promotes the starvation-induced autophagosome initiation by phosphorylation of AUTOPHAGY-RELATED GENE 1. In line with this, TOR repression leads to an elevated number of autophagosomes, whereas TOR activation inhibits autophagy under nutrient-rich conditions (Chen *et al.* 2017, Shi *et al.* 2018). If an organism has to budget its energy resources, TOR signaling itself is repressed and SnRK1 modulates the physiology according to starvation conditions (Shi *et al.* 2018). Photosynthesis-derived glucose has been claimed to be the major TOR signaling activator, however, the underlying mechanism is unknown. The inactivation of SnRK1 signaling could be an essential component of TOR regulation since SnRK1 is able to phosphorylate RAPTOR and hence interferes with TOR signaling (Nukarinen *et al.* 2016). Therefore, the idea arose that both kinases share a common subset of phosphorylation targets to sense the energy status in an antagonistic manner and thus transcriptome, metabolism, cell growth and development are adjusted (Broeckx *et al.* 2016, Li and Sheen 2016, Shi *et al.* 2018).

3. Aim of work

Light-induced transcriptome-wide reprogramming of AS pattern, next to massive adjustment of gene expression on total transcript level, contribute to the phenotypical adaptation of etiolated seedlings during the early photomorphogenesis. This study aims to understand the functional impact of single light-driven AS events and how AS responses are regulated upon illumination. To address this, AS pattern of known light-mediated AS events were analyzed in etiolated seedlings, which were kept in darkness compared to those exposed to different light conditions.

While we could demonstrate gene expression control for *RRC1* by coupled AS-NMD in etiolated seedlings, the dark-promoted *SR30.2* escapes from NMD although it displays NMD-eliciting features. Measuring RNA stability, *SR30.2* appear to have almost five times higher half-live as *SR30.1*. We proposed that nuclear retention prevents *SR30.2* from cytosolic RNA decay via NMD. To analyze the subcellular distribution of *SR30.1* and *SR30.2*, the expression level of both *SR30* mRNA isoforms were determined in nuclear and cytosolic fractions of *Arabidopsis thaliana* seedlings and *Nicotiana benthamiana* leaves expressing an *SR30* reporter. Since NMD requires translation, tagged ribosomal protein was isolated to examine the transcript abundance of the major *SR30* mRNA isoforms in the co-immunoprecipitated RNA fraction. Accordingly, *SR30* AS pattern and expression level of SR30 splice variants were measured. *SR30.3* is a less abundant mRNA isoform. It results from activation of both alternative 3' splice sites leading to an additional exon skipping event of 117 bp in exon 11 compared to *SR30.2* and accumulates in NMD mutants. To test whether *SR30.2* can be further spliced into *SR30.3* by using the remaining 3' splice site, endogenic and transgenic *SR30.3* was detected in plants overexpressing *SR30.2* cDNA.

To examined the potential regulatory role of the major red and blue light receptors in AS control, we analyzed light-trigger AS events in *phyA phyB* or *cry1 cry2* mutants, respectively, under various light regimes in Arabidopsis seedlings. Interestingly, exogenous application of sucrose or a general kinase inhibitor to etiolated seedlings completely or partly mimicked the light-triggered AS response, respectively. Therefore, we investigated the role of central energy sensor in AS control. Gene expression of SnRK1 targets *DIN1* and *DIN6* negatively correlated with light and sucrose response. To enable investigation of SnRK1 contribution in AS control, constitutive and inducible double knock-down mutants were generated and characterized including hypocotyl assays, chlorophyll measurement, mortality rate upon SnRK1 repression, and SnRK1 expression analysis on transcript and protein level. Accordingly light-responsive-ness were tested in SnRK1 mutants. Finally, we were interested in a possible contribution of the energy sensor TOR, since the kinase has been described to function opposite to SnRK1.

4. Results and discussion

The switch from skotomorphogenic to photomorphogenic growth is a highly complex light-driven, developmental process, which needs a tight regulation of gene expression. A recent study demonstrated the contribution of light-mediated AS to the tremendous transcriptional reprogramming during the early photomorphogenesis in Arabidopsis seedlings (Hartmann *et al.* 2016). Remarkably, the majority of the identified dark-promoted transcripts (77.2%) contain NMD-eliciting features whereas light exposure prompts the exclusion of these features for 61.1 % of all transcripts via usage of an alternative splice site. These data indicate a light-triggered switch from putative unproductive NMD targets, mainly abundant in darkness, to the protein-coding transcript upon illumination and thus light-triggered mRNA isoforms are stabilized. Functional relevance for AS-NMD could be shown for the putative splicing factor RRC1. The T-DNA insertion line *rrc1-2* shows defects in red light signaling characterized by an elongated hypocotyl phenotype upon red light exposure (Shikata *et al.* 2012b). The complementation with the light-induced mRNA isoform *RRC1.1* was able to reconstitute the wildtype-like hypocotyl response for *rrc1-2* in contrast to the NMD target *RRC1.2*, which accumulates under dark conditions (Hartmann *et al.* 2016). This phenotype is caused by an impaired PHYB signaling (Shikata *et al.* 2012b). The RS domain of RRC1 is important for the interaction with PHYB. Mutants lacking the functional RS domain display a similar hypocotyl phenotype and affect the splicing pattern of several SR genes in an aberrant manner (Shikata *et al.* 2012a, Shikata *et al.* 2012b). The regulation of the cassette exon might be performed by SPLICING FACTOR FOR PHYTOCHROME SIGNALING (SFPS), which was recently identified to interact with PHYB and RRC1 in nuclear photobodies. Accordingly, SFPS was shown to contribute to light-mediated AS pattern shift for *RRC1*. Hence, this complex is supposed to positively regulate PHY signaling and thus the photomorphogenesis (Xin *et al.* 2019). Next to quantitative expression control, AS can increase the functional diversity of one gene locus. Taken together, this example unveils the potential of AS as powerful mechanism for regulating gene expression to adjust the plant's metabolism and growth to light-dependent environmental changes.

Consistently, AS-NMD regulation of several splicing regulators has been reported for animals (Wollerton *et al.* 2004, Lareau *et al.* 2007b, Ni *et al.* 2007) and plants (Staiger *et al.* 2003, Wollerton *et al.* 2004, Lareau *et al.* 2007b, Ni *et al.* 2007, Schöning *et al.* 2008, Palusa and Reddy 2010, Stauffer *et al.* 2010). In Arabidopsis, the hnRNPs PTB1 and PTB2 are known to auto- and cross-regulate the splicing pattern of their pre-mRNAs (Stauffer *et al.* 2010). Elevated PTB protein level provoke the introduction of a PTC-containing cassette exon into PTB pre-mRNA and hence, the resulting transcripts are designated for RNA decay (Stauffer *et al.* 2010, Wachter *et al.* 2012b). Accordingly, transcriptome-wide AS analysis of PTB1 and

PTB2 misexpression lines uncovered a large number of potential PTB-dependent AS events despite their own pre-mRNA (Rühl *et al.* 2012). Among others, PIF6 AS pattern was affected by PTB1/2 expression and correlated with ABA-dependent seed germination. Further, GRP7 and 8 undergo a negative autoregulation via AS-NMD similar to PTB1 and 2 (Staiger *et al.* 2003, Schöning *et al.* 2008). Both circadian clock components also act in regulation of flowering time (Steffen *et al.* 2019). Combination of GRP7 knock-out and GRP8 knock-down shifted the AS ratio of *FLOWERING LOCUS M* (*FLM*) to *FLM-δ*, whereas overexpression of both GRPs favors the production of *FLM-β*. The amount of functional FLM-β was suggested to be predominantly responsible for temperature-dependent flowering induction (Sureshkumar *et al.* 2016). These instances highlight the ability of splicing regulators to auto- and cross-regulate themselves via AS-NMD to adapt their gene expression to external stimuli, however, the presence of NMD-eliciting features does not consequently entail the RNA degradation via NMD pathway suggesting the function and the mechanism of NMD is not fully understood, yet (Kalyna *et al.* 2012).

4.1. Splicing-defined subcellular localization of *SR30* transcripts determines their fate

The *SR30* pre-mRNA was identified to undergo light-mediated AS. Two major transcript types originate from usage of a constitutive or an alternative 3' splice site. Analysis of AS type distribution in a transcriptome-wide manner revealed the alternative 3' splice site to be the most frequent one in etiolated (49.6%, Hartmann *et al.* 2016) and light-grown seedlings (40.6%, Rühl *et al.* 2012) by using the same bioinformatical pipeline in both studies. However, several other RNA sequencing studies established regulated introns to be the prevalent AS type in Arabidopsis (Marquez *et al.* 2012, Mancini *et al.* 2016, Mei *et al.* 2017), monocots (Mei *et al.* 2017) and moss (Wu *et al.* 2014). Intron retention events were the second leading AS type with 22.4% of all identified AS events in our RNA sequencing data set (Hartmann *et al.* 2016). All these studies indicate a conserved preference for this splice type among the whole plant kingdom. Nevertheless, the percentage of intron retention events have been widely variable from around 24 % (Marquez *et al.* 2012) up to 59 % (Mei *et al.* 2017) between the single species mentioned above. It can be partly explained by categorization of AS types, whereas Marquez and colleagues consider ten different AS types, the other studies just distinguish between four to five AS types. Moreover, distinct bioinformatical approaches were applied to analyze the AS pattern (Marquez *et al.* 2012, Wu *et al.* 2014, Mancini *et al.* 2016) and the differences could result from usage of various plant material, developmental stages and growth conditions as demonstrated by Palusa *et al*. 2017 and Richardson *et al.* 2011. Interestingly, splice site selections were shown to be affected by splicing regulators. In fact,

PTBs were demonstrated to preferentially activate alternative 5' splice sites (Rühl *et al.* 2012), hence depending on their expression pattern, splicing regulators can shape the AS landscape.

In case of *SR30*, the usage of the upstream 3' splice site resulting in *SR30.2* is preferred in etiolated seedlings, whereas the AS pattern is strongly shifted towards *SR30.1* upon illumination by using the downstream splice site (Hartmann *et al.* 2016). Previous studies dealing with AS in light-grown seedlings have already connected *SR30* splice pattern changes with abiotic stress responses including high-light irradiation (Tanabe *et al.* 2007, Filichkin *et al.* 2010) and heat (Palusa *et al.* 2007, Filichkin *et al.* 2010). Moreover, splicing pattern of other SR proteins responded to these stimuli as well (Iida *et al.* 2004, Palusa *et al.* 2007) which might indicate a common function in abiotic stress response for SR proteins.

Interestingly, the *SR30* AS shift is reversed after 24 h of light exposure (Hartmann *et al.* 2018). Similar observations were reported by Lopato and colleagues (Lopato *et al.* 1999b). The relative transcript abundance of *SR30.1* and *.2* were analyzed during the first 20 days after germination and in different organs of Arabidopsis. Depending on plant age and tissue, *SR30* exhibit a different AS pattern. This switch could be based on a negative feedback control. Data from transient overexpression of *SR30.1* in *N. benthamiana*, which triggered the enrichment of the alternative transcript *SR30.2* (Hartmann *et al.* 2018) support a SR30 autoregulation. Similarly, overexpression of *SR30* genomic sequence in Arabidopsis caused an accumulation of *mRNA3* (corresponding to *SR30.2*) relative to *mRNA1* (*SR30.1*) when it is compared to the wild type control (Lopato *et al.* 1999b). Generation of the putative unstable transcript as response to overexpression could function as buffer system to avoid a strong accumulation of SR30 protein and thus missplicing of SR30 targets. These data support a precise and development-dependent regulation of *SR30* gene expression. Upon illumination of a skotomorphogenic seedling, the transient *SR30* AS shift towards the protein-coding transcript might contribute to the developmental transition during the photomorphogenesis.

Nevertheless, an involvement of other SR proteins cannot be excluded since cross-regulations were demonstrated for several SRs including RSZ33-dependent splicing pattern of *RS31* (Kalyna *et al.* 2006) and the interplay between RS31, RS40 and RS41 (Saile *et al*., unpublished data). This ability of SR proteins to auto-regulate themselves and cross-regulate other SR proteins opens up the possibility of a whole SR protein network to control their RNA targets.

While analyzing the sequence properties of both *SR30* isoforms, NMD-triggering features were identified within *SR30.2* (Hartmann *et al.* 2018). The usage of the upstream 3' splice site creates one PTC resulting in an extended 3' UTR with an additional intron more than 50 nt downstream of the stop codon. UTR-located introns were correlated with NMD induction and have been supposed to influence gene expression (Kertész *et al.* 2006, Kalyna *et al.* 2012, Drechsel *et al.* 2013). Therefore, we checked *SR30.2* expression in NMD mutants.

Unexpectedly, the *SR30.2* transcript level did not significantly differ between wild type and mutants although clear NMD-triggering features are present in the transcript. Moreover, mRNA half-life of *SR30.2* was strikingly enriched by a factor of 4.7 compared to *SR30.1.* The high stability of *SR30.2* argues for a limited overall RNA decay of this splice variant and supports the NMD-immunity for *SR30.2*. Translation may prevent *SR30.2* from NMD. Confocal microscopy was used to investigate a possible production of SR30.2 protein (Hartmann *et al.* 2018). A fluorescent signal for SR30.2-GFP could be experimentally proven when it is transiently expressed in protoplasts under 35S promoter. However, the usage of UTR-free constructs (Hartmann *et al.* 2018) used for this approach probably could enhance the protein production for SR30.2 since NMD features are not included. Moreover, HA_3-tag fusion proteins of *SR30* splice variants were transiently expressed in *N. benthamiana* (Hartmann *et al.* 2018). Detection of SR30.1- HA_3 resulted in a strong protein signal whereas SR30.2-HA_3 were absent or much less expressed. These results demonstrate that *SR30.2* can be translated into a protein under artificial conditions. If SR30.2 is generated during skotomorphogenesis remains elusive. Both possible proteins SR30.1 and SR30.2 would differ in the C-terminal RS domain, which is essential for protein-protein as well as protein-RNA interactions (Hartmann *et al.* 2018). Moreover, phosphorylation of the RS domain affects spliceosomal assembling and the SR protein subcellular localization (Lorkovic *et al.* 2004, Ali and Reddy 2006, Long and Caceres 2009, Mori *et al.* 2012, Zhou and Fu 2013). This opens up the possibility of two proteins with distinct functions e.g. altered RNA binding affinity regarding SR30 targets, which might affect the splice site decision. However, recent studies have assumed that AS contributes little to the proteome complexity although the majority of pre-mRNAs undergo AS (Yu *et al.* 2016, Fesenko *et al.* 2017, Tress *et al.* 2017, Chaudhary *et al.* 2019a, Chaudhary *et al.* 2019b). Consistently, detecting SR30 total protein via immunoblot resulted in a single band (Hartmann *et al.* 2018), which argues for just one SR30 protein. Nevertheless, the protein size of both theoretical proteins just differs by 12 amino acids, which makes it barely possible to distinguish them by western blot. To fully address this issue, etiolated and light-exposed seedlings should be analyzed by mass spectrometry since it is more sensitive compared to an immunological detection.

Besides translation, nuclear retention of *SR30.2* could explain its NMD-insensitivity and furthermore, the poor expression of SR30.2 protein in the above mentioned experiments. Transcripts originating from intron retention events such as *RS31* and *RS2Z33* were demonstrated to accumulate inside the nucleus (Kim *et al.* 2009, Göhring *et al.* 2014). Probably, such a compartmentation for a subset of splice variants might also exist for other AS types including *SR30*. Subcellular fractionation was performed to analyze the distribution of specific mRNA variants and revealed different expression pattern for both *SR30* isoforms (Hartmann *et al.* 2018). As predicted, *SR30.2* has been almost exclusively detectable in the

nucleus while *SR30.1* was mainly present in the cytosol (Hartmann *et al.* 2018). Additionally, the interaction of both splice variants was tested for polysome association in light-grown seedlings (Hartmann *et al.* 2018). Attachment of *SR30.1* to RIBOSOMAL PROTEIN-L18 was highly enriched whereas *SR30.2* could be poorly detected. Similarly, pronounced *SR30.1*-polysome interaction has already been reported by Palusa and Reddy (2015) for 2-week-old Arabidopsis plants. All experimental data of *SR30.2* data including nuclear enrichment, low association to polysomes and the elevated mRNA half-life time argue for nuclear retention of the dark-promoted transcript variant. Consequently, the transcript escapes from NMD since this RNA decay pathway depends on translation, and thus, it exclusively occurs in the cytosol. However, how is *SR30.2* retained and what is its purpose inside the nucleus, still remain open questions. In general, just a subset of RNAs including mRNA, ribosomal RNA and transfer RNA are regularly exported to the cytoplasm. In contrast to this, lncRNA and non-functional RNA originating from inaccurate transcription or mis-processing of functional RNA can be retained in the nucleus (Palazzo and Lee 2018). Nuclear retention or cytoplasmic export of RNAs is highly dependent on a variety of determinants such as specific *cis*-elements, splicing, post-transcriptional RNA processing and nucleotide modifications (Palazzo and Lee 2018). Interestingly, a previous publication addressed the more precise localization of different RNA isoforms and found aberrant RNAs or transcripts carrying NMD features, respectively, to be enriched in the nucleoli, whereas fully spliced transcripts were rather present in the nucleoplasm (Kim *et al.* 2009). Nucleoli are known as places of ribosomal RNA synthesis and ribosome biogenesis (Kalinina *et al.* 2018). However, this sub-nuclear compartment was connected to mRNA splicing and decay as well. Components of the EJC, which marks the exon-exon junctions (Pendle *et al.* 2005) and NMD-related proteins localize to the nuclear subcompartment (Kim *et al.* 2009) so that RNA decay reminiscent to cytosolic NMD could theoretically take place inside the nucleolus. However, the elevated mRNA half-life time of *SR30.2* argues against an active nucleolar RNA decay via NMD for this mRNA isoform. Additionally we also tested the possible RNA decay via the exosomes or exoribonuclease. Interestingly, all *SR30* transcript isoforms are degraded by alternative RNA decay mechanisms including nuclear exosomes or the cytosolic exoribonuclease 4 (XRN4) (Hartmann *et al.* 2018). The transcript level analysis revealed that *SR30.2* shows a slightly stronger accumulation than *SR30.1* in light-grown *xrn4* mutants. Accordingly it was reported that yeast XRN1 mediates glucose-dependent RNA decay of some transcripts related to metabolic processes (Braun *et al.* 2014). In this study, it was shown that XRN1 is phosphorylated by the central energy sensor SnRK1, and thus promotes RNA degradation for subset of transcript upon energy depletion. Arabidopsis XRN4 is the functional homolog to yeast XRN1 although it has a higher sequence similarity to ScXRN2 (Kastenmayer and Green 2000, Souret *et al.* 2004, Nagarajan *et al.* 2013, Nagarajan *et al.* 2019). It would be conceivable that a splice variant specific RNA decay is

triggered in response to changing energy availability which subsequently would contribute to the pronounced *SR30* AS shift upon light or sugar exposure. However, such a mechanism has not been shown so far and remains highly speculative.

The retention of a specific RNA subset could be mediated by distinct protein-RNA interactions such as uridine-rich binding proteins. In plants, these proteins preferably bind to introns, which are enriched in uridine bases (Simpson *et al.* 2004). Alternatively, sequestration of RNA binding proteins such as splicing regulators would be a plausible RNA function, which has already been described for long non-coding RNAs (Bardou *et al.* 2014). Furthermore, different degradation rates for RNA isoforms between the various plant cell compartments might lead to nuclear enrichment of certain mRNAs (Kim *et al.* 2009). Considering all possibilities, impaired export of *SR30.2* seems to the most likely scenario because of its elevated RNA stability. Further investigation regarding *SR30.2*-associated proteins would be valuable to derive a retention mechanism and/or function of the transcript.

4.2. Sequential splicing results in NMD-sensitive *SR30.3* as response to changed light conditions

Next to the two major splice variants, the less abundant *SR30.3* has attracted our attention. This transcript is highly similar to the *SR30.2* sequence except for a lack of 191 nt within the 3' UTR and 110 nt downstream of the stop codon. Contrary to *SR30.2*, the transcript level of *SR30.3* is enriched in *lba1* and *upf3-1*, hence, it seems to be targeted by NMD comparable to *SR30.1* (Hartmann *et al.* 2018). Since the high sequence similarity of *SR30.2* and *SR30.3*, we tested if *SR30.3* could originate from *SR30.2* by an additional splicing step. Therefore, we analyzed *SR30.3* transcript accumulation in Arabidopsis lines constitutively expressing either *SR30.1-HA* or *SR30.2-HA*. Using primer, which specifically detect *SR30.3* derived from the transgene, we could only verify *SR30.3* expression in *SR30.2-HA* plants suggesting *SR30.3* could arise from *SR30.2* mRNA presumably by an additional removal of a retained intronic sequence. This hypothesis is supported by an elevated *SR30.3* transcript level in etiolated seedlings overexpressing *SR30.2* (Hartmann *et al.* 2018). This splicing process is reminiscent to multi-step splicing modes such as recursive splicing in other organisms (Duff *et al.* 2015, Sibley *et al.* 2015, Gazzoli *et al.* 2016, Georgomanolis *et al.* 2016). Marquez and colleagues (2012) assumed an alternative splicing mechanism for large introns in Arabidopsis. Splice junction analysis revealed that around 70% of all identified introns were smaller than 200 nt by an average of 298 nt (median = 114 nt) (Marquez *et al.* 2012). The alternatively spliced intron in *SR30* pre-mRNA consists of 942 nt (Hartmann *et al.* 2018) and thus it is much larger than the average intron size in Arabidopsis. The longer intron might be able to trigger the two-step splicing. Nevertheless, the tenth intron of *SR30* pre-mRNA probably just represents an

exception and belongs to the 6% of introns in Arabidopsis that contain more than 900 nt (Marquez *et al.* 2012). Delayed removal of the remaining intronic sequence in *SR30.2* could generate the NMD-sensitive *SR30.3* at later stage of development such as photomorphogenesis. Such a mechanism would contribute to regulation of the nucleus-stored *SR30.2* transcript variant. Similar scenario of development-dependent post-transcriptional gene expression control by multi-step splicing was already shown for the fern *Marsilea vestita* (Boothby *et al.* 2013). Fern male microspores contain a subset of stored and partially maturated transcripts that are related to development cell differentiation and cell death. These transcripts mostly retain one intron, which has an inhibitory effect on translation during spore quiescence. During spermatogenesis of the gametophyte, the introns are removed by post-transcriptional splicing, which turns on translation and thus the gametophyte as well as spermatid differentiation (Boothby *et al.* 2013). Since ferns are evolutionary older than Arabidopsis, multiple-splicing processes might be common to vascular plants. However, if *SR30.3* originates by a two-step splicing process under natural condition to adjust *SR30* gene expression e. g. during photomorphogenesis needs to be further investigated. In theory, light exposure activates the alternative 3' splice site to generate *SR30.1*, which is still present in *SR30.2* as well. In case of *SR30.2*, the usage of the close 5' splice site generates *SR30.3.* This transcript will be exported to the cytosol to undergo NMD, and thus contributes to altered *SR30* AS ratio. Plants overexpressing either *SR30.1* or *SR30.2* exhibit an AS shift towards non-productive *SR30.2*, indicating a negative feedback loop towards the non-productive transcript isoform. Hence overall reduced transcript abundance of *SR30* splice isoforms by *SR30.2* degradation via *SR30.3* could support the generation of the protein-coding *SR30.1.* The light-activation of the downstream splice site could be triggered by specific splicing regulators. The small intron within the 3' UTR represents the only difference between *SR30.2* and *SR30.3*, and thus it might contain special sequence features responsible for nuclear *SR30.2* retention. In general, intron-associated elements including intact branch point sequence or a 5' splice site (also known as 5' splice site motif) are correlated with nuclear retention (Palazzo and Lee 2018). In human cell cultures, the nuclear export was inhibited for a substantial subset of transcripts harboring a 5' splice site at the 3' terminal exon (Lee *et al.* 2015). Further, RNA binding proteins are likely to be involved in nuclear retention of *SR30.2*. It was shown, that mature transcripts harboring a polypyrimidine-tract are kept inside the nucleus by PTB binding (Yap *et al.* 2012, Roy *et al.* 2013). Several mammalian RNA binding proteins including U1 (Takemura *et al.* 2011), hnRNP U (Hacisuleyman *et al.* 2014) and hnRNP A1 (Lévesque *et al.* 2006) were identified to promote nuclear retention of RNA. A related retention mechanism might also exist in plants and could explain the nuclear enrichment of *SR30.2* as well. Interestingly, the U1 snRNP accessory protein LETHAL UNLESS CBC7

(LUC7) was recently shown to promote terminal intron splicing in Arabidopsis as response to abiotic stresses (de Francisco Amorim *et al.* 2018). This splicing step is important for mRNA export, however the AS ratio of *SR30* was not changed in *luc* triple mutant compared to wild type. Additionally, retained transcripts tend to accumulate in dot-like structures, called speckles (Palazzo and Lee 2018). These membrane-less nuclear sub-compartments are highly dynamic protein and RNA accumulations with variable composition. Besides SR proteins, various proteins related to RNA splicing localize in these structures (Ali *et al.* 2003, Fang *et al.* 2004, Lorkovic *et al.* 2004, Tillemans *et al.* 2006, Fouquet *et al.* 2011, Xin *et al.* 2017, de Francisco Amorim *et al.* 2018), thus speckles could function as storage and assembly sites for splicing regulators in the interchromatin space (Reddy *et al.* 2012a). Moreover, speckles were shown to be places of post-transcriptional splicing in mammals as well (Dias *et al.* 2010, Girard *et al.* 2012) which would perfectly fit to our two-step-splicing model for *SR30.3*.

4.3. Splicing regulators show phosphorylation-dependent nuclear phase separation

Our localization studies of SR30.1-GFP fusion revealed that SR30 protein localizes inside the nucleoplasm and speckles (Hartmann *et al.* 2018). Similar results have been already reported for SR30 (Fang *et al.* 2004, Lorković *et al.* 2008), several other SR proteins including SR34, RS31, RSZ22, RSZ33, SC35, all SCLs (Tillemans *et al.* 2005, Lorković *et al.* 2008) and SR-like SR45 (Ali *et al.* 2003) or RRC1 (Xin *et al.* 2017, Xin *et al.* 2019). Speckles undergo constant interchange of splicing regulators with impact on their morphology including expansion, shrinking, division and budding. Fusions to fluorescent proteins and bleaching in combination with time-lapse analysis to determine the diffusion coefficient demonstrated rapid intranuclear movement and suggested intracellular shuttling for SR and SR-like proteins such as SR45 and RSZ22 (Ali *et al.* 2003, Tillemans *et al.* 2006, Zhang and Mount 2009). Interestingly, several SR proteins seem to preferentially co-localize with a distinct protein population including members of their subfamily arguing for defined recruitment of splicing regulators (Lorković *et al.* 2008). Moreover, speckle formation and morphology depends on cell cycle and developmental stage as well as physiological responses due to stresses (Reddy *et al.* 2012a). Subcellular localization of SR proteins including SR45, RS31 and RSZ22 were studied by using GFP-labelled RRM and RS domains (Tillemans *et al.* 2005, Ali and Reddy 2006). Remarkably, SR shuttling and formation of nuclear subcompartments seems to be dependent on the RS domain responsible for protein-protein interaction since deletion of the RS domain resulted in diffuse localization pattern all over the plant cell. In contrast, complementation with serine-substituted domains or a shortened RS domain restores the localization pattern to some extent (Cazalla *et al.* 2002, Tillemans *et al.* 2005, Tillemans *et al.* 2006, Twyffels *et al.* 2011, Tsugama *et al.* 2012). SR proteins can be extensively

phosphorylated at the RS domain *in planta* (Reddy 2007, Barta *et al.* 2008), e.g. by LAMMER-type kinase ARABIDOPSIS FUS3-COMPLEMENTING GENE 2 (also known as PK12/AFC2, Savaldi-Goldstein *et al.* 2003), SR protein kinases and Cdc-2-like kinases (de la Fuente van Bentem *et al.* 2006, Ding *et al.* 2006, Jeong 2017, Koutroumani *et al.* 2017). Phosphorylation inhibition by Staurosporin leads to formation of large, irregular speckles for SR45 (Ali *et al.* 2003, Ali and Reddy 2006, Mori *et al.* 2012), SR34 (Ali and Reddy 2006), RS31 and RSZ22 (Tillemans *et al.* 2005) suggesting that SR protein phosphorylation is essential for proper speckle formation. Consistently, phosphorylation-dependent localization for SR30 fused to RED FLUORESCENT PROTEIN (RFP) has been reported when it was heterologous expressed in onion epidermal cells (Mori *et al.* 2012). Application of a kinase inhibitor caused accumulation of SR30-RFP in undefined, cytoplasmatic structures and prevented nuclear localization as well as speckle formation. Note that SR30-RFP expression under control conditions revealed a nuclear and cytoplasmic fluorescent signal (Mori *et al.* 2012), which is contradicting to our observations mentioned before for SR30.1-GFP. It could be a result of the heterologous expression in onion cells, however, if SR30 shows a phosphorylation-dependent subcellular compartmentation in Arabidopsis remains to be investigated. These data suggest that phosphorylation can control the localization of splicing regulators, and thus phosphorylation status of splicing regulators probably affects the ability to participate in the splicing process. Accordingly, the LAMMER kinase PK12, which co-localizes with SR34 in Arabidopsis, were demonstrated to affect the splicing of *SR30*, *SR34* and *U1-70K* (Savaldi-Goldstein *et al.* 2003). Overexpression of the kinase shifted all AS pattern towards the shorter transcript.

4.4. Available energy sources determine AS pattern during early seedling development

4.4.1. Expression of splicing regulators show light- and sugar-dependency

Splicing regulators such as SR proteins are one of the prime candidates to be master regulators of light-mediated AS. For SR-related RRC1 was reported that it fulfils important regulatory functions during the early seedling development (Lopato *et al.* 1999b, Kalyna *et al.* 2003, Ali *et al.* 2007, Shikata *et al.* 2012b, Xin *et al.* 2017, Xin *et al.* 2019). Mutations of the splicing factor RRC1 or deletion of its RS domain caused aberrant splicing pattern for several SR proteins and reduced PHYB-dependent red light signaling (Shikata *et al.* 2012a, Shikata *et al.* 2012b). Moreover, we could demonstrate the functional impact of light-mediated AS-NMD control for the *RRC1* pre-mRNA on light-dependent hypocotyl growth. Accordingly, splicing events related to photomorphogenesis and hypocotyl elongation e.g. EARLY FLOWERING 3 and PIF3 were affected in *rrc1-3* upon light exposure (Xin *et al.* 2019).

Light-regulated AS of the *SR30* pre-mRNA promotes synthesis of the corresponding protein in etiolated seedling upon illumination (Hartmann *et al.* 2018). Besides our own analysis regarding *SR30*, AS pattern were analyzed in Arabidopsis plants grown under light-dark cycles and stress conditions. In fact, light pulses during the night (Mancini *et al.* 2016) or application of high light, heat, and salt (Palusa *et al.* 2007, Tanabe *et al.* 2007, Filichkin *et al.* 2010) favored the generation of the productive *SR30* mRNA linking *SR30* gene expression to abiotic stress responses. Further, energy depletion by applying the photosynthesis inhibitor 3-(3,4-Dichlorophenyl)-1,1-dimethylurea (DCMU) to light-grown seedlings shifted the AS pattern towards the unproductive *SR30.2* variant (Hartmann *et al.* 2016). Conversely, application of external sucrose to etiolated seedlings mimicked the light response (Hartmann *et al.* 2016). Similar energy-dependent AS of *RS31* pre-mRNA was reported (Petrillo *et al.* 2014). Taken together, *SR30* AS outcome seems to be regulated by the metabolic state of the plant (Hartmann *et al.* 2016, Hartmann *et al.* 2018). Elevated SR30 protein level might contribute to the splicing control of downstream targets under beneficial plant growth conditions besides its auto-regulation (described in 4.1.).

Next, plant development including photomorphogenesis is determined by exact expression patterns of specific growth regulators as described for *RRC1* splice variants (Hartmann *et al.* 2016, Xin *et al.* 2019). Further, the splicing regulator SR30 and the closely related SR34 were differential expressed during various stages of plant development (Lopato *et al.* 1999b, Palusa *et al.* 2007) suggesting a regulatory function for these splicing regulators in plant growth as well. *SR30.1* (indicated as mRNA1) is increased relative to *SR30.2* (mRNA3 in Lopato *et al.* 1999b, or mRNA isoform 4 in Palusa *et al.* 2007) in 3-d-old Arabidopsis seedlings grown under long-day conditions. Analyzing the *SR30* splice variants at later time points up to 15-d-old plantlet exhibit an AS shift towards *SR30.2* (Lopato *et al.* 1999b, Palusa *et al.* 2007). Additionally, investigation of reporter lines carrying promoter-GUS fusions for either SR30 or SR34 displayed β-Glucuronidase staining in pollen grains, vascular tissues and lateral roots; however, in 2-d-old seedlings *SR30* promoter activity was exclusively present in cotyledons while *SR34* promoter was only induced in hypocotyls and roots suggesting a complex tissue-specific regulation of both SR proteins (Lopato *et al.* 1999b). According to its tissue- and stage-dependent expression, overall plant development seemed to be impaired by overexpression of *SR30* resulting in larger rosette leaves, changed trichome morphology, delayed flower transition and larger flowers under long-day conditions. Interestingly, apical dominance was strongly reduced in adult *SR30* overexpressing plants under short-day conditions leading to a bushy phenotype and changed inflorescence architecture (Lopato *et al.* 1999b) connecting SR30 expression to circadian clock and auxin signaling (Covington and Harmer 2007). Accordingly, Kriechbaumer and colleagues (2012) demonstrated tissue-specific splicing for the auxin biosynthesis enzyme YUCCA4. Other SR proteins were shown

to be involved in plant growth, too (Ali *et al.* 2007, Zhang and Mount 2009, Carvalho *et al.* 2010, Reddy and Shad Ali 2011, Yan *et al.* 2017). We could demonstrate that SR30 gene expression is affected by illumination, however, light-dependent phenotypes during the early seedling development have not been observed so far. This can be explained by the functional redundancy within the SR subfamily and the absence of higher-order mutants (Hartmann *et al.* 2018). Nevertheless, *SR30* expression in fast growing and meristematic cells (Lopato *et al.* 1999b) and the transient light-responsive AS shift in etiolated seedlings (Hartmann *et al.* 2018) indicates a contribution during early seedling development.

4.4.2. Photoreceptors and retrograde signaling control different AS responses

Splicing regulators such as SR30 are likely to affect the splicing process, however, there are knowledge gaps regarding how the light signal initiates a shift in AS pattern. Recently, the involvement of photoreceptors in light-mediated AS regulation was controversially discussed (Petrillo *et al.* 2014, Shikata *et al.* 2014, Wu *et al.* 2014, Hartmann *et al.* 2016, Mancini *et al.* 2016). In general, changes in ambient light conditions are directly recognized by photoreceptors and subsequently converted into physiological responses by activation of the downstream TF network to induced light-responsive genes and to repress negative regulators of the photomorphogenesis including COP1 (Jiao *et al.* 2007, Galvao and Fankhauser 2015). Several transcriptome-wide studies dealt with the potential role of PHYs as master regulators during light-mediated AS. A comparative analysis of red light responses in wild type and PHY-deficient mutants revealed a PHY-dependency for a subset of light-regulated AS events in etiolated Arabidopsis seedlings (Shikata *et al.* 2014) and light-grown protonemata (Wu *et al.* 2014). Several components involved in mRNA splicing such as SR30, SR34a, SR34b, RS31 and U2AF65a exhibit AS pattern shifts mediated by the photoreceptors implying AS control via a PHY-splicing regulator relay (Shikata *et al.* 2014, Zhang *et al.* 2017). Under red light conditions, SFPS could connect PHY signaling with AS control since it co-localizes with PHYB, RRC1 and U2AF35A in the nucleus (Xin *et al.* 2017, Xin *et al.* 2019). SFPS-deficient mutants are affected in pre-mRNA processing of many genes involved in light signaling and photosynthesis. Accordingly, the mutations result in a diminished light responsiveness (Xin *et al.* 2019). These data give first indications of PHY-mediated splicing regulator control.

Changes of light-dependent AS pattern in etiolated seedlings have been evaluated by us as well (Hartmann *et al.* 2016). To analyze the contribution of phytochrome regarding AS shifts upon illumination, several significant light-mediated AS events were investigated in *phyA phyB* compared to wild type under different light qualities. Contrary to the analysis of Shikata and colleagues (2014), a comprehensive regulatory function for PHYs during light-mediated AS could not be derived since wild type and *phyA phyB* responded comparably upon light

exposure (Hartmann *et al.* 2016). A detailed comparison of both approaches is provided in our study (Hartmann *et al.* 2016) and revealed some explanations regarding the alleged contradictions. Interestingly, the re-analysis of RNA sequencing data from Shikata *et al.* 2014 using the bioinformatical pipeline from Hartmann *et al.* 2016 identified more AS events to be PHY-independent than PHY-dependent. Differences in light treatment (quality, intensity and duration) and splicing analysis pipeline might contribute to different outcomes of Shikata *et al.* 2014 and Hartmann *et al.* 2016. Interestingly, *phyA phyB* did not respond on AS level upon far-red light treatment indicating a clear PHY contribution under this specific light conditions (Hartmann *et al.* 2016). Notably, far-red light is unable to activate photosynthesis (Emerson and Lewis 1943, McCree 1971, Hartmann *et al.* 2016). Most likely, there are at least two signaling pathways to regulate light-mediated AS. Hence, PHY signaling might regulate a subset of genome-wide AS switches under low-light or non-photosynthetic active conditions, respectively. If these signaling pathways act in parallel or exclusively dependent on the surrounding light conditions remains unexplored. A similar operation could be also assumed for CRYs.

Other publications supported our hypothesis that PHYs function in light-dependent AS control next to other master regulators or even claimed it is PHY-independent (Petrillo *et al.* 2014, Mancini *et al.* 2016). In these studies, light-grown plants were illuminated after extended dark period (Petrillo *et al.* 2014) or treated with a light pulse within the night (Mancini *et al.* 2016), respectively. In agreement with Hartmann *et al.* 2016, AS responses were comparable between wild type, *phyA phyB* and *cry1 cry2* arguing for a photoreceptor independency. PHYA/PHYB and CRY1/CRY2 are the major photoreceptor for red and blue light perception, respectively. Nevertheless, a photoreceptor signaling via the other PHYs cannot be completely excluded since the PHY family consist of five members (Mathews and Sharrock 1997). Therefore, Mancini and colleagues (2016) investigated the red light response of *SR30* AS pattern in a *phy* quintuple mutant (*phyABCDE*). At least for this candidate event, a role of PHYs in AS control could be excluded. Similarly, other AS events might be regulated independent of PHYs. Moreover, contribution of HY5 and HYH, major downstream signaling components of all photoreceptors, were also excluded for the light-triggered AS shift of *RS31* (Petrillo *et al.* 2014). Nevertheless, photoreceptor signaling might be also activated by wavelengths distinct from the wavelength range around their individual absorption maxima (PHYs: 600 to 750 nm; CRYs: 320 to 500 nm), since PHYs absorption spectra exhibit local maxima around 363 and 414 nm, and CRYs absorption spectrum extends beyond 600 nm (Vierstra and Quail 1983, Lin *et al.* 1995, Ahmad *et al.* 2002, Galvao and Fankhauser 2015). Moreover, direct physical interactions between members of both photoreceptor families have been demonstrated (Ahmad *et al.* 1998, Más *et al.* 2000, Hughes *et al.* 2012), e.g. the light-responsive interaction of PHYB and CRY2 in nuclear speckles (Más *et al.* 2000). Next, PHYs and CRYs regulate

common downstream targets including PIFs (Martinez-Garcia *et al.* 2000, Huq *et al.* 2004, Ma *et al.* 2016, Pedmale *et al.* 2016) and COP1/SPA (Wang *et al.* 2001, Yang *et al.* 2001, Saijo *et al.* 2008, Lu *et al.* 2015, Sheerin *et al.* 2015). Therefore, PHYs and CRYs might act in common signaling pathways and could be able to at least partially compensate their signaling functions. Further investigations concerning light response in higher-order mutants blind for red and blue light signaling would be valuable to understand the molecular mechanism in more detail and overlapping absorption spectra could be excluded.

An alternative hypothesis was postulated that retrograde signaling of the chloroplast is responsible for light-mediated AS response (Petrillo *et al.* 2014) which is in line with our data (Hartmann *et al.* 2016). This assumption is based on the two following observations: First, Petrillo and colleagues were interested in the signal transduction within the seedling upon changed light conditions and performed a dissection experiment with green seedlings to analyzed the AS ratio of RS31 in cotyledons+hypocotyls and roots. Interestingly, the RS31 AS pattern did not respond to light/dark treatments in the root tissue when the root was separated before illumination or transfer to darkness, respectively. Therefore, the authors assumed a mobile signaling molecule generated in the leaves that transduce the light information from cotyledons+hypocotyl to the root (Petrillo *et al.* 2014). Our observations support this conclusion since light and sucrose trigger the same AS responses in our experiments indicating sucrose or another metabolic signal could be the shuttling molecule (Hartmann *et al.* 2016). Second, since sucrose represents one the main photosynthesis end products, the influence of photosynthesis on gene regulation were studied by application of DCMU and DBMIB (dibromothymoquinone, inhibiting the electron transport chain). The chemicals could clearly attenuate the AS response in light-grown plants (Petrillo *et al.* 2014). Similar observations were obtained for *SR30* (Hartmann *et al.* 2016, discussed in 4.4.1.). From these data, we draw the conclusion that light-mediated AS is mainly regulated via a photosynthesis-derived signal under natural conditions, whereas photoreceptor signaling might be involved under specific light conditions such as far-red light. If just one pathway or both together are activated upon light exposure remains an open question since photoreceptor and retrograde signaling are interconnected, e.g. photoreceptors determine chloroplast development (Reed *et al.* 1993, McCormac and Terry 2002, Fox *et al.* 2015). Another question will be if the photosynthesis-activated AS control can be adapted for etiolated seedlings because the final step of chlorophyll biosynthesis is dependent on light (Reinbothe *et al.* 1996) and thus, the photosynthetic capacity is limited directly upon light exposure of dark-grown plants. Accordingly, assembly of the huge protein complex for RuBisCO is initiated upon illumination (Bloom *et al.* 1983). Nevertheless, ATP supplementation is able to partly substitute the light-dependent interaction for the large subunits (Bloom *et al.* 1983). Moreover, some early publications dealing with the onset of photosynthesis upon light exposure suggested a rapid

switch to the autotrophic life style (Smith 1954, Biggins and Park 1966). In dark-grown barley, chlorophyll development, the incorporation of radioactive labelled C^{14} and oxygen production started within 1 h and speeded up continuously afterwards. Plants illuminated for 24 h reached 78% assimilation rate of light-grown ones indicating a dynamic and constant improvement of photosynthetic capacity (Smith 1954, Biggins and Park 1966). Similar results were obtained for Euglena (Stern *et al.* 1964), oat (*Avena sativa*; Blaauw-Jansen *et al.* 1950) and beans (*Phaseolus vulgaris*; Baker and Butler 1976). Moreover, the accumulation of photosystem I and II were demonstrated to appear upon the first few minutes of light exposure (Baker and Butler 1976). This earlier work proves a very prompt light-triggered activation of photosynthesis opening up the possibility of photosynthesis contribution in AS regulation although the full photosynthetic capacity might not be reached in the early time points of our experiments.

Notably, all published studies concerning light-mediated AS compose a highly complex interaction of light- and sugar signaling with impact on the plant energy status, fitness and grow behavior. It would be of high interest to address tissue- and development-specific AS responses and their consequences, e.g. if the regulation of light-dependent AS is different in cotyledons, root or even apical meristems of etiolated seedlings during light transition. Is the light-dependent AS mechanism similar to other light regimes such upon onset for plants cultivated in light/dark-cycles? What are the direct upstream regulators?

4.5. Light- and sugar-mediated AS correlate with kinase activity

4.5.1. Phosphorylation contributes to AS pattern change

Next to transcriptional induction or degradation of essential regulatory components, post-translational modifications represent an additional layer to control intracellular signaling in response to external stimuli (Millar *et al.* 2019). The covalent protein modifications are processed in a one-step reaction and thus result in a time-saving benefit compared to complex protein biosynthesis including transcription, co- and post-transcriptional RNA processing, mRNA transport, translation and folding (Chao *et al.* 2012, Blazek *et al.* 2015, Friso and van Wijk 2015, Silva-Sanchez *et al.* 2015, Millar *et al.* 2019). Phosphorylation is one of the most prominent post-translational modifications of proteins and can affect protein stability, localization, activity and interaction with binding partners (Mithoe and Menke 2011, Schonberg and Baginsky 2012, van Wijk *et al.* 2014, Silva-Sanchez *et al.* 2015). Since phosphorylation is a reversible process in which kinases and phosphatases add and remove a phosphoryl-group, respectively, it has the capacity to function as regulatory switch in signaling transduction. Remarkably, it has been predicted that plants contain double the amount of kinases as mammals implying an important role *in planta* (Manning *et al.* 2002, Champion *et al.* 2004, Zulawski *et al.* 2013). In total, 4 % of all genes in Arabidopsis encoded putative kinases

(Champion *et al.* 2004). These high number of kinases was likely achieved by successive gene duplications within the plant cell. Through sequencing of the whole Arabidopsis genome, duplicated DNA segments could be identified (Vision *et al.* 2000, Blanc *et al.* 2003). For MAPK cascades, it is assumed that around 60 % of all components originate from gene or segment duplication (Champion *et al.* 2004). Diverse large-scale phosphoproteome studies revealed the phosphorylation patterns for Arabidopsis (de la Fuente van Bentem *et al.* 2008, Duan *et al.* 2013, van Wijk *et al.* 2014, Mergner *et al.* 2020), Medicago, rice (Nakagami *et al.* 2010) and other plant species (Silva-Sanchez *et al.* 2015). However, comprehensive phosphoproteome analysis regarding light-dependent plant development such as photomorphogenesis has not been performed so far. Even though single phosphorylation events within the photosensory pathway are well characterized. Several studies demonstrated that the stability of photomorphogenic key regulators including HY5 (Hardtke *et al.* 2000), PIF1 (Shen *et al.* 2008, Paik *et al.* 2019) and PIF3 (Al-Sady *et al.* 2006, Ni *et al.* 2017) are affected by phosphorylation. In fact, phosphorylated HY5 is less targeted by COP1-triggered proteasomal degradation to ensure a small pool of HY5 protein in dark-grown seedlings (Hardtke *et al.* 2000). Moreover, recent data provided evidence that phytochromes fulfil kinase activity *in vitro* (Shin *et al.* 2016) and might be regulated by phosphorylation as well since multiple phosphorylation sites within the extended N-terminal part are present (Medzihradszky *et al.* 2013, Zhou *et al.* 2018). Light exposure initiates the addition of a phosphoryl-group to Thr104 of PHYB, which disturbs the binding to PIF3 (Nito *et al.* 2013). Corresponding to this, phosphorylation of PHYA or PHYB results in accelerated degradation or dark reversion, respectively, implying a negative regulation mechanism for both PHYs (Hoang *et al.* 2019). These examples highlight phosphorylation as additional regulatory layer of the photosensory pathway. Besides light signaling, sugar metabolism is affected by phosphorylation as well. Among others, bioinformatic analysis have assumed that nearly all key enzymes of the photorespiratory pathway are regulated by phosphorylation altering their catalytic activity as reported for RuBisCO (Hodges *et al.* 2013) along with the sucrose-phosphate synthase, which is reversibly phosphorylated in a light/dark-dependent manner to synchronize sucrose synthesis with energy availability (Huber 2007).

To strengthen our idea that phosphorylation contributes to AS control, we applied the general kinase inhibitor K252a to 6-d-old etiolated seedlings for 3 and 6 h, similarly as for light and sugar transfer experiments. The light and sugar responses were mimicked on the AS level for *SR30*, *PEAPOD2* (*PPD2*) and *MYB-LIKE DOMAIN TF* (*MYBD*) after K252a treatment, whereas AS responses for *RRC1* and *PSBP-LIKE PROTEIN1* (*PPL1*) were inhibited or displayed changes to the opposite direction (Hartmann *et al.* 2016). These data seem to appear contradicting to our hypothesis at the first glance since kinase activity inhibition does not result in a unique AS response as it was demonstrated for light- and sugar-regulated AS.

However, it rather opens up the possibility of the involvement of more than just one kinase as well as different regulations of splicing regulators by either phosphorylation-dependent activation or repression. Note that the application of K252a can cause side effects because the kinase inhibitor has a broad target spectrum (Rüegg and Gillian 1989). Drastic effects on plants morphology were reported when the kinase inhibitor is applied at high dose for a longer incubation time e.g. exposure to 1 mM K252a for 2 d cause reduced root elongation in Arabidopsis seedlings (Baskin and Wilson 1997). Short-term treatment in the µM-range restrict the impact of K252a but it still interferes with plant reaction towards external stimuli as it inhibits the hormone-triggered stomatal closure in rosette leaves (Hossain *et al.* 2011), and prevents the light- as well as pathogen-induced phosphorylation of essential components acting in photosystem II (Betterle *et al.* 2015), and plant disease resistance (Li *et al.* 2015a), respectively. To minimize the side effects, we applied the kinase inhibitor at a concentration of 4 µM for 3 to 6 h, even though unspecific effects cannot be excluded. To further analyze the possible involvement of a kinase in light- and sugar-mediated AS, investigations of AS pattern in kinase mutants are necessary, which is discussed later (see 4.5.3 and 4.5.4.). Remarkably, AS has already been connected to phosphorylation. The mammalian homolog of SR30 ASF/SF2 gets phosphorylated in its RS domain, which strengthens the interaction to the spliceosomal component U1-70K *in vitro* (Xiao and Manley 1997) and increases its splicing activity (Xiao and Manley 1998). The phosphorylation is mediated by Clk/Sty kinases, related to LAMMER type kinases. Kinase-inactive mutants of Clk2 and Clk3 form nuclear speckles and co-localize with SR proteins whereas active kinase signaling initiates a redistribution of the SR proteins within the nucleus (Colwill *et al.* 1996, Duncan *et al.* 1998). Changes in subnuclear localization of SR proteins were also reported for human cells that were incubated with purified SRPK1 (Gui *et al.* 1994). These studies suggest that released splicing regulators participate in splicing reactions during active transcription. Moreover, the phosphorylation state of SR proteins influences their capability to bind to RNA resulting in a different splice site selection in combination with altered protein-protein interactions (Xiao and Manley 1997, Shin *et al.* 2004). Subcellular localization (Huang *et al.* 2004, Sanford *et al.* 2005) and mRNA transport (Huang *et al.* 2004, Allemand *et al.* 2005) are dependent on phosphorylation as well. Accordingly, several phosphoproteins related to RNA metabolism were identified in dark-grown Arabidopsis root cells. Most of them belong to the SR family that can be regulated via conserved phosphorylation site in the RS domain probably by a common kinase (de la Fuente van Bentem *et al.* 2006, Jeong 2017). Since light and sugar strongly affect the metabolic status of the plant, it would be interesting to uncover the potential phospho-regulation of splicing regulators during dark-light transitions. First indications were reported that plant SR proteins are regulated by phosphorylation as well (Savaldi-Goldstein *et al.* 2000, Ali *et al.* 2003, Docquier *et al.* 2004, Tillemans *et al.* 2005, Shikata *et al.* 2012a, Shikata *et al.* 2012b). In fact,

the LAMMER protein kinase PK12 of *Nicotiana tabacum* physically interacts with and phosphorylates AtSR34 (Savaldi-Goldstein *et al.* 2000). Similar results were obtained for AFC2, the Arabidopsis homologue of PK12 (Golovkin and Reddy 1999, Marquez *et al.* 2012). Interestingly, PK12 phosphorylation was associated with AS. Overexpression of PK12 in Arabidopsis resulted in a pronounced AS shift towards the shorter mRNA isoform for *SR30*, *SR34* and *U1-70K*. The increased protein level of PK12 resulted in a delayed overall growth, shorter hypocotyl for etiolated seedlings and shorter roots when plants were grown in presents or absence of light (Savaldi-Goldstein *et al.* 2003). Moreover, developmental consequences of phospho-regulation were shown for SR-like SR45 (Zhang and Mount 2009). The knock-out mutant *sr45-1* show narrow petals and shorter roots compared to wild type plants. These phenotypes can be independently rescued be either introducing *SR45.1* or *SR45.2* (as introduced before in 2.3.). SR45.1 contains two predicted phosphor-sites T218 and S219, which are absent in SR45.2. Both predicted phosphor-sites were individually or together substituted with alanine and stably expressed in *sr45-1* knock-out mutant. Mutants complemented with SR45.1-S219A presented wildtype-like flowers compared *sr45-1*, whereas alanine-substitution of both phosphor-sites (SR45.1-T218A-S219A) restored the root phenotype (Zhang and Mount 2009). This study suggested that both proteins derived from *SR45* pre-mRNA are distinguished by phospho-site T218 and demonstrates that phosphorylation of a splicing regulator has impact the plant morphology.

4.5.2. Gene expression control in response to light might be processed by SnRK1

In Arabidopsis, three central energy sensor kinases are employed to regulate gene expression and metabolic processes with respect to altered energy availability (Sheen 2014). Recent studies provided evidence that these metabolic regulators including SnRK1 are strongly connected to plant development (Anderson *et al.* 2005, Baena-Gonzalez *et al.* 2007, Ren *et al.* 2011, Mair *et al.* 2015, Nukarinen *et al.* 2016, Saile *et al.* unpublished). SnRK1 represents a signal integration hub, thus the kinase affects a huge spectrum of downstream components involved in many physiological processes (Rolland *et al.* 2006, Broeckx *et al.* 2016, Baena-Gonzalez and Hanson 2017, Wurzinger *et al.* 2018). Gene expression pattern of SnRK1 targets, *DIN1* and *DIN6*, correlated with light- and sugar-dependent AS pattern shifts (Hartmann *et al.* 2016). In presence of light and sucrose, *DIN* expression levels were reduced (Baena-Gonzalez *et al.* 2007, Hartmann *et al.* 2016), which is in line with light- and sugar-repressed SnRK1 activity (Baena-Gonzalez *et al.* 2007). To decipher the SnRK1 signaling pathway, luciferase reporter assays with *DIN1* and *DIN6/ASN1* promoter sequences were performed that demonstrated a specific SnRK1-mediated activation of gene expression via G-boxes (Baena-Gonzalez *et al.* 2007). Synergistic activation of *DIN6* promoter were

demonstrated when S_1-group bZIP TFs (bZIP1, bZIP11 and bZIP53) and the C-group bZIP TF bZIP63 were co-expressed with the energy sensor, indicating DINs and bZIPs are part of SnRK1 downstream signaling under low energy conditions (Baena-Gonzalez *et al.* 2007, Mair *et al.* 2015). Next, important light signaling components such as bZIP TF HY5 and PIFs are able to bind to G-boxes (Leivar and Quail 2011, Toledo-Ortiz *et al.* 2014), which are located in many promoters of light-responsive genes as well (Giuliano *et al.* 1988, Harmer *et al.* 2000, Jiao *et al.* 2005, Chanderbali *et al.* 2010). Considering these aspects, SnRK1 might contribute to light signaling via orchestration of a TF network to adjust the metabolism to an altered energy availability; however, this interplay remains highly speculative.

4.5.3. SnRK1 is an important signal integrator in plant development

To investigate whether SnRK1 affects light-dependent seedling development, we generated stable SnRK1 knock-down mutants based on sequence information from our RNA-seq data set (Hartmann *et al.* 2016). The respective *.1* mRNA isoform is mainly expressed in etiolated seedlings, even though both SnRK1 genes encode three different mRNA isoforms according to the TAIR 10 annotation. Consequently, *SnRK1.1* and *SnRK1.2* might be regulated via AS. Important to note here, *SnRK1.1* and *SnRK1.2* represent the total RNA fraction instead of single mRNA isoforms. Differential splicing for both SnRK1 pre-mRNAs have also been proposed by Williams and colleagues (2014). Whether the other splice variants are expressed under natural conditions and if they fulfil a physiological function remains unknown at this point. Additionally, Arabidopsis encodes a third homolog SnRK1.3, however, it is expected to be not expressed and considered as a pseudogene (Baena-Gonzalez *et al.* 2007). SnRK1.1 and SnRK1.2 show a high similarity in their amino acid sequence and domain structure from which partially redundant functions were concluded (Baena-Gonzalez *et al.* 2007). Accordingly, single mutants do not show any obvious phenotypical change compared to wild type (Baena-Gonzalez *et al.* 2007, Mair *et al.* 2015, Nukarinen *et al.* 2016). We generated constitutively expressing *amiRNA* constructs, which targeted *SnRK1.1* and *SnRK1.2* in parallel. The constructs were stably transformed into Arabidopsis. Several lines were selected on Basta-containing plates for a survival rate of around 75 % suggesting a single insertion of the transgene. Unfortunately, we were not able to obtain homozygous lines in next generations. During the propagation of the three heterozygous mutant lines (c-*amiR-SnRK1-l_4, c-amiR-SnRK1-l_5 and c-amiR-SnRK1-l_22*), several developmental abnormalities appeared for small proportion of the progeny compared to wild type plants grown in parallel. The mutant plants with obvious phenotypes were delayed in growth, arrested at rosette stage and showed leaf chlorosis. Additionally, dried-out siliques were observed for some mutant plants. These strong phenotypes suggested an effective downregulation of SnRK1 expression however, premature

senescence or dried-out siliques might prevented the propagation of these plants. Accordingly, the mortality rate was determined for the progeny of heterozygous *amiR-SnRK1* lines and wild type plants. Around 20, 30 and 40 % of *c-amiR-SnRK1-I_4*, *c-amiR-SnRK1-I_5* and *c-amiR-SnRK1-I_22* were dead after 10 weeks whereas all control plants survived. Previous studies dealing with knock-down of both, *SnRK1.1* and *SnRK1.2*, reported strong developmental effects, too, resulting in lethality (Thelander *et al.* 2004, Baena-Gonzalez *et al.* 2007) or sterility (Zhang *et al.* 2001, Radchuk *et al.* 2006, Li *et al.* 2017). Remarkably, the hypocotyl length is strongly reduced for a proportion of seedlings when the progeny of heterozygous *amiR* lines is cultivated in darkness.

To further study a possible link between SnRK1 and photomorphogenesis, we used an inducible repression system to circumvent the developmental restrictions by transient knock-down of both SnRK1 kinases. Contrary to constitutive *SnRK1* repression, β-Estradiol-inducible *amiR-SnRK1* plants (*i-amiR-SnRK1-I_2* and *i-amiR-SnRK1-II_9*) developed completely normal under uninduced conditions compared to wild type (Saile *et al.*, unpublished). Similar observations were revealed by Nukarinen and colleagues (2016). Different phenotypes occurred in response to SnRK1 repression, depending on plant age at *amiR* induction and growth conditions (Baena-Gonzalez *et al.* 2007, Mair *et al.* 2015, Nukarinen *et al.* 2016). Induced, etiolated *i-amiR-SnRK1* seedlings displayed a drastically reduced hypocotyl length (Saile *et al*., unpublished) as reported for mutants of the photosensory pathway such as *cop1* (Deng *et al.* 1991) or etiolated and ethylene-treated seedlings (Yu *et al.* 2013). In absence of COP1, HY5 promotes photomorphogenesis-related gene expression leading to inhibition of hypocotyl elongation (Hardtke *et al.* 2000, Osterlund *et al.* 2000a, Osterlund *et al.* 2000b). Similar effects are caused by activation of the ethylene pathway. Perception of ethylene transcriptionally induces ETHYLENE RESPONSE FACTOR1 (Lorenzo *et al.* 2003) and WAVE-DAMPENED 5 (Sun *et al.* 2015a) resulting in shorter hypocotyls. Interestingly, light and ethylene signaling are interconnected since COP1 ubiquitinylates ETHYLENE INSENSITIVE3 (EIN3) BINDING F-BOX FACTOR 1/2 (EBF1/2), a negative regulator of ethylene signaling, and thus EBF1/2 is targeted by proteasomal degradation (Shi *et al.* 2016, Yu and Huang 2017). Further, a recent study linked ethylene recognition to the cellular energy status in light-grown plants (Kim *et al.* 2017a). Accordingly, SnRK1 activation leads to hypocotyl growth inhibition in response to energy deprivation caused by photosystem inefficiency (Kim *et al.* 2017a). Darkness promotes SnRK1 signaling as well (Baena-Gonzalez *et al.* 2007), however, seedlings grown in absence of light exhibit an elongated hypocotyl and SnRK1 repression causes a short-hypocotyl-phenotype (Saile *et al*., unpublished). The regulation of hypocotyl growth in etiolated seedlings might different since the primary goal of skotomorphogenesis is the emergence from the soil to establish photoautotrophic metabolism. Accordingly, reduced hypocotyl growth upon SnRK1 activation as described for light-grown plants would be

unfavorable. To further investigate the altered hypocotyl elongation, it would be interesting to analyze the HY5 levels upon *SnRK1* knockdown.

Induced *i-amiR-SnRK1* seedlings continuously grown under different light intensities (10, 140 and 311 µmol m^{-2} s^{-1}) showed cotyledon bleaching after 14 d on sucrose-free media (Saile *et al*., unpublished). Accelerated chlorophyll degradation was also reported for *Col-0* overexpressing SnRK1 kinase-inactive protein variants of Arabidopsis and rice under submergence conditions and in an age-dependent manner (Cho *et al.* 2012), indicating SnRK1 fulfils a conserved function as negative senescence regulator under starvation conditions. Consistently, studies using induced gene silencing to target SnRK1 reported overall delayed growth and initiation of early senescence in Arabidopsis accompanied with anthocyanin accumulation (Baena-Gonzalez *et al.* 2007, Mair *et al.* 2015, Nukarinen *et al.* 2016) or formation of abnormal filaments in moss (Thelander *et al.* 2004) whereas overexpression of SnRK1 proteins caused a delayed senescence onset (Baena-Gonzalez *et al.* 2007, Cho *et al.* 2012, Chen *et al.* 2017, Kim *et al.* 2017b). Recently, SnRK1 were shown to interact and to phosphorylate EIN3 (Kim *et al.* 2017b), which acts in leaf-senescence (Li *et al.* 2013). Phosphorylation of EIN3 triggers the destabilization of the TF and leads to delayed chlorosis as observed for SnRK1 overexpressing plants (Kim *et al.* 2017b). In line with this, SnRK1 signaling positively controls autophagy as well, which is the major recycling process and involved in chloroplast degradation during leaf senescence (Baena-Gonzalez *et al.* 2007, Chen *et al.* 2017, Soto-Burgos and Bassham 2017). Interestingly, bZIP TFs are involved in SnRK1 downstream signaling to trigger dark-induced senescence (Mair *et al.* 2015) to activated catabolic processes and maintain the energy homeostasis (Nukarinen *et al.* 2016, Pedrotti *et al.* 2018). bZIP TFs act as homo- or heterodimers in order to activate gene expression. In case of bZIP63, SnRK1-dependent phosphorylation at conserved amino acids alters bZIP63 dimerization capacity and highly promotes its heterodimerization with S_1-group bZIP TFs (Mair *et al.* 2015). Extended night conditions enhance SnRK1-triggered hyper-phosphorylation of bZIP63, whereas external sugar supply diminishes it, supporting a function of bZIP63 in energy signaling (Mair *et al.* 2015). In line with this, bZIP63 dimerization partners have already been connected to the starvation response (Hanson *et al.* 2008, Kang *et al.* 2010, Dietrich *et al.* 2011, Ma *et al.* 2011). For this reason, Mair and colleagues (2015) proposed different physiological functions dependent on bZIP dimer composition. A recent study reported that SnRK1 is recruited to the promoter of ELECTRON-TRANSFER FLAVOPROTEIN:UBIQUINONE OXIDOREDUCTASE (ETFQO) via bZIP2/bZIP63 heterodimer (Pedrotti *et al.* 2018). ETFQO is part of the branched chain amino acid catabolism, which represents an alternative respiratory pathway in mammals and plants under sugar starvation (Ishizaki *et al.* 2005, Pedrotti *et al.* 2018). The ternary SnRK1-C/S_1-bZIP complex was suggested to remodel the chromatin structure by induced acetylation and thus initiates

transcription of ETFQO (Pedrotti *et al.* 2018). Taken together, onset of senescence seems to be dependent on SnRK1 repression and the subsequent downregulation of the SnRK1 signaling pathway.

4.5.4. SnRK1 signaling correlates with AS shifts and might be regulated by light

Since AS substantially contributes to the phenotypical transition during the early photomorphogenesis, we investigate a putative SnRK1 contribution to light-dependent AS regulation. Therefore splicing pattern analysis was performed for *i-amiR-SnRK1* and wild type seedlings. We could successfully demonstrate that AS patterns for *SR30*, *RRC1* and *PPD2* were similarly shifted after SnRK1 repression in etiolated seedlings in response to light and sugar as for the controls (Hartmann *et al.* 2016, Saile *et al.*, unpublished). Etiolated seedlings grown in liquid culture showed a pronounced AS shift for *SR30* and *RRC1* after illumination for 6 h or β-Estradiol supplementation for 3 d, respectively. In case of *PPD2*, the β-Estradiol treatment was less effective than light exposure, however, SnRK1 repression revealed a clear AS pattern change. These results supports an involvement of SnRK1 in the light-mediated AS regulation. Nevertheless, the AS pattern of *MYBD* and *PPL1* were not significantly affected after induction of *amiR*s targeting *SnRK1*, indicating a more complex regulation of light-mediated AS. Interestingly, *MYBD* and *PPL1* were significantly less or not responding on AS level to red light in *phyA phyB*, respectively (Hartmann *et al.* 2016), which might pinpoint to a partial regulation of these AS events by PHYs under red light conditions. In previous studies, regulation of total transcript levels for MYB TFs was shown to be affected by components of the photosensory pathway. PHYs modified transcript abundance of MYB-related TF EARLY PHYTOCHROME RESPONSIVE1 (Kuno *et al.* 2003) and HY5 promoted the gene expression of MYBD (Nguyen *et al.* 2015). Probably MYBD gene expression is regulated on several levels by PHYs including HY5-induced gene expression and AS. Such a PHY contribution to AS control would be in line with the proposed model of PHY-dependent AS (Shikata *et al.* 2014, Wu *et al.* 2014). Since PPL1 and MYBD were identified to act during photodamage (Ishihara *et al.* 2007) and anthocyanin biosynthesis (Nguyen *et al.* 2015, Nguyen and Lee 2016), respectively, photoreceptor-mediated AS pattern changes might be part of a physiological adjustment, e.g. in response to specific light regimes. Accordingly, Hartmann and colleagues (2016) propose a similar function in light-mediated AS control for photoreceptors under low light conditions. Alternatively, SnRK1 could probably act together with light-signaling components to trigger AS pattern changes. There are indications that SnRK1 and PHYs can act within the same pathways such as regulation of anthocyanin accumulation under stress conditions (Baena-Gonzalez *et al.* 2007, Liu *et al.* 2015) or chlorophyll biosynthesis (Cho *et al.*

2016, Sheerin and Hiltbrunner 2017). Nevertheless, if SnRK1 works together with photosensory components remains highly speculative.

SnRK1 contribution to AS control upon altered illumination could involve light-regulation of the kinase itself. It would be plausible for SnRK1 that ambient light conditions are recognized via the energy status of the plant which is highly connected with photosynthesis and carbon metabolism. Extended night periods activate SnRK1 signaling including downstream bZIP63 phosphorylation as response to missing energy input in form of light (Mair *et al.* 2015). Further, Carvalho and colleagues (2016) connected SnRK1 protein stability with the energy status and demonstrated that SR45 destabilizes SnRK1 in response to sugar application by promoting proteasomal degradation of the kinase. The SnRK1 degradation rate is consistently decelerated by mutations related to the E3 ubiquitin ligase complex such as CULLIN 4 and PLEIOTROPIC REGULATORY LOCUS 1 (Bhalerao *et al.* 1999, Lee *et al.* 2008). Interestingly, light and sucrose supply to etiolated seedlings significantly decreased the expression of *SnRK1.1* and *SnRK1.2*, however, determination total protein level did not show any effect. Nevertheless, post-translational modifications possibly change SnRK1 activity in response to light. The phosphorylation status of T175 corresponds to the SnRK1 activity and could function as light-dependent switch. Accordingly, several upstream working kinases and phosphatases were identified. Phosphorylation of SnRK1 at the conserved T175 by SNRK1 ACTIVATING KINASES (SnAK1/GRIK1, SnAK2/GRIK2) promotes SnRK1 activity (Glab *et al.* 2017). In turn, SnRK1 seems to target SnAK1 and SnAK2 indicating a negative feedback control (Shen and Hanley-Bowdoin 2006, Shen *et al.* 2009, Glab *et al.* 2017). In contrast, PP2CA-type phosphatases from Arabidopsis were found inhibit SnRK1 activity (Rodrigues *et al.* 2013). Interestingly, mammalian phosphatases including PP2C and PP1, which target AMPK, do not affect SnRK1 phosphorylation (Emanuelle *et al.* 2015). However, the inhibitory effect could be restored when recombinant SnRK1 kinase was treated with rosette leaf tissue lysate that was isolated from 3-week-old Arabidopsis plants cultivated under long-day-conditions. The repressing factor was supposed to be a heat-labile protein over 30 kDa (Emanuelle *et al.* 2015), which would fit to several PP2C-type phosphatases in Arabidopsis according to TAIR10 (www.arabidopsis.org/; PP2CA, ABI1, ABI2, HAB1, HAB2; 13.10.2020).

In addition to phosphorylation, other post-translational modifications, localization or protein-protein-interactions might be involved in controlling SnRK1 action. Interestingly, one of the latest publications concerning SnRK1 combined all these aspects. It demonstrated that the interplay of α- and β-subunit is crucial for SnRK1 downstream signaling by affecting the subcellular localization (Ramon *et al.* 2019). The β-subunit contains an N-myristoylation that confers reversible attachment to the cell membrane and other proteins. Consequently, the interaction of α- and β-subunit leads to nuclear exclusion of the SnRK1 complex with impact on target gene expression. Upon energy depletion via extended night or DCMU treatment,

nuclear translocation of SnRK1α is initiated. Remarkably, an effect on target gene expression was only seen in case of promoter activation such as for *DIN6*, whereas SnRK1 target repression was unchanged (Ramon *et al.* 2019), indicating a differential regulation of SnRK1 targets or could be a result of transcript stability. The same mechanism might contribute to AS regulation via SnRK1 as well and could explain why just a subset of AS events is affected by SnRK1 repression. Next to it, Crozet and colleagues (2016) demonstrated negative feedback control of the SnRK1 complex by SUMOylation (post-translational modification through adding SMALL UBIQUITIN LIKE MODIFIERS). Kinase-inactive isoforms of SnRK1 accumulated in Arabidopsis cell culture due to inefficient protein degradation whereas SUMO mimetic isoforms of SnRK1 did not alter in their degradation rate relative to the controls. Thus, SnRK1 activity and protein stability seems to be coupled. This feedback might prevent hyperactivation of stress responses (Crozet *et al.* 2016). Further, acetylation sites were identified for SNF1 (Lin *et al.* 2009) and AMPK (Lin *et al.* 2012), however this modification has not been found so far *in planta* (Crozet *et al.* 2014).

Furthermore, sugar-phosphates inhibit SnRK1 signaling. T6P has been shown to be the most effective metabolic repressor of SnRK1 (Zhang *et al.* 2009, Delatte *et al.* 2011). The kinase activity was reduced after T6P supplementation in different tissue extracts of Arabidopsis, except for mature leaves. Kinase activity in metazoans stayed unaffected as well. Interestingly, purified SnRK1 enzyme could not be repressed by T6P *in vitro* but the effect was restored after adding the plant extracts suggesting the involvement of a co-acting factor (Zhang *et al.* 2009), probably it is the same cofactor or protein as mentioned in Emanuelle *et al*. (2015). However, overexpression of SnRK1 neutralizes the T6P effect. Similar but less pronounced results were obtained for glucose-6-phosphate (Delatte *et al.* 2011). These data point to a plant-specific, reversible, developmental stage- and tissue-specific buffer mechanisms to control SnRK1.

4.5.5. SnRK1 might alter AS decision by phosphorylation of splice regulators

Very recently, the mammalian AMPK was demonstrated to phosphorylate SR30 homologue SRSF1 (also known as ASF/SF2) in an *in vitro* kinase assay and human cell culture system (Matsumoto *et al.* 2020). More precisely, the RRM-located Ser133 is targeted by AMPK. Remarkably, the phosphorylation of this specific amino acid interrupted the interaction with RNA target sequences. For MACROPHAGE-STIMULATING PROTEIN RECEPTOR Ron, activation or repression of AMPK signaling resulted in AS shift towards inclusion or skipping of exon 11, respectively (Matsumoto *et al.* 2020). Promoted production of the exon skipping variant of *Ron* upon SRSF1 overexpression was linked to increased cell mobility, an important feature of tumor progression (Ghigna *et al.* 2005). These data strongly indicate an AMPK-

triggered splicing pattern for *Ron*. Moreover, aberrant splicing of the LAMIN A/C gene causing progeria (Hutchinson-Gilford progeria syndrome resulting in accelerated aging) and viral HIV (human immunodeficiency viruses) pre-mRNA processing were connected to AMPK activity (Finley 2015).

Protein sequence alignments of AtSR30 with HsSRSF1 show a high sequence similarity (Lopato *et al.* 1999b). Using the protein blast internet tool from NCBI (blast.ncbi.nlm.nih.gov/, 11.10.2020) revealed that 57.54 % of the protein sequences match to each other. Considering similar amino acid properties, both splicing factors are 70 % similar. Moreover, the amino acid composition 20 amino acids up- and downstream of HsSRSF1-Ser133 is almost identical to the protein sequence around AtSR30-Ser121. The amino acids at position -20, -19, -12, -1, 10 and 17 relative to the HsSRSF1-Ser133 or AtSR30-Ser121 are variable, all other within the stretch are identical or have similar amino acid properties (Fig. 2). Schaffer and colleagues (2015) previously identified three conserved AMPK phosphorylation motifs, from which the group A motif (LxxSxSxxxL) could be assigned to HsSRSF1 (Matsumoto *et al.* 2020). Similar phosphorylation site motifs were identified for SnRK1 as well (Nukarinen *et al.* 2016). It seems likely that AMPK and SnRK1 could also target AtSR30-Ser121 because of the conserved sequence, however, if SnRK1 phosphorylates SR proteins *in planta* and the impact on AS need to be addressed. SR45 has already been reported to negatively affect SnRK1 protein stability, when the plants are grown in presents of glucose (Carvalho *et al.* 2016). However if SnRK1 does only act as downstream target of SR45-mediated sugar signaling or if SnRK1 is also able to regulate the splicing factor remains unknown so far. There are currently no indications that SR45 is phosphorylated by SnRK1, however, the nuclear localization of both, SnRK1 (Williams *et al.* 2014, Jeong *et al.* 2015, Nukarinen *et al.* 2016) and SR45 (Ali *et al.* 2003, Ali and Reddy 2006), fulfil the first requirement for an interaction. Moreover, the phosphorylation status of SR45 affects its intranuclear distribution and mobility, which is important for its splicing activity (Ali *et al.* 2003, Ali and Reddy 2006). A putative SnRK1 phosphorylation site could not be identified in SR45, nevertheless, it could contain a modified phosphorylation site motif. Remarkably, phenotype of knock-out mutant *sr45-1* show a high similarity to plants inhibited in SnRK1 signaling. Hypocotyl length, cotyledon greening and expansion are drastically impaired in the mutant seedlings under glucose feeding conditions (Carvalho *et al.* 2010). Moreover, adult plants are much smaller at rosette stage and start to flower significantly later compared to wild type (Ali *et al.* 2007), which fits well to the observation for a proportion of the heterozygous, constitutive *amiR-SnRK1* lines (described before). These observations further support the idea that SnRK1 might be involved in regulation of RNA processing.

In Arabidopsis, motif analysis identified mRNA processing proteins as putative SnRK1 targets including splicing regulator CC1-like (AT2G16940) and RNA binding proteins

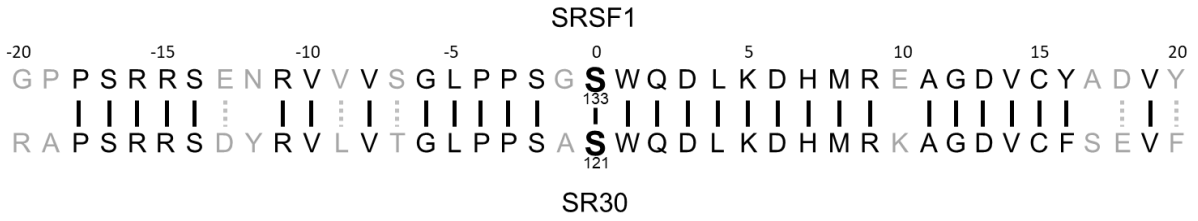

Figure 2: Protein sequence alignment for HsSRSF1 phosphorylation site to AtSR30. Shown are 20 amino acids up- and downstream of HsSRSF1-S133 and AtSR30-S121 as one-letter-code. Identical amino acids are display in black and are linked via a solid line. Gray letters indicate variable amino acid positions whereby these with similar biochemical properties were connected by an dashed line. Protein sequences were taken from www.uniprot.com to align HsSRSF1 to AtSR30 via NCBI online blast tool (https:\\blast.ncbi.nlm.nih.gov, 09.10.2020).

(AT4G17520, AT5G47210, Nukarinen *et al.* 2016). During anthers development in rice, pre-mRNA splicing is extensively regulated by phosphorylation. Interestingly, predicted SnRK1 phosphorylation targets were over-represented in this study (Ye *et al.* 2015). A direct kinase-substrate-interaction has been proven for the mRNA stability regulator PENTA and the splicing regulator GRP8 with SnRK1, respectively (Schöning *et al.* 2008, Paik *et al.* 2012, Cho *et al.* 2016). In yeast, it was shown that SNF1 affects different mRNA associated pathways, among them mRNA stability in a glucose-dependent manner. Accordingly, phosphoproteome analysis identified XRN1 to be phosphorylated by SNF1 and to promote glucose-induced decay of SNF1-regulated transcripts indicating a mRNA buffering function of the SNF1-XRN1 relay (Braun and Young 2014). XRN4 in Arabidopsis represents the homolog of yeast XRN1 and was shown by us to target SR30 (Hartmann *et al.* 2018). These correlations might pinpoint to complex SnRK1-dependent mRNA processing, however, a direct link to AS has not been described *in planta* so far. Since there are strong indications that SnRK1 regulates a network of RNA-related factors in response to changes in light conditions, we focused our investigations on SnRK1 as putative upstream regulator of light- and sugar-mediated AS.

4.5.6. Possible involvement of other kinases

Arabidopsis has more than 1000 genes encoding protein kinases that are involved in diverse physiological processes. Among them, there are numerous kinases acting in light and sugar signaling besides SnRK1. The energy sensor TOR is described as antagonistic player of SnRK1, regulating energy homeostasis under energy favorable conditions. TOR is able to integrate energy signals and activates stem cells in meristematic tissues (Xiong *et al.* 2013, Pfeiffer *et al.* 2016) to promote growth and light-mediated translation during de-etiolation (Chen *et al.* 2018). Consistently, TOR inactivation causes reduced protein biosynthesis rate of

nuclear encoded ribosomal proteins (Dobrenel *et al.* 2016). Therefore, plants impaired in TOR signaling represent a drastic reduced greening of cotyledons or chlorosis at seedling or rosette stage, respectively (Deprost *et al.* 2007, Li *et al.* 2015b, Dobrenel *et al.* 2016). Interestingly, the phosphorylation of the TOR target RIBOSOMAL PROTEIN S6 was reported to be induced by light and seems to be affected by the photosensory component COP1 (Turkina *et al.* 2011, Boex-Fontvieille *et al.* 2013, Chen *et al.* 2018). Interestingly, the photomorphogenic growth of dark-grown *cop1* seedlings is dependent on functional TOR signaling especially with regard to cotyledon opening (Chen *et al.* 2018). Since, TOR is involved in plant development and light signaling, we tested whether TOR signaling also affects light-mediated AS (Saile *et al*., unpublished). Similar to SnRK1, we analyzed AS pattern for *SR30*, *RRC1*, *PPD2* and *MYBD* in etiolated seedlings upon TOR repression relative to the controls. Surprisingly, *SR30, RRC1 and PPD2* showed an AS shift towards the light-produced splice variant when TOR signaling was impaired whereas *MYBD* AS ratio stayed unaffected (Saile *et al*., unpublished). Petrillo and colleagues (2018) have already provided evidence that TOR can regulate light- and sugar-triggered AS pattern of RS31 which fits to our data. Remarkably they could demonstrate that AS response is plant organ specific in light-grown seedlings, since TOR repression leads to unresponsiveness of RS31 AS pattern in root tissue upon sugar supplementation (Petrillo *et al.* 2018). Next to similar AS shifts, we also observed that the hypocotyl length was drastically shortened upon TOR repression as demonstrated for SnRK1 inhibition (Saile *et al.*, unpublished). These results were unexpected since both kinases have been described to work antagonistically and a cooperative action mode was never mentioned so far. However, considering similar AS pattern for selected AS events and identical hypocotyl phenotype, we suggest a similar function during early seedling development for both central energy sensors. Next steps would be to investigate whether SnRK1 and TOR signaling joint in one pathway or do they perform independently? Does a signaling hierarchy exist if both kinases participate in the signaling? There is some evidence that SnRK1 interferes with TOR signaling since the phosphorylation status of the TOR target S6 KINASE is altered in SnRK1 double mutants (Nukarinen *et al.* 2016). Furthermore, TOR was also linked to ethylene signaling (Fu *et al.* 2021) and leaf senescence (Deprost *et al.* 2007). Essential components of these pathways are also targeted by SnRK1 (see 4.5.3.). To address the TOR function in AS control in more detail, inducible *amiR-TOR* mutants should be further analyzed for AS events responding to light or sucrose. In addition, the specific TOR inhibitor AZD5088 can be used to confirm the results (Montane and Menand 2013, Pfeiffer *et al.* 2016). To examine a potential interplay of SnRK1 and TOR, TOR inhibitor could be applied to induced *i-amiR-SnRK1* mutants. When the AS pattern shift is enhanced compared to seedlings only repressed in SnRK1 signaling could provide first indications if both kinases synergistically regulate light-triggered AS. Moreover, a phosphoproteome analysis of inducible SnRK1 and TOR knock-down mutants might identify

more common phosphorylation targets as response to changed energy availability, e.g. during the early photomorphogenesis. Single phosphorylation target should be analyzed before and after kinase repression using antibodies specifically binding to the phosphorylated kinase target or using the phostag gel systems. Additionally, co-localization studies and immunoprecipitation of both kinases with the putative phosphorylation targets could be performed to proof their interaction.

Besides energy sensors, there are many kinases that are connected to light and sugar signaling on one hand and RNA metabolism on the other hand. The SUCROSE INDUCED RECEPTOR KINASE 1 (SIRK1) is activated in presence of sucrose in starved Arabidopsis seedlings (Wu *et al.* 2013). A comparative phosphoproteome study identified FAR-RED ELONGATED HYPOCOTYL 1-LIKE and NON-PHOTOTROPIC HYPOCOTYL 3 as SIRK1 targets. Additionally, several splicing-related components such as RS41 or U1-70K were identified to interact with SIRK1 kinase connecting SIRK1 to light signaling and RNA processing (Wu *et al.* 2013). Direct phosphorylation of splicing regulators by SnRK1 has not been reported so far, hence kinases targeting SR proteins could be the missing link within the regulatory network of light and sugar-mediated AS. Especially, SRPK4 (de la Fuente van Bentem *et al.* 2006), AFC2 (Golovkin and Reddy 1999) and MAPK3 and 6 (Feilner *et al.* 2005) were demonstrated to phosphorylate different SR proteins. Phosphorylation of SR proteins can affect their sub-cellular localization and splice site decision as mentioned before (Discussion point 1.1. and 1.2.). Nevertheless, if these kinases are regulated by SnRK1 or act in an energy dependent manner remains to be addressed.

4.6. Summary

In my PhD project, we could illustrate new mechanistic aspects of light-induced AS during the early photomorphogenesis. Nuclear retention enables transcripts with NMD-eliciting features to escape from this cytosolic RNA decay pathway, which was shown for dark-promoted splice variant *SR30.2*. The function of the rather stable *SR30.2* still remains elusive; however, it seems likely that RNA-protein interaction avoids the mRNA export of this mRNA isoform. Hence, *SR30.2* might sequestrate RNA-binding proteins in darkness such as splicing regulators. Further, we demonstrated that the minor mRNA isoform *SR30.3* can be derived from *SR30.2* by activation of the downstream 3' splice site in a consecutive splicing step under artificial conditions. The same 3' splice site is favored upon illumination to generate *SR30.1* from the *SR30* pre-mRNA. Both splicing events might be regulated by a common light-activated splicing regulator. *SR30.1* together with *SR30.3* are exported to the cytosol for protein biosynthesis and to undergo NMD, respectively. Hence, the production of the instable *SR30.3* would enhance the light-trigger AS shift of *SR30* towards the protein-coding transcript. Finally, the SR30 protein returns to the nucleus to participated in splicing reactions for RNA targets including its own pre-mRNA via SR30 autoregulation. This mechanism inclusive the posttranscriptional splicing step might represent an additional layer of *SR30* gene regulation and is probably transferable to other genes encoding more than two splice variants.

Moreover, phosphorylation seems to play an essential role in light-mediated AS control. Chemical inhibition of kinase signaling causes AS shifts that overlap for a subset with light-induced AS changes in etiolated seedlings. This partial correlation argues for the contribution of various kinases and probably also phosphatases to AS control. SnRK1 is a prime candidate since repression of SnRK1 signaling could be correlated with several light-induced AS pattern changes such as for *SR30*. Moreover, SnRK1 repression caused drastic phenotypes such as shortened hypocotyls of etiolated seedlings, chlorosis in light-grown seedlings and accelerated senescence for adult plants. Consistently with other publications, SnRK1 fulfills essential role in plant growth, also in early seedling development and seems to be a negative regulator of light-mediated AS. Remarkably, repression of TOR kinase revealed similar results as in case of SnRK1 mutants, although TOR is known to function antagonistically to SnRK1. Therefore, we propose that both energy sensor might work together in early photomorphogenesis.

5. References

5.1. Publications

Aghamirzaie D., Nabiyouni M., Fang Y., Klumas C., Heath L. S., Grene R. and Collakova E. (2013). "Changes in RNA Splicing in Developing Soybean (Glycine max) Embryos." Biology (Basel) **2**(4): 1311-1337.

Ahmad M., Grancher N., Heil M., Black R. C., Giovani B., Galland P. and Lardemer D. (2002). "Action spectrum for cryptochrome-dependent hypocotyl growth inhibition in Arabidopsis." Plant Physiology **129**(2): 774-785.

Ahmad M., Jarillo J. A., Smirnova O. and Cashmore A. R. (1998). "The CRY1 Blue Light Photoreceptor of Arabidopsis Interacts with Phytochrome A In Vitro." Molecular Cell **1**(7): 939-948.

Al-Sady B., Ni W., Kircher S., Schafer E. and Quail P. H. (2006). "Photoactivated phytochrome induces rapid PIF3 phosphorylation prior to proteasome-mediated degradation." Mol Cell **23**(3): 439-446.

Ali G. S., Golovkin M. and Reddy A. S. (2003). "Nuclear localization and in vivo dynamics of a plant-specific serine/arginine-rich protein." Plant J **36**(6): 883-893.

Ali G. S., Palusa S. G., Golovkin M., Prasad J., Manley J. L. and Reddy A. S. (2007). "Regulation of plant developmental processes by a novel splicing factor." PLoS One **2**(5): e471.

Ali G. S. and Reddy A. S. (2006). "ATP, phosphorylation and transcription regulate the mobility of plant splicing factors." J Cell Sci **119**(Pt 17): 3527-3538.

Allemand E., Guil S., Myers M., Moscat J., Caceres J. F. and Krainer A. R. (2005). "Regulation of heterogenous nuclear ribonucleoprotein A1 transport by phosphorylation in cells stressed by osmotic shock." Proc Natl Acad Sci U S A **102**(10): 3605-3610.

Alrahbeni T., Sartor F., Anderson J., Miedzybrodzka Z., McCaig C. and Muller B. (2015). "Full UPF3B function is critical for neuronal differentiation of neural stem cells." Mol Brain **8**: 33.

Anderson G. H., Veit B. and Hanson M. R. (2005). "The Arabidopsis AtRaptor genes are essential for post-embryonic plant growth." BMC Biol **3**: 12.

Arnold W. N. (1968). "The selection of sucrose as the translocate of higher plants." Journal of Theoretical Biology **21**(1): 13-20.

Baena-Gonzalez E. and Hanson J. (2017). "Shaping plant development through the SnRK1-TOR metabolic regulators." Curr Opin Plant Biol **35**: 152-157.

Baena-Gonzalez E., Rolland F., Thevelein J. M. and Sheen J. (2007). "A central integrator of transcription networks in plant stress and energy signalling." Nature **448**(7156): 938-942.

Bagnall D. J., King R. W. and Farquhar G. D. (1988). "Temperature-dependent feedback inhibition of photosynthesis in peanut." Planta **175**(3): 348-354.

Baker N. R. and Butler W. L. (1976). "Development of the Primary Photochemical Apparatus of Photosynthesis during Greening of Etiolated Bean Leaves." Plant Physiol **58**(4): 526-529.

Barbosa-Morais N. L., Irimia M., Pan Q., Xiong H. Y., Gueroussov S., Lee L. J., Slobodeniuc V., Kutter C., Watt S., Colak R., Kim T., Misquitta-Ali C. M., Wilson M. D., Kim P. M., Odom D. T., Frey B. J. and Blencowe B. J. (2012). "The evolutionary landscape of alternative splicing in vertebrate species." Science **338**(6114): 1587-1593.

Bardou F., Ariel F., Simpson C. G., Romero-Barrios N., Laporte P., Balzergue S., Brown J. W. and Crespi M. (2014). "Long noncoding RNA modulates alternative splicing regulators in Arabidopsis." Dev Cell **30**(2): 166-176.

Barta A., Kalyna M. and Lorkovic Z. J. (2008). "Plant SR proteins and their functions." Curr Top Microbiol Immunol **326**: 83-102.

Barta A., Kalyna M. and Reddy A. S. (2010). "Implementing a rational and consistent nomenclature for serine/arginine-rich protein splicing factors (SR proteins) in plants." Plant Cell **22**(9): 2926-2929.

Baskin T. I. and Wilson J. E. (1997). "Inhibitors of protein kinases and phosphatases alter root morphology and disorganize cortical microtubules." Plant Physiol **113**(2): 493-502.

Berget S. M., Moore C. and Sharp P. A. (1977). "Spliced segments at the 5' terminus of adenovirus 2 late mRNA." Proc Natl Acad Sci U S A **74**(8): 3171-3175.

Betterle N., Ballottari M., Baginsky S. and Bassi R. (2015). "High Light-Dependent Phosphorylation of Photosystem II Inner Antenna CP29 in Monocots Is STN7 Independent and Enhances Nonphotochemical Quenching." Plant Physiology **167**(2): 457.

Bhalerao R. P., Salchert K., Bako L., Okresz L., Szabados L., Muranaka T., Machida Y., Schell J. and Koncz C. (1999). "Regulatory interaction of PRL1 WD protein with Arabidopsis SNF1-like protein kinases." Proc Natl Acad Sci U S A **96**(9): 5322-5327.

Biggins J. and Park R. B. (1966). "CO(2) Assimilation by Etiolated Hordeum vulgare Seedlings during the Onset of Photosynthesis." Plant Physiol **41**(1): 115-118.

Blaauw-Jansen G., Komen J. G. and Thomas J. B. (1950). "On the relation between the formation of assimilatory pigments and the rate of photosynthesis in etiolated oat seedlings." Biochim Biophys Acta **5**(2): 179-185.

Blanc G., Hokamp K. and Wolfe K. H. (2003). "A recent polyploidy superimposed on older large-scale duplications in the Arabidopsis genome." Genome research **13**(2): 137-144.

Blasing O. E., Gibon Y., Gunther M., Hohne M., Morcuende R., Osuna D., Thimm O., Usadel B., Scheible W. R. and Stitt M. (2005). "Sugars and circadian regulation make major contributions to the global regulation of diurnal gene expression in Arabidopsis." Plant Cell **17**(12): 3257-3281.

Blazek M., Santisteban T. S., Zengerle R. and Meier M. (2015). "Analysis of fast protein phosphorylation kinetics in single cells on a microfluidic chip." Lab Chip **15**(3): 726-734.

Bloom M. V., Milos P. and Roy H. (1983). "Light-dependent assembly of ribulose-1,5-bisphosphate carboxylase." Proc Natl Acad Sci U S A **80**(4): 1013-1017.

Boex-Fontvieille E., Daventure M., Jossier M., Zivy M., Hodges M. and Tcherkez G. (2013). "Photosynthetic control of Arabidopsis leaf cytoplasmic translation initiation by protein phosphorylation." PLoS One **8**(7): e70692.

Boothby T. C., Zipper R. S., van der Weele C. M. and Wolniak S. M. (2013). "Removal of retained introns regulates translation in the rapidly developing gametophyte of Marsilea vestita." Dev Cell **24**(5): 517-529.

Borthwick H. A., Hendricks S. B., Parker M. W., Toole E. H. and Toole V. K. (1952). "A Reversible Photoreaction Controlling Seed Germination." Proc Natl Acad Sci U S A **38**(8): 662-666.

Bradford K. J. (1990). "A water relations analysis of seed germination rates." Plant Physiol **94**(2): 840-849.

Braun K. A., Vaga S., Dombek K. M., Fang F., Palmisano S., Aebersold R. and Young E. T. (2014). "Phosphoproteomic analysis identifies proteins involved in transcription-coupled mRNA decay as targets of Snf1 signaling." Sci Signal **7**(333): ra64.

Braunschweig U., Gueroussov S., Plocik A. M., Graveley B. R. and Blencowe B. J. (2013). "Dynamic integration of splicing within gene regulatory pathways." Cell **152**(6): 1252-1269.

Briggs W. R. and Huala E. (1999). "Blue-light photoreceptors in higher plants." Annu Rev Cell Dev Biol **15**: 33-62.

Briggs W. R. and Olney M. A. (2001). "Photoreceptors in Plant Photomorphogenesis to Date. Five Phytochromes, Two Cryptochromes, One Phototropin, and One Superchrome." Plant Physiology **125**(1): 85-88.

Broeckx T., Hulsmans S. and Rolland F. (2016). "The plant energy sensor: evolutionary conservation and divergence of SnRK1 structure, regulation, and function." J Exp Bot **67**(22): 6215-6252.

Bruns A. N., Li S., Mohannath G. and Bisaro D. M. (2019). "Phosphorylation of Arabidopsis eIF4E and eIFiso4E by SnRK1 inhibits translation." FEBS J.

Carvalho R. F., Carvalho S. D. and Duque P. (2010). "The plant-specific SR45 protein negatively regulates glucose and ABA signaling during early seedling development in Arabidopsis." Plant Physiol **154**(2): 772-783.

Carvalho R. F., Szakonyi D., Simpson C. G., Barbosa I. C., Brown J. W., Baena-Gonzalez E. and Duque P. (2016). "The Arabidopsis SR45 Splicing Factor, a Negative Regulator of Sugar Signaling, Modulates SNF1-Related Protein Kinase 1 Stability." Plant Cell **28**(8): 1910-1925.

Castillon A., Shen H. and Huq E. (2007). "Phytochrome Interacting Factors: central players in phytochrome-mediated light signaling networks." Trends Plant Sci **12**(11): 514-521.

Cazalla D., Zhu J., Manche L., Huber E., Krainer A. R. and Cáceres J. F. (2002). "Nuclear export and retention signals in the RS domain of SR proteins." Molecular and cellular biology **22**(19): 6871-6882.

Champion A., Kreis M., Mockaitis K., Picaud A. and Henry Y. (2004). "Arabidopsis kinome: after the casting." Funct Integr Genomics **4**(3): 163-187.

Chan A., Carianopol C., Tsai A. Y., Varatharajah K., Chiu R. S. and Gazzarrini S. (2017). "SnRK1 phosphorylation of FUSCA3 positively regulates embryogenesis, seed yield, and plant growth at high temperature in Arabidopsis." J Exp Bot **68**(15): 4219-4231.

Chan K. X., Phua S. Y., Crisp P., McQuinn R. and Pogson B. J. (2016). "Learning the Languages of the Chloroplast: Retrograde Signaling and Beyond." Annu Rev Plant Biol **67**: 25-53.

Chanderbali A. S., Yoo M. J., Zahn L. M., Brockington S. F., Wall P. K., Gitzendanner M. A., Albert V. A., Leebens-Mack J., Altman N. S., Ma H., dePamphilis C. W., Soltis D. E. and Soltis P. S. (2010). "Conservation and canalization of gene expression during angiosperm diversification accompany the origin and evolution of the flower." Proc Natl Acad Sci U S A **107**(52): 22570-22575.

Chao J. A., Yoon Y. J. and Singer R. H. (2012). "Imaging translation in single cells using fluorescent microscopy." Cold Spring Harb Perspect Biol **4**(11).

Chaudhary S., Jabre I., Reddy A. S. N., Staiger D. and Syed N. H. (2019a). "Perspective on Alternative Splicing and Proteome Complexity in Plants." Trends Plant Sci **24**(6): 496-506.

Chaudhary S., Khokhar W., Jabre I., Reddy A. S. N., Byrne L. J., Wilson C. M. and Syed N. H. (2019b). "Alternative Splicing and Protein Diversity: Plants Versus Animals." Front Plant Sci **10**: 708.

Chen G. H., Liu M. J., Xiong Y., Sheen J. and Wu S. H. (2018). "TOR and RPS6 transmit light signals to enhance protein translation in deetiolating Arabidopsis seedlings." Proceedings of the National Academy of Sciences of the United States of America **115**(50): 12823-12828.

Chen L., Su Z. Z., Huang L., Xia F. N., Qi H., Xie L. J., Xiao S. and Chen Q. F. (2017). "The AMP-Activated Protein Kinase KIN10 Is Involved in the Regulation of Autophagy in Arabidopsis." Frontiers in Plant Science **8**.

Cho H. Y., Wen T. N., Wang Y. T. and Shih M. C. (2016). "Quantitative phosphoproteomics of protein kinase SnRK1 regulated protein phosphorylation in Arabidopsis under submergence." J Exp Bot **67**(9): 2745-2760.

Cho Y. H., Hong J. W., Kim E. C. and Yoo S. D. (2012). "Regulatory functions of SnRK1 in stress-responsive gene expression and in plant growth and development." Plant Physiol **158**(4): 1955-1964.

Choudhary C., Kumar C., Gnad F., Nielsen M. L., Rehman M., Walther T. C., Olsen J. V. and Mann M. (2009). "Lysine acetylation targets protein complexes and co-regulates major cellular functions." Science **325**(5942): 834-840.

Chow L. T., Gelinas R. E., Broker T. R. and Roberts R. J. (1977). "An amazing sequence arrangement at the 5' ends of adenovirus 2 messenger RNA." Cell **12**(1): 1-8.

Clack T., Mathews S. and Sharrock R. A. (1994). "The phytochrome apoprotein family in Arabidopsis is encoded by five genes: the sequences and expression of PHYD and PHYE." Plant Mol Biol **25**(3): 413-427.

Colwill K., Pawson T., Andrews B., Prasad J., Manley J. L., Bell J. C. and Duncan P. I. (1996). "The Clk/Sty protein kinase phosphorylates SR splicing factors and regulates their intranuclear distribution." EMBO J **15**(2): 265-275.

Cook-Andersen H. and Wilkinson M. F. (2015). "Molecular biology: Splicing does the two-step." Nature **521**(7552): 300-301.

Covington M. F. and Harmer S. L. (2007). "The Circadian Clock Regulates Auxin Signaling and Responses in Arabidopsis." PLOS Biology **5**(8): e222.

Crozet P., Margalha L., Butowt R., Fernandes N., Elias C. A., Orosa B., Tomanov K., Teige M., Bachmair A., Sadanandom A. and Baena-Gonzalez E. (2016). "SUMOylation represses SnRK1 signaling in Arabidopsis." Plant J **85**(1): 120-133.

Crozet P., Margalha L., Confraria A., Rodrigues A., Martinho C., Adamo M., Elias C. A. and Baena-Gonzalez E. (2014). "Mechanisms of regulation of SNF1/AMPK/SnRK1 protein kinases." Front Plant Sci **5**: 190.

Dai Y., Li W. and An L. (2016). "NMD mechanism and the functions of Upf proteins in plant." Plant Cell Reports **35**(1): 5-15.

Davies S. P., Helps N. R., Cohen P. T. and Hardie D. G. (1995). "5'-AMP inhibits dephosphorylation, as well as promoting phosphorylation, of the AMP-activated protein kinase. Studies using bacterially expressed human protein phosphatase-2C alpha and native bovine protein phosphatase-2AC." FEBS Lett **377**(3): 421-425.

de Francisco Amorim M., Willing E.-M., Szabo E. X., Francisco-Mangilet A. G., Droste-Borel I., Maček B., Schneeberger K. and Laubinger S. (2018). "The U1 snRNP Subunit LUC7 Modulates Plant Development and Stress Responses via Regulation of Alternative Splicing." The Plant Cell **30**(11): 2838-2854.

de la Fuente van Bentem S., Anrather D., Dohnal I., Roitinger E., Csaszar E., Joore J., Buijnink J., Carreri A., Forzani C., Lorkovic Z. J., Barta A., Lecourieux D., Verhounig A., Jonak C. and Hirt H. (2008). "Site-specific phosphorylation profiling of Arabidopsis proteins by mass spectrometry and peptide chip analysis." J Proteome Res **7**(6): 2458-2470.

de la Fuente van Bentem S., Anrather D., Roitinger E., Djamei A., Hufnagl T., Barta A., Csaszar E., Dohnal I., Lecourieux D. and Hirt H. (2006). "Phosphoproteomics reveals extensive in vivo phosphorylation of Arabidopsis proteins involved in RNA metabolism." Nucleic Acids Res **34**(11): 3267-3278.

Delatte T. L., Sedijani P., Kondou Y., Matsui M., de Jong G. J., Somsen G. W., Wiese-Klinkenberg A., Primavesi L. F., Paul M. J. and Schluepmann H. (2011). "Growth arrest by trehalose-6-phosphate: an astonishing case of primary metabolite control over growth by way of the SnRK1 signaling pathway." Plant Physiol **157**(1): 160-174.

Deng X. W., Caspar T. and Quail P. H. (1991). "cop1: a regulatory locus involved in light-controlled development and gene expression in Arabidopsis." Genes Dev **5**(7): 1172-1182.

Deprost D., Yao L., Sormani R., Moreau M., Leterreux G., Nicolai M., Bedu M., Robaglia C. and Meyer C. (2007). "The Arabidopsis TOR kinase links plant growth, yield, stress resistance and mRNA translation." EMBO Rep **8**(9): 864-870.

Dias A. P., Dufu K., Lei H. and Reed R. (2010). "A role for TREX components in the release of spliced mRNA from nuclear speckle domains." Nat Commun **1**: 97.

Dietrich K., Weltmeier F., Ehlert A., Weiste C., Stahl M., Harter K. and Droge-Laser W. (2011). "Heterodimers of the Arabidopsis transcription factors bZIP1 and bZIP53 reprogram amino acid metabolism during low energy stress." Plant Cell **23**(1): 381-395.

Dijkwel P. P., Kock P., Bezemer R., Weisbeek P. J. and Smeekens S. (1996). "Sucrose Represses the Developmentally Controlled Transient Activation of the Plastocyanin Gene in Arabidopsis thaliana Seedlings." Plant Physiol **110**(2): 455-463.

Ding J. H., Zhong X. Y., Hagopian J. C., Cruz M. M., Ghosh G., Feramisco J., Adams J. A. and Fu X. D. (2006). "Regulated cellular partitioning of SR protein-specific kinases in mammalian cells." Mol Biol Cell **17**(2): 876-885.

Dobrenel T., Mancera-Martinez E., Forzani C., Azzopardi M., Davanture M., Moreau M., Schepetilnikov M., Chicher J., Langella O., Zivy M., Robaglia C., Ryabova L. A., Hanson J. and Meyer C. (2016). "The Arabidopsis TOR Kinase Specifically Regulates the Expression of Nuclear Genes Coding for Plastidic Ribosomal Proteins and the Phosphorylation of the Cytosolic Ribosomal Protein S6." Front Plant Sci **7**: 1611.

Docquier S., Tillemans V., Deltour R. and Motte P. (2004). "Nuclear bodies and compartmentalization of pre-mRNA splicing factors in higher plants." Chromosoma **112**(5): 255-266.

Drechsel G., Kahles A., Kesarwani A. K., Stauffer E., Behr J., Drewe P., Ratsch G. and Wachter A. (2013). "Nonsense-mediated decay of alternative precursor mRNA splicing variants is a major determinant of the Arabidopsis steady state transcriptome." Plant Cell **25**(10): 3726-3742.

Duan G., Walther D. and Schulze W. X. (2013). "Reconstruction and analysis of nutrient-induced phosphorylation networks in Arabidopsis thaliana." Front Plant Sci **4**: 540.

Duff M. O., Olson S., Wei X., Garrett S. C., Osman A., Bolisetty M., Plocik A., Celniker S. E. and Graveley B. R. (2015). "Genome-wide identification of zero nucleotide recursive splicing in Drosophila." Nature **521**(7552): 376-379.

Duncan P. I., Stojdl D. F., Marius R. M., Scheit K. H. and Bell J. C. (1998). "The Clk2 and Clk3 Dual-Specificity Protein Kinases Regulate the Intranuclear Distribution of SR Proteins and Influence Pre-mRNA Splicing." Experimental Cell Research **241**(2): 300-308.

Eastmond P. J., Van Dijken A. J. H., Spielman M., Kerr A., Tissier A. F., Dickinson H. G., Jones J. D. G., Smeekens S. C. and Graham I. A. (2002). "Trehalose-6-phosphate synthase 1, which catalyses the first step in trehalose synthesis, is essential for Arabidopsis embryo maturation." The Plant Journal **29**(2): 225-235.

Eberle A. B., Stalder L., Mathys H., Orozco R. Z. and Muhlemann O. (2008). "Posttranscriptional gene regulation by spatial rearrangement of the 3' untranslated region." PLoS Biol **6**(4): e92.

Edmond V., Moysan E., Khochbin S., Matthias P., Brambilla C., Brambilla E., Gazzeri S. and Eymin B. (2011). "Acetylation and phosphorylation of SRSF2 control cell fate decision in response to cisplatin." EMBO J **30**(3): 510-523.

Emanuelle S., Hossain M. I., Moller I. E., Pedersen H. L., van de Meene A. M., Doblin M. S., Koay A., Oakhill J. S., Scott J. W., Willats W. G., Kemp B. E., Bacic A., Gooley P. R. and Stapleton D. I. (2015). "SnRK1 from Arabidopsis thaliana is an atypical AMPK." Plant J **82**(2): 183-192.

Emerson R. and Lewis C. M. (1943). "The Dependence of the Quantum Yield of Chlorella Photosynthesis on Wave Lenghth of Light." American Journal of Botany **30**(3): 165-178.

Erwin J. (1991). "TEMPERATURE AND LIGHT EFFECTS ON SEED GERMINATION." **40**: 16.

Fang Y., Hearn S. and Spector D. L. (2004). "Tissue-specific expression and dynamic organization of SR splicing factors in Arabidopsis." Mol Biol Cell **15**(6): 2664-2673.

Fankhauser C. and Chory J. (1997). "Light control of plant development." Annu Rev Cell Dev Biol **13**: 203-229.

Feilner T., Hultschig C., Lee J., Meyer S., Immink R. G., Koenig A., Possling A., Seitz H., Beveridge A., Scheel D., Cahill D. J., Lehrach H., Kreutzberger J. and Kersten B. (2005). "High throughput identification of potential Arabidopsis mitogen-activated protein kinases substrates." Mol Cell Proteomics **4**(10): 1558-1568.

Feng C. M., Qiu Y., Van Buskirk E. K., Yang E. J. and Chen M. (2014). "Light-regulated gene repositioning in Arabidopsis." Nat Commun **5**: 3027.

Feng L., Raza M. A., Li Z., Chen Y., Khalid M. H. B., Du J., Liu W., Wu X., Song C., Yu L., Zhang Z., Yuan S., Yang W. and Yang F. (2019). "The Influence of Light Intensity and Leaf Movement on Photosynthesis Characteristics and Carbon Balance of Soybean." Frontiers in Plant Science **9**(1952).

Fesenko I., Khazigaleeva R., Kirov I., Kniazev A., Glushenko O., Babalyan K., Arapidi G., Shashkova T., Butenko I., Zgoda V., Anufrieva K., Seredina A., Filippova A. and Govorun V. (2017). "Alternative splicing shapes transcriptome but not proteome diversity in Physcomitrella patens." Sci Rep **7**(1): 2698.

Figueroa C. M. and Lunn J. E. (2016). "A Tale of Two Sugars: Trehalose 6-Phosphate and Sucrose." Plant Physiol **172**(1): 7-27.

Filichkin S. A., Priest H. D., Givan S. A., Shen R., Bryant D. W., Fox S. E., Wong W. K. and Mockler T. C. (2010). "Genome-wide mapping of alternative splicing in Arabidopsis thaliana." Genome Res **20**(1): 45-58.

Finley J. (2015). "Reactivation of latently infected HIV-1 viral reservoirs and correction of aberrant alternative splicing in the LMNA gene via AMPK activation: Common mechanism of action linking HIV-1 latency and Hutchinson-Gilford progeria syndrome." Med Hypotheses **85**(3): 320-332.

Folta K. M. and Maruhnich S. A. (2007). "Green light: a signal to slow down or stop." J Exp Bot **58**(12): 3099-3111.

Fouquet R., Martin F., Fajardo D. S., Gault C. M., Gómez E., Tseung C.-W., Policht T., Hueros G. and Settles A. M. (2011). "Maize Rough Endosperm3 Encodes an RNA Splicing Factor Required for Endosperm Cell Differentiation and Has a Nonautonomous Effect on Embryo Development." The Plant Cell **23**(12): 4280-4297.

Fox A. R., Barberini M. L., Ploschuk E. L., Muschietti J. P. and Mazzella M. A. (2015). "A proteome map of a quadruple photoreceptor mutant sustains its severe photosynthetic deficient phenotype." J Plant Physiol **185**: 13-23.

Fredeen A. L., Gamon J. A. and Field C. B. (1991). "Responses of photosynthesis and carbohydrate-partitioning to limitations in nitrogen and water availability in field-grown sunflower*." Plant, Cell & Environment **14**(9): 963-970.

Friso G. and van Wijk K. J. (2015). "Posttranslational Protein Modifications in Plant Metabolism." Plant Physiol **169**(3): 1469-1487.

Fu G., Condon K. C., Epton M. J., Gong P., Jin L., Condon G. C., Morrison N. I., Dafa'alla T. H. and Alphey L. (2007). "Female-specific insect lethality engineered using alternative splicing." Nat Biotechnol **25**(3): 353-357.

Fu L., Liu Y., Qin G., Wu P., Zi H., Xu Z., Zhao X., Wang Y., Li Y., Yang S., Peng C., Wong C. C. L., Yoo S.-D., Zuo Z., Liu R., Cho Y.-H. and Xiong Y. (2021). "The TOR–EIN2 axis mediates nuclear signalling to modulate plant growth." Nature.

Fujiki Y., Ito M., Nishida I. and Watanabe A. (2000). "Multiple signaling pathways in gene expression during sugar starvation. Pharmacological analysis of din gene expression in suspension-cultured cells of Arabidopsis." Plant Physiol **124**(3): 1139-1148.

Fujiki Y., Yoshikawa Y., Sato T., Inada N., Ito M., Nishida I. and Watanabe A. (2001). "Dark-inducible genes from Arabidopsis thaliana are associated with leaf senescence and repressed by sugars." Physiol Plant **111**(3): 345-352.

Galvao V. C. and Fankhauser C. (2015). "Sensing the light environment in plants: photoreceptors and early signaling steps." Curr Opin Neurobiol **34**: 46-53.

Gazzoli I., Pulyakhina I., Verwey N. E., Ariyurek Y., Laros J. F. J., t Hoen P. A. C. and Aartsma-Rus A. (2016). "Non-sequential and multi-step splicing of the dystrophin transcript." RNA Biology **13**(3): 290-305.

Ge H. and Manley J. L. (1990). "A protein factor, ASF, controls cell-specific alternative splicing of SV40 early pre-mRNA in vitro." Cell **62**(1): 25-34.

Georgomanolis T., Sofiadis K. and Papantonis A. (2016). "Cutting a Long Intron Short: Recursive Splicing and Its Implications." Front Physiol **7**: 598.

Gest H. (1988). "Sun-beams, cucumbers, and purple bacteria : Historical milestones in early studies of photosynthesis revisited." Photosynth Res **19**(3): 287-308.

Gest H. (2000). "Bicentenary homage to Dr Jan Ingen-Housz, MD (1730-1799), pioneer of photosynthesis research." Photosynth Res **63**(2): 183-190.

Ghigna C., Giordano S., Shen H., Benvenuto F., Castiglioni F., Comoglio P. M., Green M. R., Riva S. and Biamonti G. (2005). "Cell Motility Is Controlled by SF2/ASF through Alternative Splicing of the Ron Protooncogene." Molecular Cell **20**(6): 881-890.

Girard C., Will C. L., Peng J., Makarov E. M., Kastner B., Lemm I., Urlaub H., Hartmuth K. and Lührmann R. (2012). "Post-transcriptional spliceosomes are retained in nuclear speckles until splicing completion." Nat Commun **3**: 994.

Giuliano G., Pichersky E., Malik V. S., Timko M. P., Scolnik P. A. and Cashmore A. R. (1988). "An evolutionarily conserved protein binding sequence upstream of a plant light-regulated gene." Proc Natl Acad Sci U S A **85**(19): 7089-7093.

Glab N., Oury C., Guerinier T., Domenichini S., Crozet P., Thomas M., Vidal J. and Hodges M. (2017). "The impact of Arabidopsis thaliana SNF1-related-kinase 1 (SnRK1)-activating kinase 1 (SnAK1) and SnAK2 on SnRK1 phosphorylation status: characterization of a SnAK double mutant." Plant J **89**(5): 1031-1041.

Gloggnitzer J., Akimcheva S., Srinivasan A., Kusenda B., Riehs N., Stampfl H., Bautor J., Dekrout B., Jonak C., Jimenez-Gomez J. M., Parker J. E. and Riha K. (2014). "Nonsense-mediated mRNA decay modulates immune receptor levels to regulate plant antibacterial defense." Cell Host Microbe **16**(3): 376-390.

Godoy Herz M. A., Kubaczka M. G., Brzyzek G., Servi L., Krzyszton M., Simpson C., Brown J., Swiezewski S., Petrillo E. and Kornblihtt A. R. (2019). "Light Regulates Plant Alternative Splicing through the Control of Transcriptional Elongation." Mol Cell **73**(5): 1066-1074 e1063.

Göhring J., Jacak J. and Barta A. (2014). "Imaging of Endogenous Messenger RNA Splice Variants in Living Cells Reveals Nuclear Retention of Transcripts Inaccessible to Nonsense-Mediated Decay in <em>Arabidopsis</em&gt." The Plant Cell **26**(2): 754.

Golovkin M. and Reddy A. S. (1999). "An SC35-like protein and a novel serine/arginine-rich protein interact with Arabidopsis U1-70K protein." J Biol Chem **274**(51): 36428-36438.

Gomez L. D., Gilday A., Feil R., Lunn J. E. and Graham I. A. (2010). "AtTPS1-mediated trehalose 6-phosphate synthesis is essential for embryogenic and vegetative growth and responsiveness to ABA in germinating seeds and stomatal guard cells." Plant J **64**(1): 1-13.

Graveley B. R. (2005). "Mutually Exclusive Splicing of the Insect Dscam Pre-mRNA Directed by Competing Intronic RNA Secondary Structures." Cell **123**(1): 65-73.

Graveley B. R. and Maniatis T. (1998). "Arginine/serine-rich domains of SR proteins can function as activators of pre-mRNA splicing." Mol Cell **1**(5): 765-771.

Gui J.-F., Lane W. S. and Fu X.-D. (1994). "A serine kinase regulates intracellular localization of splicing factors in the cell cycle." Nature **369**(6482): 678-682.

Gupta S., Wang B. B., Stryker G. A., Zanetti M. E. and Lal S. K. (2005). "Two novel arginine/serine (SR) proteins in maize are differentially spliced and utilize non-canonical splice sites." Biochim Biophys Acta **1728**(3): 105-114.

Hachet O. and Ephrussi A. (2004). "Splicing of oskar RNA in the nucleus is coupled to its cytoplasmic localization." Nature **428**(6986): 959-963.

Hacisuleyman E., Goff L. A., Trapnell C., Williams A., Henao-Mejia J., Sun L., McClanahan P., Hendrickson D. G., Sauvageau M., Kelley D. R., Morse M., Engreitz J., Lander E. S., Guttman M., Lodish H. F., Flavell R., Raj A. and Rinn J. L. (2014). "Topological organization of multichromosomal regions by the long intergenic noncoding RNA Firre." Nature Structural & Molecular Biology **21**(2): 198-206.

Hanaoka H., Noda T., Shirano Y., Kato T., Hayashi H., Shibata D., Tabata S. and Ohsumi Y. (2002). "Leaf senescence and starvation-induced chlorosis are accelerated by the disruption of an Arabidopsis autophagy gene." Plant Physiol **129**(3): 1181-1193.

Hanson J., Hanssen M., Wiese A., Hendriks M. M. and Smeekens S. (2008). "The sucrose regulated transcription factor bZIP11 affects amino acid metabolism by regulating the expression of ASPARAGINE SYNTHETASE1 and PROLINE DEHYDROGENASE2." Plant J **53**(6): 935-949.

Hardtke C. S., Gohda K., Osterlund M. T., Oyama T., Okada K. and Deng X. W. (2000). "HY5 stability and activity in arabidopsis is regulated by phosphorylation in its COP1 binding domain." EMBO J **19**(18): 4997-5006.

Harmer S. L., Hogenesch J. B., Straume M., Chang H. S., Han B., Zhu T., Wang X., Kreps J. A. and Kay S. A. (2000). "Orchestrated transcription of key pathways in Arabidopsis by the circadian clock." Science **290**(5499): 2110-2113.

Hartmann L., Drewe-Boß P., Wießner T., Wagner G., Geue S., Lee H. C., Obermüller D. M., Kahles A., Behr J., Sinz F. H., Rätsch G. and Wachter A. (2016). "Alternative Splicing Substantially Diversifies the Transcriptome during Early Photomorphogenesis and Correlates with the Energy Availability in Arabidopsis." Plant Cell **28**(11): 2715-2734.

Hartmann L., Wießner T. and Wachter A. (2018). "Subcellular Compartmentation of Alternatively-Spliced Transcripts Defines SERINE/ARGININE-RICH PROTEIN 30 Expression." Plant Physiology: pp.01260.02017.

Hatton A. R., Subramaniam V. and Lopez A. J. (1998). "Generation of alternative Ultrabithorax isoforms and stepwise removal of a large intron by resplicing at exon-exon junctions." Mol Cell **2**(6): 787-796.

Hausler R. E., Heinrichs L., Schmitz J. and Flugge U. I. (2014). "How sugars might coordinate chloroplast and nuclear gene expression during acclimation to high light intensities." Mol Plant **7**(7): 1121-1137.

Heitman J., Movva N. R. and Hall M. N. (1991). "Targets for cell cycle arrest by the immunosuppressant rapamycin in yeast." Science **253**(5022): 905-909.

Hernando C. E., Garcia C. and Mateos J. L. (2017). "Casting Away the Shadows: Elucidating the Role of Light-mediated Posttranscriptional Control in Plants." Photochem Photobiol **93**(3): 656-665.

Heschel M. S., Selby J., Butler C., Whitelam G. C., Sharrock R. A. and Donohue K. (2007). "A new role for phytochromes in temperature-dependent germination." New Phytol **174**(4): 735-741.

Hinterberger M., Pettersson I. and Steitz J. A. (1983). "Isolation of small nuclear ribonucleoproteins containing U1, U2, U4, U5, and U6 RNAs." J Biol Chem **258**(4): 2604-2613.

Hoang Q. T. N., Han Y. J. and Kim J. I. (2019). "Plant Phytochromes and their Phosphorylation." International journal of molecular sciences **20**(14).

Hodges M., Jossier M., Boex-Fontvieille E. and Tcherkez G. (2013). "Protein phosphorylation and photorespiration." Plant Biol (Stuttg) **15**(4): 694-706.

Horne-Badovinac S. and Bilder D. (2008). "Dynein regulates epithelial polarity and the apical localization of stardust A mRNA." PLoS Genet **4**(1): e8.

Hossain M. A., Munemasa S., Nakamura Y., Mori I. C. and Murata Y. (2011). "K252a-sensitive protein kinases but not okadaic acid-sensitive protein phosphatases regulate methyl jasmonate-induced cytosolic Ca2+ oscillation in guard cells of Arabidopsis thaliana." Journal of Plant Physiology **168**(16): 1901-1908.

Howard J. M. and Sanford J. R. (2015). "The RNAissance family: SR proteins as multifaceted regulators of gene expression." Wiley Interdiscip Rev RNA **6**(1): 93-110.

Huang Y., Yario T. A. and Steitz J. A. (2004). "A molecular link between SR protein dephosphorylation and mRNA export." Proc Natl Acad Sci U S A **101**(26): 9666-9670.

Huber S. C. (2007). "Exploring the role of protein phosphorylation in plants: from signalling to metabolism." Biochem Soc Trans **35**(Pt 1): 28-32.

Hughes R. M., Vrana J. D., Song J. and Tucker C. L. (2012). "Light-dependent, dark-promoted interaction between Arabidopsis cryptochrome 1 and phytochrome B proteins." The Journal of biological chemistry **287**(26): 22165-22172.

Huq E., Al-Sady B., Hudson M., Kim C., Apel K. and Quail P. H. (2004). "Phytochrome-interacting factor 1 is a critical bHLH regulator of chlorophyll biosynthesis." Science **305**(5692): 1937-1941.

Hwang J. and Maquat L. E. (2011). "Nonsense-mediated mRNA decay (NMD) in animal embryogenesis: to die or not to die, that is the question." Curr Opin Genet Dev **21**(4): 422-430.

Iida K. and Go M. (2006). "Survey of conserved alternative splicing events of mRNAs encoding SR proteins in land plants." Mol Biol Evol **23**(5): 1085-1094.

Iida K., Seki M., Sakurai T., Satou M., Akiyama K., Toyoda T., Konagaya A. and Shinozaki K. (2004). "Genome-wide analysis of alternative pre-mRNA splicing in Arabidopsis thaliana based on full-length cDNA sequences." Nucleic Acids Res **32**(17): 5096-5103.

Iñiguez L. P., Ramírez M., Barbazuk W. B. and Hernández G. (2017). "Identification and analysis of alternative splicing events in Phaseolus vulgaris and Glycine max." BMC Genomics **18**(1): 650.

Ishihara S., Takabayashi A., Ido K., Endo T., Ifuku K. and Sato F. (2007). "Distinct functions for the two PsbP-like proteins PPL1 and PPL2 in the chloroplast thylakoid lumen of Arabidopsis." Plant Physiol **145**(3): 668-679.

Ishizaki K., Larson T. R., Schauer N., Fernie A. R., Graham I. A. and Leaver C. J. (2005). "The critical role of Arabidopsis electron-transfer flavoprotein:ubiquinone oxidoreductase during dark-induced starvation." The Plant Cell **17**(9): 2587-2600.

Isken O. and Maquat L. E. (2007). "Quality control of eukaryotic mRNA: safeguarding cells from abnormal mRNA function." Genes Dev **21**(15): 1833-1856.

Isshiki M., Tsumoto A. and Shimamoto K. (2006). "The serine/arginine-rich protein family in rice plays important roles in constitutive and alternative splicing of pre-mRNA." Plant Cell **18**(1): 146-158.

James A. B., Syed N. H., Bordage S., Marshall J., Nimmo G. A., Jenkins G. I., Herzyk P., Brown J. W. and Nimmo H. G. (2012). "Alternative splicing mediates responses of the Arabidopsis circadian clock to temperature changes." Plant Cell **24**(3): 961-981.

Jeong E. Y., Seo P. J., Woo J. C. and Park C. M. (2015). "AKIN10 delays flowering by inactivating IDD8 transcription factor through protein phosphorylation in Arabidopsis." BMC Plant Biol **15**: 110.

Jeong S. (2017). "SR Proteins: Binders, Regulators, and Connectors of RNA." Mol Cells **40**(1): 1-9.

Jiao Y., Lau O. S. and Deng X. W. (2007). "Light-regulated transcriptional networks in higher plants." Nat Rev Genet **8**(3): 217-230.

Jiao Y., Ma L., Strickland E. and Deng X. W. (2005). "Conservation and divergence of light-regulated genome expression patterns during seedling development in rice and Arabidopsis." Plant Cell **17**(12): 3239-3256.

Johnson M. P. (2016). "Photosynthesis." Essays in biochemistry **60**(3): 255-273.

Jung K.-H., Bartley L. E., Cao P., Canlas P. E. and Ronald P. C. (2009). "Analysis of Alternatively Spliced Rice Transcripts Using Microarray Data." Rice **2**(1): 44-55.

Kaiserli E., Paldi K., O'Donnell L., Batalov O., Pedmale U. V., Nusinow D. A., Kay S. A. and Chory J. (2015). "Integration of Light and Photoperiodic Signaling in Transcriptional Nuclear Foci." Dev Cell **35**(3): 311-321.

Kalinina N. O., Makarova S., Makhotenko A., Love A. J. and Taliansky M. (2018). "The Multiple Functions of the Nucleolus in Plant Development, Disease and Stress Responses." Front Plant Sci **9**: 132.

Kalyna M., Lopato S. and Barta A. (2003). "Ectopic expression of atRSZ33 reveals its function in splicing and causes pleiotropic changes in development." Mol Biol Cell **14**(9): 3565-3577.

Kalyna M., Lopato S., Voronin V. and Barta A. (2006). "Evolutionary conservation and regulation of particular alternative splicing events in plant SR proteins." Nucleic Acids Res **34**(16): 4395-4405.

Kalyna M., Simpson C. G., Syed N. H., Lewandowska D., Marquez Y., Kusenda B., Marshall J., Fuller J., Cardle L., McNicol J., Dinh H. Q., Barta A. and Brown J. W. (2012). "Alternative splicing and nonsense-mediated decay modulate expression of important regulatory genes in Arabidopsis." Nucleic Acids Res **40**(6): 2454-2469.

Kami C., Lorrain S., Hornitschek P. and Fankhauser C. (2010). "Light-Regulated Plant Growth and Development." Plant Development **91**: 29-66.

Kang S. G., Price J., Lin P. C., Hong J. C. and Jang J. C. (2010). "The arabidopsis bZIP1 transcription factor is involved in sugar signaling, protein networking, and DNA binding." Mol Plant **3**(2): 361-373.

Kanopka A., Muhlemann O. and Akusjarvi G. (1996). "Inhibition by SR proteins of splicing of a regulated adenovirus pre-mRNA." Nature **381**(6582): 535-538.

Karam R., Lou C. H., Kroeger H., Huang L., Lin J. H. and Wilkinson M. F. (2015). "The unfolded protein response is shaped by the NMD pathway." EMBO Rep **16**(5): 599-609.

Karousis E. D., Nasif S. and Muhlemann O. (2016). "Nonsense-mediated mRNA decay: novel mechanistic insights and biological impact." Wiley Interdiscip Rev RNA **7**(5): 661-682.

Kastenmayer J. P. and Green P. J. (2000). "Novel features of the XRN-family in Arabidopsis: evidence that AtXRN4, one of several orthologs of nuclear Xrn2p/Rat1p, functions in the cytoplasm." Proc Natl Acad Sci U S A **97**(25): 13985-13990.

Kelemen O., Convertini P., Zhang Z., Wen Y., Shen M., Falaleeva M. and Stamm S. (2013). "Function of alternative splicing." Gene **514**(1): 1-30.

Kendrick R. E. and Frankland B. (1969). "Photocontrol of germination in Amaranthus caudatus." Planta **85**(4): 326-339.

Kendrick R. E. and Heeringa G. H. (1986). "Photosensitivity of Rumex-Obtusifolius Seeds for Stimulation of Germination - Influence of Light and Temperature." Physiologia Plantarum **67**(2): 275-278.

Kertész S., Kerényi Z., Mérai Z., Bartos I., Pálfy T., Barta E. and Silhavy D. (2006). "Both introns and long 3'-UTRs operate as cis-acting elements to trigger nonsense-mediated decay in plants." Nucleic Acids Res **34**(21): 6147-6157.

Khodor Y. L., Rodriguez J., Abruzzi K. C., Tang C. H. A., Marr M. T. and Rosbash M. (2011). "Nascent-seq indicates widespread cotranscriptional pre-mRNA splicing in Drosophila." Genes & Development **25**(23): 2502-2512.

Kim G. D., Cho Y. H. and Yoo S. D. (2017a). "Phytohormone ethylene-responsive Arabidopsis organ growth under light is in the fine regulation of Photosystem II deficiency-inducible AKIN10 expression." Sci Rep **7**(1): 2767.

Kim G. D., Cho Y. H. and Yoo S. D. (2017b). "Regulatory Functions of Cellular Energy Sensor SNF1-Related Kinase1 for Leaf Senescence Delay through ETHYLENE-INSENSITIVE3 Repression." Sci Rep **7**(1): 3193.

Kim J. Y., Song J. T. and Seo H. S. (2017c). "COP1 regulates plant growth and development in response to light at the post-translational level." J Exp Bot **68**(17): 4737-4748.

Kim S. H., Koroleva O. A., Lewandowska D., Pendle A. F., Clark G. P., Simpson C. G., Shaw P. J. and Brown J. W. (2009). "Aberrant mRNA transcripts and the nonsense-mediated decay proteins UPF2 and UPF3 are enriched in the Arabidopsis nucleolus." Plant Cell **21**(7): 2045-2057.

Kircher S., Kozma-Bognar L., Kim L., Adam E., Harter K., Schafer E. and Nagy F. (1999). "Light quality-dependent nuclear import of the plant photoreceptors phytochrome A and B." Plant Cell **11**(8): 1445-1456.

Kleiner O., Kircher S., Harter K. and Batschauer A. (1999). "Nuclear localization of the Arabidopsis blue light receptor cryptochrome 2." Plant J **19**(3): 289-296.

Kliebenstein D. J., Lim J. E., Landry L. G. and Last R. L. (2002). "Arabidopsis UVR8 regulates ultraviolet-B signal transduction and tolerance and contains sequence similarity to human regulator of chromatin condensation 1." Plant Physiol **130**(1): 234-243.

Kolbe A., Tiessen A., Schluepmann H., Paul M., Ulrich S. and Geigenberger P. (2005). "Trehalose 6-phosphate regulates starch synthesis via posttranslational redox activation of ADP-glucose pyrophosphorylase." Proc Natl Acad Sci U S A **102**(31): 11118-11123.

Koutroumani M., Papadopoulos G. E., Vlassi M., Nikolakaki E. and Giannakouros T. (2017). "Evidence for disulfide bonds in SR Protein Kinase 1 (SRPK1) that are required for activity and nuclear localization." PLoS One **12**(2): e0171328.

Krainer A. R., Conway G. C. and Kozak D. (1990). "Purification and characterization of pre-mRNA splicing factor SF2 from HeLa cells." Genes Dev **4**(7): 1158-1171.

Krapp A., Hofmann B., Schäfer C. and Stitt M. (1993). "Regulation of the expression of rbcS and other photosynthetic genes by carbohydrates: a mechanism for the 'sink regulation' of photosynthesis?" The Plant Journal **3**(6): 817-828.

Kriechbaumer V., Wang P., Hawes C. and Abell B. M. (2012). "Alternative splicing of the auxin biosynthesis gene YUCCA4 determines its subcellular compartmentation." Plant J **70**(2): 292-302.

Kuno N., Moller S. G., Shinomura T., Xu X., Chua N. H. and Furuya M. (2003). "The novel MYB protein EARLY-PHYTOCHROME-RESPONSIVE1 is a component of a slave circadian oscillator in Arabidopsis." Plant Cell **15**(10): 2476-2488.

Laloum T., Martín G. and Duque P. (2018). "Alternative Splicing Control of Abiotic Stress Responses." Trends Plant Sci **23**(2): 140-150.

Lareau L. F., Brooks A. N., Soergel D. A., Meng Q. and Brenner S. E. (2007a). "The coupling of alternative splicing and nonsense-mediated mRNA decay." Adv Exp Med Biol **623**: 190-211.

Lareau L. F., Inada M., Green R. E., Wengrod J. C. and Brenner S. E. (2007b). "Unproductive splicing of SR genes associated with highly conserved and ultraconserved DNA elements." Nature **446**(7138): 926-929.

Laurie S., McKibbin R. S. and Halford N. G. (2003). "Antisense SNF1-related (SnRK1) protein kinase gene represses transient activity of an alpha-amylase (alpha-Amy2) gene promoter in cultured wheat embryos." J Exp Bot **54**(383): 739-747.

Le Hir H., Gatfield D., Braun I. C., Forler D. and Izaurralde E. (2001). "The protein Mago provides a link between splicing and mRNA localization." EMBO Rep **2**(12): 1119-1124.

Le Sommer C., Lesimple M., Mereau A., Menoret S., Allo M. R. and Hardy S. (2005). "PTB regulates the processing of a 3'-terminal exon by repressing both splicing and polyadenylation." Mol Cell Biol **25**(21): 9595-9607.

Lee E. S., Akef A., Mahadevan K. and Palazzo A. F. (2015). "The consensus 5' splice site motif inhibits mRNA nuclear export." PLoS One **10**(3): e0122743.

Lee J.-S. and Daie J. (1997). "End-Product Repression of Genes Involving Carbon Metabolism in Photosynthetically Active Leaves of Sugarbeet." Plant and Cell Physiology **38**(8): 887-894.

Lee J. H., Terzaghi W., Gusmaroli G., Charron J. B., Yoon H. J., Chen H., He Y. J., Xiong Y. and Deng X. W. (2008). "Characterization of Arabidopsis and rice DWD proteins and their roles as substrate receptors for CUL4-RING E3 ubiquitin ligases." Plant Cell **20**(1): 152-167.

Lee Y. and Rio D. C. (2015). "Mechanisms and Regulation of Alternative Pre-mRNA Splicing." Annu Rev Biochem **84**: 291-323.

Leivar P., Monte E., Oka Y., Liu T., Carle C., Castillon A., Huq E. and Quail P. H. (2008). "Multiple phytochrome-interacting bHLH transcription factors repress premature seedling photomorphogenesis in darkness." Curr Biol **18**(23): 1815-1823.

Leivar P. and Quail P. H. (2011). "PIFs: pivotal components in a cellular signaling hub." Trends Plant Sci **16**(1): 19-28.

Leivar P., Tepperman J. M., Monte E., Calderon R. H., Liu T. L. and Quail P. H. (2009). "Definition of early transcriptional circuitry involved in light-induced reversal of PIF-imposed repression of photomorphogenesis in young Arabidopsis seedlings." Plant Cell **21**(11): 3535-3553.

Lerner M. R., Boyle J. A., Mount S. M., Wolin S. L. and Steitz J. A. (1980). "Are snRNPs involved in splicing?" Nature **283**(5743): 220-224.

Lerner M. R. and Steitz J. A. (1979). "Antibodies to small nuclear RNAs complexed with proteins are produced by patients with systemic lupus erythematosus." Proc Natl Acad Sci U S A **76**(11): 5495-5499.

Lévesque K., Halvorsen M., Abrahamyan L., Chatel-Chaix L., Poupon V., Gordon H., DesGroseillers L., Gatignol A. and Mouland A. J. (2006). "Trafficking of HIV-1 RNA is Mediated by Heterogeneous Nuclear Ribonucleoprotein A2 Expression and Impacts on Viral Assembly." Traffic **7**(9): 1177-1193.

Lewis B. P., Green R. E. and Brenner S. E. (2003). "Evidence for the widespread coupling of alternative splicing and nonsense-mediated mRNA decay in humans." Proceedings of the National Academy of Sciences of the United States of America **100**(1): 189-192.

Li B., Jiang S., Yu X., Cheng C., Chen S., Cheng Y., Yuan J. S., Jiang D., He P. and Shan L. (2015a). "Phosphorylation of Trihelix Transcriptional Repressor ASR3 by MAP KINASE4 Negatively Regulates Arabidopsis Immunity." The Plant Cell **27**(3): 839.

Li D. D., Guan H., Li F., Liu C. Z., Dong Y. X., Zhang X. S. and Gao X. Q. (2017). "Arabidopsis shaker pollen inward K(+) channel SPIK functions in SnRK1 complex-regulated pollen hydration on the stigma." J Integr Plant Biol **59**(9): 604-611.

Li L. and Sheen J. (2016). "Dynamic and diverse sugar signaling." Curr Opin Plant Biol **33**: 116-125.

Li L., Song Y., Wang K., Dong P., Zhang X., Li F., Li Z. and Ren M. (2015b). "TOR-inhibitor insensitive-1 (TRIN1) regulates cotyledons greening in Arabidopsis." Front Plant Sci **6**: 861.

Li T., Shi Y., Wang P., Guachalla L. M., Sun B., Joerss T., Chen Y. S., Groth M., Krueger A., Platzer M., Yang Y. G., Rudolph K. L. and Wang Z. Q. (2015c). "Smg6/Est1 licenses

embryonic stem cell differentiation via nonsense-mediated mRNA decay." EMBO J **34**(12): 1630-1647.

Li Y., Varala K. and Hudson M. E. (2014). "A survey of the small RNA population during far-red light-induced apical hook opening." Front Plant Sci **5**: 156.

Li Z. H., Peng J. Y., Wen X. and Guo H. W. (2013). "ETHYLENE-INSENSITIVE3 Is a Senescence-Associated Gene That Accelerates Age-Dependent Leaf Senescence by Directly Repressing miR164 Transcription in Arabidopsis." Plant Cell **25**(9): 3311-3328.

Lin C., Robertson D. E., Ahmad M., Raibekas A. A., Jorns M. S., Dutton P. L. and Cashmore A. R. (1995). "Association of flavin adenine dinucleotide with the Arabidopsis blue light receptor CRY1." Science **269**(5226): 968.

Lin C. and Shalitin D. (2003). "Cryptochrome structure and signal transduction." Annu Rev Plant Biol **54**: 469-496.

Lin Y. Y., Kiihl S., Suhail Y., Liu S. Y., Chou Y. H., Kuang Z., Lu J. Y., Khor C. N., Lin C. L., Bader J. S., Irizarry R. and Boeke J. D. (2012). "Functional dissection of lysine deacetylases reveals that HDAC1 and p300 regulate AMPK." Nature **482**(7384): 251-255.

Lin Y. Y., Lu J. Y., Zhang J., Walter W., Dang W., Wan J., Tao S. C., Qian J., Zhao Y., Boeke J. D., Berger S. L. and Zhu H. (2009). "Protein acetylation microarray reveals that NuA4 controls key metabolic target regulating gluconeogenesis." Cell **136**(6): 1073-1084.

Liu Z., Zhang Y., Wang J., Li P., Zhao C., Chen Y. and Bi Y. (2015). "Phytochrome-interacting factors PIF4 and PIF5 negatively regulate anthocyanin biosynthesis under red light in Arabidopsis seedlings." Plant Sci **238**: 64-72.

Long J. C. and Caceres J. F. (2009). "The SR protein family of splicing factors: master regulators of gene expression." Biochem J **417**(1): 15-27.

Lopato S., Forstner C., Kalyna M., Hilscher J., Langhammer U., Indrapichate K., Lorkovic Z. J. and Barta A. (2002). "Network of interactions of a novel plant-specific Arg/Ser-rich protein, atRSZ33, with atSC35-like splicing factors." J Biol Chem **277**(42): 39989-39998.

Lopato S., Gattoni R., Fabini G., Stevenin J. and Barta A. (1999a). "A novel family of plant splicing factors with a Zn knuckle motif: examination of RNA binding and splicing activities." Plant Mol Biol **39**(4): 761-773.

Lopato S., Kalyna M., Dorner S., Kobayashi R., Krainer A. R. and Barta A. (1999b). "atSRp30, one of two SF2/ASF-like proteins from Arabidopsis thaliana, regulates splicing of specific plant genes." Genes Dev **13**(8): 987-1001.

Lopato S., Mayeda A., Krainer A. R. and Barta A. (1996a). "Pre-mRNA splicing in plants: characterization of Ser/Arg splicing factors." Proc Natl Acad Sci U S A **93**(7): 3074-3079.

Lopato S., Waigmann E. and Barta A. (1996b). "Characterization of a novel arginine/serine-rich splicing factor in Arabidopsis." Plant Cell **8**(12): 2255-2264.

Lorenzo O., Piqueras R., Sánchez-Serrano J. J. and Solano R. (2003). "ETHYLENE RESPONSE FACTOR1 integrates signals from ethylene and jasmonate pathways in plant defense." Plant Cell **15**(1): 165-178.

Lorković Z. J., Hilscher J. and Barta A. (2008). "Co-localisation studies of Arabidopsis SR splicing factors reveal different types of speckles in plant cell nuclei." Experimental Cell Research **314**(17): 3175-3186.

Lorkovic Z. J., Lopato S., Pexa M., Lehner R. and Barta A. (2004). "Interactions of Arabidopsis RS domain containing cyclophilins with SR proteins and U1 and U11 small nuclear ribonucleoprotein-specific proteins suggest their involvement in pre-mRNA Splicing." J Biol Chem **279**(32): 33890-33898.

Lorrain S., Allen T., Duek P. D., Whitelam G. C. and Fankhauser C. (2008). "Phytochrome-mediated inhibition of shade avoidance involves degradation of growth-promoting bHLH transcription factors." Plant J **53**(2): 312-323.

Lu C. A., Lin C. C., Lee K. W., Chen J. L., Huang L. F., Ho S. L., Liu H. J., Hsing Y. I. and Yu S. M. (2007). "The SnRK1A protein kinase plays a key role in sugar signaling during germination and seedling growth of rice." Plant Cell **19**(8): 2484-2499.

Lu X. D., Zhou C. M., Xu P. B., Luo Q., Lian H. L. and Yang H. Q. (2015). "Red-light-dependent interaction of phyB with SPA1 promotes COP1-SPA1 dissociation and photomorphogenic development in Arabidopsis." Mol Plant **8**(3): 467-478.

Lunn J. E., Feil R., Hendriks J. H., Gibon Y., Morcuende R., Osuna D., Scheible W. R., Carillo P., Hajirezaei M. R. and Stitt M. (2006). "Sugar-induced increases in trehalose 6-phosphate are correlated with redox activation of ADPglucose pyrophosphorylase and higher rates of starch synthesis in Arabidopsis thaliana." Biochem J **397**(1): 139-148.

Luo Q., Lian H. L., He S. B., Li L., Jia K. P. and Yang H. Q. (2014). "COP1 and phyB Physically Interact with PIL1 to Regulate Its Stability and Photomorphogenic Development in Arabidopsis." Plant Cell **26**(6): 2441-2456.

Lykke-Andersen S. and Jensen T. H. (2015). "Nonsense-mediated mRNA decay: an intricate machinery that shapes transcriptomes." Nat Rev Mol Cell Biol **16**(11): 665-677.

Ma D., Li X., Guo Y., Chu J., Fang S., Yan C., Noel J. P. and Liu H. (2016). "Cryptochrome 1 interacts with PIF4 to regulate high temperature-mediated hypocotyl elongation in response to blue light." Proc Natl Acad Sci U S A **113**(1): 224-229.

Ma J., Hanssen M., Lundgren K., Hernandez L., Delatte T., Ehlert A., Liu C. M., Schluepmann H., Droge-Laser W., Moritz T., Smeekens S. and Hanson J. (2011). "The sucrose-regulated Arabidopsis transcription factor bZIP11 reprograms metabolism and regulates trehalose metabolism." New Phytol **191**(3): 733-745.

Ma L., Li J., Qu L., Hager J., Chen Z., Zhao H. and Deng X. W. (2001). "Light control of Arabidopsis development entails coordinated regulation of genome expression and cellular pathways." Plant Cell **13**(12): 2589-2607.

Ma Z., Hu X., Cai W., Huang W., Zhou X., Luo Q., Yang H., Wang J. and Huang J. (2014). "Arabidopsis miR171-targeted scarecrow-like proteins bind to GT cis-elements and mediate gibberellin-regulated chlorophyll biosynthesis under light conditions." PLoS Genet **10**(8): e1004519.

Mair A., Pedrotti L., Wurzinger B., Anrather D., Simeunovic A., Weiste C., Valerio C., Dietrich K., Kirchler T., Nagele T., Vicente Carbajosa J., Hanson J., Baena-Gonzalez E., Chaban C., Weckwerth W., Droge-Laser W. and Teige M. (2015). "SnRK1-triggered switch of bZIP63 dimerization mediates the low-energy response in plants." Elife **4**.

Mancinelli A. L., Yaniv Z. and Smith P. (1967). "Phytochrome and Seed Germination. I. Temperature Dependence and Relative P(FR) Levels in the Germination of Dark-germinating Tomato Seeds." Plant Physiol **42**(3): 333-337.

Mancini E., Sanchez S. E., Romanowski A., Schlaen R. G., Sanchez-Lamas M., Cerdan P. D. and Yanovsky M. J. (2016). "Acute Effects of Light on Alternative Splicing in Light-Grown Plants." Photochem Photobiol **92**(1): 126-133.

Manley J. L. and Krainer A. R. (2010). "A rational nomenclature for serine/arginine-rich protein splicing factors (SR proteins)." Genes Dev **24**(11): 1073-1074.

Manning G., Whyte D. B., Martinez R., Hunter T. and Sudarsanam S. (2002). "The protein kinase complement of the human genome." Science **298**(5600): 1912-1934.

Mano S., Hayashi M. and Nishimura M. (1999). "Light regulates alternative splicing of hydroxypyruvate reductase in pumpkin." The Plant Journal **17**(3): 309-320.

Mano S., Hayashi M. and Nishimura M. (2000). "A leaf-peroxisomal protein, hydroxypyruvate reductase, is produced by light-regulated alternative splicing." Cell Biochemistry and Biophysics **32**(1): 147-154.

Mano S., Yamaguchi K., Hayashi M. and Nishimura M. (1997). "Stromal and thylakoid-bound ascorbate peroxidases are produced by alternative splicing in pumpkin 1The nucleotide sequence data reported in this paper will appear in the DDBJ, EMBL and GenBank nucleotide sequence databases with the accession number D88420.1." FEBS Letters **413**(1): 21-26.

Markelz N. H., Costich D. E. and Brutnell T. P. (2003). "Photomorphogenic responses in maize seedling development." Plant Physiol **133**(4): 1578-1591.

Marquez Y., Brown J. W., Simpson C., Barta A. and Kalyna M. (2012). "Transcriptome survey reveals increased complexity of the alternative splicing landscape in Arabidopsis." Genome Res **22**(6): 1184-1195.

Marquez Y., Hopfler M., Ayatollahi Z., Barta A. and Kalyna M. (2015). "Unmasking alternative splicing inside protein-coding exons defines exitrons and their role in proteome plasticity." Genome Res **25**(7): 995-1007.

Martinez-Garcia J. F., Huq E. and Quail P. H. (2000). "Direct targeting of light signals to a promoter element-bound transcription factor." Science **288**(5467): 859-863.

Más P., Devlin P. F., Panda S. and Kay S. A. (2000). "Functional interaction of phytochrome B and cryptochrome 2." Nature **408**(6809): 207-211.

Mathews S. and Sharrock R. A. (1997). "Phytochrome gene diversity." Plant, Cell & Environment **20**(6): 666-671.

Matsumoto E., Akiyama K., Saito T., Matsumoto Y., Kobayashi K.-I., Inoue J., Yamamoto Y. and Suzuki T. (2020). "AMP-activated protein kinase regulates alternative pre-mRNA splicing by phosphorylation of SRSF1." Biochemical Journal **477**(12): 2237-2248.

McCormac A. C. and Terry M. J. (2002). "Light-signalling pathways leading to the co-ordinated expression of HEMA1 and Lhcb during chloroplast development in Arabidopsis thaliana." Plant J **32**(4): 549-559.

McCree K. J. (1971). "The action spectrum, absorptance and quantum yield of photosynthesis in crop plants." Agricultural Meteorology **9**: 191-216.

McIlwain D. R., Pan Q., Reilly P. T., Elia A. J., McCracken S., Wakeham A. C., Itie-Youten A., Blencowe B. J. and Mak T. W. (2010). "Smg1 is required for embryogenesis and regulates diverse genes via alternative splicing coupled to nonsense-mediated mRNA decay." Proc Natl Acad Sci U S A **107**(27): 12186-12191.

Medzihradszky M., Bindics J., Ádám É., Viczián A., Klement É., Lorrain S., Gyula P., Mérai Z., Fankhauser C., Medzihradszky K. F., Kunkel T., Schäfer E. and Nagy F. (2013). "Phosphorylation of phytochrome B inhibits light-induced signaling via accelerated dark reversion in Arabidopsis." Plant Cell **25**(2): 535-544.

Mei W., Boatwright L., Feng G., Schnable J. C. and Barbazuk W. B. (2017). "Evolutionarily Conserved Alternative Splicing Across Monocots." Genetics **207**(2): 465-480.

Menand B., Desnos T., Nussaume L., Berger F., Bouchez D., Meyer C. and Robaglia C. (2002). "Expression and disruption of the Arabidopsis TOR (target of rapamycin) gene." Proc Natl Acad Sci U S A **99**(9): 6422-6427.

Mergner J., Frejno M., List M., Papacek M., Chen X., Chaudhary A., Samaras P., Richter S., Shikata H., Messerer M., Lang D., Altmann S., Cyprys P., Zolg D. P., Mathieson T., Bantscheff M., Hazarika R. R., Schmidt T., Dawid C., Dunkel A., Hofmann T., Sprunck S., Falter-Braun P., Johannes F., Mayer K. F. X., Jürgens G., Wilhelm M., Baumbach J., Grill E., Schneitz K., Schwechheimer C. and Kuster B. (2020). "Mass-spectrometry-based draft of the Arabidopsis proteome." Nature **579**(7799): 409-414.

Merkin J., Russell C., Chen P. and Burge C. B. (2012). "Evolutionary dynamics of gene and isoform regulation in Mammalian tissues." Science **338**(6114): 1593-1599.

Millar A. H., Heazlewood J. L., Giglione C., Holdsworth M. J., Bachmair A. and Schulze W. X. (2019). "The Scope, Functions, and Dynamics of Posttranslational Protein Modifications." Annu Rev Plant Biol **70**: 119-151.

Mithoe S. C. and Menke F. L. (2011). "Phosphoproteomics perspective on plant signal transduction and tyrosine phosphorylation." Phytochemistry **72**(10): 997-1006.

Montane M. H. and Menand B. (2013). "ATP-competitive mTOR kinase inhibitors delay plant growth by triggering early differentiation of meristematic cells but no developmental patterning change." J Exp Bot **64**(14): 4361-4374.

Monte E., Tepperman J. M., Al-Sady B., Kaczorowski K. A., Alonso J. M., Ecker J. R., Li X., Zhang Y. and Quail P. H. (2004). "The phytochrome-interacting transcription factor, PIF3, acts early, selectively, and positively in light-induced chloroplast development." Proc Natl Acad Sci U S A **101**(46): 16091-16098.

Mori T., Yoshimura K., Nosaka R., Sakuyama H., Koike Y., Tanabe N., Maruta T., Tamoi M. and Shigeoka S. (2012). "Subcellular and subnuclear distribution of high-light responsive serine/arginine-rich proteins, atSR45a and atSR30, in Arabidopsis thaliana." Biosci Biotechnol Biochem **76**(11): 2075-2081.

Nagarajan V. K., Jones C. I., Newbury S. F. and Green P. J. (2013). "XRN 5'-->3' exoribonucleases: structure, mechanisms and functions." Biochim Biophys Acta **1829**(6-7): 590-603.

Nagarajan V. K., Kukulich P. M., von Hagel B. and Green P. J. (2019). "RNA degradomes reveal substrates and importance for dark and nitrogen stress responses of Arabidopsis XRN4." Nucleic Acids Res **47**(17): 9216-9230.

Nakagami H., Sugiyama N., Mochida K., Daudi A., Yoshida Y., Toyoda T., Tomita M., Ishihama Y. and Shirasu K. (2010). "Large-scale comparative phosphoproteomics identifies conserved phosphorylation sites in plants." Plant Physiol **153**(3): 1161-1174.

Nguyen N. H., Jeong C. Y., Kang G. H., Yoo S. D., Hong S. W. and Lee H. (2015). "MYBD employed by HY5 increases anthocyanin accumulation via repression of MYBL2 in Arabidopsis." Plant J **84**(6): 1192-1205.

Nguyen N. H. and Lee H. (2016). "MYB-related transcription factors function as regulators of the circadian clock and anthocyanin biosynthesis in Arabidopsis." Plant Signal Behav **11**(3): e1139278.

Ni J. Z., Grate L., Donohue J. P., Preston C., Nobida N., O'Brien G., Shiue L., Clark T. A., Blume J. E. and Ares M., Jr. (2007). "Ultraconserved elements are associated with homeostatic control of splicing regulators by alternative splicing and nonsense-mediated decay." Genes Dev **21**(6): 708-718.

Ni W., Xu S. L., Gonzalez-Grandio E., Chalkley R. J., Huhmer A. F. R., Burlingame A. L., Wang Z. Y. and Quail P. H. (2017). "PPKs mediate direct signal transfer from phytochrome photoreceptors to transcription factor PIF3." Nat Commun **8**: 15236.

Nicholson P., Yepiskoposyan H., Metze S., Zamudio Orozco R., Kleinschmidt N. and Muhlemann O. (2010). "Nonsense-mediated mRNA decay in human cells: mechanistic insights, functions beyond quality control and the double-life of NMD factors." Cell Mol Life Sci **67**(5): 677-700.

Nikas I. P., Themistocleous S. C., Paschou S. A., Tsamis K. I. and Ryu H. S. (2019). "Serine-Arginine Protein Kinase 1 (SRPK1) as a Prognostic Factor and Potential Therapeutic Target in Cancer: Current Evidence and Future Perspectives." Cells **9**(1): 19.

Nilsen T. W. and Graveley B. R. (2010). "Expansion of the eukaryotic proteome by alternative splicing." Nature **463**(7280): 457-463.

Nito K., Wong Catherine C. L., Yates John R. and Chory J. (2013). "Tyrosine Phosphorylation Regulates the Activity of Phytochrome Photoreceptors." Cell Reports **3**(6): 1970-1979.

Nott A., Jung H.-S., Koussevitzky S. and Chory J. (2006). "PLASTID-TO-NUCLEUS RETROGRADE SIGNALING." Annual Review of Plant Biology **57**(1): 739-759.

Nukarinen E., Nagele T., Pedrotti L., Wurzinger B., Mair A., Landgraf R., Bornke F., Hanson J., Teige M., Baena-Gonzalez E., Droge-Laser W. and Weckwerth W. (2016). "Quantitative phosphoproteomics reveals the role of the AMPK plant ortholog SnRK1 as a metabolic master regulator under energy deprivation." Sci Rep **6**: 31697.

Oh E., Kim J., Park E., Kim J. I., Kang C. and Choi G. (2004). "PIL5, a phytochrome-interacting basic helix-loop-helix protein, is a key negative regulator of seed germination in Arabidopsis thaliana." Plant Cell **16**(11): 3045-3058.

Oh E., Yamaguchi S., Kamiya Y., Bae G., Chung W.-I. and Choi G. (2006). "Light activates the degradation of PIL5 protein to promote seed germination through gibberellin in Arabidopsis." The Plant Journal **47**(1): 124-139.

Osterlund M. T., Hardtke C. S., Wei N. and Deng X. W. (2000a). "Targeted destabilization of HY5 during light-regulated development of Arabidopsis." Nature **405**(6785): 462-466.

Osterlund M. T., Wei N. and Deng X. W. (2000b). "The roles of photoreceptor systems and the COP1-targeted destabilization of HY5 in light control of Arabidopsis seedling development." Plant Physiol **124**(4): 1520-1524.

Oszvald M., Primavesi L. F., Griffiths C. A., Cohn J., Basu S. S., Nuccio M. L. and Paul M. J. (2018). "Trehalose 6-Phosphate Regulates Photosynthesis and Assimilate Partitioning in Reproductive Tissue." Plant Physiology **176**(4): 2623-2638.

Padgett R. A., Konarska M. M., Grabowski P. J., Hardy S. F. and Sharp P. A. (1984). "Lariat RNA's as intermediates and products in the splicing of messenger RNA precursors." Science **225**(4665): 898-903.

Paik I., Chen F., Ngoc Pham V., Zhu L., Kim J.-I. and Huq E. (2019). "A phyB-PIF1-SPA1 kinase regulatory complex promotes photomorphogenesis in Arabidopsis." Nature Communications **10**(1): 4216.

Paik I., Yang S. and Choi G. (2012). "Phytochrome regulates translation of mRNA in the cytosol." Proc Natl Acad Sci U S A **109**(4): 1335-1340.

Pajoro A., Severing E., Angenent G. C. and Immink R. G. H. (2017). "Histone H3 lysine 36 methylation affects temperature-induced alternative splicing and flowering in plants." Genome Biology **18**(1): 102.

Palazzo A. F. and Lee E. S. (2018). "Sequence Determinants for Nuclear Retention and Cytoplasmic Export of mRNAs and lncRNAs." Frontiers in genetics **9**: 440.

Palusa S. G., Ali G. S. and Reddy A. S. (2007). "Alternative splicing of pre-mRNAs of Arabidopsis serine/arginine-rich proteins: regulation by hormones and stresses." Plant J **49**(6): 1091-1107.

Palusa S. G. and Reddy A. S. (2010). "Extensive coupling of alternative splicing of pre-mRNAs of serine/arginine (SR) genes with nonsense-mediated decay." New Phytol **185**(1): 83-89.

Palusa S. G. and Reddy A. S. (2015). "Differential recruitment of splice variants from SR pre-mRNAs to polysomes during development and in response to stresses." Plant Cell Physiol **56**(3): 421-427.

Pan Q., Shai O., Lee L. J., Frey B. J. and Blencowe B. J. (2008). "Deep surveying of alternative splicing complexity in the human transcriptome by high-throughput sequencing." Nat Genet **40**(12): 1413-1415.

Park J. W. and Graveley B. R. (2007). "Complex alternative splicing." Advances in experimental medicine and biology **623**: 50-63.

Paul M. J. and Foyer C. H. (2001). "Sink regulation of photosynthesis." Journal of Experimental Botany **52**(360): 1383-1400.

Peccarelli M. and Kebaara B. W. (2014). "Regulation of natural mRNAs by the nonsense-mediated mRNA decay pathway." Eukaryot Cell **13**(9): 1126-1135.

Pedmale Ullas V., Huang S.-shan C., Zander M., Cole Benjamin J., Hetzel J., Ljung K., Reis Pedro A. B., Sridevi P., Nito K., Nery Joseph R., Ecker Joseph R. and Chory J. (2016). "Cryptochromes Interact Directly with PIFs to Control Plant Growth in Limiting Blue Light." Cell **164**(1): 233-245.

Pedrotti L., Weiste C., Nägele T., Wolf E., Lorenzin F., Dietrich K., Mair A., Weckwerth W., Teige M., Baena-González E. and Dröge-Laser W. (2018). "Snf1-RELATED KINASE1-Controlled C/S(1)-bZIP Signaling Activates Alternative Mitochondrial Metabolic Pathways to Ensure Plant Survival in Extended Darkness." The Plant Cell **30**(2): 495-509.

Pego J. V., Kortstee A. J., Huijser C. and Smeekens S. C. (2000). "Photosynthesis, sugars and the regulation of gene expression." J Exp Bot **51 Spec No**: 407-416.

Peltz S. W., Brown A. H. and Jacobson A. (1993). "mRNA destabilization triggered by premature translational termination depends on at least three cis-acting sequence elements and one trans-acting factor." Genes Dev **7**(9): 1737-1754.

Pendle A. F., Clark G. P., Boon R., Lewandowska D., Lam Y. W., Andersen J., Mann M., Lamond A. I., Brown J. W. and Shaw P. J. (2005). "Proteomic analysis of the Arabidopsis nucleolus suggests novel nucleolar functions." Mol Biol Cell **16**(1): 260-269.

Perrella G. and Kaiserli E. (2016). "Light behind the curtain: photoregulation of nuclear architecture and chromatin dynamics in plants." New Phytol **212**(4): 908-919.

Petrillo E., Godoy Herz M. A., Fuchs A., Reifer D., Fuller J., Yanovsky M. J., Simpson C., Brown J. W., Barta A., Kalyna M. and Kornblihtt A. R. (2014). "A chloroplast retrograde signal regulates nuclear alternative splicing." Science **344**(6182): 427-430.

Petrillo E., Riegler S., Fuchs A., Servi L., Godoy Herz M. A., Kubaczka M. G., Venhuizen P., Schweighofer A., Kornblihtt A. R., Simpson C., Brown J. W. S., Meyer C., Kalyna M. and Barta A. (2018). "Remote control of alternative splicing in roots through TOR kinase." bioRxiv: 472126.

Pfeiffer A., Janocha D., Dong Y., Medzihradszky A., Schone S., Daum G., Suzaki T., Forner J., Langenecker T., Rempel E., Schmid M., Wirtz M., Hell R. and Lohmann J. U. (2016). "Integration of light and metabolic signals for stem cell activation at the shoot apical meristem." Elife **5**.

Pham V. N., Kathare P. K. and Huq E. (2018). "Phytochromes and Phytochrome Interacting Factors." Plant Physiol **176**(2): 1025-1038.

Radchuk R., Emery R. J., Weier D., Vigeolas H., Geigenberger P., Lunn J. E., Feil R., Weschke W. and Weber H. (2010). "Sucrose non-fermenting kinase 1 (SnRK1) coordinates metabolic and hormonal signals during pea cotyledon growth and differentiation." Plant J **61**(2): 324-338.

Radchuk R., Radchuk V., Weschke W., Borisjuk L. and Weber H. (2006). "Repressing the expression of the SUCROSE NONFERMENTING-1-RELATED PROTEIN KINASE gene in pea embryo causes pleiotropic defects of maturation similar to an abscisic acid-insensitive phenotype." Plant Physiol **140**(1): 263-278.

Ramani A. K., Calarco J. A., Pan Q., Mavandadi S., Wang Y., Nelson A. C., Lee L. J., Morris Q., Blencowe B. J., Zhen M. and Fraser A. G. (2011). "Genome-wide analysis of alternative splicing in Caenorhabditis elegans." Genome Res **21**(2): 342-348.

Ramon M., Dang T. V. T., Broeckx T., Hulsmans S., Crepin N., Sheen J. and Rolland F. A. (2019). "Default activation and nuclear translocation of the plant cellular energy sensor SnRK1 regulate metabolic stress responses and development." Plant Cell.

Rayson S., Arciga-Reyes L., Wootton L., De Torres Zabala M., Truman W., Graham N., Grant M. and Davies B. (2012). "A role for nonsense-mediated mRNA decay in plants: pathogen responses are induced in Arabidopsis thaliana NMD mutants." PLoS One **7**(2): e31917.

Reddy A. S. (2007). "Alternative splicing of pre-messenger RNAs in plants in the genomic era." Annu Rev Plant Biol **58**: 267-294.

Reddy A. S., Day I. S., Gohring J. and Barta A. (2012a). "Localization and dynamics of nuclear speckles in plants." Plant Physiol **158**(1): 67-77.

Reddy A. S., Marquez Y., Kalyna M. and Barta A. (2013). "Complexity of the alternative splicing landscape in plants." Plant Cell **25**(10): 3657-3683.

Reddy A. S., Rogers M. F., Richardson D. N., Hamilton M. and Ben-Hur A. (2012b). "Deciphering the plant splicing code: experimental and computational approaches for predicting alternative splicing and splicing regulatory elements." Front Plant Sci **3**: 18.

Reddy A. S. and Shad Ali G. (2011). "Plant serine/arginine-rich proteins: roles in precursor messenger RNA splicing, plant development, and stress responses." Wiley Interdiscip Rev RNA **2**(6): 875-889.

Reed J. W., Nagpal P., Poole D. S., Furuya M. and Chory J. (1993). "Mutations in the gene for the red/far-red light receptor phytochrome B alter cell elongation and physiological responses throughout Arabidopsis development." Plant Cell **5**(2): 147-157.

Reinbothe S., Reinbothe C., Lebedev N. and Apel K. (1996). "PORA and PORB, Two Light-Dependent Protochlorophyllide-Reducing Enzymes of Angiosperm Chlorophyll Biosynthesis." The Plant Cell **8**(5): 763-769.

Ren M., Qiu S., Venglat P., Xiang D., Feng L., Selvaraj G. and Datla R. (2011). "Target of rapamycin regulates development and ribosomal RNA expression through kinase domain in Arabidopsis." Plant Physiol **155**(3): 1367-1382.

Richardson D. N., Rogers M. F., Labadorf A., Ben-Hur A., Guo H., Paterson A. H. and Reddy A. S. (2011). "Comparative analysis of serine/arginine-rich proteins across 27 eukaryotes: insights into sub-family classification and extent of alternative splicing." PLoS One **6**(9): e24542.

Rockwell N. C., Su Y. S. and Lagarias J. C. (2006). "Phytochrome structure and signaling mechanisms." Annu Rev Plant Biol **57**: 837-858.

Rodermel S. (2001). "Pathways of plastid-to-nucleus signaling." Trends in Plant Science **6**(10): 471-478.

Rodrigues A., Adamo M., Crozet P., Margalha L., Confraria A., Martinho C., Elias A., Rabissi A., Lumbreras V., Gonzalez-Guzman M., Antoni R., Rodriguez P. L. and Baena-Gonzalez E. (2013). "ABI1 and PP2CA Phosphatases Are Negative Regulators of Snf1-Related Protein Kinase1 Signaling in Arabidopsis." Plant Cell **25**(10): 3871-3884.

Rogers J. and Wall R. (1980). "A mechanism for RNA splicing." Proc Natl Acad Sci U S A **77**(4): 1877-1879.

Rolland F., Baena-Gonzalez E. and Sheen J. (2006). "Sugar sensing and signaling in plants: conserved and novel mechanisms." Annu Rev Plant Biol **57**: 675-709.

Roth-Bejerano N., Koller D. and Negbi M. (1966). "Mediation of phytochrome in the inductive action of low temperature on dark germination of lettuce seed at supra-optimal temperature." Plant Physiol **41**(6): 962-964.

Roth M. B., Zahler A. M. and Stolk J. A. (1991). "A conserved family of nuclear phosphoproteins localized to sites of polymerase II transcription." J Cell Biol **115**(3): 587-596.

Roy D., Bhanja Chowdhury J. and Ghosh S. (2013). "Polypyrimidine tract binding protein (PTB) associates with intronic and exonic domains to squelch nuclear export of unspliced RNA." FEBS Lett **587**(23): 3802-3807.

Ruckle M. E., DeMarco S. M. and Larkin R. M. (2007). "Plastid signals remodel light signaling networks and are essential for efficient chloroplast biogenesis in Arabidopsis." Plant Cell **19**(12): 3944-3960.

Ruckle M. E. and Larkin R. M. (2009). "Plastid signals that affect photomorphogenesis in Arabidopsis thaliana are dependent on GENOMES UNCOUPLED 1 and cryptochrome 1." New Phytol **182**(2): 367-379.

Rüegg U. T. and Gillian B. (1989). "Staurosporine, K-252 and UCN-01: potent but nonspecific inhibitors of protein kinases." Trends in Pharmacological Sciences **10**(6): 218-220.

Rühl C., Stauffer E., Kahles A., Wagner G., Drechsel G., Rätsch G. and Wachter A. (2012). "Polypyrimidine Tract Binding Protein Homologs from Arabidopsis Are Key Regulators of Alternative Splicing with Implications in Fundamental Developmental Processes." The Plant Cell **24**(11): 4360.

Ruskin B., Krainer A. R., Maniatis T. and Green M. R. (1984). "Excision of an intact intron as a novel lariat structure during pre-mRNA splicing in vitro." Cell **38**(1): 317-331.

Sabatini D. M., Erdjument-Bromage H., Lui M., Tempst P. and Snyder S. H. (1994). "RAFT1: a mammalian protein that binds to FKBP12 in a rapamycin-dependent fashion and is homologous to yeast TORs." Cell **78**(1): 35-43.

Saijo Y., Zhu D., Li J., Rubio V., Zhou Z., Shen Y., Hoecker U., Wang H. and Deng X. W. (2008). "Arabidopsis COP1/SPA1 complex and FHY1/FHY3 associate with distinct phosphorylated forms of phytochrome A in balancing light signaling." Mol Cell **31**(4): 607-613.

Sakamoto K. and Nagatani A. (1996). "Nuclear localization activity of phytochrome B." Plant J **10**(5): 859-868.

Sakuraba Y., Jeong J., Kang M.-Y., Kim J., Paek N.-C. and Choi G. (2014). "Phytochrome-interacting transcription factors PIF4 and PIF5 induce leaf senescence in Arabidopsis." Nature Communications **5**(1): 4636.

Saldi T., Cortazar M. A., Sheridan R. M. and Bentley D. L. (2016). "Coupling of RNA Polymerase II Transcription Elongation with Pre-mRNA Splicing." J Mol Biol **428**(12): 2623-2635.

Sanchez-Retuerta C., Suarez-Lopez P. and Henriques R. (2018). "Under a New Light: Regulation of Light-Dependent Pathways by Non-coding RNAs." Front Plant Sci **9**: 962.

Sanford J. R., Ellis J. D., Cazalla D. and Caceres J. F. (2005). "Reversible phosphorylation differentially affects nuclear and cytoplasmic functions of splicing factor 2/alternative splicing factor." Proc Natl Acad Sci U S A **102**(42): 15042-15047.

Savaldi-Goldstein S., Aviv D., Davydov O. and Fluhr R. (2003). "Alternative splicing modulation by a LAMMER kinase impinges on developmental and transcriptome expression." Plant Cell **15**(4): 926-938.

Savaldi-Goldstein S., Sessa G. and Fluhr R. (2000). "The ethylene-inducible PK12 kinase mediates the phosphorylation of SR splicing factors." Plant J **21**(1): 91-96.

Schaffer Bethany E., Levin Rebecca S., Hertz Nicholas T., Maures Travis J., Schoof Michael L., Hollstein Pablo E., Benayoun Bérénice A., Banko Max R., Shaw Reuben J., Shokat Kevan M. and Brunet A. (2015). "Identification of AMPK Phosphorylation Sites Reveals a Network of Proteins Involved in Cell Invasion and Facilitates Large-Scale Substrate Prediction." Cell Metabolism **22**(5): 907-921.

Schaffer R., Landgraf J., Accerbi M., Simon V., Larson M. and Wisman E. (2001). "Microarray Analysis of Diurnal and Circadian-Regulated Genes in Arabidopsis." The Plant Cell **13**(1): 113-123.

Schluepmann H., Pellny T., van Dijken A., Smeekens S. and Paul M. (2003). "Trehalose 6-phosphate is indispensable for carbohydrate utilization and growth in Arabidopsis thaliana." Proc Natl Acad Sci U S A **100**(11): 6849-6854.

Schonberg A. and Baginsky S. (2012). "Signal integration by chloroplast phosphorylation networks: an update." Front Plant Sci **3**: 256.

Schoning J. C., Streitner C., Meyer I. M., Gao Y. and Staiger D. (2008). "Reciprocal regulation of glycine-rich RNA-binding proteins via an interlocked feedback loop coupling alternative splicing to nonsense-mediated decay in Arabidopsis." Nucleic Acids Res **36**(22): 6977-6987.

Schöning J. C., Streitner C., Meyer I. M., Gao Y. and Staiger D. (2008). "Reciprocal regulation of glycine-rich RNA-binding proteins via an interlocked feedback loop coupling alternative splicing to nonsense-mediated decay in Arabidopsis." Nucleic Acids Research **36**(22): 6977-6987.

Schumann T., Paul S., Melzer M., Dörmann P. and Jahns P. (2017). "Plant Growth under Natural Light Conditions Provides Highly Flexible Short-Term Acclimation Properties toward High Light Stress." Frontiers in Plant Science **8**(681).

Schweingruber C., Rufener S. C., Zund D., Yamashita A. and Muhlemann O. (2013). "Nonsense-mediated mRNA decay - mechanisms of substrate mRNA recognition and degradation in mammalian cells." Biochim Biophys Acta **1829**(6-7): 612-623.

Sehgal S. N., Baker H. and Vezina C. (1975). "Rapamycin (AY-22,989), a new antifungal antibiotic. II. Fermentation, isolation and characterization." J Antibiot (Tokyo) **28**(10): 727-732.

Seo H. S., Yang J. Y., Ishikawa M., Bolle C., Ballesteros M. L. and Chua N. H. (2003). "LAF1 ubiquitination by COP1 controls photomorphogenesis and is stimulated by SPA1." Nature **423**(6943): 995-999.

Sharrock R. A. and Quail P. H. (1989). "Novel phytochrome sequences in Arabidopsis thaliana: structure, evolution, and differential expression of a plant regulatory photoreceptor family." Genes Dev **3**(11): 1745-1757.

Shaul O. (2015). "Unique Aspects of Plant Nonsense-Mediated mRNA Decay." Trends Plant Sci **20**(11): 767-779.

Sheen J. (2014). "Master Regulators in Plant Glucose Signaling Networks." J Plant Biol **57**(2): 67-79.

Sheerin D. J. and Hiltbrunner A. (2017). "Molecular mechanisms and ecological function of far-red light signalling." Plant Cell Environ **40**(11): 2509-2529.

Sheerin D. J., Menon C., zur Oven-Krockhaus S., Enderle B., Zhu L., Johnen P., Schleifenbaum F., Stierhof Y. D., Huq E. and Hiltbrunner A. (2015). "Light-activated phytochrome A and B interact with members of the SPA family to promote photomorphogenesis in Arabidopsis by reorganizing the COP1/SPA complex." Plant Cell **27**(1): 189-201.

Shen H., Zhu L., Castillon A., Majee M., Downie B. and Huq E. (2008). "Light-induced phosphorylation and degradation of the negative regulator PHYTOCHROME-INTERACTING FACTOR1 from Arabidopsis depend upon its direct physical interactions with photoactivated phytochromes." Plant Cell **20**(6): 1586-1602.

Shen W., Dallas M. B., Goshe M. B. and Hanley-Bowdoin L. (2014). "SnRK1 phosphorylation of AL2 delays Cabbage leaf curl virus infection in Arabidopsis." J Virol **88**(18): 10598-10612.

Shen W. and Hanley-Bowdoin L. (2006). "Geminivirus infection up-regulates the expression of two Arabidopsis protein kinases related to yeast SNF1- and mammalian AMPK-activating kinases." Plant Physiol **142**(4): 1642-1655.

Shen W., Reyes M. I. and Hanley-Bowdoin L. (2009). "Arabidopsis protein kinases GRIK1 and GRIK2 specifically activate SnRK1 by phosphorylating its activation loop." Plant Physiol **150**(2): 996-1005.

Shepard P. J. and Hertel K. J. (2009). "The SR protein family." Genome Biol **10**(10): 242.

Shi H., Liu R., Xue C., Shen X., Wei N., Deng Xing W. and Zhong S. (2016). "Seedlings Transduce the Depth and Mechanical Pressure of Covering Soil Using COP1 and Ethylene to Regulate EBF1/EBF2 for Soil Emergence." Current Biology **26**(2): 139-149.

Shi L., Wu Y. and Sheen J. (2018). "TOR signaling in plants: conservation and innovation." Development **145**(13).

Shi Y. (2017). "Mechanistic insights into precursor messenger RNA splicing by the spliceosome." Nat Rev Mol Cell Biol **18**(11): 655-670.

Shikata H., Hanada K., Ushijima T., Nakashima M., Suzuki Y. and Matsushita T. (2014). "Phytochrome controls alternative splicing to mediate light responses in Arabidopsis." Proc Natl Acad Sci U S A **111**(52): 18781-18786.

Shikata H., Nakashima M., Matsuoka K. and Matsushita T. (2012a). "Deletion of the RS domain of RRC1 impairs phytochrome B signaling in Arabidopsis." Plant Signal Behav **7**(8): 933-936.

Shikata H., Shibata M., Ushijima T., Nakashima M., Kong S. G., Matsuoka K., Lin C. and Matsushita T. (2012b). "The RS domain of Arabidopsis splicing factor RRC1 is required for phytochrome B signal transduction." Plant J **70**(5): 727-738.

Shin A. Y., Han Y. J., Baek A., Ahn T., Kim S. Y., Nguyen T. S., Son M., Lee K. W., Shen Y., Song P. S. and Kim J. I. (2016). "Evidence that phytochrome functions as a protein kinase in plant light signalling." Nat Commun **7**: 11545.

Shin C., Feng Y. and Manley J. L. (2004). "Dephosphorylated SRp38 acts as a splicing repressor in response to heat shock." Nature **427**(6974): 553-558.

Sibley C. R., Emmett W., Blazquez L., Faro A., Haberman N., Briese M., Trabzuni D., Ryten M., Weale M. E., Hardy J., Modic M., Curk T., Wilson S. W., Plagnol V. and Ule J. (2015). "Recursive splicing in long vertebrate genes." Nature **521**(7552): 371-375.

Sibout R., Sukumar P., Hettiarachchi C., Holm M., Muday G. K. and Hardtke C. S. (2006). "Opposite Root Growth Phenotypes of hy5 versus hy5 hyh Mutants Correlate with Increased Constitutive Auxin Signaling." PLOS Genetics **2**(11): e202.

Siebel C. W. and Guthrie C. (1996). "The essential yeast RNA binding protein Np13p is methylated." Proc Natl Acad Sci U S A **93**(24): 13641-13646.

Silva-Sanchez C., Li H. and Chen S. (2015). "Recent advances and challenges in plant phosphoproteomics." Proteomics **15**(5-6): 1127-1141.

Simpson C. G., Fuller J., Maronova M., Kalyna M., Davidson D., McNicol J., Barta A. and Brown J. W. (2008). "Monitoring changes in alternative precursor messenger RNA splicing in multiple gene transcripts." Plant J **53**(6): 1035-1048.

Simpson C. G., Jennings S. N., Clark G. P., Thow G. and Brown J. W. S. (2004). "Dual functionality of a plant U-rich intronic sequence element." The Plant Journal **37**(1): 82-91.

Sinha R., Allemand E., Zhang Z., Karni R., Myers M. P. and Krainer A. R. (2010). "Arginine methylation controls the subcellular localization and functions of the oncoprotein splicing factor SF2/ASF." Mol Cell Biol **30**(11): 2762-2774.

Smeekens S., Ma J., Hanson J. and Rolland F. (2010). "Sugar signals and molecular networks controlling plant growth." Curr Opin Plant Biol **13**(3): 274-279.

Smith A. M., Zeeman S. C. and Smith S. M. (2005). "Starch degradation." Annu Rev Plant Biol **56**: 73-98.

Smith J. H. (1954). "The Development of Chlorophyll and Oxygen-evolving Power in Etiolated Barley Leaves When Illuminated." Plant Physiol **29**(2): 143-148.

Somers D. E., Schultz T. F., Milnamow M. and Kay S. A. (2000). "ZEITLUPE encodes a novel clock-associated PAS protein from Arabidopsis." Cell **101**(3): 319-329.

Soto-Burgos J. and Bassham D. C. (2017). "SnRK1 activates autophagy via the TOR signaling pathway in Arabidopsis thaliana." PLoS One **12**(8): e0182591.

Souret F. F., Kastenmayer J. P. and Green P. J. (2004). "AtXRN4 degrades mRNA in Arabidopsis and its substrates include selected miRNA targets." Mol Cell **15**(2): 173-183.

Srinivasan A., Jimenez-Gomez J. M., Fornara F., Soppe W. J. and Brambilla V. (2016). "Alternative splicing enhances transcriptome complexity in desiccating seeds." J Integr Plant Biol **58**(12): 947-958.

Staiger D. and Brown J. W. (2013). "Alternative splicing at the intersection of biological timing, development, and stress responses." Plant Cell **25**(10): 3640-3656.

Staiger D., Zecca L., Wieczorek Kirk D. A., Apel K. and Eckstein L. (2003). "The circadian clock regulated RNA-binding protein AtGRP7 autoregulates its expression by influencing alternative splicing of its own pre-mRNA." Plant J **33**(2): 361-371.

Staknis D. and Reed R. (1994). "SR proteins promote the first specific recognition of Pre-mRNA and are present together with the U1 small nuclear ribonucleoprotein particle in a general splicing enhancer complex." Mol Cell Biol **14**(11): 7670-7682.

Stauffer E., Westermann A., Wagner G. and Wachter A. (2010). "Polypyrimidine tract-binding protein homologues from Arabidopsis underlie regulatory circuits based on alternative splicing and downstream control." Plant J **64**(2): 243-255.

Steffen A., Elgner M. and Staiger D. (2019). "Regulation of Flowering Time by the RNA-Binding Proteins AtGRP7 and AtGRP8." Plant Cell Physiol **60**(9): 2040-2050.

Stein O. and Granot D. (2019). "An Overview of Sucrose Synthases in Plants." Front Plant Sci **10**: 95.

Stern A. I., Schiff J. A. and Epstein H. T. (1964). "Studies of Chloroplast Development in Euglena. V. Pigment Biosynthesis, Photosynthetic Oxygen Evolution and Carbon Dioxide Fixation during Chloroplast Development." Plant Physiol **39**(2): 220-226.

Stitt M. (1991). "Rising CO2 levels and their potential significance for carbon flow in photosynthetic cells." Plant, Cell & Environment **14**(8): 741-762.

Sugnet C. W., Kent W. J., Ares M., Jr. and Haussler D. (2004). "Transcriptome and genome conservation of alternative splicing events in humans and mice." Pac Symp Biocomput: 66-77.

Sun J., Ma Q. and Mao T. (2015a). "Ethylene Regulates the Arabidopsis Microtubule-Associated Protein WAVE-DAMPENED2-LIKE5 in Etiolated Hypocotyl Elongation." Plant Physiol **169**(1): 325-337.

Sun W., Xu X. H., Wu X., Wang Y., Lu X., Sun H. and Xie X. (2015b). "Genome-wide identification of microRNAs and their targets in wild type and phyB mutant provides a key link between microRNAs and the phyB-mediated light signaling pathway in rice." Front Plant Sci **6**: 372.

Sun Y. and Xiao H. (2015). "Identification of alternative splicing events by RNA sequencing in early growth tomato fruits." BMC Genomics **16**: 948.

Sureshkumar S., Dent C., Seleznev A., Tasset C. and Balasubramanian S. (2016). "Nonsense-mediated mRNA decay modulates FLM-dependent thermosensory flowering response in Arabidopsis." Nat Plants **2**(5): 16055.

Syed N. H., Kalyna M., Marquez Y., Barta A. and Brown J. W. (2012). "Alternative splicing in plants--coming of age." Trends Plant Sci **17**(10): 616-623.

Takano M., Inagaki N., Xie X., Yuzurihara N., Hihara F., Ishizuka T., Yano M., Nishimura M., Miyao A., Hirochika H. and Shinomura T. (2005). "Distinct and cooperative functions of phytochromes A, B, and C in the control of deetiolation and flowering in rice." Plant Cell **17**(12): 3311-3325.

Takemura R., Takeiwa T., Taniguchi I., McCloskey A. and Ohno M. (2011). "Multiple factors in the early splicing complex are involved in the nuclear retention of pre-mRNAs in mammalian cells." Genes to Cells **16**(10): 1035-1049.

Tanabe N., Yoshimura K., Kimura A., Yabuta Y. and Shigeoka S. (2007). "Differential expression of alternatively spliced mRNAs of Arabidopsis SR protein homologs, atSR30 and atSR45a, in response to environmental stress." Plant Cell Physiol **48**(7): 1036-1049.

Taylorson R. B. and Hendricks S. B. (1972). "Interactions of light and a temperature shift on seed germination." Plant Physiol **49**(2): 127-130.

Telonis-Scott M., Kopp A., Wayne M. L., Nuzhdin S. V. and McIntyre L. M. (2009). "Sex-Specific Splicing in Drosophila: Widespread Occurrence, Tissue Specificity and Evolutionary Conservation." Genetics **181**(2): 421-434.

Tepperman J. M., Zhu T., Chang H. S., Wang X. and Quail P. H. (2001). "Multiple transcription-factor genes are early targets of phytochrome A signaling." Proc Natl Acad Sci U S A **98**(16): 9437-9442.

Terzaghi W. B. and Cashmore A. R. (1995). "Photomorphogenesis. Seeing the light in plant development." Curr Biol **5**(5): 466-468.

Thatcher S. R., Zhou W., Leonard A., Wang B. B., Beatty M., Zastrow-Hayes G., Zhao X., Baumgarten A. and Li B. (2014). "Genome-wide analysis of alternative splicing in Zea mays: landscape and genetic regulation." Plant Cell **26**(9): 3472-3487.

Thelander M., Olsson T. and Ronne H. (2004). "Snf1-related protein kinase 1 is needed for growth in a normal day-night light cycle." EMBO J **23**(8): 1900-1910.

Tillemans V., Dispa L., Remacle C., Collinge M. and Motte P. (2005). "Functional distribution and dynamics of Arabidopsis SR splicing factors in living plant cells." Plant J **41**(4): 567-582.

Tillemans V., Leponce I., Rausin G., Dispa L. and Motte P. (2006). "Insights into nuclear organization in plants as revealed by the dynamic distribution of Arabidopsis SR splicing factors." Plant Cell **18**(11): 3218-3234.

Toledo-Ortiz G., Johansson H., Lee K. P., Bou-Torrent J., Stewart K., Steel G., Rodriguez-Concepcion M. and Halliday K. J. (2014). "The HY5-PIF regulatory module coordinates light and temperature control of photosynthetic gene transcription." PLoS Genet **10**(6): e1004416.

Toole E. H., Toole V. K., Borthwick H. A. and Hendricks S. B. (1955). "Interaction of Temperature and Light in Germination of Seeds." Plant Physiol **30**(5): 473-478.

Tress M. L., Abascal F. and Valencia A. (2017). "Alternative Splicing May Not Be the Key to Proteome Complexity." Trends Biochem Sci **42**(2): 98-110.

Tsai A. Y. and Gazzarrini S. (2012). "AKIN10 and FUSCA3 interact to control lateral organ development and phase transitions in Arabidopsis." Plant J **69**(5): 809-821.

Tsai H. L., Li Y. H., Hsieh W. P., Lin M. C., Ahn J. H. and Wu S. H. (2014). "HUA ENHANCER1 is involved in posttranscriptional regulation of positive and negative regulators in Arabidopsis photomorphogenesis." Plant Cell **26**(7): 2858-2872.

Tsugama D., Liu S. and Takano T. (2012). "A putative myristoylated 2C-type protein phosphatase, PP2C74, interacts with SnRK1 in Arabidopsis." FEBS Lett **586**(6): 693-698.

Tung K.-F., Pan C.-Y., Chen C.-H. and Lin W.-c. (2020). "Top-ranked expressed gene transcripts of human protein-coding genes investigated with GTEx dataset." Scientific Reports **10**(1): 16245.

Turkina M. V., Klang Arstrand H. and Vener A. V. (2011). "Differential phosphorylation of ribosomal proteins in Arabidopsis thaliana plants during day and night." PLoS One **6**(12): e29307.

Twyffels L., Gueydan C. and Kruys V. (2011). "Shuttling SR proteins: more than splicing factors." FEBS J **278**(18): 3246-3255.

van Dijken A. J., Schluepmann H. and Smeekens S. C. (2004). "Arabidopsis trehalose-6-phosphate synthase 1 is essential for normal vegetative growth and transition to flowering." Plant Physiol **135**(2): 969-977.

Van Oosten J.-J. and Besford R. T. (1995). "Some relationships between the gas exchange, biochemistry and molecular biology of photosynthesis during leaf development of tomato plants after transfer to different carbon dioxide concentrations." Plant, Cell & Environment **18**(11): 1253-1266.

Van Oosten J.-J., Wilkins D. and Besford R. T. (1994). "Regulation of the expression of photosynthetic nuclear genes by CO2 is mimicked by regulation by carbohydrates: a mechanism for the acclimation of photosynthesis to high CO2?" Plant, Cell & Environment **17**(8): 913-923.

van Wijk K. J., Friso G., Walther D. and Schulze W. X. (2014). "Meta-Analysis of Arabidopsis thaliana Phospho-Proteomics Data Reveals Compartmentalization of Phosphorylation Motifs." Plant Cell **26**(6): 2367-2389.

Vierstra R. D. and Quail P. H. (1983). "Photochemistry of 124 kilodalton Avena phytochrome in vitro." Plant Physiol **72**(1): 264-267.

Vision T. J., Brown D. G. and Tanksley S. D. (2000). "The origins of genomic duplications in Arabidopsis." Science **290**(5499): 2114-2117.

Wachter A. (2010). "Riboswitch-mediated control of gene expression in eukaryotes." RNA Biol **7**(1): 67-76.

Wachter A. and Hartmann L. (2014). "NMD: nonsense-mediated defense." Cell Host Microbe **16**(3): 273-275.

Wachter A., Ruhl C. and Stauffer E. (2012a). "The Role of Polypyrimidine Tract-Binding Proteins and Other hnRNP Proteins in Plant Splicing Regulation." Front Plant Sci **3**: 81.

Wachter A., Rühl C. and Stauffer E. (2012b). "The Role of Polypyrimidine Tract-Binding Proteins and Other hnRNP Proteins in Plant Splicing Regulation." Frontiers in Plant Science **3**(81).

Wahl M. C., Will C. L. and Luhrmann R. (2009). "The spliceosome: design principles of a dynamic RNP machine." Cell **136**(4): 701-718.

Wang H., Ma L. G., Li J. M., Zhao H. Y. and Deng X. W. (2001). "Direct interaction of Arabidopsis cryptochromes with COP1 in light control development." Science **294**(5540): 154-158.

Wang L., Mai Y. X., Zhang Y. C., Luo Q. and Yang H. Q. (2010). "MicroRNA171c-targeted SCL6-II, SCL6-III, and SCL6-IV genes regulate shoot branching in Arabidopsis." Mol Plant **3**(5): 794-806.

Wang Z. and Burge C. B. (2008). "Splicing regulation: from a parts list of regulatory elements to an integrated splicing code." RNA **14**(5): 802-813.

Whitelam G. (1995). "Plant photomorphogenesis: a green light for cryptochrome research." Curr Biol **5**(12): 1351-1353.

Whitelam G. C., Patel S. and Devlin P. F. (1998). "Phytochromes and photomorphogenesis in Arabidopsis." Philos Trans R Soc Lond B Biol Sci **353**(1374): 1445-1453.

Wilkinson M. E., Charenton C. and Nagai K. (2019). "RNA Splicing by the Spliceosome." Annu Rev Biochem.

Will C. L. and Luhrmann R. (2011). "Spliceosome structure and function." Cold Spring Harb Perspect Biol **3**(7).

Williams S. P., Rangarajan P., Donahue J. L., Hess J. E. and Gillaspy G. E. (2014). "Regulation of Sucrose non-Fermenting Related Kinase 1 genes in Arabidopsis thaliana." Front Plant Sci **5**: 324.

Witten J. T. and Ule J. (2011). "Understanding splicing regulation through RNA splicing maps." Trends Genet **27**(3): 89-97.

Wollerton M. C., Gooding C., Wagner E. J., Garcia-Blanco M. A. and Smith C. W. (2004). "Autoregulation of polypyrimidine tract binding protein by alternative splicing leading to nonsense-mediated decay." Mol Cell **13**(1): 91-100.

Wu G. and Spalding E. P. (2007). "Separate functions for nuclear and cytoplasmic cryptochrome 1 during photomorphogenesis of Arabidopsis seedlings." Proc Natl Acad Sci U S A **104**(47): 18813-18818.

Wu H. P., Su Y. S., Chen H. C., Chen Y. R., Wu C. C., Lin W. D. and Tu S. L. (2014). "Genome-wide analysis of light-regulated alternative splicing mediated by photoreceptors in Physcomitrella patens." Genome Biol **15**(1): R10.

Wu X. N., Sanchez Rodriguez C., Pertl-Obermeyer H., Obermeyer G. and Schulze W. X. (2013). "Sucrose-induced receptor kinase SIRK1 regulates a plasma membrane aquaporin in Arabidopsis." Mol Cell Proteomics **12**(10): 2856-2873.

Wurzinger B., Nukarinen E., Nagele T., Weckwerth W. and Teige M. (2018). "The SnRK1 Kinase as Central Mediator of Energy Signaling between Different Organelles." Plant Physiol **176**(2): 1085-1094.

Xiao S. H. and Manley J. L. (1997). "Phosphorylation of the ASF/SF2 RS domain affects both protein-protein and protein-RNA interactions and is necessary for splicing." Genes Dev **11**(3): 334-344.

Xiao S. H. and Manley J. L. (1998). "Phosphorylation-dephosphorylation differentially affects activities of splicing factor ASF/SF2." EMBO J **17**(21): 6359-6367.

Xin R., Kathare P. K. and Huq E. (2019). "Coordinated Regulation of Pre-mRNA Splicing by the SFPS-RRC1 Complex to Promote Photomorphogenesis." Plant Cell **31**(9): 2052-2069.

Xin R., Zhu L., Salome P. A., Mancini E., Marshall C. M., Harmon F. G., Yanovsky M. J., Weigel D. and Huq E. (2017). "SPF45-related splicing factor for phytochrome signaling promotes photomorphogenesis by regulating pre-mRNA splicing in Arabidopsis." Proc Natl Acad Sci U S A **114**(33): E7018-E7027.

Xiong Y., McCormack M., Li L., Hall Q., Xiang C. and Sheen J. (2013). "Glucose-TOR signalling reprograms the transcriptome and activates meristems." Nature **496**(7444): 181-186.

Yadav U. P., Ivakov A., Feil R., Duan G. Y., Walther D., Giavalisco P., Piques M., Carillo P., Hubberten H. M., Stitt M. and Lunn J. E. (2014). "The sucrose-trehalose 6-phosphate

(Tre6P) nexus: specificity and mechanisms of sucrose signalling by Tre6P." J Exp Bot **65**(4): 1051-1068.

Yan Q., Xia X., Sun Z. and Fang Y. (2017). "Depletion of Arabidopsis SC35 and SC35-like serine/arginine-rich proteins affects the transcription and splicing of a subset of genes." PLoS Genet **13**(3): e1006663.

Yang F., Liu Q., Cheng Y., Feng L., Wu X., Fan Y., Raza M. A., Wang X., Yong T., Liu W., Liu J., Du J., Shu K. and Yang W. (2020). "Low red/far-red ratio as a signal promotes carbon assimilation of soybean seedlings by increasing the photosynthetic capacity." BMC Plant Biology **20**(1): 148.

Yang H.-Q., Tang R.-H. and Cashmore A. R. (2001). "The Signaling Mechanism of Arabidopsis CRY1 Involves Direct Interaction with COP1." The Plant Cell **13**(12): 2573.

Yang S., Tang F. and Zhu H. (2014). "Alternative Splicing in Plant Immunity." International journal of molecular sciences **15**(6).

Yap K., Lim Z. Q., Khandelia P., Friedman B. and Makeyev E. V. (2012). "Coordinated regulation of neuronal mRNA steady-state levels through developmentally controlled intron retention." Genes Dev **26**(11): 1209-1223.

Ye J., Zhang Z., Long H., Zhang Z., Hong Y., Zhang X., You C., Liang W., Ma H. and Lu P. (2015). "Proteomic and phosphoproteomic analyses reveal extensive phosphorylation of regulatory proteins in developing rice anthers." Plant J **84**(3): 527-544.

Yu H., Tian C., Yu Y. and Jiao Y. (2016). "Transcriptome Survey of the Contribution of Alternative Splicing to Proteome Diversity in Arabidopsis thaliana." Mol Plant **9**(5): 749-752.

Yu Y. and Huang R. (2017). "Integration of Ethylene and Light Signaling Affects Hypocotyl Growth in Arabidopsis." Front Plant Sci **8**: 57.

Yu Y., Wang J., Zhang Z., Quan R., Zhang H., Deng X. W., Ma L. and Huang R. (2013). "Ethylene Promotes Hypocotyl Growth and HY5 Degradation by Enhancing the Movement of COP1 to the Nucleus in the Light." PLOS Genetics **9**(12): e1004025.

Zahler A. M. and Roth M. B. (1995). "Distinct functions of SR proteins in recruitment of U1 small nuclear ribonucleoprotein to alternative 5' splice sites." Proc Natl Acad Sci U S A **92**(7): 2642-2646.

Zhang G., Guo G., Hu X., Zhang Y., Li Q., Li R., Zhuang R., Lu Z., He Z., Fang X., Chen L., Tian W., Tao Y., Kristiansen K., Zhang X., Li S., Yang H., Wang J. and Wang J. (2010). "Deep RNA sequencing at single base-pair resolution reveals high complexity of the rice transcriptome." Genome Res **20**(5): 646-654.

Zhang H., Lin C. and Gu L. (2017). "Light Regulation of Alternative Pre-mRNA Splicing in Plants." Photochem Photobiol **93**(1): 159-165.

Zhang Q., Zhang X., Wang S., Tan C., Zhou G. and Li C. (2016). "Involvement of Alternative Splicing in Barley Seed Germination." PLoS One **11**(3): e0152824.

Zhang X. N. and Mount S. M. (2009). "Two alternatively spliced isoforms of the Arabidopsis SR45 protein have distinct roles during normal plant development." Plant Physiol **150**(3): 1450-1458.

Zhang Y., Primavesi L. F., Jhurreea D., Andralojc P. J., Mitchell R. A., Powers S. J., Schluepmann H., Delatte T., Wingler A. and Paul M. J. (2009). "Inhibition of SNF1-related protein kinase1 activity and regulation of metabolic pathways by trehalose-6-phosphate." Plant Physiol **149**(4): 1860-1871.

Zhang Y., Shewry P. R., Jones H., Barcelo P., Lazzeri P. A. and Halford N. G. (2001). "Expression of antisense SnRK1 protein kinase sequence causes abnormal pollen development and male sterility in transgenic barley." Plant J **28**(4): 431-441.

Zhou D. X., Kim Y. J., Li Y. F., Carol P. and Mache R. (1998). "COP1b, an isoform of COP1 generated by alternative splicing, has a negative effect on COP1 function in regulating light-dependent seedling development in Arabidopsis." Mol Gen Genet **257**(4): 387-391.

Zhou Y., Yang L., Duan J., Cheng J., Shen Y., Wang X., Han R., Li H., Li Z., Wang L., Terzaghi W., Zhu D., Chen H., Deng X. W. and Li J. (2018). "Hinge region of Arabidopsis phyA plays an important role in regulating phyA function." Proceedings of the National Academy of Sciences **115**(50): E11864-E11873.

Zhou Z. and Fu X. D. (2013). "Regulation of splicing by SR proteins and SR protein-specific kinases." Chromosoma **122**(3): 191-207.

Zulawski M., Braginets R. and Schulze W. X. (2013). "PhosPhAt goes kinases--searchable protein kinase target information in the plant phosphorylation site database PhosPhAt." Nucleic Acids Res **41**(Database issue): D1176-1184.

5.2. Cited books

Voet D., Voet J., Pratt C. “Lehrbuch der Biochemie” (2010)
zweite, aktualisierte und erweiterte Auflage
WILEY-VCH Verlag GmbH & Co. KGaA
ISBN: 978-3-527-32667-9

5.3. Internet pages

The Arabidopsis Information Resource (TAIR) on **www.arabidopsis.org:**

ABI1 (AT4G26080)
https://www.arabidopsis.org/servlets/TairObject?type=locus&name=AT4g26080, 13.10.2020

ABI2 (AT5G57050)
https://www.arabidopsis.org/servlets/TairObject?type=locus&name=AT5g57050, 13.10.2020

HAB1 (AT1G72770)
https://www.arabidopsis.org/servlets/TairObject?type=locus&name=AT1g72770, 13.10.2020

HAB2 AT1G17550
https://www.arabidopsis.org/servlets/TairObject?type=locus&name=AT1g17550, 13.10.2020

SnRK1.1 (AT3G01090)
https://www.arabidopsis.org/servlets/TairObject?id=40447&type=locus, 30.09.2020

SnRK1.2 (AT3G29160)
https://www.arabidopsis.org/servlets/TairObject?id=39165&type=locus, 30.09.2020

PP2CA (AT3G11410)
https://www.arabidopsis.org/servlets/TairObject?type=locus&name=AT3g11410, 13.10.2020

Arabidopsis information portal (ARAPORT) on **www.araport.org:**

SnRK1.1 (AT3G01090)
https://bar.utoronto.ca/thalemine/report.do?id=4815425&trail=%7c4815425, 30.09.2020

SnRK1.2 (AT3G29160)
https://bar.utoronto.ca/thalemine/report.do?id=5021245&trail=%7c5021245, 30.09.2020

UniProt on **www.uniprot.org**:

HsSRSF1 (HGNC:10780)[1]
https://www.uniprot.org/uniprot/Q07955, 09.10.2020

SR30 (AT1G09140)
https://www.uniprot.org/uniprot/Q9XFR5, 09.10.2020

Standard Protein Blast online tool on **https://blast.ncbi.nlm.nih.gov**

Protein sequence alignment of HsSRSF1 and AtSR20, blastp suite-2sequences
https://blast.ncbi.nlm.nih.gov/Blast.cgi?PROGRAM=blastp&PAGE_TYPE=BlastSearch&LINK_LOC=blasthome, 09.10.2020

[1] **HGNC ID**
HUGO gene nomenclature ID, is a unique ID for each human gene, independent of gene labels including label changes (https://www.genenames.org/data/gene-symbol-report/#!/hgnc_id/HGNC:10780, 04.03.2021)

IV. Appendix

IV.1. Project-based publications and manuscripts

IV.1.1. Publication in 2016

"Alternative Splicing Substantially Diversifies the Transcriptome during Early Photomorphogenesis and Correlates with the Energy Availability in Arabidopsis."

- Authors:
  Hartmann L.*, Drewe-Boß P., Wießner T., Wagner G., Geue S., Lee H. C., Obermüller D. M., Kahles A., Behr J., Sinz F. H., Rätsch G. and Wachter A.

- Journal: Plant Cell 28(11): 2715-2734

- Publication date: November 2016

The Plant Cell, Vol. 28: 2715–2734, November 2016, www.plantcell.org

LARGE-SCALE BIOLOGY ARTICLE

Alternative Splicing Substantially Diversifies the Transcriptome during Early Photomorphogenesis and Correlates with the Energy Availability in Arabidopsis

Lisa Hartmann,[a] Philipp Drewe-Boß,[b,c] Theresa Wießner,[a] Gabriele Wagner,[a] Sascha Geue,[a] Hsin-Chieh Lee,[a] Dominik M. Obermüller,[a] André Kahles,[b] Jonas Behr,[b] Fabian H. Sinz,[d,1] Gunnar Rätsch,[b,e] and Andreas Wachter[a,2]

[a] Center for Plant Molecular Biology (ZMBP), University of Tübingen, 72076 Tübingen, Germany
[b] Computational Biology Center, Memorial Sloan Kettering Cancer Center, New York, New York 10065
[c] Berlin Institute for Medical Systems Biology, Max Delbrück Center for Molecular Medicine, 13092 Berlin, Germany
[d] Institute for Neurobiology, University of Tübingen, 72076 Tübingen, Germany
[e] Department of Computer Science, ETH Zürich, 8006 Zürich, Switzerland

ORCID IDs: 0000-0003-3494-2269 (L.H.); 0000-0002-1288-1322 (J.B.); 0000-0002-1348-9736 (F.H.S.); 0000-0002-3132-5161 (A.W.)

Plants use light as source of energy and information to detect diurnal rhythms and seasonal changes. Sensing changing light conditions is critical to adjust plant metabolism and to initiate developmental transitions. Here, we analyzed transcriptome-wide alterations in gene expression and alternative splicing (AS) of etiolated seedlings undergoing photomorphogenesis upon exposure to blue, red, or white light. Our analysis revealed massive transcriptome reprogramming as reflected by differential expression of ~20% of all genes and changes in several hundred AS events. For more than 60% of all regulated AS events, light promoted the production of a presumably protein-coding variant at the expense of an mRNA with nonsense-mediated decay-triggering features. Accordingly, AS of the putative splicing factor *REDUCED RED-LIGHT RESPONSES IN CRY1CRY2 BACKGROUND1*, previously identified as a red light signaling component, was shifted to the functional variant under light. Downstream analyses of candidate AS events pointed at a role of photoreceptor signaling only in monochromatic but not in white light. Furthermore, we demonstrated similar AS changes upon light exposure and exogenous sugar supply, with a critical involvement of kinase signaling. We propose that AS is an integration point of signaling pathways that sense and transmit information regarding the energy availability in plants.

INTRODUCTION

Photosynthetic organisms use light as a source of energy, which perpetually fluctuates under natural conditions due to the day-night rhythm, seasonal variation, and nonperiodic changes depending on diverse environmental factors. Thus, sensing light and triggering adequate responses is of utmost importance for the survival and reproductive success of photoautotrophs. Plants have evolved complex light signaling mechanisms to adjust numerous aspects of their physiology and development (Jiao et al., 2007; Franklin and Quail, 2010; Kami et al., 2010; Galvão and Fankhauser, 2015), including seedling germination, deetiolation of dark-grown seedlings, entrainment of the circadian clock, chloroplast movement, stomatal opening, phototropism, shade avoidance, and the timing of flowering.

Higher plants possess at least five classes of photoreceptors mediating responses to different light qualities: red and far-red light can be sensed by phytochromes (PHYs) (Bae and Choi, 2008), blue and UV-A radiation are mainly detected by cryptochromes (CRYs; Lin and Shalitin, 2003), phototropins (Briggs and Christie, 2002), as well as members of the ZEITLUPE family (Somers et al., 2000; Imaizumi et al., 2003), while UV-B light is detected by the receptor UVR8 (Rizzini et al., 2011; Heijde and Ulm, 2012). Many of the light-regulated processes are responsive to different light qualities and photoreceptor types and require integration with additional signaling pathways determining plant development and adaptation. Further information on the light status is perceived in the chloroplast by means of photosynthesis, which has been demonstrated to regulate gene expression in different compartments, including retrograde signaling from the plastid to the nucleus (Foyer et al., 2012). Importantly, retrograde and photoreceptor-mediated signaling are interconnected to enable a coordinated response (Ruckle and Larkin, 2009; Estavillo et al., 2011; Lepistö and Rintamäki, 2012; Ruckle et al., 2012).

Plant adaptation to altered light conditions can result in massive changes in plant physiology and growth, e.g., deetiolation of dark-grown seedlings entails reduced hypocotyl elongation, opening of the apical hook, and both expansion and greening of the cotyledons (Franklin and Quail, 2010; Kami et al., 2010). The molecular mechanisms underlying these phenotypic adaptations have been intensively studied, revealing complex light-regulated transcriptional networks (Jiao et al., 2007) as well as other modes of gene activity

[1] Current address: Baylor College of Medicine, Department of Neuroscience, One Baylor Plaza, Houston, TX 77030.
[2] Address correspondence to awachter@zmbp.uni-tuebingen.de.
The author responsible for distribution of materials integral to the findings presented in this article in accordance with the policy described in the Instructions for Authors (www.plantcell.org) is: Andreas Wachter (awachter@zmbp.uni-tuebingen.de).
www.plantcell.org/cgi/doi/10.1105/tpc.16.00508

control. Major aspects of light signaling occur within the nucleus, into which PHYs are translocated upon light activation (Nagatani, 2004). However, light signaling has also been shown to include translational control in the cytosol (Liu et al., 2012b; Paik et al., 2012).

Early steps in light signaling include inactivation of negative regulators such as PHYTOCHROME INTERACTING FACTORs (Duek and Fankhauser, 2005; Monte et al., 2007), DE-ETIOLATED1, and CONSTITUTIVE PHOTOMORPHOGENIC1 (Lau and Deng, 2012). Subsequently, photomorphogenesis-promoting transcription factors are expressed, resulting in the activation of downstream transcriptional networks (Hoecker, 2005; Bae and Choi, 2008). Furthermore, light signaling can alter histone marks and change chromatin organization (van Zanten et al., 2010; Fisher and Franklin, 2011). Light-induced switching from skoto- to photomorphogenesis is accompanied by fundamentally altered gene expression patterns. For instance, more than 20% of all genes in rice (*Oryza sativa*) and *Arabidopsis thaliana* are differentially expressed in dark-grown compared with light-exposed seedlings (Ma et al., 2001; Tepperman et al., 2001; Jiao et al., 2005, 2007).

Earlier studies mainly considered quantitative changes in gene expression upon altered light signaling. However, it is now becoming evident that alternative precursor mRNA (pre-mRNA) processing substantially increases transcriptome complexity and can play an important role in modulating gene expression in response to internal and external cues. Among these mechanisms, alternative pre-mRNA splicing (AS) is particularly widespread in higher eukaryotes including plants, affecting more than 60% of all intron-containing genes in Arabidopsis (Filichkin et al., 2010; Marquez et al., 2012). While regulation and functions of most AS events remain to be addressed, compelling evidence for the relevance of selected AS instances in plant physiological responses has been provided (Syed et al., 2012; Reddy et al., 2013; Staiger and Brown, 2013). For example, intricate links between the circadian clock and AS regulation were uncovered in Arabidopsis (Sanchez et al., 2010; Staiger and Green, 2011; James et al., 2012; Wang et al., 2012).

AS is perfectly suited to coordinately regulate gene expression and might play an important role in plant light signaling as well. This hypothesis is supported by the functional analysis of selected AS events and previously described effects of light conditions on AS in different plant species. For the PHY-specific type 5 phosphatase, two protein variants with distinct subcellular localization patterns are derived from AS of the corresponding pre-mRNA (de la Fuente van Bentem et al., 2003). In the case of a homolog of the light-regulatory transcription factor LONG HYPOCOTYL5 (HY5), HY5-HOMOLOG, AS generates transcript variants encoding protein versions with different stabilities (Sibout et al., 2006). However, the regulation of these AS events and their putative role in light signaling were not investigated. Examples for the influence of light conditions on AS include genes encoding an ascorbate peroxidase (Mano et al., 1997) as well as a hydroxypyruvate reductase (Mano et al., 1999) in *Cucurbita* sp (pumpkin), and high-light-modulated AS for homologs of the family of serine/arginine-rich (SR) splicing factors from Arabidopsis (Tanabe et al., 2007). Comparisons of AS profiles for light- versus dark-grown rice seedlings using microarrays (Jung et al., 2009) and for Arabidopsis seedlings with a high-resolution RT-PCR panel (Simpson et al., 2008) indicated that light-mediated changes in AS patterns might affect the expression of numerous genes. This notion was further supported by recent studies using RNA sequencing (RNA-seq) to deduce light-regulated AS patterns in a transcriptome-wide manner in the moss *Physcomitrella patens* (Wu et al., 2014), etiolated Arabidopsis seedlings (Shikata et al., 2014), and light-grown Arabidopsis plants (Mancini et al., 2016). Interestingly, Wu et al. (2014) and Shikata et al. (2014) reported PHY signaling acting upstream of light-regulated AS. By contrast, AS patterns for a subset of genes in Arabidopsis exposed to alternating light/dark conditions changed independent of photoreceptors (Petrillo et al., 2014a, 2014b; Mancini et al., 2016). These findings raise the intriguing questions whether independent signaling pathways in light-regulated AS exist and how AS changes can contribute to plant adaptation to altered light conditions. The identification of the SR-like splicing factor REDUCED RED-LIGHT RESPONSES IN CRY1CRY2 BACKGROUND1 (RRC1) as a novel component of PHYB signaling uncovered a further connection between light signaling and AS (Shikata et al., 2012a, 2012b). The *rrc1* mutant was impaired in the PHYB-dependent light response and showed AS changes for several SR genes (Shikata et al., 2012b). RRC1 functioning in light signaling was dependent on its C-terminal arginine/serine-rich (RS) region (Shikata et al., 2012a). Given that the RS domain of splicing factors is assumed to play an important role in spliceosome assembly (Reddy et al., 2013), it can be anticipated that RRC1 acts in PHYB signaling via light-regulated AS of downstream targets.

In this work, we analyzed transcriptome-wide gene expression and AS changes in etiolated Arabidopsis seedlings exposed to blue, red, and white light. Our study revealed that light signals trigger rapid AS responses of numerous genes, including splicing factors and other functional groups. Among these candidates was *RRC1*, which was previously shown to play a role in PHYB signaling. The light signaling phenotype of an *rrc1* mutant could only be complemented with the splicing variant that is upregulated upon light exposure, indicating the presence of a self-reinforcing circuit. Based on AS analyses under different light conditions, the major photoreceptors for blue and red light play no essential role in regulating these events during photomorphogenesis in white light. Interestingly, the AS output was similarly changed by light and sugar feeding in darkness and depended on kinase signaling. Our data also revealed a correlation between the AS output and expression of target genes of SUCROSE-NON-FERMENTATION1-RELATED KINASE1, a central integrator of plant energy signaling.

RESULTS

Dark-Grown Seedlings Display Numerous AS Changes upon Exposure to Blue, Red, or White Light

Previous studies have established massive transcriptomic reprogramming in the switch from skoto- to photomorphogenesis (Jiao et al., 2007). To investigate the potential impact of AS on gene expression in response to altered light conditions, we analyzed transcriptomes of Arabidopsis seedlings grown for 6 d in darkness and exposed for 1 or 6 h to blue, red, or white light by RNA-seq. Two replicate samples for each time point and light quality, as well as corresponding dark controls were generated. Mapping of the

100-bp reads to the Arabidopsis genome (TAIR10 annotation) resulted in 86.0 to 207.6 × 10^6 reads per time point, based on the two replicate samples each (Supplemental Table 1). AS events were extracted from TAIR10 and complemented by unannotated events that were found in our data resulting in 56,270 AS events. To determine quantitative changes in AS and gene expression, a previously established and validated computational pipeline was applied (Rühl et al., 2012; Drechsel et al., 2013; Drewe et al., 2013; Supplemental Data Sets 1 and 2). Upon 1 h exposure to blue (~6 μmol m^{-2} s^{-1}) or red light (~14 μmol m^{-2} s^{-1}) at intensities that, based on previous publications (Laubinger et al., 2004; Shen et al. (2007)), are expected to result in overall saturating effects on hypocotyl elongation, 81 AS events derived from 51 genes were significantly altered (false discovery rate [FDR] < 0.1; this FDR value is generally used unless otherwise mentioned; Supplemental Figure 1A). The number of AS changes massively increased after 6 h blue or red light illumination (Figures 1A and 1B). Additional AS shifts were detected upon exposure to white light (~130 μmol m^{-2} s^{-1}), representing more natural light conditions. Considering all three light settings, 700 AS events associated with 311 genes were significantly altered upon 6 h light exposure. As the rate of change in transcript steady state levels depends on transcript stability, early AS shifts will only be detectable for relatively unstable transcripts. We found only few consistent AS changes when comparing the 1- and 6-h time points for blue and red light (Supplemental Data Set 1). This limited overlap can be explained by overall weak AS changes at the early time point and the activation of downstream signaling cascades at 6 h versus 1 h light exposure. To investigate the potential role of AS in all of these light-regulatory processes, we focused our further analysis on the 6 h time point. We noticed that the AS responses for the three light qualities showed only a partial overlap, independent of the FDR cutoff value (Supplemental Figure 1B). While blue and red light primarily elicit CRY and PHY photoreceptor signaling, respectively, both signaling pathways should become active in response to white light. Thus, most of the AS changes observed in response to monochromatic light were also expected to be present upon white light exposure. To reduce the effect of AS fluctuation between samples, which is expected to be most prevalent for low-abundant splicing variants with few supporting reads, and to select for AS events that are more likely biologically relevant, we included an additional filter for effect size (change in splicing index [SI] > 0.05; Supplemental Figure 1C and Supplemental Data Set 3). Addition of the SI filter reduced the number of detected events, while the overlap between the different light qualities was still limited. We assumed that this might be caused by a too stringent FDR filter. Therefore, we considered next all events with an FDR < 0.1 in at least one color and then filtered for SI > 0.05 (Figure 1C). Applying this filter strategy resulted in strongly overlapping patterns of AS changes for all three light qualities, with 87.5 to 98.0% of all events altered in one color being also affected in at least one more light condition (Figure 1C). The majority of AS events were changed under all three light regimes, indicating common AS responses. Red light caused fewer significantly altered events upon FDR filtering and a lower median SI change of 0.079 compared with 0.137 and 0.136 in blue and white light, respectively (Supplemental Data Set 3). Red light thus had an overall weaker effect on AS than blue and white light. Both the occurrence of mostly common AS changes in response to different light qualities and, for some AS events, weaker quantitative effects of red light were confirmed by the validation experiments (see below).

Of all 56,270 AS events detected in this analysis, 46.9, 22.4, 21.2, and 9.5% corresponded to alternative 3′ splice sites, regulated introns (varying rate of intron retention/splicing), alternative 5′ splice sites, and regulated exons (cassette exons), respectively (Supplemental Figure 2A). The AS analysis in this work is based on a heuristic method, and it was demonstrated to compare favorably to related approaches (Kahles et al., 2016). Similar frequencies of the different AS types have been observed in previous studies using the same, but also with different AS analysis pipelines, and are also found for the TAIR10 annotation (Supplemental Table 2). According to these data sets, alternative 3′ splice sites are most abundant, whereas a previous survey of AS in Arabidopsis identified intron retention as the prevalent AS type (Marquez et al., 2012). These discrepancies most likely result from using different computational approaches for defining splicing variants, including many low-abundant isoforms that might not be biologically relevant. Indeed, a very different distribution was found for the 700 light-regulated AS events: cassette exons and regulated introns were enriched, representing 18.0 and 37.1%, respectively, of all AS events altered in response to at least one light quality, while lower fractions of alternative 3′ (27.3%) and 5′ (17.6%) splice sites were observed. Among the light-regulated AS events, we also identified several exitrons (Supplemental Table 3), a class of cryptic introns that reside within the coding region of transcripts (Marquez et al., 2015). Analyzing the direction of the shift for the AS events that were significantly altered in response to at least one light quality, we observed strong biases for the intron retention and cassette exon events (Supplemental Figure 2B). In 74% of the significantly changed intron retention events, light triggered a shift toward the spliced, i.e., shorter transcript variant, while in 67% of the cassette exons a relative increase of the skipping variant was detected. Proportions of alternative up- and downstream 5′ and 3′ splice site usage, respectively, were also elevated in response to light, but this effect was less pronounced than for the other two AS types. To assess the potential consequences of light-regulated AS on the expression of the corresponding genes, we compared the positions of all events to those displaying significant changes (Supplemental Figure 2C and Supplemental Data Sets 4A to 4D). For the light-regulated AS events, the fractions of events associated either with the coding sequence or the 3′ untranslated region (UTR) were decreased and increased, respectively, in comparison to all events. For all subsets, however, most of the AS events overlapped with the coding sequence. Based on their positions within the pre-mRNAs, light-triggered AS events can affect the coding and regulation potential of the resulting mRNAs.

Previous studies have revealed widespread coupling of AS and nonsense-mediated decay (NMD) in Arabidopsis (Kalyna et al., 2012; Drechsel et al., 2013). To assess the prevalence of coupled AS-NMD in the context of light regulation, the occurrence of NMD-triggering features in the corresponding splicing variants was analyzed. To this end, the AS events were integrated into the representative transcript isoform from TAIR10, followed by the detection of upstream open reading frames, premature termination codons (PTCs), and long 3′ UTRs (Supplemental Data Sets 4A

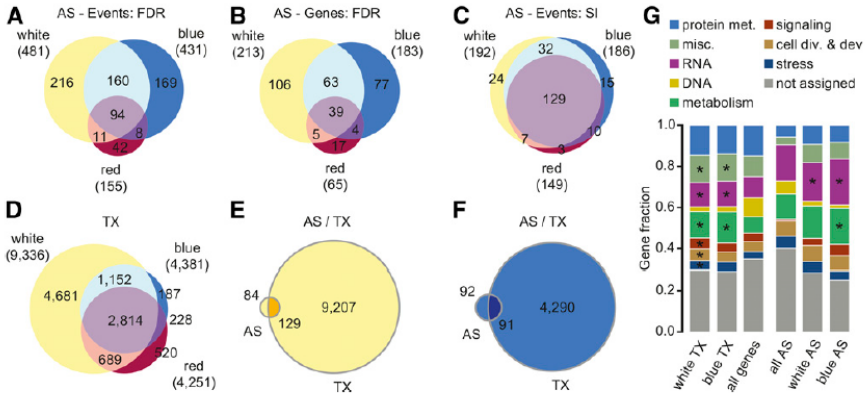

Figure 1. Changes in AS and Gene Expression in the Course of Photomorphogenesis Triggered by Blue, Red, and White Light.

(A) and **(B)** Venn diagrams showing the numbers of significantly altered AS events **(A)** and the corresponding numbers of genes affected **(B)** upon 6 h exposure to blue (~6 μmol m^{-2} s^{-1}), red (~14 μmol m^{-2} s^{-1}), and white (~130 μmol m^{-2} s^{-1}) light (FDR < 0.1). Events or genes showing changes in opposing directions under two light conditions were excluded. Total numbers of events/genes changing under each light condition are given in parentheses.
(C) Venn diagram of significantly altered AS events after 6 h light exposure upon additional filtering based on the effect size (change in SI > 0.05). Only events with an FDR < 0.1 under at least one light condition were considered for SI analysis. Events with SI changes in opposite directions under two conditions were excluded. Events are grouped according to their SI only.
(D) Venn diagram of genes changing in total expression (TX) upon 6 h exposure to blue, red, and white light (FDR ≤ 0.1). Total numbers of genes changing under each light condition are given in parentheses.
(E) and **(F)** Genes exhibiting changes in AS, TX, or both upon 6 h white **(E)** and blue **(F)** light exposure.
(G) Gene Ontology term analysis of genes undergoing AS or TX changes, upon 6 h white or blue light exposure compared with all AS events detected and all genes in MapMan, respectively. met., metabolism; misc., miscellaneous; cell div. and dev, cell division and development; asterisks indicate terms overrepresented compared with all AS events and all genes in MapMan, respectively, with Bonferroni-corrected P < 0.05.

to 4D). Remarkably, 77.2% of all light-regulated AS events exhibit NMD features within the splicing isoform that is relatively more abundant in the dark samples. Furthermore, 61.1% of all events showed a relative switch from a putative NMD target to a non-NMD-regulated transcript variant upon light exposure. The corresponding fractions were even larger when only considering events within the coding sequence, which accounted for most NMD-triggering features in those transcripts. Further evidence for coupling of light-regulated AS and NMD was provided by comparing the sets of significant events from this study and from a previous analysis upon NMD impairment (Drechsel et al., 2013): ~10% of all light-regulated events have previously been established to involve NMD control (Supplemental Data Sets 4E to 4G). Notably, the seedlings analyzed in this and the previous work substantially differed in their developmental stage and growth conditions. The frequency of coupled AS-NMD was analyzed in light-grown seedlings, while this study revealed that most of the light-regulated AS-NMD events showed downregulation of the putative NMD form in light. Thus, the overlap might be even higher when analyzing seedlings cultivated under identical conditions. In conclusion, light-triggered AS typically mediates a switch from a presumably NMD-regulated transcript to a protein-coding alternative variant, enabling the activation of gene expression in the transition from skoto- to photomorphogenesis.

The RNA-seq data were also analyzed for differential gene expression (Anders and Huber, 2010; FDR ≤ 0.1; Supplemental Data Set 2). In line with previous findings (Jiao et al., 2007), a substantial fraction of all genes were significantly up- or downregulated in response to light (Figure 1D; Supplemental Figure 3). Out of 33,602 genes in the TAIR10 annotation, 23,432 genes were expressed in our data set when considering all samples (FDR ≤ 0.1; method based on Gan et al., 2011). Furthermore, 10,271 (43.8%) of the expressed genes showed altered transcript levels in response to at least one light quality for the 6 h time point. White, blue, and red light changed the expression of 9336, 4381, and 4251 genes, respectively. When setting a threshold of an at least 2-fold change in transcript levels, 3439, 2406, and 2020 were differentially expressed upon seedling exposure to white, blue, and red light, respectively. This adds up to a total number of 4310 genes, corresponding to 18.4% of all expressed genes. Patterns of differential gene expression in response to blue and red light showed a huge overlap and most of the changes in transcript levels upon illumination with monochromatic light were also detected under white light. Furthermore, blue and red light affected the expression of a comparable number of genes, while on the level of AS red light was less effective than blue light. Moreover, many transcriptional changes were only found in response to white light, possibly as part of an adaptive program that is not activated by weak, monochromatic light. When considering differential expression separately for up- and downregulated genes, slightly more genes were induced than repressed at the 6 h time point. We also analyzed differential gene expression for the samples exposed to light for 1 h (Supplemental Figure 3). In line with the observations on the level of AS, fewer changes were detected for the 1 h compared with the 6 h time point. For this earlier time point, the number of induced genes was

approximately twice the number of downregulated ones. Fewer down- than upregulated genes cannot only be explained by a lower number of repressed than induced genes, but also by the stability of the transcripts: A significant decrease in steady state transcript levels as a result of diminished transcription within 1 h is expected to be detectable only for highly unstable transcripts.

To test if light affects both expression levels and AS of genes, the corresponding gene lists were compared separately for white, blue, and red light (Figures 1E and 1F; Supplemental Figure 1D). For all light qualities, a substantial fraction of the genes showing changes in AS had unchanged total transcript levels. Given that AS can contribute to quantitative gene control, for example by generating destabilized NMD targets (Drechsel et al., 2013), the number of light-regulated genes displaying both altered AS and differential gene expression in a splicing-independent manner might be even smaller. In summary, the altered light status triggers complex transcriptome reprogramming, involving changes in both gene expression and, for a smaller, mostly distinct set of genes, AS.

Analyzing the functional categories of genes associated with light-regulated AS revealed an overrepresentation of the terms "RNA" and "metabolism" for blue light and "RNA" for white light (Figure 1G; Supplemental Data Set 5). The overrepresentation of the "RNA" category is in line with previous publications (Filichkin et al., 2010; Rühl et al., 2012; Drechsel et al., 2013), showing extensive regulated AS for genes involved in RNA metabolism. Since numerous intergenic regions are expressed in an NMD-regulated manner (Drechsel et al., 2013), we compared read accumulation in intergenic regions for the dark- and light-exposed samples (Supplemental Data Set 6). Several of these transcriptional units were found to overlap with previously identified long intergenic RNAs (Liu et al., 2012a). Read coverage for some of these regions differed substantially between the light conditions tested here. However, total expression levels were low in most cases and further studies are required to test the functional relevance of these transcripts.

Finally, to rule out the occurrence of rhythmic expression in the absence of light, transcript levels of circadian genes were analyzed in the dark and light samples (Supplemental Table 4). When comparing the 0 and 6 h dark samples, no significant change was detectable for any of the genes. By contrast, light altered the expression of several of these genes, in line with the known role of light in influencing circadian expression patterns (Jiao et al., 2007).

Validation of Light-Regulated AS Events

We next selected candidates from the list of light-regulated AS events for an independent experimental validation (Figure 2). This selection covered different functional categories of genes, including splicing factors (Figures 2A to 2D), putative transcription factors (Figures 2E to 2G), and a photosynthetic component (Figure 2H). All of the candidate events were confirmed, in line with the high validation rate observed in previous studies that applied the same pipeline for AS analysis (Rühl et al., 2012; Drechsel et al., 2013). For some genes, several AS events were detected and we focused our analysis on the major splicing variants, which were also sequenced (Supplemental Figure 4). For all events, the AS ratios were changed in response to blue, red, and white light. However, the extent of splicing change differed for some candidates (Figure 2). For those candidates, white light generally caused the strongest AS shifts. Furthermore, for three out of nine candidates, a weaker change in response to red compared with blue and white light was observed. These findings are in agreement with differences in the SI changes for the three light qualities from the RNA-seq data.

Light-Regulated AS of *RRC1* Results in a Self-Enforcing Circuit

Previous work had identified the putative splicing factor RRC1 as a novel component of PHY-dependent light signaling (Shikata et al., 2012b). Interestingly, our RNA-seq data suggested that the inclusion of the third exon of *RRC1* is regulated in a light-dependent manner (Figure 3A). Analyzing the AS pattern of this region via RT-PCR supported the notion that blue, red, and white light caused a shift toward the inclusion variant compared with dark samples (Figure 3B). Separate quantitation of the two splicing variants revealed that light exposure resulted in slightly elevated levels of the representative *RRC1.1* variant and diminished amounts of *RRC1.2* (Supplemental Figure 5A). Opposite changes in the levels of the two splicing variants were also observed for the light-regulated event in *SR30* (Supplemental Figure 5B), indicating that those shifts in splicing variant ratios are caused by AS and not by an altered transcript turnover rate. The exon skipping variant *RRC1.2* gives rise to a frame shift, resulting in a PTC two exons further downstream. We therefore assumed that this AS variant is targeted by NMD, which was corroborated by its accumulation in two mutants impaired in NMD activity (Figure 3C).

To test the functional significance of light-regulated AS of *RRC1*, complementation of the *rrc1-2* mutant, carrying a T-DNA insertion (Figure 3A) and previously described as a knockdown allele (Shikata et al., 2012b), was performed. Subsequently, we determined hypocotyl lengths of seedlings grown in red light or darkness (Figure 3D). Median hypocotyl lengths in darkness were similar for all tested lines (Supplemental Figure 6A) and lengths measured in red light were normalized to the average dark value for each line to correct for a potential light-independent growth phenotype. In line with the previous report by Shikata et al. (2012b) and the role of RRC1 as a positive regulator of light signaling, *rrc1-2* had longer hypocotyls than the wild type (Figure 3D). This phenotype could be rescued upon complementation with the splicing variant *RRC1.1*, but not *RRC1.2*, under control of the constitutive 35S promoter. Complementation with a corresponding genomic construct also resulted in significantly shorter hypocotyls compared with the *rrc1-2* mutant, even though the median length was still slightly elevated compared with the wild type. The differences in hypocotyl lengths when comparing complementation with *RRC1.1* and the genomic construct might be caused by varying levels of overexpression (Supplemental Figure 6B). Analysis of the *RRC1* levels for the two splicing variants and total transcripts confirmed robust and specific expression of the constructs in all transgenic lines. However, the genomic construct resulted in massive overaccumulation of *RRC1* transcripts compared with a more moderate increase in the cDNA lines. To exclude an effect of using a strong constitutive promoter for the complementation, the constructs based on the two AS

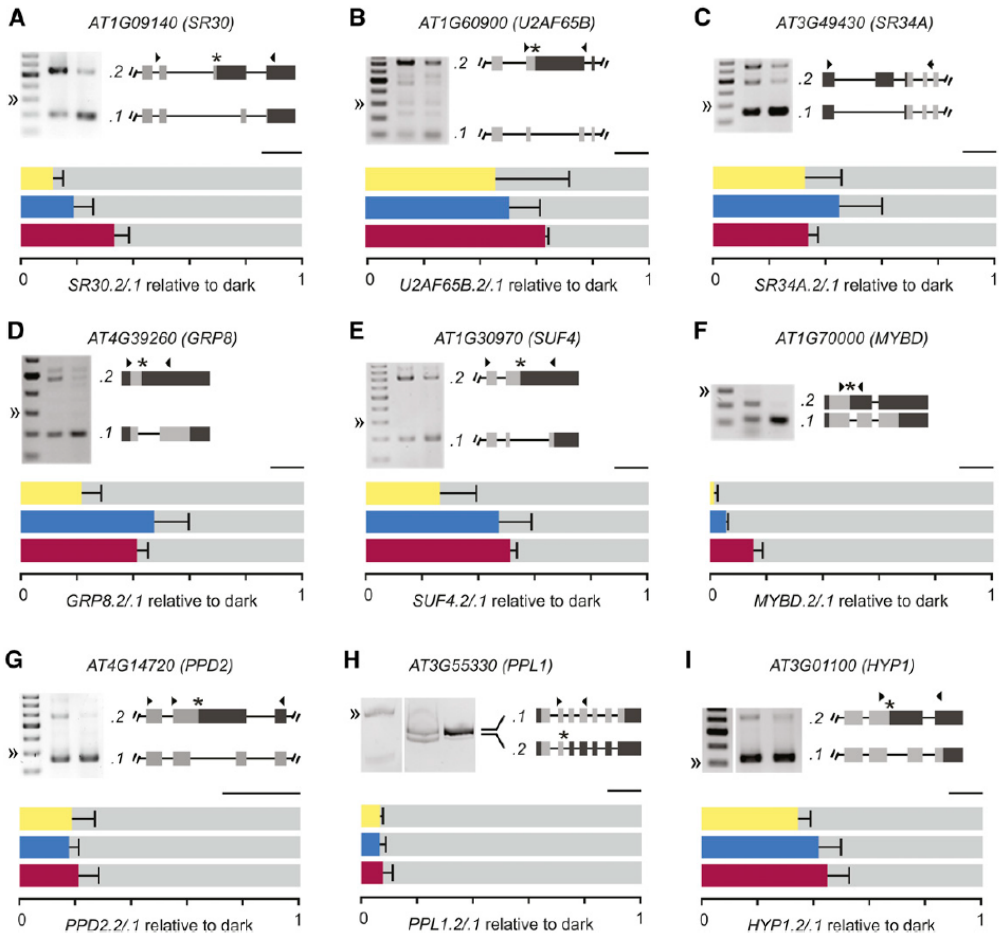

Figure 2. Validation of Light-Dependent AS in Genes from Different Functional Categories.

Splicing variants of genes encoding splicing factors (**[A]** to **[D]**), putative transcription factors (**[E]** to **[G]**), a photosynthetic component **(H)**, and a hypothetical chloroplast protein **(I)** were coamplified from samples grown in darkness and collected at 0 h or after 6 h exposure to white (~130 μmol m^{-2} s^{-1}), blue (~6 μmol m^{-2} s^{-1}), or red (~18 μmol m^{-2} s^{-1}) light (top, middle, and bottom bars) and quantified using a Bioanalyzer. Shown are representative agarose gels with double arrowheads pointing at 300 bp of a DNA size ladder with 100-bp increments, and PCR products from 0 h (left) and 6 h white light (right) samples. The variants quantified are labeled (*.1* or *.2*), and partial (**[A]** to **[C]**, **[E]**, **[G]**, and **[I]**) or full (**[D]**, **[F]**, and **[H]**) gene models are shown with introns represented by lines and exons by boxes. Regions colored in dark gray are UTRs, and asterisks mark the introduction of a premature termination codon. Solid arrowheads show the positions of the primers used, and the arrow in **(C)** indicates a splice-junction-spanning primer. Bars give average relative splice form ratios with the ratio in darkness set to 1, as indicated by the light-gray background bar for each color. Error bars are SD, $n = 3$. Scale bars beneath the models represent 500 bp.

variants were also expressed in the wild-type background. None of these lines displayed altered hypocotyl lengths compared with the wild type (Supplemental Figures 6C to 6E). Moreover, immunoblot analysis allowed the detection of a protein corresponding to the splicing variant *RRC1.1*, but not *RRC1.2* (Supplemental Figure 6F), further suggesting that the exon skipping variant is subject to NMD and does not lead to RRC1 protein. In line with the transcript data, protein levels were much higher in the plants expressing the genomic construct compared with complementation with the *RRC1.1* construct. The strong overexpression of *RRC1* upon complementation with the genomic construct might result in perturbed downstream signaling, which would explain the only partial rescue of the hypocotyl elongation phenotype in case of this construct. To exclude such effects, the *rrc1-2* mutant was also complemented with constructs under control of the *RRC1* promoter. Indeed, the genomic *RRC1* sequence under control of the endogenous promoter fully rescued the mutant phenotype (Supplemental Figures 7A and 7B). Expressing the two *RRC1* splicing variants under control of the endogenous promoter resulted in transcript levels that were substantially lower than in the wild type, possibly due to the absence of introns (Supplemental Figure 7C). Accordingly, functional complementation of the hypocotyl phenotype was found only for the *RRC1.1* line with the highest expression (Supplemental Figure

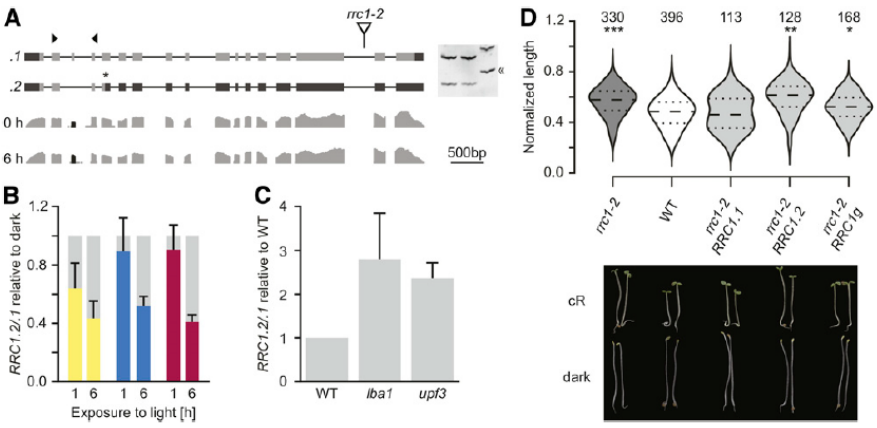

Figure 3. Light Promotes AS of *RRC1* to the Variant Required for Functioning in Phytochrome Signaling.

(A) Models of *RRC1* major splicing variants showing exons as boxes and introns as lines. UTRs are dark gray. The positions of the coamplification primers are given by arrowheads, and the insertion site of the T-DNA in the *rrc1-2* mutant is indicated. The asterisk marks the introduction of a premature termination codon in the *RRC1.2* variant. The coamplified PCR products in 0 h (left) and 6 h white light (right) samples separated on a gel are shown with the double arrowhead pointing at 100 bp of a 50-bp ladder. Transcript models are aligned to corresponding amplification products. Below the transcript models, coverage plots show representative RNA-seq results for a 0 h and 6 h light sample. The alternatively spliced region is shown in black.

(B) Confirmation of light-dependent AS under ~130 μmol m^{-2} s^{-1} white (left), ~6 μmol m^{-2} s^{-1} blue (middle), and ~18 μmol m^{-2} s^{-1} red (right) light. Splicing variants were coamplified from samples grown in darkness for 6 d and collected at 0 h or after 1 h or 6 h exposure to light, and quantified using a Bioanalyzer. Bars give average splice form ratios with the ratio in darkness set to 1. Error bars are SD, $n = 3$.

(C) Splicing variants were coamplified from etiolated wild-type plants, or indicated NMD-deficient mutants, and quantified as in **(B)**. Ratio in the wild type is

(D) Violin plots showing the distribution of the relative hypocotyl lengths measured in red light (~10 μmol m^{-2} s^{-1}) for *rrc1-2*, wild-type, and complementation lines (top). In each violin, the dashed line represents the median, and the dotted lines the quartiles. All hypocotyls were normalized to the average length in darkness of each line. Complementation constructs express tagged splicing variants (*.1* or *.2*) or the genomic sequence (*g*) under control of the CaMV 35S promoter. Asterisks indicate P values from Mood's median test compared with the wild type: *$P < 10^{-2}$, **$P < 10^{-11}$, and ***$P < 10^{-17}$. Exact P values for all comparisons are provided in Supplemental Figure 6E; *n* is indicated above each genotype. For each complementation construct, three independent F1 lines were each analyzed once in a total of three independent experiments. Bottom panel shows representative seedlings from hypocotyl assays in darkness and under red light (cR).

7D). As expected, none of the *RRC1.2* lines showed a rescue of the mutant phenotype. Taken together, light-stimulated inclusion of the cassette exon represents a mechanism to induce functional *RRC1* expression, thereby increasing the levels of a positive regulator of light signaling.

Contribution of Photoreceptors to AS Changes during Photomorphogenesis

Recent studies in *P. patens* (Wu et al., 2014) and etiolated Arabidopsis seedlings (Shikata et al., 2014) suggested a major role of PHY photoreceptors in red light-dependent AS, whereas altered AS patterns in leaves subjected to varying light conditions were attributed to retrograde signaling (Petrillo et al., 2014b). These seemingly controversial findings may result from different experimental settings and suggest that various factors can influence AS patterns under changing light conditions. To further address this intriguing aspect, we first compared the AS patterns of five confirmed candidates in etiolated wild-type and *phyA phyB* double mutant seedlings upon illumination with white light (Figure 4A). For all events, very similar patterns of light-induced AS changes in the comparison of wild-type and *phyA phyB* mutant seedlings were observed; significant differences between the wild type and the mutant were only found for single events and time points and did not correlate with the overall light response. Interestingly, seedling growth on sugar-containing medium, as in the RNA-seq experiment, shifted the AS ratio into the same direction as light (Figure 4A, right panels). The relative change upon 6 h of light exposure, however, was identical for seedlings grown without and with external sugar supply and also did not differ between the wild type and *phyA phyB* (Supplemental Figure 8).

Our data did not provide evidence for a critical role of the two major red light photoreceptors PHYA and PHYB in triggering AS changes upon exposure to white light. Given that white light could trigger AS via red and blue light signaling, we next analyzed changes in AS upon exposure to red light (Figure 4B; Supplemental Figure 8). For four out of five events, red light resulted in an AS change in both wild-type and *phyA phyB* seedlings. Interestingly, the mutant showed a significantly weaker red light response than the wild type for *MYBD*. Furthermore, the AS ratio of *PPL1* was not significantly changed in comparison of darkness and red light in the mutant. These data suggested the existence of alternative pathways controlling light-triggered AS and that a contribution of PHYA/PHYB only becomes detectable for some

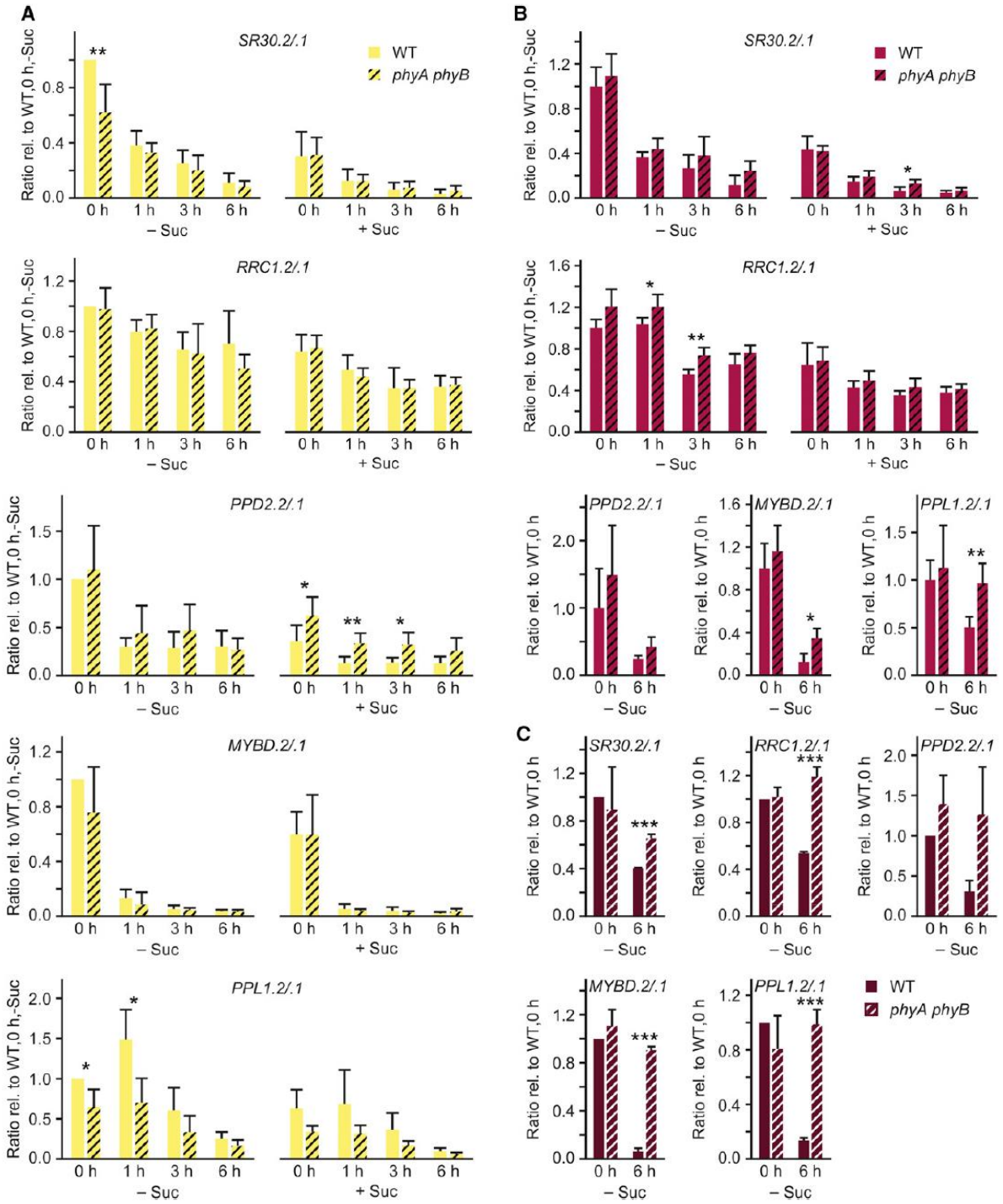

Figure 4. Contribution of Phytochrome A/B Signaling to AS Control Becomes Visible in Red and Far-Red, but Not in White Light.

Etiolated seedlings grown on plates with or without 2% sucrose for 6 d were exposed to ~130 μmol m^{-2} s^{-1} white **(A)**, ~28 μmol m^{-2} s^{-1} red **(B)**, or ~15 μmol m^{-2} s^{-1} far-red **(C)** light for the indicated periods. Splice variants were coamplified and quantified using a Bioanalyzer. AS ratios in **(A)** and **(C)** were

events under red light. We therefore assumed that exposure of seedlings to far-red light, which triggers PHYA signaling but does not support photosynthesis and the associated signaling, should result in more distinct AS responses in wild-type and *phyA phyB* seedlings. Far-red light caused an AS shift of all tested events in the wild type, albeit quantitative changes for *SR30* were substantially lower than under white light (Figure 4C; Supplemental Figure 8). Remarkably, no or only very weak effects of far-red on the AS pattern in the mutant was detected, revealing the dependency on PHY under this particular light condition.

The differences in AS responses under white, red, and far-red light highlight the occurrence of multiple signaling pathways and that the major PHYs A and B are not essential in this process under white light. Besides PHY signaling, white light also activates the blue light-responsive cryptochrome photoreceptors. To test for a potential role of CRYs, AS changes upon exposure to white light were compared between wild-type and *cry1 cry2* mutant seedlings. All tested events showed the same white light response in wild-type and *cry1 cry2* seedlings (Figure 5A; Supplemental Figure 8). Overall similar AS changes in wild-type and *cry1 cry2* seedlings were also detected upon blue light exposure (Figure 5B). The relative AS changes between darkness and 6 h blue light were slightly more pronounced in the wild type than in the mutant (Supplemental Figure 8); however, this quantitative difference was statistically significant only for *SR30*. Taken together, neither PHYA/B-dependent red light signaling nor CRY-mediated blue light signaling are essential in causing the AS changes in etiolated seedlings exposed to white light. This observation could be explained by alternate signaling through either PHYs or CRYs; in this case, however, no AS changes would be expected upon red and blue light exposure of the *phyA phyB* and *cry1 cry2* mutant, respectively. While a role of other photoreceptor types cannot be fully excluded, it seems more likely that another, photoreceptor-independent signaling pathway is involved in light-responsive AS during photomorphogenesis.

Illumination of etiolated seedlings will not only activate photoreceptor signaling and photosynthesis, but also entrain the expression of circadian regulators. Previous reports revealed intricate links between the circadian clock and AS in plants (Sanchez et al., 2010; James et al., 2012). To address a potential impact of circadian regulators, we tested light-triggered AS in mutants defective in different components of the circadian clock (Supplemental Figure 9). Only for the *prr7-3 prr9-1* double mutant a slightly weaker AS change was seen in case of *RRC1*, suggesting that overall circadian regulators do not play a major role in the control of these AS events in the early phase of photomorphogenesis.

AS Output Correlates with the Plant's Energy Supply

Analysis of the light-responsive AS in etiolated seedlings revealed that not only light, but also the growth conditions had a major impact on the splicing outcome. Etiolated seedlings grown on sucrose-containing medium had AS ratios shifted into the same direction as observed for seedlings grown without sucrose and exposed for 6 h to light (Figures 4 and 5). To further dissect how light and sugar can alter AS patterns, wild-type seedlings grown in darkness and on sugar-free medium were transferred to liquid medium with or without sugar and kept in darkness or exposed to white light. To account for the osmotic effect of sugar supplementation, an additional control with an equimolar concentration of mannitol was included. No significant change in AS was detected upon 1 h incubation in darkness when comparing medium without supplement, with mannitol, and with sucrose (Figure 6A). In line with the previous findings, light exposure resulted in a pronounced AS shift already after 1 h of illumination. Interestingly, at the 6 h time point, the sugar-treated and dark-kept seedlings showed a pronounced AS shift in the same direction and of a similar extent as observed in light without sugar supply. For several events, the presence of both sugar and light caused an even stronger AS shift than the single treatments (Supplemental Table 5).

Many of the light-induced AS events are expected to be coupled to NMD. To test if the AS shift under these conditions might be, at least to some extent, a consequence of altered NMD activity, we compared the AS response to light and sucrose in etiolated wild-type and NMD mutant seedlings. Analysis of three predicted AS-NMD events revealed identical AS shifts in wild-type and *lba1* seedlings upon exposure to light and sucrose (Supplemental Figure 10), irrespective of the accumulation of the predicted NMD variant in the *lba1* mutant. These data and the separate quantitation of splicing variants (Supplemental Figure 5) indicate that the changes occur on the level of AS and not downstream of it.

The strong effect of sucrose feeding on the AS output is in line with a previous study, suggesting that retrograde signaling contributes to AS control in light-grown plants (Petrillo et al., 2014b). Accordingly, light-mediated AS is suppressed in green plants upon chemical inhibition of photosynthesis by DCMU (Petrillo et al., 2014b; Supplemental Figure 11). Treatment of etiolated seedlings with the same inhibitor also slightly weakened, yet did not completely abolish the AS shift in our study (Supplemental Figure 11). The weaker suppression of light-mediated AS by DCMU in etiolated seedlings might be explained by the absence of an active photosynthesis apparatus. Indeed, different effects of DCMU on light- and dark-grown plants have been described before (Mancinelli, 1994). Alternatively, upon disruption of photosynthesis, photoreceptor-mediated AS control might become detectable in etiolated seedlings, but not in light-grown plants.

We next tested the effect of different sugars on the AS output. Treatment of etiolated seedlings with sucrose, glucose, or trehalose in the absence or presence of light revealed that sucrose was most effective (Figure 6B). Exposure to 0.2% sucrose caused

Figure 4. (continued).

normalized to the one measured for the corresponding wild type at 0 h on plates without sucrose, separately for each replicate of wild-type and *phyA phyB* sample sets. In **(B)**, ratios were normalized to the mean value of the wild-type replicates at 0 h (− Suc). Displayed are mean values + SD **([A]**, $n = 5$ to 7 for *SR30* and *RRC1*; other candidates: $n = 3$; **[B]**, $n = 4$ for *SR30*; other candidates $n = 3$; **[C]**, $n = 3$). P values: *P < 0.05, **P < 0.01, ***P < 0.001, comparing the wild type and *phyA phyB* in an independent *t* test, or, if the wild type is set to 1, in a one-sample *t* test.

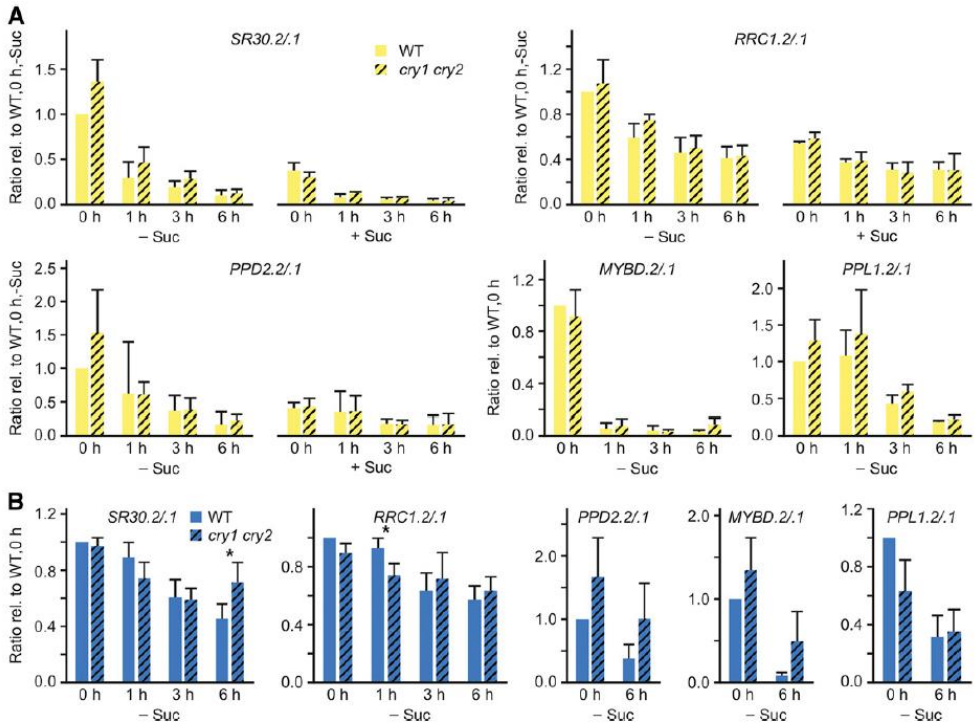

Figure 5. AS Shifts in Response to White Light Are Comparable in Wild-Type and *cry1 cry2* Seedlings.

Etiolated seedlings grown on plates with or without 2% sucrose for 6 d were exposed to ~130 μmol m^{-2} s^{-1} white **(A)** or ~4 μmol m^{-2} s^{-1} blue **(B)** light for the indicated periods. Splice variants of the indicated genes were coamplified and quantified using a Bioanalyzer. AS ratios were normalized to the one measured for wild-type at 0 h on plates without sucrose. Displayed are mean values + SD ($n = 3$ to 4). Statistical comparison of the wild type and *cry1 cry2* using independent *t* test, or, if the wild type is set to 1, in a one-sample *t* test (*$P < 0.05$).

a strong AS shift, which was further enhanced in the presence of 2% sucrose (Figure 6B). Glucose feeding caused a slightly weaker AS shift than sucrose. We also treated seedlings with trehalose to trigger accumulation of trehalose 6-phosphate (Schluepmann et al., 2004), which has previously been described as a signal for carbon availability (Schluepmann et al., 2012); however, trehalose exposure had only a minor effect on the splicing outcome. Based on these findings, we postulate that the AS output might be regulated in response to the plant's energy supply, possibly mediated by the level of sucrose, the major transport form of photoassimilates.

Upstream Signaling Involved in Light- and Sugar-Mediated AS Changes

Both sugar feeding and light-driven photosynthesis alter the plant's energy signaling, which might be an integration point resulting in the AS changes observed here. Independently acting systems for sensing the plant's energy status have been described, including HEXOKINASE1 (HXK1) and SUCROSE-NON-FERMENTATION1-RELATED KINASE1 (SnRK1; Sheen, 2014). To test their potential relevance under the conditions of our experiments, transcript levels of *HXK1*, *CHLOROPHYLL A/B BINDING PROTEIN1* (*CAB1*), which is known to be induced by light (Brusslan and Tobin, 1992), and the SnRK1 targets *DARK INDUCED1* (*DIN1*) and *DIN6* were measured in seedlings transferred to control or supplemented media and incubated for 6 h in light or darkness (Figure 6C; Supplemental Figure 12). Expression levels of *HXK1* were unaffected by both sugar and light, while *CAB1* transcript levels were elevated only in response to light. However, *DIN1* and *DIN6* levels correlated with the AS pattern shifts, altering in response to sugar and light. *DIN1* and *DIN6* transcript levels were reduced in response to light and, to an even greater extent, upon sugar exposure. As for the AS shifts, the maximum effect was visible when both sugar and light were supplied. The light- and sugar-responsive expression patterns of *DIN1* and *DIN6* are in agreement with previous reports (Thum et al., 2003; Baena-González et al., 2007).

The resemblance of the AS and DIN expression changes in response to light and sugar application would be in line with a coupling of these processes, which we first tested using a *snrk1.1* mutant. Molecular characterization of the *snrk1.1-3* mutant revealed that the T-DNA insertion resulted in an altered transcript and no detectable SnRK1.1 protein (Supplemental Figures 13 and 14). Comparing the AS patterns in etiolated wild-type and *snrk1.1-3* seedlings showed a slightly different sugar

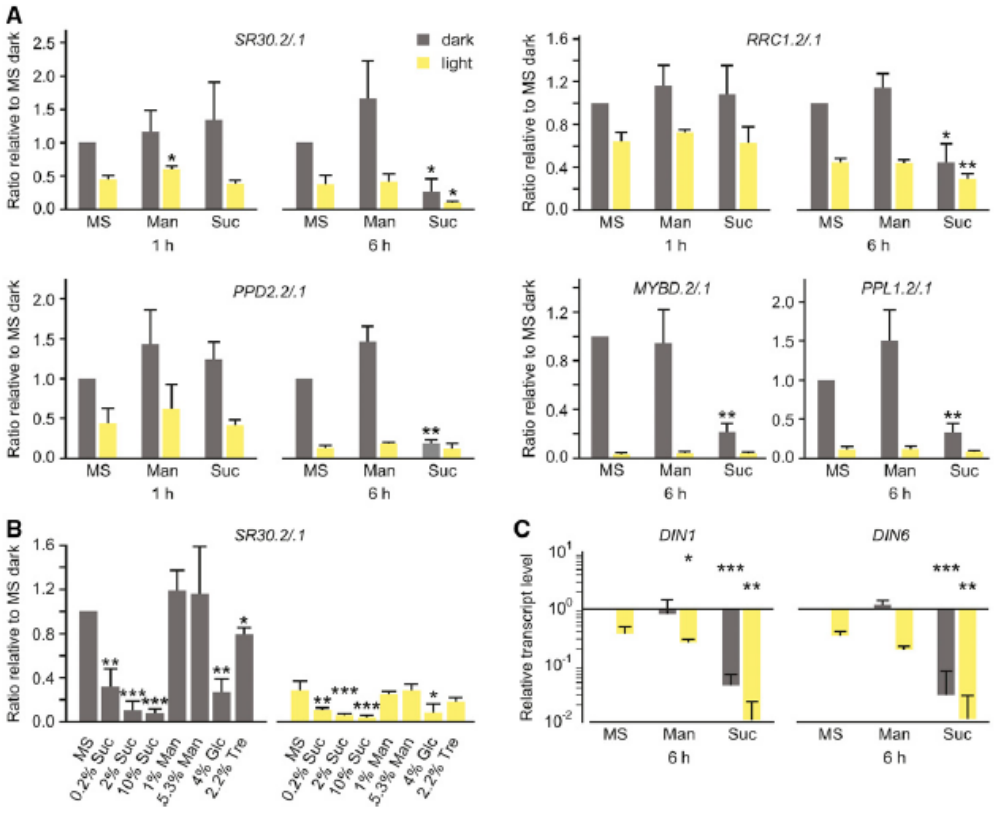

Figure 6. Sucrose and Light Cause Comparable AS Shifts.

(A) Seedlings were grown in darkness for 6 d and afterwards incubated in control medium (MS), mannitol (Man), or sucrose (Suc) solutions for 1 or 6 h in darkness or ~130 μmol m^{-2} s^{-1} white light. Alternative splice forms were coamplified and quantified using a Bioanalyzer. Ratios were normalized to the corresponding control samples in darkness. Color scheme for dark (gray) and light (yellow) samples applies to all panels. Displayed are mean values ($n = 3$). Error bars are SD; P values: *P < 0.05, **P < 0.01, and ***P < 0.001 comparing mannitol and sucrose to the MS light and dark samples, respectively. Tests are independent *t* tests when not tested against 1, and one-sample *t* test when tested against 1. Detailed results from the statistical analysis are provided in Supplemental Table 5.
(B) AS analysis of *SR30* in seedlings grown in darkness and incubated in control medium (MS), sucrose (Suc), mannitol (Man), glucose (Glc), or trehalose (Tre) solutions for 6 h in darkness or ~130 μmol m^{-2} s^{-1} white light. Data are normalized to MS sample in darkness. Displayed are mean values ($n = 3$ to 5) + SD. Statistical comparison between MS and different sugars as detailed in **(A)**; dark and light samples were analyzed separately.
(C) RT-qPCR analysis of transcript levels for SnRK1.1 targets. Sample description and data normalization, depiction, and statistical analysis as described in **(A)**. Data displayed on a log scale.

response in darkness (Supplemental Figure 15A). However, both the AS and DIN expression responses (Supplemental Figure 15B) were overall similar in wild-type and mutant seedlings, suggesting remaining activity of the mutant allele or functional redundancy of the two close homologs SnRK1.1 and SnRK1.2. In line with this notion, previous studies have shown that the *snrk1.1-3* mutant does not have an obvious growth phenotype (Mair et al., 2015) and that plants are impaired in development and stress responses only upon transient knockdown of both SnRK1.1 and SnRK1.2 (Baena-González et al., 2007).

Signaling through SnRK1 is dependent on its kinase activity and can be disrupted by treatment with the kinase inhibitor K252a (Baena-González et al., 2007). Thus, chemical inhibition of SnRK1 is expected to mimic its inactivation under conditions of increased energy availability. However, it should be noted that K252a has a broad target spectrum, resulting in the inhibition of various kinases, and not exclusively SnRK1. Treatment of etiolated seedlings with K252a in the dark changed the AS ratio for *SR30*, *PPD2*, and *MYBD* as sucrose supply or light exposure did (Figure 7). Furthermore, in the presence of K252a, the effect of sucrose supply in darkness on the AS ratio of *SR30* and *PPD2* was significantly enhanced compared with the corresponding controls without inhibitor. An additional effect of K252a on the AS ratio was also observed for some of the light-treated samples. In the case of *RRC1* and *PPL1*, K252a treatment changed AS into the opposite direction compared with sucrose and light treatment. These different AS responses could be explained by the involvement of distinct sets of splicing factors and their regulation upon inhibitor treatment in a SnRK1-dependent and -independent manner, in line with the broad target spectrum of K252a. Thus, generation of

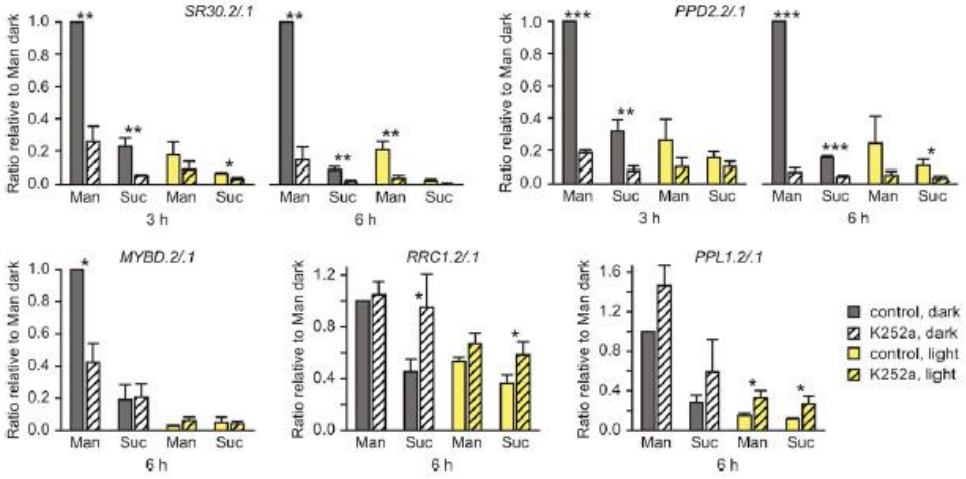

Figure 7. Light- and Sucrose-Regulated AS Involves Kinase Signaling.

Wild-type seedlings were grown in darkness and then incubated in control medium (mannitol [Man]) or sucrose (Suc) solution for 3 or 6 h in darkness or ~130 μmol m^{-2} s^{-1} white light. Incubation was performed in the absence (control) or presence of the kinase inhibitor K252a. AS ratios were determined as described before and are normalized to corresponding Man dark samples. Displayed are mean values + SD ($n = 3$); P values: *P < 0.05, **P < 0.01, and ***P < 0.001 comparing control and K252a treatment. Significant differences determined using independent *t* tests when not tested against 1, and one-sample *t* test when tested against 1.

a mutant specifically impaired in both SnRK1.1 and SnRK1.2 activities will be needed to test for a direct role of SnRK1 signaling in these splicing pattern changes. Taken together, our data suggest that in plants AS represents an integration point of multiple signaling pathways that are responsive to altered energy availability.

DISCUSSION

Photomorphogenesis Induces Complex Transcriptome Changes on the Levels of Gene Expression and AS

Previous microarray studies revealed that a substantial proportion of the Arabidopsis genome is expressed in a light-dependent manner (Ma et al., 2001; Tepperman et al., 2001; Jiao et al., 2005, 2007). Genome-wide profiling based on oligonucleotide microarrays suggested that ~20% of all genes from Arabidopsis and rice are differentially expressed in comparison of seedlings undergoing skoto- or photomorphogenesis (Jiao et al., 2005). In this study, we used RNA-seq to determine transcriptome profiles in the early phase of photomorphogenesis, induced by exposure of etiolated Arabidopsis seedlings to blue, red, or white light. We found that 18.4% of all expressed genes show an at least 2-fold increase or decrease of total transcript levels in response to 6 h light exposure for one or several light conditions. Accordingly, the extent of light-modulated gene expression seems to be comparable in the transition phase and upon constant growth in different light regimes. When comparing different light qualities, blue and red light affected similar numbers of genes, with a substantial gene overlap. This observation is in agreement with previous studies showing that only relatively few genes are specifically regulated by monochromatic light (Ma et al., 2001; Jiao et al., 2005). Furthermore, we found that most of the genes showing altered expression upon exposure to blue and red light, but also many additional genes, were responsive to white light. The finding that white light is most effective can be explained by the activation of both blue and red light signaling as well as by the higher intensity of white light, which was used to analyze the seedling response under standard illumination conditions.

Analysis of our RNA-seq data further revealed that the photomorphogenic response is not only accompanied by differential expression of numerous genes but also involves massive AS changes. Illuminating etiolated seedlings for 6 h caused significant changes in 700 AS events under at least one light condition. Upon additional filtering for the effect size, most regulated AS events were altered under all three light conditions. Interestingly, several AS events showed weaker quantitative changes under red light compared with blue and white light. We used intensities of blue and red light that are expected to overall saturate the effect on hypocotyl elongation. However, this does not exclude that stronger and/or additional AS shifts may be detected upon exposure of etiolated seedlings to monochromatic light of higher intensities due to photoreceptor-dependent and -independent signaling. Comparison of the sets of genes displaying light-modulated gene expression and AS highlighted the existence of mostly distinct and few common targets. This overlap might be even lower, considering that many AS variants from Arabidopsis have been reported to be targeted by NMD (Kalyna et al., 2012; Drechsel et al., 2013). Accordingly, AS shifts affecting the formation of destabilized transcripts are also expected to change total steady state transcript levels.

To test for a role of coupled AS-NMD in light-responsive gene control, we analyzed which types of AS events are affected and whether this has an effect on the presence of NMD-triggering features. Instances of light-regulated AS were enriched for intron retention and cassette exon events, both of which are known to frequently introduce NMD target features (Kalyna et al., 2012; Drechsel et al., 2013). For example, splicing factors from the family of POLYPYRIMIDINE TRACT BINDING PROTEINS, such as PTB1 and PTB2 from Arabidopsis, activate inclusion of so-called poison exons in their corresponding pre-mRNAs, thereby introducing PTCs and rendering the transcripts sensitive to NMD (Stauffer et al., 2010). The auto- and cross-regulatory mechanism allows balancing of gene expression based on coupled AS-NMD and has been frequently observed for splicing factors from animals and plants (Staiger et al., 2003; Lareau et al., 2007; Isken and Maquat, 2008; Schöning et al., 2008; Palusa and Reddy, 2010; Wachter et al., 2012). Regarding the direction of AS changes, the majority of light-regulated cassette exon and intron retention events resulted in skipping and splicing, respectively, upon light exposure. Interestingly, a previous study in *P. patens* showed the opposite effect for intron retention events, i.e., preferential intron retention upon light exposure (Wu et al., 2014).

Based on the predominant AS shifts observed in our study, we anticipated that light exposure reduces the number of transcripts containing NMD-triggering features. Implementing the AS events into the corresponding full-length transcripts further corroborated this assumption: 77.2% of the light-responsive AS events exhibited NMD target features for the splicing variants being relatively more abundant in darkness. Furthermore, 61.1% of the significant events showed a light-dependent relative shift from a splicing variant containing NMD-eliciting features to an mRNA without such characteristics. It will be interesting to test how many of these transcripts are indeed regulated by NMD, and to what extent accumulation of the corresponding proteins is affected by the changes in AS-NMD. Based on the large number of light-regulated AS events affecting the presence of NMD target features, it seems likely that the expression of numerous genes can be restricted by the formation of NMD-regulated splicing variants in darkness, whereas light shifts the AS outcome toward a more stable mRNA and translation into the corresponding factors. The involvement of coupled AS-NMD in light-triggered processes further expands the functions of NMD, which is increasingly recognized as an important regulator of physiological transcripts besides its role in RNA surveillance (Drechsel et al., 2013; Karam et al., 2013; Gloggnitzer et al., 2014; Sureshkumar et al., 2016). Furthermore, alternative strategies for preventing the translation of unproductive transcripts have been described in plants, in particular nuclear retention of intron-containing transcripts (Göhring et al., 2014). Thus, different mechanisms might contribute to the regulation of gene expression by targeting AS variants predominantly produced in etiolated seedlings.

Light-Dependent AS Defines Expression of Splicing Factors and Is Critical for Light Signaling

The genes containing light-dependent AS events showed an overrepresentation of the functional category "RNA," including several splicing factors. This observation is in line with previous studies showing extensive and regulated AS for the pre-mRNAs of many splicing factors (Reddy and Shad Ali, 2011; Syed et al., 2012; Wachter et al., 2012; Reddy et al., 2013; Staiger and Brown, 2013; Mancini et al., 2016), which allows quantitative gene control by coupling to NMD (see above) but might also increase their functional diversity. Interestingly, among our candidates was RRC1, a putative splicing factor that had previously been identified as a component of PHYB signaling (Shikata et al., 2012a, 2012b). Here, we demonstrated that the corresponding AS event gives rise to one splicing variant that is degraded via NMD, whereas light promotes the formation of the transcript resulting in RRC1 protein. Complementation experiments using an *rrc1* mutant revealed that only the light-induced splicing variant is able to rescue the mutant defect in red light signaling. Accordingly, generation of this PHY signaling component is limited due to coupled AS-NMD in darkness. The light-mediated AS change is expected to allow increased formation of the RRC1 protein, which, because of its function as a positive regulator of PHY signaling, should further enhance the light response. Previous work showed that the C-terminal arginine/serine-rich (RS) domain of RRC1 is required for its function in PHYB signaling (Shikata et al., 2012a, 2012b). In general, the RS domain of splicing factors is critical for their splicing regulatory activity (Graveley, 2000; Reddy and Shad Ali, 2011). Hypomorphic *rrc1* mutants lacking the RS domain displayed AS changes for several SR genes (Shikata et al., 2012b), indicating that RRC1 might be directly involved in the regulation of these AS events. Future work needs to address whether RRC1 is a key regulator of downstream light-modulated AS events and what the molecular links to red light signaling are. Analyzing the sequence context of light-regulated AS events identified several enriched motifs (Supplemental Table 6), which might serve as binding sites for RRC1 or other splicing factors involved in this process.

AS Is a Converging Point for Processes Affecting Plant Energy Signaling

Our study revealed that AS of numerous genes is altered upon illumination of etiolated seedlings and, in the case of *RRC1*, can modulate light signaling. To gain a better understanding of light-triggered AS, the upstream regulatory components need to be identified. Two recent studies analyzing light-induced AS in *P. patens* (Wu et al., 2014) and etiolated Arabidopsis seedlings (Shikata et al., 2014) suggested the involvement of PHY photoreceptors. Notably, comparison of AS changes in wild-type and *phyA phyB* mutants upon exposure to red light actually identified a larger number of PHY-independent than PHY-dependent events (Shikata et al., 2014; Supplemental Data Set 7): Upon 1 h red light exposure, 1505 and 1714 genes were reported to give rise to PHY-dependent and PHY-independent AS events, respectively. An even lower fraction of PHY-dependent AS events were found upon 3 h red light exposure, triggering AS changes in 1116 and 2098 genes in a PHY-dependent and PHY-independent manner, respectively. Surprisingly, most of the events defined to be PHY-dependent were changed only after 1 or 3 h, raising the question of what the functions of numerous, short-lived AS changes might be. Analysis of the data from Shikata et al. (2014) using our pipeline detected far fewer AS changes and an increase in the number of

events from the 1 h to the 3 h time point (Supplemental Data Set 7). The latter is expected, as changes in RNA steady state levels are limited by the RNA stability and as a consequence of downstream signaling. Both the order of magnitude of regulated AS events and an increase in detectable AS changes over time are in agreement with the results from our RNA-seq data. Shikata et al. (2014) defined AS events to be PHY-dependent when the direction of change was identical in the comparison of dark versus light in the wild type and *phyA phyB* versus the wild type in light. We used an alternative constraint for calling events PHY-dependent, which is the occurrence of light-induced AS in the wild type, but not in the *phyA phyB* mutant. Using this definition and our analysis pipeline, we identified 329 PHY-dependent and 11 PHY-independent AS changes upon 3 h of red light exposure from the RNA-seq data generated by Shikata et al. (2014) (Supplemental Data Set 7). Thus, according to our analysis, almost all AS changes detected upon exposure to red light of this intensity are PHY-dependent.

By contrast, light-triggered AS changes in plants grown in light/dark cycles were shown to be independent of photoreceptors (Petrillo et al., 2014b; Mancini et al., 2016). Based on our data, the PHYA/B and CRY photoreceptors also play no major role in AS control during photomorphogenesis in normal light conditions. AS changes in response to white light were identical in the wild type compared with *phyA phyB* and *cry1 cry2* mutants, which are defective in the major red and blue light receptors, respectively. Analysis of red-light-responsive AS for a splicing factor gene in a *phy* quintuple mutant from Arabidopsis also excluded, at least in light-grown plants, a role of the other PHYs in this process (Mancini et al., 2016). We observed that a contribution of PHYA/B to light-mediated AS is only detectable under red and far-red light. For most candidates, AS changes in response to red light were less pronounced in *phyA phyB* than in the wild type. Similarly, blue light induced slightly weaker AS shifts in *cry1 cry2* compared with the wild type, albeit this difference was not statistically significant for most events. An even weaker or no AS shift in *phyA phyB* seedlings exposed to red light was shown in the validation experiments from Shikata et al. (2014). Moreover, our analysis of the RNA-seq data from Shikata et al. (2014) revealed that 97% of the AS changes in red light are PHY-dependent (see above). The varying degree of PHY-mediated AS control upon exposure to red light can most likely be attributed to the use of different light intensities, as 8.3 and ~28 $\mu mol\, m^{-2}\, s^{-1}$ red light, respectively, was used by Shikata et al. (2014) and in our corresponding downstream analyses. Higher intensities of red light might result in an increased PHY response, but also enhance PHY-independent signaling. Accordingly, a stronger activation of photosynthesis at higher light intensities might explain the reduced PHY-dependency of the AS changes under this condition. Furthermore, we found that in response to far-red light, most AS events were unchanged in the *phyA phyB* mutant, while wild-type seedlings showed similar AS shifts as under white light. Taken together, our data suggest that PHYs and presumably also CRYs can induce AS changes; however, this effect becomes detectable only in artificial monochromatic light conditions. Accordingly, alternative signaling routes must exist and are active under more natural, white light conditions, outweighing the effect photoreceptors have on AS.

Based on our findings, we propose that AS changes during photomorphogenesis in regular light conditions are primarily controlled by a metabolic signal that is derived from photosynthesis. A major role of PHYA/B and CRY photoreceptors only becomes visible under light conditions that do not, or only to a minor extent, support photosynthesis, namely, far-red light and relatively weak red light. Moreover, sugar feeding in darkness had a similar effect on the splicing patterns as light exposure. In line with our findings for etiolated seedlings, AS changes in light-grown plants were reported to depend on retrograde signaling from the chloroplast to the nucleus (Petrillo et al., 2014b). In contrast to light-grown plants, etiolated seedlings do not possess a fully developed photosynthesis system. This raises the question of how much time etiolated seedlings need to set up photosynthesis and thereby alter metabolic signaling. While we are not aware of studies reporting the onset of photosynthesis in Arabidopsis seedlings undergoing photomorphogenesis, previous reports on other plant species suggested that photochemical activity of the photosystems is already detectable a few minutes after illumination of etiolated seedlings (Baker and Butler, 1976). In barley (*Hordeum vulgare*), the first CO_2 assimilates were detected 1 h after light exposure (Biggins and Park, 1966). Accordingly, we assume that photosynthesis is activated within the first hours of light exposure, resulting in altered metabolic signaling and changing AS patterns. Interestingly, previous studies described metabolic repression of photoreceptor signaling (Sheen, 1990; Harter et al., 1993; Dijkwel et al., 1997), which might further limit the role of photoreceptors in the light regulation of AS under photosynthesis-competent conditions. The crosstalk between carbon and light signaling can also substantially change during plant development, as reported for the sugar- and light-responsive transcript levels of three genes in etiolated seedlings compared with light-grown plants (Thum et al., 2003). Similarly, the contribution of different signaling pathways in light-mediated AS might be altered during photomorphogenesis.

Testing the effect of different sugars, we observed that exogenous supply of sucrose caused the most pronounced AS shifts. Exposure of etiolated seedlings to both light and sugar resulted in even stronger AS shifts than the single treatments for most events. This finding can be explained by the existence of independent signaling pathways. Alternatively, the single treatments may not have resulted in saturated responses, e.g., as a consequence of limited photosynthesis or inefficient sugar uptake and transport in the seedlings. Taking into account that already the single treatments resulted in very pronounced AS changes for most candidates, further work will need to examine whether an even stronger AS shift is of functional relevance. At least some of the AS events might allow a gradual response due to the integration of multiple signaling pathways.

Furthermore, we demonstrated that the AS patterns correlated with the expression of *DIN* genes, which are targets of SnRK1, a central integrator of energy and stress signaling (Sheen, 2014). Previous work revealed inactivation of SnRK1 under conditions of high energy availability, in particular under light or upon sugar feeding in darkness (Baena-González et al., 2007; Sheen, 2014). Interestingly, we found for several genes that chemical inhibition of kinases caused similar AS shifts as supply of light or sugar, suggesting an important role of phosphorylation in the upstream signaling. However, as the kinase inhibitor used in our study is not specific for SnRK1 and because of the probable functional

redundancy of SnRK1.1 and SnRK1.2, further work will be required to test a direct link between SnRK1 signaling and light-/sugar-triggered AS changes. Notably, a role of AS in sugar responses is also supported by the findings that the splicing factor SR45 negatively regulates glucose signaling (Carvalho et al., 2010) and modulates SnRK1 protein stability in Arabidopsis (Carvalho et al., 2016). SnRK1-mediated metabolic adjustment has been described to involve direct phosphorylation of key enzymes in metabolism (Sugden et al., 1999; Harthill et al., 2006) and differential transcriptional programs (Polge and Thomas, 2007; Baena-González and Sheen, 2008; Mair et al., 2015). Based on our findings, changes in the AS program, mediated through SnRK1 and/or other kinases, might provide an additional and powerful means to adjust metabolism to the plant energy supply.

METHODS

Plant Cultivation and Experiments

Generally, seeds were sterilized in 3.75% NaClO and 0.01% Triton X-100 and plated on 0.5× MS medium containing 0.8% phytoagar (Duchefa) with or without 2% sucrose added. Sucrose-containing medium was used for the RNA-seq and validation (Figures 2 and 3) experiments. The experiments with the photoreceptor mutants (Figures 4 and 5) were performed in parallel with seedlings grown on medium with and without sugar as indicated. Seeds were stratified for at least 2 d at 4°C, then germination was induced in white light for 2 h. Seedlings were grown in darkness for 6 d and then exposed to white, red, blue, or far-red light or kept in darkness for the indicated period. Darkness samples were taken in green light.

For hypocotyl assays, seeds were plated singly on plates without sucrose. After the initial 2 h light exposure, plates were placed in red light or in darkness for 6 d. The lines to be compared were grown on the same plates. Seeds were the same age. Seedlings were scanned after transfer to 0.5× MS plates with 1.5% agar. The length of scanned seedlings was measured using ImageJ (Schneider et al., 2012). All relative hypocotyl lengths are normalized to the average length of each line grown in darkness.

For transfer experiments and sugar treatments (Figures 6 and 7), seeds were plated densely on medium without sucrose and grown in darkness for 6 d after initial light exposure. Seedlings were transferred to liquid 0.5× MS medium without or with sugar supplementation under green light and incubated in white light or darkness for the indicated periods. For kinase inhibition, 4 μM K252a (dissolved in DMSO) was added; the corresponding mock sample was treated with DMSO only.

For DCMU treatment, light-grown seedlings were cultivated under long-day conditions in white light for 6 d on sucrose-free 0.5× MS plates. Subsequently, seedlings were transferred to 100 μM DCMU (stock dissolved in ethanol) or mock solution containing an equivalent concentration of ethanol, followed by 6 h incubation in darkness or white light. Etiolated seedlings were grown for 6 d in liquid medium (0.5× MS without sucrose) and darkness, followed by DCMU or mock treatment as described for the light-grown seedlings.

The following lines have been used in different experiments: *rrc1-2* (SALK_121526C, N667179), *lba1* (Yoine et al., 2006), *upf3-1* (SALK_025175), *lhy-null* (Yakir et al., 2009), *toc1-101* (Kikis et al., 2005), *prr7-3 prr9-1* (Farré et al., 2005), *phyA-211 phyB-9* (*phyA phyB*), *cry1-304 cry2-1* (*cry1 cry2*), and *snrk1.1-3* (GABI_579E09; Mair et al., 2015).

Light Conditions

Continuous white light had an intensity of ~130 μmol m^{-2} s^{-1}. For monochromatic light LED fields (Flora LED; CLF Plant Climatics) were used. Specifications: blue 420 to 550 nm, maximum (max) 463 nm, full width at half maximum (FWHM) 22.2 nm; far-red 680 to 790 nm, max 742 nm, FWHM 23.8 nm; red 620 to 730 nm, max 671 nm, FWHM 25 nm. Light intensities are provided in figure legends and have been measured with a Skye SKR1850, using the far-red channel for far red, and photosynthetically active radiation for blue, red, and white light. Red light intensity of ~10 μmol m^{-2} s^{-1} for hypocotyl assays was achieved by stacking plates with a layer of white paper between them.

RNA-Seq Analyses

Seedlings were grown in darkness for 6 d, then sampled (0h), or exposed to light for 1 (1h) or 6 h (6h), or kept in darkness for 6 h before sampling (6hD). RNA was extracted using the EURx GeneMATRIX Universal RNA purification kit. Starting from 4 μg total RNA, libraries were prepared using the Illumina TruSeq Kit v2 Box A mostly according to the manufacturer's instructions (Sample Preparation v2 Guide, September 2012). The PCR step was performed using only half the template in a reaction volume of 34 μL, and the libraries were subsequently purified on a 2% agarose gel. After cutting a band of appropriate size from the gel for each library, the DNA was extracted using the Qiagen MinElute gel extraction kit. Concentrations were determined using the Agilent 2100 Bioanalyzer with the DNA 1000 kit. RNA-seq libraries were prepared using the Illumina TruSeq kit and sequenced single end with 101-bp read length and a 7-bp index read on the HiSeq 2000, equipped with on-instrument HCS version 1.5.15 and real-time analysis (RTA) version 1.13. Cluster generation was performed on a cBot (recipe: SR_Amp_Lin_Block_Hyb_v8.0; Illumina) using a flow cell v3 and reagents from TruSeq SR Cluster Kits v3 (Illumina) according to the manufacturer's instructions. The final library DNA concentration was 7 to 8 pM on the flow cell. Samples were duplexed or quadruplexed using the adapters 012, 006, 019, and 005 (Supplemental Table 1). Each sample was run in biological duplicates.

We used a previously established pipeline for alignment, splice event calling, and analyses (Rühl et al., 2012; Drechsel et al., 2013). In short, RNA-seq reads were aligned to the TAIR10 reference genome using PALMapper (Jean et al., 2010) in two steps. First, an alignment was performed to discover novel splice junctions. Second, the novel splice junctions were included in the alignment to obtain a splice-sensitive alignment. Subsequently, novel splice events were called using SplAdder (Kahles et al., 2016), as also described by Drechsel et al. (2013). Read counts and differential AS events were determined using rDiff (Drewe et al., 2013). Differential gene expression was analyzed using DESeq (Anders and Huber, 2010). For a detailed description of parameter settings, see Computational Parameter Settings in the Supplemental Methods. To estimate the biological variance and thus determine accurate FDRs, the analyses of differential AS events and differential gene expression were performed jointly on all replicates of the samples that were to be compared.

For filtering the results, AS events with an FDR value below a certain threshold were required to not show changes in the opposite direction in any other light condition, i.e., (B_up < FDR and R_down > FDR and W_down > FDR) or (B_down < FDR and R_up > FDR and W_up > FDR) for events changing significantly in blue light. Data analysis was done using Excel (Microsoft) or Python (Anaconda distribution 2.1.0; Continuum Analytics) with SciPy (Jones et al., 2001), NumPy (van der Walt et al., 2011), Pandas (McKinney, 2010), Matplotlib (Hunter, 2007), IPython (Pérez and Granger, 2007), or DataJoint (Yatsenko et al., 2015).

Functional clustering using the MapMan software (Thimm et al., 2004) was done as previously described (Rühl et al., 2012; Drechsel et al., 2013) and as detailed in Supplemental Data Set 5. Extraction of NMD features and analysis of intergenic regions were performed as described by Drechsel et al. (2013).

The RNA-seq data described by Shikata et al. (2014) were kindly provided by Kousuke Hanada. Trimming was performed as described by Shikata et al. (2014). Subsequently, the data were analyzed as described for our RNA-seq data. In our analysis of the data described by Shikata et al.

(2014), we considered both read ends of the paired-end reads as two independent single-end reads.

Calculation of Splicing Index and Event Filtering

For determination of effect sizes, the SI was calculated for each event and light condition. SI is the ratio of the number of spliced alignments supporting the longer isoform, divided by all spliced alignments corresponding to this event. In case of intron retention events, the SI was determined as the average intron coverage divided by the average intron coverage plus the spliced alignments spanning the respective intron. As the reliability of the SI depends on the number of available alignments, no SI index was calculated when fewer than 10 isoform-specific reads were available. SI values for an event of the category "old" were only computed when the event could be confirmed in the respective read library, that is there was a sufficient number of alignments present in the new libraries to call the event.

For comparison of SI values of significantly changed AS events, the following filters were applied: All relevant replicates need to be assigned an SI value, and the variation in SI between replicates needs to be <0.25. Furthermore, to exclude splicing variants of low abundance or with minor changes, only those events with SI changes >0.05 were considered as having changed between dark and light samples. When combining data from different light qualities, events with opposite changes in SI >0.05 were excluded.

RNA Extraction, RT-qPCR, and PCR Product Analyses

RNA was extracted using the Universal RNA purification kit (EURx) with an on-column DNase digest as instructed by the manufacturer. Reverse transcription was done with RevertAid Premium (Thermo Fisher) or using AMV Reverse Transcriptase Native (EURx) for light-grown sets of wild-type and NMD mutant seedlings. The maximum volume of RNA template possible and a dT_{20} primer were used following the manufacturers' instructions.

RT-qPCRs were performed as described previously (Stauffer et al., 2010). In short, the Bio-Rad CFX384 real-time PCR system and MESA GREEN qPCR Mastermix Plus (Eurogentec) were used. *PP2A* (*AT1G13320*) transcript levels were measured for normalization.

RT-PCR fragments were separated and visualized on ethidium bromide-stained agarose or polyacrylamide gels. Isoform concentrations were measured using the Agilent 2100 Bioanalyzer with the DNA1000 kit. Oligonucleotides used are listed in Supplemental Table 7. Gel pictures were enhanced using the Adobe Photoshop autocontrast function.

Splice variants were subcloned using the pGEM-T Vector System I (Promega) or StrataClone PCR cloning kit (Agilent) and sequenced, or sequenced directly.

Statistical Analysis

Number of biological replicates (*n*), types of error bars, and statistical analyses are defined in the figure legends.

Cloning Procedures

RRC1 overexpression constructs are based on the vector pGWB612 (Nakamura et al., 2010). Oligonucleotide sequences are listed in Supplemental Table 7. Coding sequences of the splicing variants, with the 3′ UTR included, were amplified from cDNA, and the genomic sequence of *RRC1* was amplified from genomic DNA using primers 22/23 and recombined using the Gateway system (Invitrogen) into pDONR207, after PCR extension of the attachment sites with primers 24/25. Subsequently, *RRC1* sequences were recombined into pGWB612. For the complementation constructs under control of the endogenous promoter, an *RRC1* 1013-bp putative promoter fragment including the 5′ UTR was amplified using primers 26/27 and exchanged with the 35S promoter of pGWB612 using *Hin*dIII/*Xba*I. Subsequently, the cDNA or genomic sequence was introduced as for the overexpression constructs.

Plant Transformation

Arabidopsis plants were stably transformed by the floral dip method (Clough and Bent, 1998).

Protein Extraction and Immunoblot Analyses

For immunoblot analyses, proteins were extracted as described previously (Rühl et al., 2012), using the following buffers: RRC1 protein was extracted using a denaturing buffer as previously described (Shikata et al., 2012b) with Complete (Roche) as protease inhibitor. SnRK1.1 protein was extracted using 50 mM Tris-HCl (pH 7.5), 150 mM NaCl, 0.1% (v/v) Tween 20, and 0.1% (v/v) β-mercaptoethanol. All extracts were cleared by centrifugation for ~20 min at 15,000*g* and 4°C. SDS-PAGE and semidry immunoblotting were performed according to standard protocols. For detection, the following commercial antibodies were used: mouse α-HA (Sigma-Aldrich), rabbit α-SnRK1.1 (Agrisera), α-mouse-peroxidase (Sigma-Aldrich), α-rabbit-peroxidase (Sigma-Aldrich). Chemiluminescence detection used Super Signal West Dura (Pierce).

Data Access

Visualization of RNA-seq data is available at http://gbrowse.cbio.mskcc.org/gb/gbrowse/r403PAS/

Accession Numbers

RNA-seq data have been deposited in the Gene Expression Omnibus repository (http://www.ncbi.nlm.nih.gov/geo) under accession number GSE70575. A list of all analyzed genes is provided in Supplemental Data Sets 1 and 2.

Supplemental Data

Supplemental Figure 1. Light-Triggered AS Changes Using Different Filter Criteria.

Supplemental Figure 2. Properties of AS Events.

Supplemental Figure 3. Light-Dependent Changes in Total Transcript Levels.

Supplemental Figure 4. Sequences of Splicing Variants Identified.

Supplemental Figure 5. Changes in Splicing Variant Levels of *RRC1* and *SR30* in Response to White, Blue, and Red Light.

Supplemental Figure 6. Overexpression of *RRC1* Does Not Affect Hypocotyl Length.

Supplemental Figure 7. Complementation of the *rrc1-2* Mutant Using Constructs under Control of the Endogenous Promoter.

Supplemental Figure 8. AS Shifts in Response to White Light Are Comparable in the Wild Type and Photoreceptor Mutants.

Supplemental Figure 9. Circadian Regulators Do Not Majorly Influence Light-Dependent AS of Select Candidates.

Supplemental Figure 10. Light- and Sucrose-Triggered AS Changes Are Comparable in Wild-Type and NMD Mutant Seedlings.

Supplemental Figure 11. DCMU Treatment Reduces Light-Dependent AS Changes in Light- and Dark-Grown Arabidopsis Seedlings.

Supplemental Figure 12. Transcript Levels of *HXK1* and *CAB1* in Response to Sucrose and Light.

Supplemental Figure 13. Analysis of the T-DNA Insertion Mutant *snrk1.1-3*.

Supplemental Figure 14. Genomic, Transcript, and Protein Sequences for the Wild-Type *SnRK1.1* and the Mutant *snrk1.1-3* Alleles.

Supplemental Figure 15. AS Patterns and *DIN* Expression in the *snrk1.1-3* Mutant.

Supplemental Table 1. Alignment Statistics for RNA-Seq Data.

Supplemental Table 2. Frequencies of AS Types in Different Data Sets.

Supplemental Table 3. Light-Regulated AS Events of "Exitron" Type.

Supplemental Table 4. Genes Underlying Circadian Regulation Are Not Differentially Expressed in Darkness.

Supplemental Table 5. Statistical Comparison of AS Changes in Response to Light and Sugar.

Supplemental Table 6. Motifs Enriched in Light-Regulated AS Events.

Supplemental Table 7. Sequences of DNA Oligonucleotides.

Supplemental Methods. Computational Parameter Settings.

The following materials have been deposited in the DRYAD repository under accession number http://dx.doi.org/10.5061/dryad.4nt0f.

Supplemental Data Set 1. Computational Analysis of Transcriptome-Wide AS.

Supplemental Data Set 2. Computational Analysis of Transcriptome-Wide Differential Gene Expression.

Supplemental Data Set 3. Splicing Index Analysis.

Supplemental Data Set 4. Analysis of NMD Target Features and Overlap between NMD- and Light-Regulated AS.

Supplemental Data Set 5. Categorization of Light-Regulated and Reference Gene Sets into Functional Subgroups.

Supplemental Data Set 6. Expressed Intergenic Regions.

Supplemental Data Set 7. Computational Analysis of Transcriptome-Wide AS Changes in Response to Red Light Based on the Data from Shikata et al. (2014).

ACKNOWLEDGMENTS

We thank Christa Lanz, Jens Riexinger, and the Genome Center (Max Planck Institute for Developmental Biology) for performing the Illumina sequencing and Vipin T. Sreedharan for visualization of the RNA-seq data in GBrowse. We thank the Nottingham Arabidopsis Stock Centre for providing seeds of the *rrc1*, *lba1*, and *upf3* mutants described in this work. Andreas Hiltbrunner provided seeds of the *phyA phyB* and *cry1 cry2* mutants, Hugh G. Nimmo and Allan James provided circadian mutants, and Elena Baena-Gonzalez provided the *snrk1.1-3* mutant. We also thank Gabriele Drechsel for help with MapMan, Anja Possart and Virtudes Mira-Rodado for help with the LED fields, Natalie Faiss for technical support, and Andreas Hiltbrunner, Sascha Laubinger, and Klaus Harter for discussion of our findings. Furthermore, we thank the central facilities of the Center for Plant Molecular Biology (University of Tübingen), the Max Planck Society, the Memorial Sloan Kettering Cancer Center, and the ETH Zürich. This work was supported by the German Research Foundation (Deutsche Forschungsgemeinschaft) (WA 2167/4-1, SFB#1101, TP C03) and a Heisenberg fellowship (WA 2167/8-1) to A.W., RA1894/2-1 to G.R., and by the Memorial Sloan Kettering Cancer Center and ETH Zürich to G.R.

AUTHOR CONTRIBUTIONS

L.H., P.D.-B., G.R., and A.W. designed research. L.H., T.W., G.W., S.G., H.-C.L., and D.M.O. performed experiments. P.D.-B., A.K., J.B., L.H., and F.H.S. performed computational analyses. A.W. and L.H. wrote the manuscript. All authors contributed to data analysis and discussion.

Received June 23, 2016; revised October 7, 2016; accepted October 31, 2016; published November 1, 2016.

REFERENCES

Anders, S., and Huber, W. (2010). Differential expression analysis for sequence count data. Genome Biol. **11:** R106.

Bae, G., and Choi, G. (2008). Decoding of light signals by plant phytochromes and their interacting proteins. Annu. Rev. Plant Biol. **59:** 281–311.

Baena-González, E., and Sheen, J. (2008). Convergent energy and stress signaling. Trends Plant Sci. **13:** 474–482.

Baena-González, E., Rolland, F., Thevelein, J.M., and Sheen, J. (2007). A central integrator of transcription networks in plant stress and energy signalling. Nature **448:** 938–942.

Baker, N.R., and Butler, W.L. (1976). Development of the primary photochemical apparatus of photosynthesis during greening of etiolated bean leaves. Plant Physiol. **58:** 526–529.

Biggins, J., and Park, R.B. (1966). CO_2 assimilation by etiolated *Hordeum vulgare* seedlings during the onset of photosynthesis. Plant Physiol. **41:** 115–118.

Briggs, W.R., and Christie, J.M. (2002). Phototropins 1 and 2: versatile plant blue-light receptors. Trends Plant Sci. **7:** 204–210.

Brusslan, J.A., and Tobin, E.M. (1992). Light-independent developmental regulation of cab gene expression in *Arabidopsis thaliana* seedlings. Proc. Natl. Acad. Sci. USA **89:** 7791–7795.

Carvalho, R.F., Carvalho, S.D., and Duque, P. (2010). The plant-specific SR45 protein negatively regulates glucose and ABA signaling during early seedling development in Arabidopsis. Plant Physiol. **154:** 772–783.

Carvalho, R.F., Szakonyi, D., Simpson, C.G., Barbosa, I.C., Brown, J.W., Baena-González, E., and Duque, P. (2016). The Arabidopsis SR45 splicing factor, a negative regulator of sugar signaling, modulates SNF1-Related Protein Kinase 1 stability. Plant Cell **28:** 1910–1925.

Clough, S.J., and Bent, A.F. (1998). Floral dip: a simplified method for Agrobacterium-mediated transformation of *Arabidopsis thaliana*. Plant J. **16:** 735–743.

de la Fuente van Bentem, S., Vossen, J.H., Vermeer, J.E., de Vroomen, M.J., Gadella, T.W., Jr., Haring, M.A., and Cornelissen, B.J. (2003). The subcellular localization of plant protein phosphatase 5 isoforms is determined by alternative splicing. Plant Physiol. **133:** 702–712.

Dijkwel, P.P., Huijser, C., Weisbeek, P.J., Chua, N.H., and Smeekens, S.C. (1997). Sucrose control of phytochrome A signaling in Arabidopsis. Plant Cell **9:** 583–595.

Drechsel, G., Kahles, A., Kesarwani, A.K., Stauffer, E., Behr, J., Drewe, P., Rätsch, G., and Wachter, A. (2013). Nonsense-mediated decay of alternative precursor mRNA splicing variants is a major determinant of the Arabidopsis steady state transcriptome. Plant Cell **25:** 3726–3742.

Drewe, P., Stegle, O., Hartmann, L., Kahles, A., Bohnert, R., Wachter, A., Borgwardt, K., and Rätsch, G. (2013). Accurate detection of differential RNA processing. Nucleic Acids Res. **41:** 5189–5198.

Duek, P.D., and Fankhauser, C. (2005). bHLH class transcription factors take centre stage in phytochrome signalling. Trends Plant Sci. **10:** 51–54.

Estavillo, G.M., et al. (2011). Evidence for a SAL1-PAP chloroplast retrograde pathway that functions in drought and high light signaling in Arabidopsis. Plant Cell **23:** 3992–4012.

Farré, E.M., Harmer, S.L., Harmon, F.G., Yanovsky, M.J., and Kay, S.A. (2005). Overlapping and distinct roles of PRR7 and PRR9 in the Arabidopsis circadian clock. Curr. Biol. **15:** 47–54.

Filichkin, S.A., Priest, H.D., Givan, S.A., Shen, R., Bryant, D.W., Fox, S.E., Wong, W.K., and Mockler, T.C. (2010). Genome-wide mapping of alternative splicing in *Arabidopsis thaliana*. Genome Res. **20:** 45–58.

Fisher, A.J., and Franklin, K.A. (2011). Chromatin remodelling in plant light signalling. Physiol. Plant. **142:** 305–313.

Foyer, C.H., Neukermans, J., Queval, G., Noctor, G., and Harbinson, J. (2012). Photosynthetic control of electron transport and the regulation of gene expression. J. Exp. Bot. **63:** 1637–1661.

Franklin, K.A., and Quail, P.H. (2010). Phytochrome functions in Arabidopsis development. J. Exp. Bot. **61:** 11–24.

Galvão, V.C., and Fankhauser, C. (2015). Sensing the light environment in plants: photoreceptors and early signaling steps. Curr. Opin. Neurobiol. **34:** 46–53.

Gan, X., et al. (2011). Multiple reference genomes and transcriptomes for *Arabidopsis thaliana*. Nature **477:** 419–423.

Gloggnitzer, J., Akimcheva, S., Srinivasan, A., Kusenda, B., Riehs, N., Stampfl, H., Bautor, J., Dekrout, B., Jonak, C., Jiménez-Gómez, J.M., Parker, J.E., and Riha, K. (2014). Nonsense-mediated mRNA decay modulates immune receptor levels to regulate plant antibacterial defense. Cell Host Microbe **16:** 376–390.

Göhring, J., Jacak, J., and Barta, A. (2014). Imaging of endogenous messenger RNA splice variants in living cells reveals nuclear retention of transcripts inaccessible to nonsense-mediated decay in Arabidopsis. Plant Cell **26:** 754–764.

Graveley, B.R. (2000). Sorting out the complexity of SR protein functions. RNA **6:** 1197–1211.

Harter, K., Talke-Messerer, C., Barz, W., and Schäfer, E. (1993). Light- and sucrose-dependent gene expression in photomixotrophic cell suspension cultures and protoplasts of rape (*Brassica napus* L.). Plant J. **4:** 507–516.

Harthill, J.E., Meek, S.E., Morrice, N., Peggie, M.W., Borch, J., Wong, B.H., and Mackintosh, C. (2006). Phosphorylation and 14-3-3 binding of Arabidopsis trehalose-phosphate synthase 5 in response to 2-deoxyglucose. Plant J. **47:** 211–223.

Heijde, M., and Ulm, R. (2012). UV-B photoreceptor-mediated signalling in plants. Trends Plant Sci. **17:** 230–237.

Hoecker, U. (2005). Regulated proteolysis in light signaling. Curr. Opin. Plant Biol. **8:** 469–476.

Hunter, J.D. (2007). Matplotlib: A 2D Graphics Environment. Comput. Sci. Eng. **9:** 90–95.

Imaizumi, T., Tran, H.G., Swartz, T.E., Briggs, W.R., and Kay, S.A. (2003). FKF1 is essential for photoperiodic-specific light signalling in Arabidopsis. Nature **426:** 302–306.

Isken, O., and Maquat, L.E. (2008). The multiple lives of NMD factors: balancing roles in gene and genome regulation. Nat. Rev. Genet. **9:** 699–712.

James, A.B., Syed, N.H., Bordage, S., Marshall, J., Nimmo, G.A., Jenkins, G.I., Herzyk, P., Brown, J.W., and Nimmo, H.G. (2012). Alternative splicing mediates responses of the Arabidopsis circadian clock to temperature changes. Plant Cell **24:** 961–981.

Jean, G., Kahles, A., Sreedharan, V.T., De Bona, F., and Rätsch, G. (2010). RNA-Seq read alignments with PALMapper. Curr. Protoc. Bioinformatics **11:** http://dx.doi.org/10.1002/0471250953.bi1106s32.

Jiao, Y., Lau, O.S., and Deng, X.W. (2007). Light-regulated transcriptional networks in higher plants. Nat. Rev. Genet. **8:** 217–230.

Jiao, Y., Ma, L., Strickland, E., and Deng, X.W. (2005). Conservation and divergence of light-regulated genome expression patterns during seedling development in rice and Arabidopsis. Plant Cell **17:** 3239–3256.

Jones, E., et al. (2001). SciPy: Open Source Scientific Tools for Python, 2001. http://www.scipy.org/.

Jung, K.-H., Bartley, L., Cao, P., Canlas, P., and Ronald, P. (2009). Analysis of alternatively spliced rice transcripts using microarray data. Rice (NY) **2:** 44–55.

Kahles, A., Ong, C.S., Zhong, Y., and Rätsch, G. (2016). SplAdder: identification, quantification and testing of alternative splicing events from RNA-Seq data. Bioinformatics **32:** 1840–1847.

Kalyna, M., et al. (2012). Alternative splicing and nonsense-mediated decay modulate expression of important regulatory genes in Arabidopsis. Nucleic Acids Res. **40:** 2454–2469.

Kami, C., Lorrain, S., Hornitschek, P., and Fankhauser, C. (2010). Light-regulated plant growth and development. Curr. Top. Dev. Biol. **91:** 29–66.

Karam, R., Wengrod, J., Gardner, L.B., and Wilkinson, M.F. (2013). Regulation of nonsense-mediated mRNA decay: implications for physiology and disease. Biochim. Biophys. Acta **1829:** 624–633.

Kikis, E.A., Khanna, R., and Quail, P.H. (2005). ELF4 is a phytochrome-regulated component of a negative-feedback loop involving the central oscillator components CCA1 and LHY. Plant J. **44:** 300–313.

Lareau, L.F., Inada, M., Green, R.E., Wengrod, J.C., and Brenner, S.E. (2007). Unproductive splicing of SR genes associated with highly conserved and ultraconserved DNA elements. Nature **446:** 926–929.

Lau, O.S., and Deng, X.W. (2012). The photomorphogenic repressors COP1 and DET1: 20 years later. Trends Plant Sci. **17:** 584–593.

Laubinger, S., Fittinghoff, K., and Hoecker, U. (2004). The SPA quartet: a family of WD-repeat proteins with a central role in suppression of photomorphogenesis in arabidopsis. Plant Cell **16:** 2293–2306.

Lepistö, A., and Rintamäki, E. (2012). Coordination of plastid and light signaling pathways upon development of Arabidopsis leaves under various photoperiods. Mol. Plant **5:** 799–816.

Lin, C., and Shalitin, D. (2003). Cryptochrome structure and signal transduction. Annu. Rev. Plant Biol. **54:** 469–496.

Liu, J., Jung, C., Xu, J., Wang, H., Deng, S., Bernad, L., Arenas-Huertero, C., and Chua, N.H. (2012a). Genome-wide analysis uncovers regulation of long intergenic noncoding RNAs in Arabidopsis. Plant Cell **24:** 4333–4345.

Liu, M.J., Wu, S.H., Chen, H.M., and Wu, S.H. (2012b). Widespread translational control contributes to the regulation of Arabidopsis photomorphogenesis. Mol. Syst. Biol. **8:** 566.

Ma, L., Li, J., Qu, L., Hager, J., Chen, Z., Zhao, H., and Deng, X.W. (2001). Light control of Arabidopsis development entails coordinated regulation of genome expression and cellular pathways. Plant Cell **13:** 2589–2607.

Mair, A., et al. (2015). SnRK1-triggered switch of bZIP63 dimerization mediates the low-energy response in plants. eLife **4:** 489–498.

Mancinelli, A. (1994). The physiology of phytochrome action. In Photomorphogenesis in Plants, 2nd ed, K.G. Kendrick, ed (Dordrecht, The Netherlands: Kluwer Academic Publishers), pp. 211–269.

Mancini, E., Sanchez, S.E., Romanowski, A., Schlaen, R.G., Sanchez-Lamas, M., Cerdán, P.D., and Yanovsky, M.J. (2016). Acute effects of light on alternative splicing in light-grown plants. Photochem. Photobiol. **92:** 126–133.

Mano, S., Hayashi, M., and Nishimura, M. (1999). Light regulates alternative splicing of hydroxypyruvate reductase in pumpkin. Plant J. **17:** 309–320.

Mano, S., Yamaguchi, K., Hayashi, M., and Nishimura, M. (1997). Stromal and thylakoid-bound ascorbate peroxidases are produced by alternative splicing in pumpkin. FEBS Lett. **413:** 21–26.

Marquez, Y., Brown, J.W., Simpson, C., Barta, A., and Kalyna, M. (2012). Transcriptome survey reveals increased complexity of the alternative splicing landscape in Arabidopsis. Genome Res. **22:** 1184–1195.

Marquez, Y., Höpfler, M., Ayatollahi, Z., Barta, A., and Kalyna, M. (2015). Unmasking alternative splicing inside protein-coding exons defines exitrons and their role in proteome plasticity. Genome Res. **25:** 995–1007.

McKinney, W. (2010). Data Structures for Statistical Computing in Python. In Proceedings of the 9th Python in Science Conference, pp. 51–56.

Monte, E., Al-Sady, B., Leivar, P., and Quail, P.H. (2007). Out of the dark: how the PIFs are unmasking a dual temporal mechanism of phytochrome signalling. J. Exp. Bot. **58:** 3125–3133.

Nagatani, A. (2004). Light-regulated nuclear localization of phytochromes. Curr. Opin. Plant Biol. **7:** 708–711.

Nakamura, S., Mano, S., Tanaka, Y., Ohnishi, M., Nakamori, C., Araki, M., Niwa, T., Nishimura, M., Kaminaka, H., Nakagawa, T., Sato, Y., and Ishiguro, S. (2010). Gateway binary vectors with the bialaphos resistance gene, bar, as a selection marker for plant transformation. Biosci. Biotechnol. Biochem. **74:** 1315–1319.

Paik, I., Yang, S., and Choi, G. (2012). Phytochrome regulates translation of mRNA in the cytosol. Proc. Natl. Acad. Sci. USA **109:** 1335–1340.

Palusa, S.G., and Reddy, A.S. (2010). Extensive coupling of alternative splicing of pre-mRNAs of serine/arginine (SR) genes with nonsense-mediated decay. New Phytol. **185:** 83–89.

Pérez, F., and Granger, B.E. (2007). IPython: A system for interactive scientific computing. J. Comput. Sci. Eng. **9:** 21–29.

Petrillo, E., Godoy Herz, M.A., Barta, A., Kalyna, M., and Kornblihtt, A.R. (2014a). Let there be light: regulation of gene expression in plants. RNA Biol. **11:** 1215–1220.

Petrillo, E., Godoy Herz, M.A., Fuchs, A., Reifer, D., Fuller, J., Yanovsky, M.J., Simpson, C., Brown, J.W., Barta, A., Kalyna, M., and Kornblihtt, A.R. (2014b). A chloroplast retrograde signal regulates nuclear alternative splicing. Science **344:** 427–430.

Polge, C., and Thomas, M. (2007). SNF1/AMPK/SnRK1 kinases, global regulators at the heart of energy control? Trends Plant Sci. **12:** 20–28.

Reddy, A.S., and Shad Ali, G. (2011). Plant serine/arginine-rich proteins: roles in precursor messenger RNA splicing, plant development, and stress responses. Wiley Interdiscip. Rev. RNA **2:** 875–889.

Reddy, A.S., Marquez, Y., Kalyna, M., and Barta, A. (2013). Complexity of the alternative splicing landscape in plants. Plant Cell **25:** 3657–3683.

Rizzini, L., Favory, J.J., Cloix, C., Faggionato, D., O'Hara, A., Kaiserli, E., Baumeister, R., Schäfer, E., Nagy, F., Jenkins, G.I., and Ulm, R. (2011). Perception of UV-B by the Arabidopsis UVR8 protein. Science **332:** 103–106.

Ruckle, M.E., and Larkin, R.M. (2009). Plastid signals that affect photomorphogenesis in *Arabidopsis thaliana* are dependent on GENOMES UNCOUPLED 1 and cryptochrome 1. New Phytol. **182:** 367–379.

Ruckle, M.E., Burgoon, L.D., Lawrence, L.A., Sinkler, C.A., and Larkin, R.M. (2012). Plastids are major regulators of light signaling in Arabidopsis. Plant Physiol. **159:** 366–390.

Rühl, C., Stauffer, E., Kahles, A., Wagner, G., Drechsel, G., Rätsch, G., and Wachter, A. (2012). Polypyrimidine tract binding protein homologs from Arabidopsis are key regulators of alternative splicing with implications in fundamental developmental processes. Plant Cell **24:** 4360–4375.

Sanchez, S.E., et al. (2010). A methyl transferase links the circadian clock to the regulation of alternative splicing. Nature **468:** 112–116.

Schluepmann, H., van Dijken, A., Aghdasi, M., Wobbes, B., Paul, M., and Smeekens, S. (2004). Trehalose mediated growth inhibition of Arabidopsis seedlings is due to trehalose-6-phosphate accumulation. Plant Physiol. **135:** 879–890.

Schluepmann, H., Berke, L., and Sanchez-Perez, G.F. (2012). Metabolism control over growth: a case for trehalose-6-phosphate in plants. J. Exp. Bot. **63:** 3379–3390.

Schneider, C.A., Rasband, W.S., and Eliceiri, K.W. (2012). NIH Image to ImageJ: 25 years of image analysis. Nat. Methods **9:** 671–675.

Schöning, J.C., Streitner, C., Meyer, I.M., Gao, Y., and Staiger, D. (2008). Reciprocal regulation of glycine-rich RNA-binding proteins via an interlocked feedback loop coupling alternative splicing to nonsense-mediated decay in Arabidopsis. Nucleic Acids Res. **36:** 6977–6987.

Sheen, J. (1990). Metabolic repression of transcription in higher plants. Plant Cell **2:** 1027–1038.

Sheen, J. (2014). Master regulators in plant glucose signaling networks. J. Plant Biol. **57:** 67–79.

Shen, H., Luong, P., and Huq, E. (2007). The F-box protein MAX2 functions as a positive regulator of photomorphogenesis in Arabidopsis. Plant Physiol. **145:** 1471–1483.

Shikata, H., Nakashima, M., Matsuoka, K., and Matsushita, T. (2012a). Deletion of the RS domain of RRC1 impairs phytochrome B signaling in Arabidopsis. Plant Signal. Behav. **7:** 933–936.

Shikata, H., Hanada, K., Ushijima, T., Nakashima, M., Suzuki, Y., and Matsushita, T. (2014). Phytochrome controls alternative splicing to mediate light responses in Arabidopsis. Proc. Natl. Acad. Sci. USA **111:** 18781–18786.

Shikata, H., Shibata, M., Ushijima, T., Nakashima, M., Kong, S.-G., Matsuoka, K., Lin, C., and Matsushita, T. (2012b). The RS domain of Arabidopsis splicing factor RRC1 is required for phytochrome B signal transduction. Plant J. **70:** 727–738.

Sibout, R., Sukumar, P., Hettiarachchi, C., Holm, M., Muday, G.K., and Hardtke, C.S. (2006). Opposite root growth phenotypes of hy5 versus hy5 hyh mutants correlate with increased constitutive auxin signaling. PLoS Genet. **2:** e202.

Simpson, C.G., Fuller, J., Maronova, M., Kalyna, M., Davidson, D., McNicol, J., Barta, A., and Brown, J.W. (2008). Monitoring changes in alternative precursor messenger RNA splicing in multiple gene transcripts. Plant J. **53:** 1035–1048.

Somers, D.E., Schultz, T.F., Milnamow, M., and Kay, S.A. (2000). ZEITLUPE encodes a novel clock-associated PAS protein from Arabidopsis. Cell **101:** 319–329.

Staiger, D., and Green, R. (2011). RNA-based regulation in the plant circadian clock. Trends Plant Sci. **16:** 517–523.

Staiger, D., and Brown, J.W. (2013). Alternative splicing at the intersection of biological timing, development, and stress responses. Plant Cell **25:** 3640–3656.

Staiger, D., Zecca, L., Wieczorek Kirk, D.A., Apel, K., and Eckstein, L. (2003). The circadian clock regulated RNA-binding protein AtGRP7 autoregulates its expression by influencing alternative splicing of its own pre-mRNA. Plant J. **33:** 361–371.

Stauffer, E., Westermann, A., Wagner, G., and Wachter, A. (2010). Polypyrimidine tract-binding protein homologues from Arabidopsis underlie regulatory circuits based on alternative splicing and downstream control. Plant J. **64:** 243–255.

Sugden, C., Donaghy, P.G., Halford, N.G., and Hardie, D.G. (1999). Two SNF1-related protein kinases from spinach leaf phosphorylate and inactivate 3-hydroxy-3-methylglutaryl-coenzyme A reductase, nitrate reductase, and sucrose phosphate synthase in vitro. Plant Physiol. **120:** 257–274.

Sureshkumar, S., Dent, C., Seleznev, A., Tasset, C., and Balasubramanian, S. (2016). Nonsense-mediated mRNA decay

modulates FLM-dependent thermosensory flowering response in Arabidopsis. Nat. Plants **2:** 16055.

Syed, N.H., Kalyna, M., Marquez, Y., Barta, A., and Brown, J.W. (2012). Alternative splicing in plants–coming of age. Trends Plant Sci. **17:** 616–623.

Tanabe, N., Yoshimura, K., Kimura, A., Yabuta, Y., and Shigeoka, S. (2007). Differential expression of alternatively spliced mRNAs of Arabidopsis SR protein homologs, atSR30 and atSR45a, in response to environmental stress. Plant Cell Physiol. **48:** 1036–1049.

Tepperman, J.M., Zhu, T., Chang, H.S., Wang, X., and Quail, P.H. (2001). Multiple transcription-factor genes are early targets of phytochrome A signaling. Proc. Natl. Acad. Sci. USA **98:** 9437–9442.

Thimm, O., Bläsing, O., Gibon, Y., Nagel, A., Meyer, S., Krüger, P., Selbig, J., Müller, L.A., Rhee, S.Y., and Stitt, M. (2004). MAPMAN: a user-driven tool to display genomics data sets onto diagrams of metabolic pathways and other biological processes. Plant J. **37:** 914–939.

Thum, K.E., Shasha, D.E., Lejay, L.V., and Coruzzi, G.M. (2003). Light- and carbon-signaling pathways. Modeling circuits of interactions. Plant Physiol. **132:** 440–452.

van der Walt, S., Colbert, S.C., and Varoquaux, G. (2011). The NumPy array: A structure for efficient numerical computation. Comput. Sci. Eng. **13:** 22–30.

van Zanten, M., Tessadori, F., McLoughlin, F., Smith, R., Millenaar, F.F., van Driel, R., Voesenek, L.A., Peeters, A.J., and Fransz, P. (2010). Photoreceptors CRYTOCHROME2 and phytochrome B control chromatin compaction in Arabidopsis. Plant Physiol. **154:** 1686–1696.

Wachter, A., Rühl, C., and Stauffer, E. (2012). The role of polypyrimidine tract-binding proteins and other hnRNP proteins in plant splicing regulation. Front. Plant Sci. **3:** 81.

Wang, X., et al. (2012). SKIP is a component of the spliceosome linking alternative splicing and the circadian clock in Arabidopsis. Plant Cell **24:** 3278–3295.

Wu, H.P., Su, Y.S., Chen, H.C., Chen, Y.R., Wu, C.C., Lin, W.D., and Tu, S.L. (2014). Genome-wide analysis of light-regulated alternative splicing mediated by photoreceptors in *Physcomitrella patens*. Genome Biol. **15:** R10.

Yakir, E., Hilman, D., Kron, I., Hassidim, M., Melamed-Book, N., and Green, R.M. (2009). Posttranslational regulation of CIRCADIAN CLOCK ASSOCIATED1 in the circadian oscillator of Arabidopsis. Plant Physiol. **150:** 844–857.

Yatsenko, D., Reimer, J., Ecker, A.S., Walker, E.Y., Sinz, F.H., Berens, P., Hoenselaar, A., Cotton, R.J., Siapas, A.G., and Tolias, A.S. (2015). DataJoint: managing big scientific data using MATLAB or Python. bioRxiv, http://dx.doi.org/doi/10.1101/031658.

Yoine, M., Nishii, T., and Nakamura, K. (2006). Arabidopsis UPF1 RNA helicase for nonsense-mediated mRNA decay is involved in seed size control and is essential for growth. Plant Cell Physiol. **47:** 572–580.

IV.1.2. Publication in 2018

"Subcellular Compartmentation of Alternatively Spliced Transcripts Defines SERINE/ARGININE-RICH PROTEIN30 Expression"

- Authors:
  Hartmann L.*, Wiessner T.* and Wachter A.

- Journal: Plant Physiol 176(4): 2886-2903

- Publication data: April 2018

Subcellular Compartmentation of Alternatively Spliced Transcripts Defines *SERINE/ARGININE-RICH PROTEIN30* Expression[1][OPEN]

Lisa Hartmann,[2] Theresa Wießner,[2] and Andreas Wachter[3]

Center for Plant Molecular Biology (ZMBP), University of Tübingen, 72076 Tübingen, Germany

ORCID IDs: 0000-0003-3494-2269 (L.H.); 0000-0002-3132-5161 (A.W.).

Alternative splicing (AS) is prevalent in higher eukaryotes, and generation of different AS variants is tightly regulated. Widespread AS occurs in response to altered light conditions and plays a critical role in seedling photomorphogenesis, but despite its frequency and effect on plant development, the functional role of AS remains unknown for most splicing variants. Here, we characterized the light-dependent AS variants of the gene encoding the splicing regulator Ser/Arg-rich protein SR30 in Arabidopsis (*Arabidopsis thaliana*). We demonstrated that the splicing variant *SR30.2*, which is predominantly produced in darkness, is enriched within the nucleus and strongly depleted from ribosomes. Light-induced AS from a downstream 3′ splice site gives rise to *SR30.1*, which is exported to the cytosol and translated, coinciding with SR30 protein accumulation upon seedling illumination. Constitutive expression of SR30.1 and SR30.2 fused to fluorescent proteins revealed their identical subcellular localization in the nucleoplasm and nuclear speckles. Furthermore, expression of either variant shifted splicing of a genomic *SR30* reporter toward *SR30.2*, suggesting that an autoregulatory feedback loop affects *SR30* splicing. We provide evidence that *SR30.2* can be further spliced and, unlike *SR30.2*, the resulting cassette exon variant *SR30.3* is sensitive to nonsense-mediated decay. Our work delivers insight into the complex and compartmentalized RNA processing mechanisms that control the expression of the splicing regulator SR30 in a light-dependent manner.

Maturation of eukaryotic mRNAs involves intricate co- and posttranscriptional RNA processing, which has critical functions in regulating gene expression and diversifying the transcriptome. Among several mechanisms, alternative precursor mRNA splicing (AS) in particular generates many transcript variants by removing distinct intronic regions and joining the resulting exons. Deep analysis of transcriptomes via high-throughput RNA sequencing (RNA-seq) has revealed that a major fraction of all intron-containing genes from higher eukaryotes generates AS variants. In humans, more than 95% of multiexon genes display AS (Pan et al., 2008). The prevalence of AS has also been demonstrated for other eukaryotes including plants (Reddy et al., 2013; Staiger and Brown, 2013), with current estimates of ~61% and ~42% of intron-containing genes giving rise to AS variants in the model plants Arabidopsis (*Arabidopsis thaliana*; Marquez et al., 2012) and *Brachypodium distachyon* (Mandadi and Scholthof, 2015), respectively.

Besides its pivotal role in increasing the coding and regulatory capacity of the transcriptome, AS fine-tunes gene expression by varying the output ratios of splicing variants. The full extent of AS regulation likely exceeds the current estimates, as the production of many transcript variants can be specifically controlled under certain conditions, such as cell and tissue types, developmental stages, and in response to stresses and other environmental factors (Reddy et al., 2013; Staiger and Brown, 2013). The enormous advancement of RNA-seq now allows profiling of this diversity at high depth and spatiotemporal resolution, which is expected to provide important insight into mechanisms and biological functions of AS. For example, comparing the transcriptome patterns between different maize (*Zea mays*) tissues via single molecule long-read sequencing revealed mutually exclusive exon inclusions as the dominant AS type in the endosperm, while regulated intron retention prevailed in other tissues (Wang et al., 2016) and has also been previously described as the most frequent AS type in plants (Filichkin et al., 2010; Marquez et al., 2012; Reddy et al., 2013; Staiger and Brown, 2013).

[1] This work was funded by the German Research Foundation (DFG), with grants WA 2167/4-1, CRC#1101 (C03), and a Heisenberg fellowship (WA 2167/8-1).

[2] These authors contributed equally to the article.

[3] Address correspondence to awachter@zmbp.uni-tuebingen.de.

The author responsible for distribution of materials integral to the findings presented in this article in accordance with the policy described in the Instructions for Authors (www.plantphysiol.org) is: Andreas Wachter (awachter@zmbp.uni-tuebingen.de).

A.W. and L.H. conceived the project; all authors contributed to experimental design; L.H. and T.W. performed the experiments; A.W. supervised the experiments and all authors contributed to data analysis; A.W. wrote the article with contributions from the other authors.

[OPEN] Articles can be viewed without a subscription.

www.plantphysiol.org/cgi/doi/10.1104/pp.17.01260

The generation of AS variants depends on the presence of competing splice sites. Various mechanisms regulate splice site availability and the recruitment of spliceosomal factors as well as splicing regulators to cis-regulatory elements, ultimately defining splice site usage and the AS output. Critical determinants are the regulated formation of mRNA structures (Wachter, 2010, 2014; Wachter et al., 2012; Liu et al., 2015), the recruitment of splicing factors/regulators by components of the transcriptional machinery and associated factors or chromatin marks (Braunschweig et al., 2013), and kinetic coupling between transcription and splicing (Braunschweig et al., 2013; Dolata et al., 2015). Furthermore, the protein level and activity of transacting factors involved in AS decisions is controlled by various means, including expression levels, AS of their own precursor mRNAs (pre-mRNAs), and subcellular protein localization (Wachter et al., 2012; Reddy et al., 2013).

Ser/Arg-rich (SR) proteins and heterogeneous ribonucleoprotein (hnRNP) proteins are two major groups of RNA-binding proteins that are present in animals and plants (Chen and Manley, 2009; Wachter et al., 2012; Reddy et al., 2013). Studies in Arabidopsis demonstrate widespread AS regulatory functions for the hnRNP proteins GLY-RICH PROTEIN7 (GRP7) and GRP8 (Streitner et al., 2012), POLYPYRIMIDINE TRACT BINDING PROTEIN1 (PTB1) and PTB2 (Rühl et al., 2012), RZ-1B/RZ-1C (Wu et al., 2016), and the SR-like protein SR45 (Carvalho et al., 2016). Furthermore, binding motifs required for AS control by SR45 (Day et al., 2012) and the SC35-LIKE33 (SCL33; Thomas et al., 2012) have been identified in single target pre-mRNAs. Recently, transcriptome-wide approaches for profiling interaction sites of RNA binding proteins have been established in plants (Meyer et al., 2017; Xing et al., 2015; Zhang et al., 2015) and are expected to considerably accelerate the discovery of novel AS targets and binding motifs for the large number of potential plant AS regulators.

While it is well established that manifold AS changes are triggered by diverse developmental signals and external cues, few AS events have been functionally characterized in plants. In Arabidopsis, many AS variants are targeted by nonsense-mediated decay (NMD; Kalyna et al., 2012; Drechsel et al., 2013). Coupling of AS and NMD enables quantitative gene control, which is particularly common in the auto- and cross-regulation of splicing regulators, including Arabidopsis SR proteins (Kalyna et al., 2006), GRP7/8 (Staiger et al., 2003; Schöning et al., 2008), and PTBs (Stauffer et al., 2010). Moreover, for some AS events, it has been shown that the splicing variants generate functionally distinct proteins. For example, Kriechbaumer et al. (2012) have demonstrated that tissue-specific AS allows targeting the auxin biosynthetic component YUCCA4 to the endoplasmic reticulum in flowers and to the cytosol in all other examined tissues. Organ-specific AS has also been revealed for the pre-mRNA of the ZINC-INDUCED FACILITATOR-LIKE1 (ZIFL1) transporter (Remy et al., 2013). This AS event causes differential targeting of ZIFL1 to the vacuolar and plasma membrane in root and guard cells, respectively, with specific functions in auxin transport and stomatal movement-dependent drought tolerance. AS of the *PHYTOCHROME INTERACTING FACTOR6* is involved in the regulation of seed germination (Penfield et al., 2010; Rühl et al., 2012).

AS also represents a powerful mechanism to coordinate the expression of sets of genes. Studies in animals demonstrate that specific AS programs underlie certain aspects of neuronal development (Li et al., 2014; Gueroussov et al., 2015; Traunmüller et al., 2016). Furthermore, cell cycle progression is accompanied by periodic AS programs and depends on an SR protein kinase in human cells (Dominguez et al., 2016). In plants, few studies have profiled developmentally controlled AS in a transcriptome-wide manner and at high spatiotemporal resolution. Li et al. (2016) have provided a high-resolution expression map of the Arabidopsis root, covering different cell types and developmental stages. Interestingly, their data also support a role of coordinated AS programs in cell differentiation, while no evidence for AS-mediated cell-type specification has been observed. Furthermore, transcriptome analyses in the course of photomorphogenesis have revealed widespread AS changes within few hours of light exposure of etiolated Arabidopsis seedlings (Shikata et al., 2014; Hartmann et al., 2016). Interestingly, more than 60% of the regulated AS events show a switch from a presumably nonproductive variant in darkness to a probably protein-coding variant in light (Hartmann et al., 2016), thereby allowing to ramp up expression of critical factors. Experimental evidence for such regulation has been provided for the positive light signaling component REDUCED RED-LIGHT RESPONSES IN CRY1CRY2 BACKGROUND1 (Shikata et al., 2012), which displays an AS switch from an NMD target in darkness to a protein-coding transcript variant in light (Hartmann et al., 2016). Furthermore, evidence was provided that photomorphogenesis is promoted by light-dependent AS of *SPA1-RELATED3* (Shikata et al., 2014) due to light-triggered formation of a dominant-negative version of this repressor of photomorphogenesis.

Critical functions of AS in many aspects of plant development and stress responses can also be deduced from the complex phenotypes of splicing regulator mutants (Staiger and Brown, 2013), albeit some of the defects might not result from AS but be linked to other RNA metabolic functions of these factors. Several reports highlight an important role of AS in regulating the plant circadian clock. Accordingly, extensive and temperature-dependent AS has been demonstrated for clock genes from Arabidopsis (James et al., 2012; Filichkin et al., 2015), and mutations in the PROTEIN ARG METHYL TRANSFERASE5 (Sanchez et al., 2010) and the splicing factor SNW/SKI-INTERACTING PROTEIN (Wang et al., 2012) alter circadian rhythms due to mis-splicing of clock genes. Misexpression of SR protein genes results in various changes in plant

morphology (Lopato et al., 1999; Kalyna et al., 2003; Ali et al., 2007). Interestingly, several SR and hnRNP protein mutants show altered flowering time (Staiger and Green, 2011; Staiger and Brown, 2013), and a recent report provides evidence for regulation of *FLOWERING LOCUS M* via coupled AS-NMD (Sureshkumar et al., 2016).

The *SR* genes from Arabidopsis are subject to extensive AS regulation, which is modulated in response to hormone treatment and in particular abiotic stresses, such as extreme temperatures, salt stress, and high light (Palusa et al., 2007; Tanabe et al., 2007; Filichkin et al., 2010). Many AS variants derived from the *SR* genes are subject to NMD (Palusa and Reddy, 2010; Kalyna et al., 2012), and differential splicing variant recruitment to polysomes has been observed during development and in response to stresses (Palusa and Reddy, 2015). Interestingly, in the case of the SR-like factor SR45, distinct biological functions of the two AS variants have been demonstrated by complementing a mutant in a splicing variant-specific manner (Zhang and Mount, 2009). While the mutant shows defects in petal development and root growth, complementation with *SR45.1* and *SR45.2* specifically rescues the petal and root phenotype, respectively. However, for most *SR* genes, the specific function of their transcript variants and the impact of AS on gene expression remain unknown.

Here, we functionally characterized light-regulated AS of the *SR30* gene. In dark-grown seedlings, splicing from an alternative upstream 3′ splice site resulted in predominant generation of *SR30.2*, which was enriched in nuclear fractions and depleted in cytosolic fractions. Furthermore, only a minor fraction of *SR30.2* was found to be associated with ribosomes. Light exposure triggered usage of a downstream 3′ splice site, generating *SR30.1*, which is efficiently exported from the nucleus and translated in the cytosol. In line with the distinct subcellular distribution patterns of their mRNAs, the SR30.1 protein accumulated to significant levels, while SR30.2 was not detectable in Arabidopsis plants. Constitutive expression of the two protein isoforms in transient expression systems revealed identical localization patterns of fluorescent protein fusions in the nucleus and similar AS regulation of an *SR30*-based splicing reporter. Besides the major AS variants *SR30.1* and *SR30.2*, we detected the minor cassette exon variant *SR30.3* that is generated by utilizing both alternative 3′ splice sites. *SR30.3* was targeted by NMD, while *SR30.2* was NMD immune. Furthermore, the *SR30.2* cDNA sequence expressed from a transgene could be further spliced to *SR30.3*. Our findings highlight a complex interplay of nuclear and cytosolic processing events in the regulation of *SR30* expression.

RESULTS

Light Induces a Rapid and Transient AS Shift for the Splicing Factor Gene *SR30*

Transcriptome-wide AS profiling of etiolated Arabidopsis seedlings either exposed to different light qualities for 6 h or retained in darkness revealed several hundred AS event changes in response to illumination (Hartmann et al., 2016). Interestingly, the majority of regulated AS events display a switch from a presumably unproductive transcript in darkness to a likely protein-coding variant in light (Hartmann et al., 2016). To understand the regulation and potential impact of this apparently frequent mode of AS shift, AS of *SR30* was functionally characterized. Two major *SR30* variants are generated by AS in etiolated seedlings. *SR30.1* was predominantly produced upon light exposure and encodes the annotated full-length SR30 protein (Fig. 1A; Supplemental Fig. S1). In darkness, *SR30.2* was the major isoform, which results from usage of an upstream 3′ splice site. The additional sequence included in *SR30.2* gives rise to a premature termination codon. Therefore, *SR30.2* contains an extended 3′ untranslated region (UTR) and an intron positioned downstream of the stop codon, features known to be able to trigger NMD in plants (Kerényi et al., 2008).

The levels of these two major *SR30* variants were first measured in etiolated seedlings after various periods of exposure to white light (Fig. 1B). Interestingly, a trend of reciprocal changes in the levels of *SR30.1* and *SR30.2* was already visible after 0.5 h of light exposure. Maximum and minimum levels of *SR30.1* and *SR30.2*, respectively, were reached upon 6 h of white light treatment. Levels of *SR30* splicing variants remained unchanged when seedlings were kept in darkness. These data showed a rapid and transient AS response of *SR30* to white light. Furthermore, reciprocal changes in *SR30.1* and *SR30.2* suggested that the changes occur directly on the level of AS, rather than resulting from light-induced changes in stability of one transcript variant. Illuminating etiolated seedlings with blue (Fig. 1C) and red (Fig. 1D) light also triggered opposite changes in steady state levels of *SR30.1* and *SR30.2*, consistent with the earlier report of similar AS changes in response to different light qualities (Hartmann et al., 2016).

Switching between *SR30* Splicing Variants Regulates Gene Expression

Based on the analysis of transcript features, we expected that *SR30.1* encodes a full-length protein, whereas the presence of a long 3′ UTR as well as a 3′ UTR-located intron in *SR30.2* should trigger NMD. However, analyzing transcript steady state levels in the NMD-impaired mutants *low-beta-amylase1* (*lba1*; Yoine et al., 2006) and *up-frameshift3-1* (*upf3-1*; Hori and Watanabe, 2005) revealed comparable levels of both *SR30.1* and *SR30.2* in the wild type and mutant lines (Fig. 2A). Our analysis also included the minor AS variant *SR30.3*, which we identified by sequencing RT-PCR products from *SR30* and which results from usage of the same alternative 3′ splice site as in *SR30.2* but has an additional splicing event in the region retained in *SR30.2* (Fig. 1A; Supplemental Fig. S1). In contrast to *SR30.2*, *SR30.3* accumulated in the NMD-

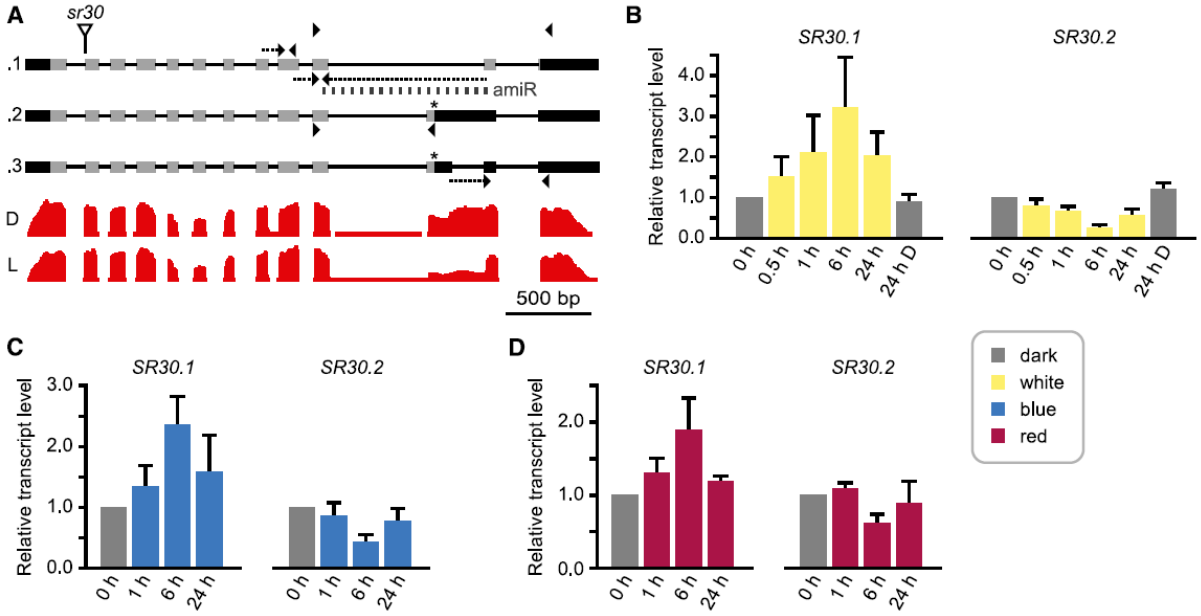

Figure 1. Light exposure triggers opposite changes in levels of major *SR30* splicing variants. A, Gene model of *SR30* including splicing variants analyzed in this work. Primers binding within one exon are shown as arrowheads, whereas arrows with dotted lines indicate primer binding sites spanning splice junctions. The topmost pair are coamplification primers used in downstream analyses, while the primer pair directly above the first variant was used to measure total *SR30* transcripts. Below each variant, the positions of primers used in RT-qPCR for detection of the corresponding splicing variants are indicated. Lines and boxes depict introns and exons, respectively; UTRs and cds are indicated by black and gray shading, respectively. Gray dashed line indicates binding site of artificial microRNA (amiR) spanning a specific splice junction of *SR30.1*. The triangle points at the T-DNA insertion site of *sr30*. Underneath the gene models, representative coverage plots are shown from a previous RNA-seq study (Hartmann et al., 2016) for dark (D) and 6-h white light (L). B to D, Splicing variants were quantified using RT-qPCR in seedlings exposed to white (B), blue (C), or red (D) light for indicated periods. Levels are relative to total *SR30* transcripts and normalized to the 0 h sample. D, Dark; mean values + SD ($n = 3–7$ for white and $n = 3$ for blue and red light).

impaired samples relative to the wild type (Fig. 2A). In line with its NMD insensitivity, *SR30.2* displayed a rather high stability, with a half-life of 7.65 h upon transcriptional inhibition (Fig. 2B). Interestingly, *SR30.1* was considerably less stable, displaying a half-life of 1.60 h.

NMD requires translation of its target mRNAs. Thus, a process withholding *SR30.2* from translation could impart immunity to NMD despite the presence of strong NMD-eliciting features. For example, retaining *SR30.2* within the nucleus would prevent its translation and NMD targeting. We therefore examined the distribution of splicing variants in RNA isolated from total samples, cytosol-enriched fractions, and nuclei (Fig. 2, C–E). Purity of the fractions was confirmed by exclusive detection of the nuclear and cytosolic marker proteins histone and UDP-Glc pyrophosphorylase (UGPase), respectively (Fig. 2C). The ratio of *SR30.2/.1* was increased in nuclei compared to total fractions, supporting the theory of impaired nuclear export of *SR30.2* (Fig. 2, D and E). Levels of *SR30.1* and *SR30.2* were also quantified separately in the samples from the fractionation experiment. Compared to the total sample, *SR30.2* was depleted and enriched in the cytosolic and nuclear fraction, respectively (Fig. 2F). We also analyzed ratios of AS variants from *SERRATED LEAVES AND EARLY FLOWERING* (*SEF*) and *RS2Z33*, which have been previously reported to generate AS transcripts that accumulate in the nucleus as a consequence of intron retention (Göhring et al., 2014). The AS ratios of these controls shifted even more toward the longer variant in the nuclear fraction (Fig. 2E), possibly due to more efficient nuclear retention of the intron-retained transcripts compared to *SR30.2*.

To test whether nuclear accumulation of *SR30.2* occurs in a species-specific manner, we transiently expressed a splicing reporter based on the genomic sequence of *SR30* from Arabidopsis in *Nicotiana benthamiana* (see Fig. 5 for reporter diagram and splicing). The reporter gave rise to the same AS variants *SR30.1* and *SR30.2* as in Arabidopsis, and the levels of these transcripts were analyzed in total and fractionated samples. Again, diminished and elevated levels of *SR30.2* were observed in cytosolic and nuclear fractions, respectively (Fig. 2G). When considering both the cytosolic enrichment and nuclear depletion of *SR30.1*,

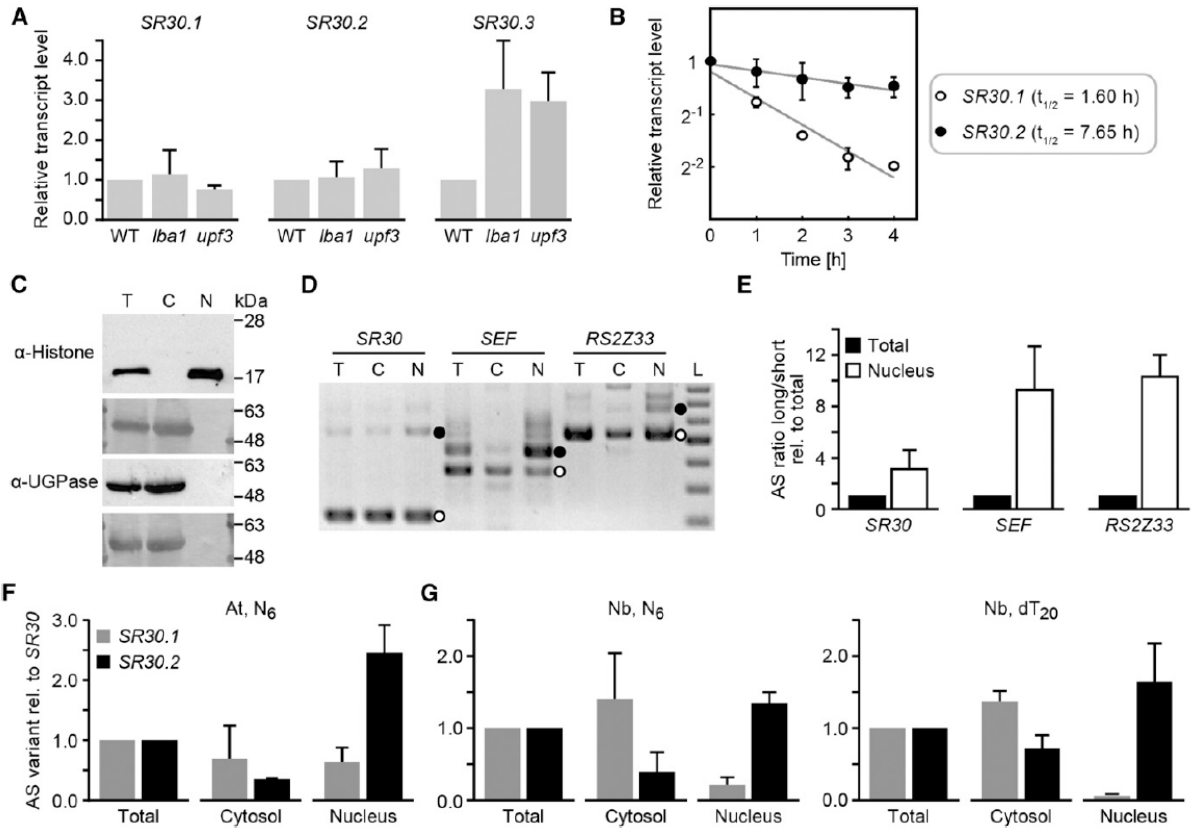

Figure 2. The *SR30.2* variant is relatively stable and enriched in the nucleus. A, *SR30* transcript levels determined via RT-qPCR in 10-d-old green wild-type, *lba1*, or *upf3* seedlings, relative to total *SR30* and the wild type. Mean values + SD; $n = 3$. B, Analysis of *SR30.1* and *SR30.2* RNA stability in 7-d-old Arabidopsis seedlings upon addition of cordycepin. Transcript levels were measured using RT-qPCR and normalized to a stable actin reference. Mean values ± SD are displayed on a $\log_2$ axis; $n = 3$. Half-lives based on exponential regression curves. C, Immunoblot analysis of total (T), cytosolic (C), and nuclear (N) fractions, with histone H3 and UGPase being detected as nuclear and cytosolic markers, respectively. Amidoblack staining shown beneath immunosignals; positions of relevant size marker bands are indicated. D, Coamplification of AS variants for *SR30*, *SEF*, and *RS2Z33* from fractions described in C. Bands corresponding to fragments used for quantitation are marked with white and black dots next to nuclear samples. L, size ladder consisting of DNAs in 100-bp increments from 200 to 800 bp. E, Ratios of long to short AS variants in nuclear fractions relative to total fractions. Mean values + SD; $n = 3$. F and G, Levels of *SR30* AS variants relative to total *SR30* determined via RT-qPCR in indicated fractions from Arabidopsis (At) seedlings (F) and *N. benthamiana* (Nb) leaves expressing an *SR30* reporter (G), using N_6 (left) or dT_{20} (right) for cDNA generation. Mean values + SD; $n = 3$.

the differences in subcellular distribution of the two splicing variants were particularly obvious. We obtained similar results when random hexamer or oligo(dT) primers were used for priming in reverse transcription (Fig. 2G), suggesting that the differential compartmentation of *SR30.1* and *SR30.2* is not explained by the presence of a major fraction of nonpolyadenylated transcripts.

Given the differential subcellular distribution of *SR30* splicing variants and its potential impact on their cellular fate, we analyzed variant levels in mutants defective in nuclear and cytosolic RNA degradation (Supplemental Fig. S2). Mutants with defects in the exosomal core components SUPPRESSOR OF PAS2 2/RRP4 (*sop2-1*) and mRNA TRANSPORT3 (*mtr3*) or a nuclear exosome factor (*hua-enhancer2-4*, *hen2-4*) had an ~2-fold increase in *SR30.1* and *SR30.2* levels; an even stronger accumulation was seen for the cassette exon variant *SR30.3*. In line with the increased levels of the individual splicing variants, total *SR30* transcript levels were also elevated in these mutants. As expected, the *mtr4-1* mutant impaired in nucleolar exosome function showed wild-type-like levels for all *SR30* transcript types. Unchanged steady state levels of all *SR30* transcripts were also observed in a *superkiller* (*ski*) mutant that is defective in a factor contributing to cytoplasmic exosome function. Besides exosome mutants affected in 3′-5′ decay, we also tested a potential role of 5′-3′ exoribonucleases (XRNs) in the degradation of *SR30* transcripts (Supplemental Fig. S2).

A single mutant in the cytoplasmic XRN4 accumulated higher levels of all *SR30* splicing variants. The increase was approximately 2-, 3-, and 4-fold for *SR30.1*, *SR30.2*, and *SR30.3*, respectively. Double mutants impaired in XRN4 and the nucleolar XRN2 or the nucleoplasmic XRN3 showed similar results as the single *xrn4* mutant, suggesting a major role of cytoplasmic but not nuclear 5′-3′ decay. Furthermore, we analyzed the *fiery1-6* (*fry1-6*) mutant, in which the activity of all three XRNs is reduced (Gy et al., 2007). In line with the data from the *xrn* mutants, the variant *SR30.3* strongly overaccumulated in the *fry1-6* seedlings. However, levels of *SR30.1* and *SR30.2* were higher and lower, respectively, in *fry1-6* relative to the *xrn* mutants, possibly due to a change in AS of *SR30* in the *fry1-6* mutant that shows several phenotypical abnormalities. Taken together, our data indicated that both nucleoplasmic 3′-5′ and cytoplasmic 5′-3′ decay contribute to the degradation of all three *SR30* splicing variants. The stronger accumulation of the *SR30.3* variant can be explained by a major impact of RNA turnover on the steady state level of this low abundant splicing variant.

The nuclear enrichment of *SR30.2* and its NMD immunity indicated that at least a substantial fraction of this AS variant did not undergo translation. We directly tested this hypothesis by isolating ribosomes and analyzing the distribution of *SR30* splicing variants in total and ribosomal fractions. Ribosomes were purified via immunoprecipitation from an Arabidopsis transgenic line expressing an epitope-tagged version of the ribosomal protein L18 (RPL18; Zanetti et al., 2005; Mustroph et al., 2013). Successful and specific immunoprecipitation was confirmed by immunoblot detection of the tagged ribosomal protein (Fig. 3A). Coamplification of *SR30.1* and *SR30.2* indicated a weak ribosomal association of *SR30.2* (Fig. 3B), which was confirmed by quantification of the individual splicing variants (Fig. 3C). *SR30.2* was strongly depleted in the ribosomal sample compared to the input, irrespective of the use of random hexamers or oligo(dT) primers for reverse transcription. In contrast, strong ribosomal association was detected for *SR30.1*.

We next investigated whether the small fraction of *SR30.2* transcripts associated with ribosomes gave rise to detectable amounts of a corresponding protein. Constitutive expression of epitope-tagged constructs based on the coding sequences (cds; Fig. 3D) or cDNAs including 5′ and 3′ UTRs (Fig. 3E) of *SR30.1* and *SR30.2* in *N. benthamiana* resulted in robust protein accumulation for SR30.1. In contrast, no or much weaker protein signals were detected upon expression of the constructs based on *SR30.2*. *SR30.1* and *SR30.2* are predicted to encode proteins of 30.4 and 29.1 kDa, respectively, and the triple HA tag is expected to increase protein size by ~3 kDa. The expression of both constructs resulted in immunosignals of similar M_r slightly above 40 kDa. Immunoblot detection using an affinity-purified antibody that was raised against the recombinant full-length SR30.2 protein confirmed the results obtained with the tag-specific antibody (Fig. 3E).

Considering that the expression via infiltration assays of *N. benthamiana* leaves represents an artificial and transient system, we also tested SR30 protein accumulation in Arabidopsis wild-type and stably transformed lines. Immunoprecipitation followed by immunoblot analysis with the SR30 antibody resulted in a double band of ~40 kDa for wild-type Arabidopsis seedlings (Fig. 3, F and G). The lower signal was absent in a transgenic line expressing an artificial microRNA (amiR) directed against *SR30.1* (Fig. 3G; Supplemental Table S1) as well as in the T-DNA insertion line *sr30* (Supplemental Fig. S3, A–C), which was expected to be impaired in the expression of any SR30 protein. Accordingly, the lower signal of the double band in wild-type plants can be assigned to the SR30 protein. Furthermore, SR30 protein detection in transgenic lines expressing tagged versions of the cDNAs from *SR30.1* and *SR30.2* (Supplemental Table S1) resulted in an additional, upward shifted signal for *SR30.1* (Fig. 3F). This signal was also detectable using a tag-specific antibody. In contrast, no construct-specific protein signal was observed in the case of *SR30.2* overexpression, in line with our finding of low or undetectable accumulation of this protein upon transient expression. The upper signal of the double band detected in wild-type and transgenic seedlings may represent an unspecific signal or cross-detection of a related SR protein. Given the pronounced AS shift of *SR30* during photomorphogenesis, we also analyzed SR30 protein levels in etiolated seedlings exposed to light for different periods as well as in light-grown seedlings. The specific SR30 signal was weakest in etiolated seedlings and became stronger with the duration of light exposure (Supplemental Fig. S3C), in agreement with a light-induced switch to the protein-coding variant *SR30.1*. Taken together, our data indicated that light-mediated AS of *SR30* mainly functions in quantitative gene control, whereas no evidence for significant accumulation of the alternative protein SR30.2 in wild-type samples was found.

Proteins Encoded by the *SR30* Variants Show Comparable Nuclear Localization and Splicing Regulatory Functions

Immunological detection of the proteins generated upon transgenic expression of the *SR30* variants revealed that *SR30.2* results in substantially weaker signals than *SR30.1*, irrespective of the presence or absence of the UTRs. The proteins encoded by the two major AS variants of *SR30* differ only in their C termini. Due to upstream 3′ splice site usage, *SR30.2* possibly encodes a protein that is 12 amino acids shorter than SR30.1 and that ends with a specific sequence of 10 amino acids. To test if AS of *SR30* enables not only quantitative control of gene expression but can also give rise to potentially functionally distinct proteins under any condition, we first analyzed the subcellular localization of both protein variants. Reporter constructs containing fusions of the cds from *SR30.1* or *SR30.2* and yellow or cyan fluorescent protein were transiently expressed in Arabidopsis protoplasts, followed

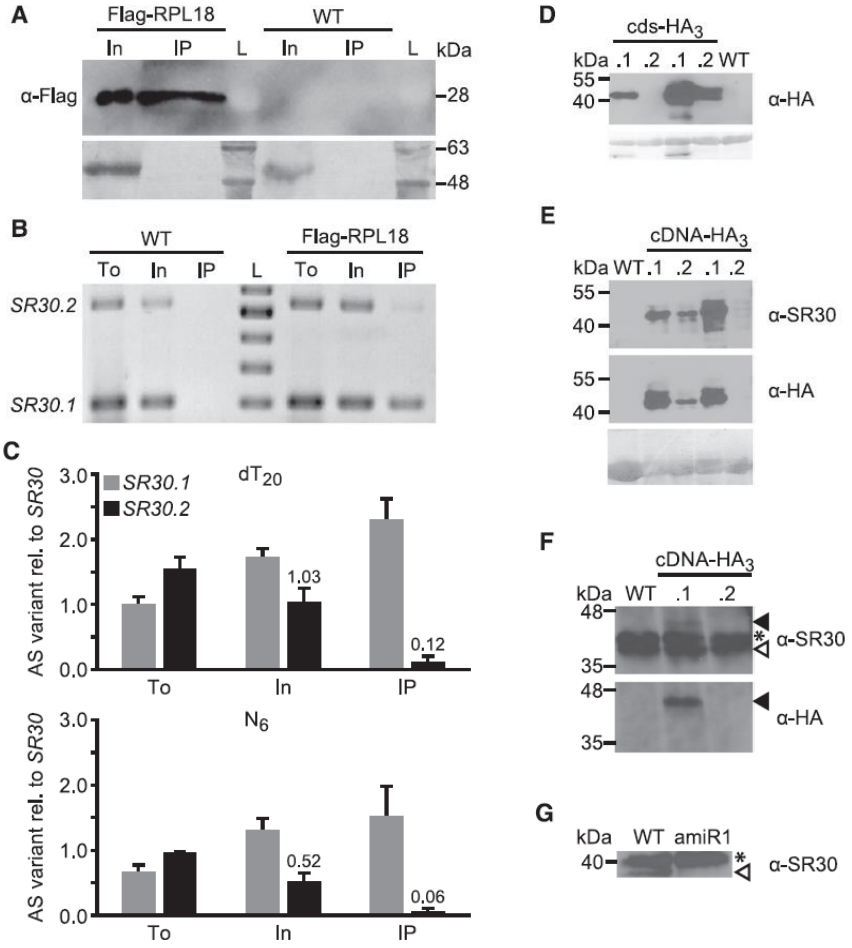

Figure 3. Splicing to *SR30.2* results in diminished protein production. A, Immunoblot detection of Flag-tagged RPL18 in input (In) and immunoprecipitation (IP) fractions of 10-d-old green Arabidopsis seedlings from indicated genotypes. Twenty micrograms of total protein of In (~0.1% of In) and 6% of IP sample was loaded. L, ladder containing proteins of indicated sizes. Upper and lower panels depict immune signal and amidoblack staining, respectively. B, RT-PCR coamplification of *SR30.1*/*.2* from total RNA preparation (To; standard RNA extraction directly from freshly frozen material) and samples described in A. L, size ladder consisting of DNAs in 100-bp increments from 200 to 600 bp. C, Levels of *SR30.1* and *SR30.2* were determined via RT-qPCR in samples described before and are depicted relative to total *SR30* transcripts and normalized to a total sample from the wild type. Reverse transcription of RNAs performed with dT_{20} (top) or N_6 (bottom) primers. Mean values + SD; $n = 3$. Values for *SR30.2* in relevant In and IP fractions are provided. D and E, Immunoblot detection of HA-tagged SR30.1 and SR30.2 in *N. benthamiana* upon transient expression of constructs based on the cds (D) or the cDNAs with 5′ and 3′ UTRs (E). Each sample pair came from corresponding leaf halves. WT, Noninfiltrated leaf. Fifteen micrograms of total protein each (D) or fresh weight equivalents (E) were loaded; lower panels show amidoblack staining as the loading control. F and G, Immunoblot analysis upon immunoprecipitation with α-SR30 from 10-d-old green wild-type or transgenic Arabidopsis seedlings, expressing indicated cDNA-HA_3 constructs (F) or an amiR construct targeting *SR30.1* (G). Fresh weight equivalents were loaded; cross-detection band (asterisk) serves as the loading control. Open arrowheads indicate endogenous SR30, and closed arrowheads in (F) mark tagged SR30.1.

by in vivo imaging. Note that UTR-free constructs were used for constitutive expression in an artificial and transient assay and that inspection of fluorescence in individual protoplasts does not allow a quantitative comparison of the accumulation for the two SR30 variants. Both SR30.1-YFP and SR30.2-YFP were detectable and colocalized with the marker construct NLS-DsRED in the nucleus (Fig. 4A; Supplemental Fig. S4A). Colocalization studies of SR30.1 and SR30.2 reporter fusions showed completely overlapping signal patterns (Fig. 4, B–D). Within the nucleus, the fusion proteins generally localized in the nucleoplasm, while they were absent from the nucleoli. In some protoplasts, both fusion proteins also accumulated in nuclear speckles (Fig. 4D). To test if the presence of a fluorescent protein tag in the localization constructs affected the accumulation of the corresponding

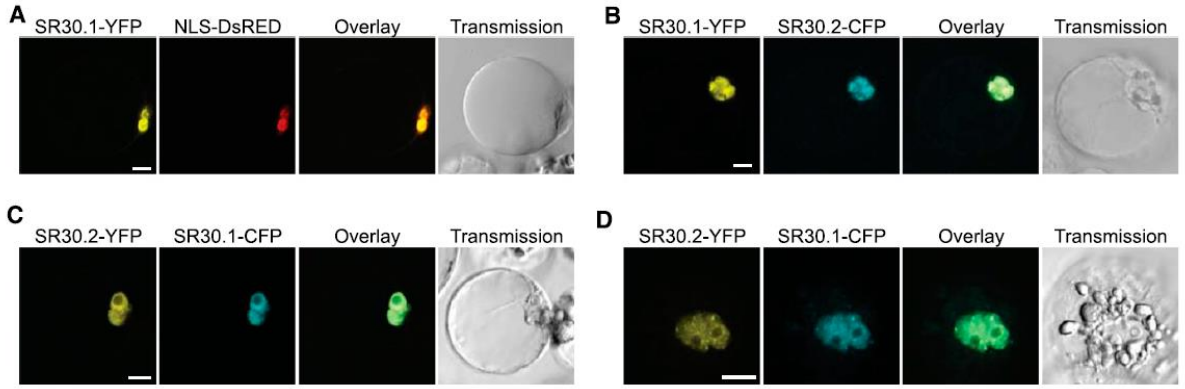

Figure 4. Fluorescent protein fusions of SR30.1 and SR30.2 both localize to the nucleus in Arabidopsis protoplasts. A, A construct containing the cds of *SR30.1* fused to *YFP* was transiently coexpressed with the nuclear marker NLS-DsRED in Arabidopsis protoplasts, followed by imaging using confocal microscopy. B and C, Colocalization of SR30.1 and SR30.2 fusions. D, Colocalization of SR30.2-YFP and SR30.1-CFP in the nucleoplasm and speckles. Bars = 10 μm in all panels.

fusion proteins and to be able to compare their levels quantitatively, we transiently expressed the reporter fusions in *N. benthamiana*, followed by immunoblot analysis. In agreement with the previous immunoblots, the fusions containing SR30.1 resulted in strong protein signals, whereas the SR30.2 fusions were not detected or were barely detectable (Supplemental Fig. S4B). SR30.1-Y/CFP was detected as two bands with a size of ~70 kDa. This corresponded to a size shift of approximately 10 kDa above the theoretical size, as we observed for the other SR30 immunosignals. Taken together, our data suggested that *SR30.2* resulted in considerably lower protein accumulation than *SR30.1*, most likely as a consequence of the nuclear retention of *SR30.2*. While we cannot exclude that other parameters, such as the degree of protein extractability, contributed to the differences in strength of the immunosignals between SR30.1 and SR30.2, the very small fraction of *SR30.2* associated with ribosomes suggested that its low level of translation was the main cause for our observation.

Previous work indicated that SR30 can regulate AS of its own pre-mRNA, as overexpressing *SR30* results in an altered AS output for the endogenous *SR30* locus (Lopato et al., 1999). However, effects of the proteins potentially encoded by the two AS variants of *SR30* have not been compared. To allow a quantitative comparison, a splicing reporter based on the genomic sequence of *SR30* and containing a tag sequence for specific detection (Fig. 5A) was coexpressed with cds constructs of *SR30.1* and *SR30.2*. Interestingly, both SR30.1 and SR30.2 shifted reporter splicing toward the *SR30.2* transcript version (Fig. 5B). Quantitation of the data revealed that the two SR30 variants displayed a comparable splicing regulatory activity (Fig. 5C). In summary, enforcing the expression of the two protein variants using a strong constitutive promoter and omitting the UTRs did not provide evidence that AS of *SR30* can give rise to functionally distinct proteins.

The *SR30.2* Transcript Can Be Further Spliced

A substantial fraction of *SR30.2* transcripts was found in the nucleus, where these transcripts may be subject to further processing including degradation. Interestingly, light-induced AS of *SR30* not only led to an altered ratio of *SR30.1/SR30.2*, but also caused significant changes for several cassette exon events in the

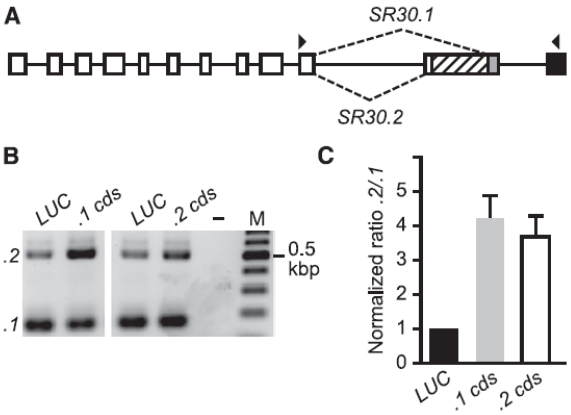

Figure 5. Both SR30.1 and SR30.2 can alter splicing of the *SR30* pre-mRNA. A, Gene model of the reporter used for the splicing assay. Exons are shown as boxes and introns as lines. White, cds; hatched, 3′ UTR in *SR30.2*; gray, cds in *SR30.1* and 3′ UTR in *SR30.2*; black, HA-tag. Arrowheads indicate binding positions of primers for coamplification of resulting splicing variants. With the exception of the HA-tag, model is drawn to scale. B, RT-PCR products upon coamplification of splicing variants *SR30.1* and *SR30.2* from the reporter coexpressed with a control protein (luciferase [LUC]) or the cds of *SR30.1* and *SR30.2*. Shown is representative agarose gel including a no template control (–) and DNA size ladder (M) with 100-bp increments. C, Ratio quantification using a Bioanalyzer for splicing variants displayed in B and normalized to the control (LUC). Mean values + SE; n = 14 to 15.

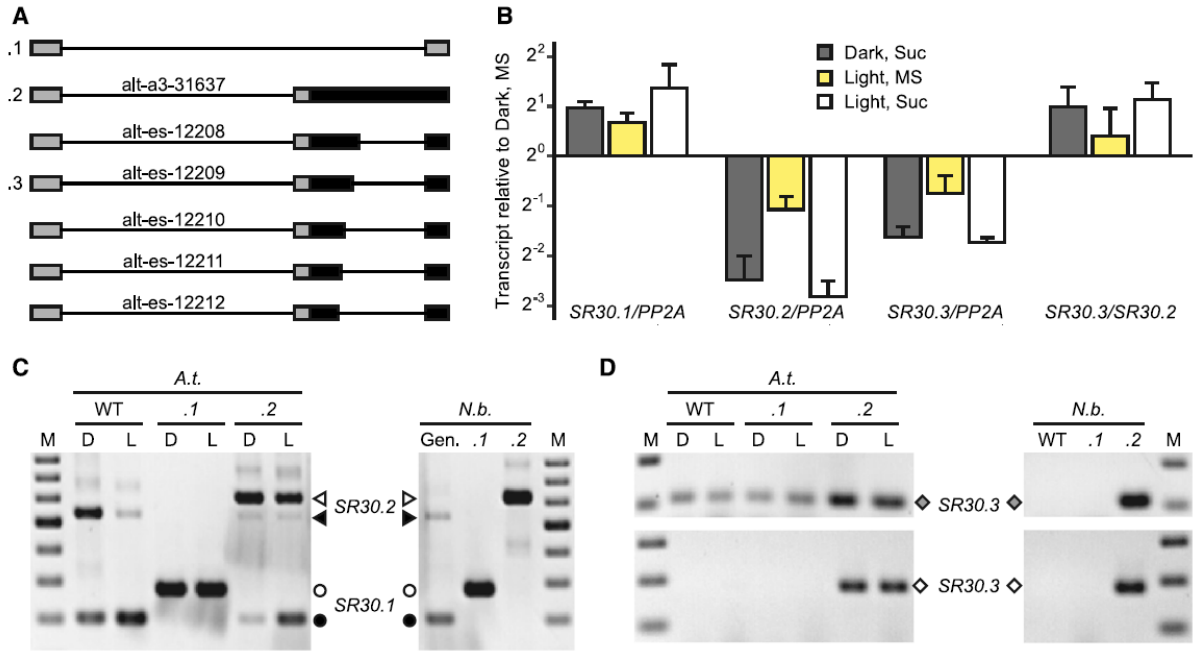

Figure 6. *SR30.2* can be further spliced to *SR30.3*. A, Partial models of *SR30* alternative splicing variants that were previously identified (Hartmann et al., 2016) to be significantly altered relative to *SR30.1* upon light exposure of etiolated seedlings. Lines and boxes correspond to introns and exons, respectively. Gray and black fills indicate coding sequence and 3′ UTR, respectively; AS event identifiers from previous study (Hartmann et al., 2016) are provided. B, Levels of *SR30* splicing variants relative to reference *PP2A* and ratio *SR30.3/SR30.2* were determined using RT-qPCR from *lba1* seedlings grown for 6 d in darkness and then retained in darkness or exposed for 6 h to white light in liquid control medium (MS) or medium containing 2% Suc. Data normalized to corresponding values from seedlings kept in dark and MS. Mean values + SD; $n = 3$ for sugar and light treatments and $n = 2$ for dark/MS controls. C, RT-PCR products upon coamplification of *SR30.1* (circles) and *SR30.2* (arrowheads) from Arabidopsis (A.t.) seedlings grown for 6 d in dark (D) or under long-day conditions (L) or *N. benthamiana* (N.b.) leaves transformed with *SR30* constructs. Transformation results in constitutive expression of cDNA constructs (*.1* and *.2*) based on the corresponding Arabidopsis *SR30* variants or the genomic Arabidopsis *SR30* sequence (Gen.). Black symbols indicate positions of products corresponding to endogenous splicing variants, and white symbols point at transgene-derived products that are size-shifted due to the presence of a tag. Size marker (M) consists of DNAs in 100-bp increments, with the lowest band representing 200 bp. D, RT-PCR products upon amplification of *SR30.3* (indicated by diamonds), either from the endogenous locus and transgene (upper gel) or specifically from the transgene (lower gel). Samples as in C, with added nontransformed wild-type control for *N. benthamiana*. Size marker in 100-bp increments; top bands correspond to 200 and 300 bp in upper and lower gels, respectively.

same region (Fig. 6A; data from Hartmann et al., 2016). The cassette exons result from two splicing events using both alternative 3′ splice sites, whereas for *SR30.1* and *SR30.2* only the downstream and upstream 3′ splice site, respectively, are used. The five cassette exon variants include *SR30.3* and differ only in their 5′ splice site within the region that is retained in *SR30.2* and intronic for *SR30.1* (Fig. 6A; Supplemental Fig. S5). The corresponding cassette exons are 165, 147, 127, 117, and 112 bp in size. Three of the cassette exon events (alt-es-12209/12210/12211) have been previously identified as being regulated by NMD (Drechsel et al., 2013). NMD targeting of *SR30.3* (alt-es-12209) was confirmed in this study (Fig. 2A). Based on the coverage plots from the RNA-seq data and the absence of bands corresponding to the cassette exon variants in RT-PCR reactions coamplifying *SR30.1* and *SR30.2*, we concluded that the steady state levels of the cassette exon variants were relatively low. Their low abundance can result from minor usage of the corresponding splice sites and/or high transcript turnover, in line with NMD targeting of *SR30.3* and its strong overaccumulation in RNA degradation mutants. Remarkably, further splicing of *SR30.2* might produce the cassette exon variants and thereby induce nuclear export and cytoplasmic decay of these transcripts. In support of such a route for generating the cassette exon variants, no splicing variants were observed that retained the intron upstream of the cassette exons or were derived from using alternative 5′ or 3′ splice sites in this upstream region.

To investigate how AS of *SR30* affects the generation of the various splicing variants, their levels were analyzed in dark-grown seedlings as well as upon light and/or sugar treatment, based on the previous

observation that both signals trigger AS for *SR30* and other genes (Hartmann et al., 2016). We used seedlings of wild type and the NMD-impaired mutant *lba1*, in which the NMD target *SR30.3* overaccumulated relative to the wild type, while levels of *SR30.1* and *SR30.2* were not affected (Fig. 2A). In line with our previous observations (Hartmann et al., 2016), both light and sugar exposure caused an increase of *SR30.1* and a concomitant reduction of *SR30.2* in *lba1* seedlings (Fig. 6B; Supplemental Fig. S6A). *SR30.3* was used as a proxy for the cassette exon variants, as measuring them collectively by RT-qPCR without detecting *SR30.2* is not possible. Interestingly, levels of *SR30.3* were also reduced in sugar- and light-treated seedlings (Fig. 6B). The reduction in *SR30.3* was less pronounced than for *SR30.2*, as also reflected by an increased ratio of *SR30.3*/*SR30.2* upon sugar and light treatment (Fig. 6B). The increased ratio of *SR30.3*/*SR30.2* in sugar-/light-treated samples may result from further splicing of *SR30.2* to the cassette exon variants; this AS ratio change is in line with the activation of the downstream 3′ splice site, which is also used for splicing of the pre-mRNA to *SR30.1* under these conditions. As an alternative to the generation of the cassette exon variants from the mature *SR30.2* mRNA, these transcripts may also originate directly from splicing of the pre-mRNA. Similar light- and sugar-induced changes in the levels of the individual *SR30* variants were observed for wild-type seedlings (Supplemental Fig. S6B). However, changes in the *SR30.3*/*SR30.2* ratios were less pronounced in the wild type compared to *lba1* seedlings, possibly due to different turnover rates of *SR30.3*.

We next tested whether *SR30.3* can be spliced from a cDNA corresponding to the *SR30.2* sequence or if the authentic pre-mRNA context is required. Therefore, *SR30* AS patterns were determined in Arabidopsis seedlings and infiltrated *N. benthamiana* leaves expressing constructs based on *SR30.1* or *SR30.2*. Coamplification with primers spanning the alternatively spliced region of *SR30* detected endogenous *SR30.1* and *SR30.2* in wild-type Arabidopsis seedlings, with the light-dependent differences in the ratios as described before (Fig. 6C, left). In Arabidopsis seedlings transformed with 35S promoter-driven constructs based on the *SR30.1* or *SR30.2* cDNAs, the main signal corresponded to the respective transgene, independent of the light condition. This observation further substantiated the conclusion that light-dependent changes in the levels of *SR30* transcript variants resulted from AS and not altered transcript turnover rates. The products derived from the transgene and the endogenous locus could be distinguished by their size difference; due to the presence of a tag in the constructs, the corresponding RT-PCR products were larger than those derived from the endogenous *SR30* locus. In the lines overexpressing *SR30.2*, the endogenous *SR30.1* and its light induction was still visible, while endogenous *SR30.2* was not detected in the lines overproducing *SR30.1* (Fig. 6C, left). This is likely due to the fact that *SR30.1* and *SR30.2* accumulated to different extents. In *N. benthamiana* leaves transiently expressing a construct based on the genomic sequence of *SR30* from Arabidopsis (Fig. 6C, right), both major *SR30* splicing variants were detected. In contrast, leaves expressing the cDNA constructs allowed only detection of the respective variants. We next used these samples to examine whether the *SR30.2* cDNA can be further processed to *SR30.3*. Using a primer combination that can detect *SR30.3* produced both from the endogenous *SR30* locus and the transgene (Fig. 6D, upper panel) resulted in detection of this variant in all Arabidopsis samples and *N. benthamiana* leaves expressing *SR30.2*. Furthermore, the level of *SR30.3* was strongly increased upon *SR30.2* overexpression, while *SR30.1* overexpression had no effect on the accumulation of the cassette exon variant in the stably transformed Arabidopsis lines (Supplemental Fig. S6C). To support direct processing of *SR30.2* to *SR30.3*, we used a tag-specific primer in combination with an *SR30.3*-specific primer. Indeed, *SR30.3* production from the transgene was found in all samples expressing the *SR30.2* construct (Fig. 6D, lower panel). This splicing event from *SR30.2* to *SR30.3* is expected to trigger nuclear export of the transcript, followed by its translation and degradation via NMD, which may represent a major route of its turnover. Additional work is needed to test if our finding of further splicing of a transgene-derived *SR30.2* variant also applies to generation of the corresponding *SR30* transcripts from the endogenous locus. Interestingly, inspection of AS patterns for several other *SR* genes revealed the occurrence of similar AS events within long introns as for *SR30*, suggesting that related splicing mechanisms may be more common (Supplemental Fig. S7).

DISCUSSION

Regulation of *SR30* Expression via Alternative RNA Processing in the Nucleus and Cytosol

We have demonstrated in this study that light-regulated AS controls expression of *SR30* by creating splicing variants that show distinct subcellular distribution patterns and are degraded via different mechanisms (Fig. 7). In the presence of light, usage of the downstream 3′ splice site generates *SR30.1*, which is exported to the cytosol and translated into the corresponding splicing regulator. In darkness, splicing from the upstream 3′ splice site produces *SR30.2*, which is enriched in the nucleus and depleted from the cytosolic fraction. The nuclear enrichment of *SR30.2* is in line with its weak ribosomal association and NMD immunity, despite the presence of a premature termination codon and long 3′ UTR, both of which are NMD-triggering features. The nuclear enrichment of *SR30.2* can result from either impaired export of this splicing variant into the cytoplasm or accelerated turnover in the cytoplasm. Given that *SR30.2* accumulates only slightly stronger than *SR30.1* in cytoplasmic RNA decay mutants and that *SR30.2* is significantly more stable than *SR30.1*, we think that impaired nuclear export of *SR30.2* is mainly responsible for our observations. Additionally, the minor variant *SR30.3* retaining a cassette exon within

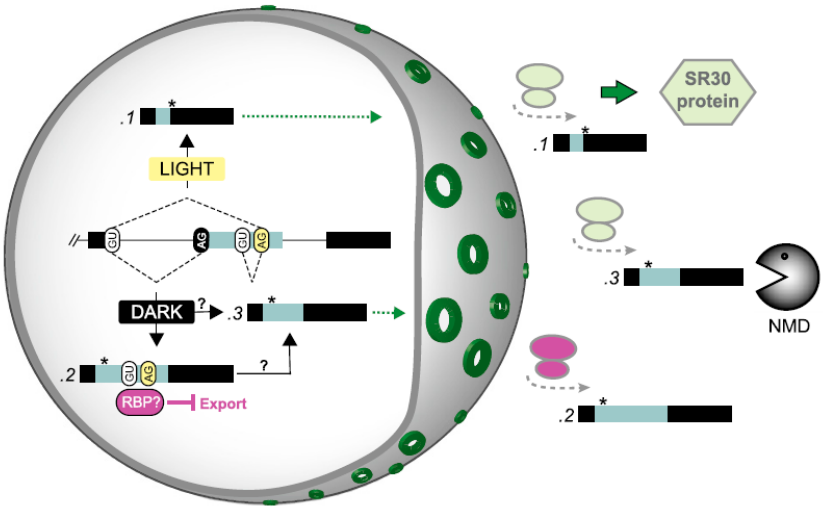

Figure 7. Model of *SR30* regulation via AS and downstream processes. Boxes and lines depict exons and introns, respectively, of *SR30* transcripts, for which only the part from the exon upstream of the alternatively spliced region to the 3′ end of the mRNAs is displayed. Asterisks depict positions of first in-frame translational stop codons for each mRNA. RBP indicates a putative RNA-binding protein. Dark-gray shape represents nuclear envelope with pores for export (green rings). Active translation is indicated by light-green ribosome symbols. Magenta indicates impairment of the corresponding process.

the alternatively spliced region has been detected. Based on the currently available data, generation of *SR30.3* by splicing of the primary pre-mRNA as well as consecutive splicing of the *SR30.2* mRNA seem plausible (see discussion below). NMD targeting of *SR30.3* and, according to published RNA-seq data (Drechsel et al., 2013), other cassette exon variants of *SR30* implies that these mRNAs are exported from the nucleus and translated. Based on our results, we propose that regulated AS of *SR30* allows rapid adjustment of the expression of this splicing regulator to ambient light conditions.

Our findings reveal an unexpected complexity of AS variant formation and downstream regulatory processes. The observation of nuclear enrichment of a splicing variant resulting from alternative 3′ splice site usage in the *SR30* pre-mRNA suggests that many other AS events may affect nuclear export of the corresponding splicing variants. A previous study reported nuclear accumulation of intron-retained transcripts (Göhring et al., 2014); however, our data show that splicing from an alternative 3′ splice site can similarly affect the subcellular distribution of mRNAs. Intron retention and alternative 3′ splice site usage have been described as the most common types of AS in plants, with varying frequencies in different studies (Marquez et al., 2012; Rühl et al., 2012; Hartmann et al., 2016). Furthermore, it seems likely that other AS types, such as splicing from alternative 5′ splice sites, can also prevent efficient nuclear export of the corresponding splicing variants. Nuclear enrichment of certain AS variants has also been observed in a previous study comparing the transcript profiles in libraries constructed from Arabidopsis whole cells, nuclei, and nucleoli (Kim et al., 2009). Interestingly, it was reported that many of these AS variants are enriched in the nucleolus compared to the nucleoplasm (Kim et al., 2009). In contrast to *SR30.2*, however, several of the nucleolus-enriched AS variants that were further analyzed by Kim et al. (2009) showed NMD targeting. Thus, specific regulation of mRNA transport within and export from the nucleus must occur. One possible scenario is that a particular RNA-binding protein associated with a completely or partially retained intron of a splicing variant prevents its nuclear export (Fig. 7). The nuclear retained transcripts may then be subjected to degradation in this compartment. Alternatively, removal of the corresponding protein factor, e.g. as a result of further processing, may enable export of the mRNA into the cytosol at a later point.

Possible Alternative Routes for the Generation of the *SR30.3* Variant

We have shown that a transgene-derived cDNA corresponding to the fully spliced *SR30.2* sequence can be further spliced to *SR30.3*. Several observations are in line with the hypothesis that endogenous *SR30.3* and the other cassette exon variants can also be generated by consecutive splicing of *SR30.2*, as opposed to independent removal of the two introns flanking the cassette exons from the pre-mRNA. First, no splicing variants have been identified in which the intron downstream of the cassette exon has been removed while the upstream intron is still present. Second, for all cassette exon variants, the splice sites used for removal of the upstream intron conform to the sites specifying *SR30.2*, while various 5′ splice sites are used for splicing of the intron downstream of the cassette exon. Regulation of AS in this region can be explained by the presence of two competing 3′ splice sites. In darkness, the upstream 3′ splice site is preferred, resulting in formation of *SR30.2*. Light and sugar signals trigger formation of *SR30.1* by activating the downstream 3′ splice site, e.g. by binding of a negative or positive splicing regulator, respectively, near the up- and

downstream 3′ splice site. Due to usage of the identical 5′ splice site, generation of the two major splicing forms *SR30.1* and *SR30.2* is mutually exclusive. However, *SR30.2* still contains a substantial portion of the sequence that is intronic for *SR30.1*, including the 3′ splice site. Therefore, in a second step, splicing of *SR30.2* to the cassette exon variants could occur, independent of the other introns. Such a consecutive splicing mechanism giving rise to the *SR30* cassette exon variants would be reminiscent of recursive splicing that was first described for the *ULTRABITHORAX* gene in *Drosophila melanogaster* (Hatton et al., 1998). In this example, a large intron is not spliced as a single unit, but in a sequential manner by recreating 5′ splice sites after splicing. Recently, further examples of recursive splicing events, involving generation of zero nucleotide exons, have been described for *D. melanogaster* (Duff et al., 2015). Identification of recursive splicing in vertebrate genes (Sibley et al., 2015) demonstrated that this mechanism is not restricted to *D. melanogaster*. Interestingly, all of the recursive splicing events found in human can result in cassette exon inclusion (Cook-Andersen and Wilkinson, 2015; Sibley et al., 2015), equivalent to the proposed consecutive splicing events resulting in *SR30.3*. In the first step, the intron upstream of the cassette exon is spliced out. In the second step, splicing from a 5′ splice site either at the start of the cassette exon or downstream of it results in removal and inclusion of the cassette exon, respectively. Like *SR30.3*, most of the cassette exon variants resulting from recursive splicing in vertebrate genes are targeted by NMD (Sibley et al., 2015). Interestingly, the regulated intron in *SR30* and the corresponding introns from other *SR* genes showing *SR30*-like AS patterns are exceptionally long, with 942 nucleotides for *SR30* and ranging from 765 to 1100 nucleotides for the other cases (Supplemental Fig. S7). In contrast, the average intron length in Arabidopsis is only 165 nucleotides according to TAIR10 (Lamesch et al., 2012). Accordingly, these long introns may have specifically evolved to allow gene regulation via mechanisms related to those proposed in this work. Further work is needed to be able to distinguish between the alternative routes of cassette exon variant formation for these *SR* genes, involving either activation of multiple AS sites on the pre-mRNA or consecutive splicing of mRNAs. Given the low steady state levels of *SR30.3* and the other cassette exon variants, its relevance for the regulation of *SR30* expression also remains open. In light of NMD targeting of these splicing variants and the strong accumulation of *SR30.3* in exosome and *xrn* mutants, however, it is possible that a substantial fraction of all *SR30* pre-mRNAs is spliced to the cassette exon isoforms, which do not accumulate due to rapid turnover.

In case the *SR30* pre-mRNA is spliced consecutively, the timing of the two splicing events will be of particular interest. Previous work indicated that posttranscriptional splicing can be activated on demand. Boothby et al. (2013) demonstrated that splicing of retained introns allows regulation of translation during gametophyte development in the fern *Marsilea vestita*. Our AS analysis revealed a slight increase in the ratio *SR30.3*/*SR30.2* in light- and sugar-treated seedlings compared to dark controls. This AS ratio change and the increased formation of *SR30.1* are in line with an activation of the downstream 3′ splice site upon light and sugar availability. Moreover, *SR30.2* may not only function in gene regulation by being withheld from translation, but could also fulfill specific functions in the nucleus. For example, this splicing variant may sequester or assemble splicing regulators and thereby affect the AS outcome of other pre-mRNAs, similar to what has been described for a long noncoding RNA in Arabidopsis. This long noncoding RNA can interact with nuclear speckle RNA-binding proteins and thereby alter the AS outcome of their target pre-mRNAs (Bardou et al., 2014). Further splicing of *SR30.2* may also compete with nuclear decay of this splicing variant. Precedence for such a mechanism comes from the identification of exosome mutants as suppressors of a splicing-defective allele of *PASTICCINO2* (*PAS2*; Hématy et al., 2016). The suppressor mutants *sop1*, *sop2*, and *sop3* displayed an accumulation of an intron-retaining *pas2-1* isoform, which probably allowed increased splicing to a variant complementing the *pas2-1* phenotype. Our analysis of *SR30* transcript levels in exosome and *xrn* mutants indicated that both nucleoplasmic 3′-5′ and cytoplasmic 5′-3′ decay contributed to the turnover of all three variants. Accordingly, the two pathways may compensate for a defect in one of their components in the corresponding mutants. The observation of cytosolic and nucleoplasmic turnover for *SR30.2* and *SR30.3*, respectively, is of particular interest, as it points to the existence of additional mechanisms limiting their accumulation. Specifically, some *SR30.3* transcripts are already targeted for degradation in the nucleus before they can be exported to the cytoplasm, and *SR30.2* mRNAs escaping the nucleus are subjected to XRN4-mediated decay in the cytoplasm. However, given that *SR30.2* accumulates only slightly more than *SR30.1* in the *xrn* mutants and as *SR30.2* shows a much higher stability than *SR30.1*, we think it is unlikely that alternative turnover rates alone can explain the differential subcellular distribution patterns of the two splicing variants. The NMD immunity of *SR30.2* also is in line with our model that most of this transcript variant is not available for translation in the cytoplasm, albeit additional mechanisms suppressing translation of this splicing variant may exist.

Distinct Subcellular Localization of *SR30* mRNA Variants

Key to the specific fates of the *SR30* splicing variants is their distinct subcellular distribution. Regulated localization of RNAs within the cell is found from bacteria to higher eukaryotes and emerging evidence suggests its frequent occurrence (Chin and Lécuyer, 2017). A first direct link between mRNA localization and splicing was provided in *D. melanogaster* for the

OSKAR mRNA, which needs to contain the first intron of the pre-mRNA and be spliced in it, in order to correctly localize to the posterior pole of the oocyte cytoplasm. Subsequent studies identified the molecular mechanisms of this splicing requirement, including deposition of the exon junction complex (Newmark and Boswell, 1994; Mohr et al., 2001; van Eeden et al., 2001; Hachet and Ephrussi, 2004; Palacios et al., 2004) and formation of an RNA structural element defining the localization of the *OSKAR* mRNA (Ghosh et al., 2012). Furthermore, evidence has been provided that AS is used to achieve distinct subcellular localization of the mature mRNA variants (Chin and Lécuyer, 2017). However, with the exception of the study by Göhring et al. (2014), most of our current knowledge on splicing-dependent RNA localization is based on studies in animal systems. Our finding of nuclear retention of *SR30.2* provides a good starting point for further investigating the molecular basis of the subcellular localization of this splicing variant, e.g. by searching for protein factors that are specifically associated with *SR30.2* and not the other *SR30* AS variants or by mapping the critical RNA region.

While our data indicated that the major portion of *SR30.2* is retained within the nucleus, a small fraction was also detectable in the cytosolic fraction. The amount in the cytosol may still be an overestimation, as some of these mRNAs can originate from nuclei that ruptured during the fractionation experiment. Indeed, very little *SR30.2* was detected on purified ribosomes, in agreement with a previous study that systematically examined the association of *SR* splicing variants with ribosomes (Palusa and Reddy, 2015). The weak ribosomal association explains why no corresponding protein variant was detectable upon constitutive expression of this cDNA in stably transformed Arabidopsis. Even enforced expression in transient assays yielded no or very low amount of SR30.2 protein, while SR30.1 always accumulated to high levels. Taken together, these data suggest that either *SR30.2* is almost fully retained in the nucleus, or, in case some export to the cytosol occurs, an additional mechanism may actively restrain this transcript variant from translation. The full absence of translation of this splicing variant is also supported by its NMD immunity, despite the presence of strong NMD-eliciting features. NMD immunity of *SR30.2* has been demonstrated by analyzing the levels of the individual *SR30* variants in two NMD-impaired mutants, *lba1* (Yoine et al., 2006) and *upf3* (Hori and Watanabe, 2005), in this study and a previous transcriptome-wide comparison of AS patterns between controls and four different types of NMD impairment (Drechsel et al., 2013). In contrast, another study suggested that *SR30.2* is an NMD target, based on an increased ratio of *SR30.2/SR30.1* in a *upf3* mutant compared to the wild type (Palusa and Reddy, 2010). However, as this previous study only considered the AS ratio change in a single mutant, and since many signals can alter AS of the *SR30* pre-mRNA (also see below), a change on the level of AS rather than transcript turnover seems to be a more likely explanation for the observation by Palusa and Reddy (2010). In summary, our data strongly suggest that the AS switch in *SR30* functions in quantitative control of gene expression. Remarkably, the protein-coding variant *SR30.1* is subject to rapid decay. This high turnover rate enables a fast change in transcript steady state levels upon shifting the AS of the *SR30* pre-mRNA, quickly adjusting expression of this splicing regulator.

Fine-Tuning *SR30* Expression via AS in Development and Stress Response

AS of the *SR30* pre-mRNA is tightly regulated during development and in response to stresses. We have shown in a previous study (Hartmann et al., 2016) and this report that AS of *SR30* is regulated in response to light and sugar availability. In darkness, mainly *SR30.2* is generated, whereas light and sugar trigger predominant splicing to the protein-coding variant *SR30.1*. Profiling the response over a period of 24 h suggested that this AS switch reaches its maximum at ~6 h and then is partially reverted, possibly as part of a feedback loop. Changes in *SR30* AS have also been observed during development of light-grown seedlings and in comparison of different plant tissues (Lopato et al., 1999; Palusa et al., 2007). Furthermore, several studies demonstrate that the AS output of *SR30* is highly responsive to stress, with heat (Palusa et al., 2007; Filichkin et al., 2010), high light (Tanabe et al., 2007; Filichkin et al., 2010), and NaCl (Tanabe et al., 2007; Filichkin et al., 2010) all resulting in a shift toward *SR30.1*.

Generation of an antibody raised against the endogenous SR30 protein allowed us to demonstrate that the light-induced shift in splicing to *SR30.1* correlates with increased SR30 protein levels, being most pronounced in the comparison of dark- and light-grown plants. Both endogenous SR30 and several transgene-derived tagged versions of it were detected at an apparent M_r that is ~10 kDa above the theoretical size. A similar shift in the size of the SR30 protein upon immunodetection was previously reported and phosphatase treatment has been described to cause faster migration of the protein (Lopato et al., 1999). An elevated apparent M_r has also been observed for other related factors (Golovkin and Reddy, 1998; Ali et al., 2003).

Our subcellular localization studies using fluorescent protein fusions of SR30.1 confirmed its previously reported presence in the nucleoplasm and nuclear speckles (Fang et al., 2004; Lorković et al., 2004), a pattern also observed for several other SR proteins (Fang et al., 2004; Lorković et al., 2004; Tillemans et al., 2005) and SR45 (Ali et al., 2003). In another study, subcellular distribution of At-SR30.1 fused to red fluorescent protein has been examined in onion epidermal cells (Mori et al., 2012). In contrast to our findings in Arabidopsis, a substantial proportion of the fusion protein was present in the cytosol of onion epidermal cells, possibly due to the heterologous expression. Interestingly, chemical inhibition of phosphorylation

suppressed nuclear localization of the SR30 protein fusion, which accumulated under these conditions in large structures within the cytosol (Mori et al., 2012). Further work will be needed to determine if interference with phosphorylation similarly affects SR30 localization in Arabidopsis. Furthermore, we observed that the extent of speckle localization varied between cells, which is in line with the highly dynamic nature of nuclear speckles formed by several SR- and SR-like proteins (Ali et al., 2003; Fang et al., 2004; Tillemans et al., 2005, 2006). Enforcing expression of SR30.2 revealed an identical localization of the fluorescent protein fusion in the nuclear compartments as observed for SR30.1.

Constitutive overexpression of a genomic construct of *SR30* has been previously shown to result mainly in splicing to the *SR30.2* variant (Lopato et al., 1999), possibly as part of a feedback control on the AS level, as it has been demonstrated for other splicing regulators, e.g. GRPs (Staiger et al., 2003; Schöning et al., 2008) and PTBs (Stauffer et al., 2010; Wachter et al., 2012). Coexpressing a genomic *SR30* construct with the cds of the major *SR30* splicing variants allowed us to corroborate the assumption of an AS shift toward *SR30.2* under conditions of elevated SR30 protein levels. Remarkably, constitutive coexpression of SR30.1 or SR30.2 with the splicing reporter similarly shifted its AS to the unproductive variant. Based on the comparable splicing regulatory effect and subcellular localization of the artificially expressed SR30.1 and SR30.2, distinct functions of these variants seem unlikely, even if the SR30.2 protein were generated in planta under any condition. In contrast, splicing variant-specific complementation of defects in petal development and root growth has been found for the *sr45-1* mutant (Zhang and Mount, 2009).

Feedback control of SR30 expression on the level of AS can also explain the transient AS response to light and other changes in growth conditions. Accordingly, a shift in AS to *SR30.1* is expected to result in elevated levels and activity of SR30 protein, which in turn should alter splicing of the *SR30* pre-mRNA toward the unproductive *SR30.2* variant. Furthermore, evidence for SR30-mediated AS regulation of its homolog SR34 and other genes has been previously provided, based on changes in their splicing patterns in the *SR30* overexpression lines (Lopato et al., 1999). A recent study aiming at elucidating the physiological functions of SR proteins generated multiple mutants for all subfamilies of SR proteins (Yan et al., 2017). While a quintuple mutant in SC35 and SCL genes displays pleiotropic alterations in plant morphology and development, no phenotypic changes were observed for the other mutants, including the *sr* quadruple mutant that is supposedly defective in the expression of the related factors *SR34*, *SR34a*, *SR34b*, and *SR30*. However, our analysis of the T-DNA insertion line SALK_116747C in *SR30*, which was used by Yan et al. (2017), revealed no difference in the *SR30* expression pattern compared to the wild type (Supplemental Fig. S3A), suggesting that the *sr* quadruple mutant generated by Yan et al. (2017) is, at least for *SR30*, not a knockout. Besides analyzing full knockout mutants, it will be of interest to examine phenotypes of *sr* mutants under specific growth conditions including stress regimes. In line with a critical function of *SR30*, its overexpression resulted in several morphological and developmental defects, including late flowering, reduced apical dominance, and changes in rosette leaf size (Lopato et al., 1999). This finding underscores the importance of tight regulation of *SR30* expression, which we have demonstrated in this work to be based on the intricate interplay of nuclear and cytosolic events in RNA metabolism.

MATERIALS AND METHODS

Plant Cultivation and Experiments

Arabidopsis (*Arabidopsis thaliana*) Col-0 seeds sterilized in 3.75% NaOCl and 0.01% Triton X-100 were grown on or in 0.5× Murashige and Skoog (MS) medium with supplements added as described below. Solid medium contained 0.8% phytoagar (Duchefa). Upon stratification for at least 2 d at 4°C, germination was induced in white light for 2 h. All darkness samples were taken in green light. For light experiments (Fig. 1), seeds were plated on solid medium containing 2% Suc. Six-day-old, dark-grown seedlings were exposed to white, blue, or red light, or kept in darkness for the indicated period. For transfer experiments (Fig. 6B), seedlings were grown on solid medium without Suc and kept in darkness for 6 d after induction of germination. Under green light, seedlings were transferred to liquid 0.5× MS medium with or without supplements as indicated and incubated in darkness or light for the time stated. For the RNA half-life assay (Fig. 2B), seedlings were cultivated in 100 mL liquid medium under long-day conditions on a shaker at 115 rpm for 7 d. The seedlings were rinsed with water, transferred into 150 μg/mL cordycepin (Sigma-Aldrich) solution, and then sampled after 1, 2, 3, and 4 h. For the other experiments, seedlings were cultivated for the indicated time under long-day conditions on solid medium containing 2% Suc.

Light Conditions

Continuous white light was used at an intensity of ~130 μmol m^{-2} s^{-1}. Monochromatic light from LED fields (Flora LED; CLF Plant Climatics) had the following specifications: blue 420 to 550 nm, maximum at 463 nm, full width at half maximum 22.2 nm, intensity ~6 μmol m^{-2} s^{-1}; red 620 to 730 nm, maximum at 671 nm, full width at half maximum 25 nm, intensity ~18 μmol m^{-2} s^{-1}. Intensities were measured with a Skye SKR1850 (Skye Instruments) and are limited to photosynthetically active radiation.

Subcellular Fractionation

Subcellular fractionation was performed according to a protocol provided by M. Amorim and S. Laubinger (de Francisco Amorim et al., 2017). Briefly, 2 g of plant material was ground under liquid nitrogen cooling and suspended in 4 mL HONDA buffer (20 mM HEPES, KOH, pH 7.4, 0.44 M Suc, 1.25% Ficoll 400, 2.5% Dextran T40, 10 mM $MgCl_2$, 0.5% Triton X-100, 1 mM PMSF, 5 mM DTT, 50 units/mL RiboLock [Thermo Fisher Scientific], and 1× Complete protease inhibitor [Roche]). All following steps were performed at 4°C. The sample plus 1 mL HONDA buffer used for rinsing was filtered through Miracloth (Calbiochem; 22–25 μm), resulting in the total fraction. The sample was centrifuged at 1,500*g* for 10 min to separate the nuclei and the cytosolic fraction. The supernatant was transferred into a fresh tube and centrifuged at 13,000*g* for 15 min. The resulting supernatant corresponded to the cytosolic fraction. The pellet from the 1,500*g* centrifugation was resuspended in 1 mL HONDA buffer using a Pasteur pipette and centrifuged at 1,800*g* for 5 min. This washing step was repeated four to five times until the supernatant became clear. Finally, the pellet was suspended in 400 μL HONDA buffer (nuclei fraction). Three hundred and one hundred microliters were used for RNA and protein extraction, respectively. Samples taken for RNA isolation were thoroughly mixed with 2 volumes of 8 M guanidinium hydrochloride and 3 volumes of 100% ethanol. The RNA was precipitated over night at −20°C and pelleted at 16,000*g* for

50 min. The supernatant was removed, the pellet was dried at room temperature for 20 min and used for RNA isolation using a column-based system as described below. Protein samples were mixed with 5× SDS sample buffer (0.3 M Tris-HCl, pH 6.8, 50% glycerol, 5% SDS, 0.05% bromophenol blue, and 100 mM DTT) and denatured at 95°C for 5 min.

Ribosome Immunoprecipitation

Ribosome immunoprecipitation was conducted based on a protocol from Mustroph et al. (2013). Briefly, 2 g of seedlings was ground under liquid nitrogen cooling and mixed with 5 mL polysome extraction buffer (200 mM Tris-HCl, pH 9.0, 200 mM KCl, 25 mM EGTA, 36 mM $MgCl_2$, 5 mM DTT, 50 μg/mL cycloheximide, 50 μg/mL chloramphenicol, 0.5 mg/mL heparin, 1% Triton X-100, 1% Tween 20, 1% Brij-35, 1% IGEPAL CA-630, 2% polyethylene glycol 400, 1% deoxycholic acid, 1 mM PMSF, and 50 units/mL RiboLock). All subsequent steps were performed at 4°C. The sample was centrifuged at 16,000*g* for 15 min, followed by filtration of the supernatant through Miracloth (Calbiochem; 22–25 μm) and another centrifugation step at 16,000*g* for 15 min. The input sample was taken from the supernatant. One hundred and fifty microliters of Protein G coupled Dynabeads (Life Technologies) was washed twice with 1.5 mL washing buffer (WB; 200 mM Tris-HCl, pH 9.0, 200 mM KCl, 25 mM EGTA, 36 mM $MgCl_2$, 5 mM DTT, 50 μg/mL cycloheximide, 50 μg/mL chloramphenicol, and 50 units/mL RiboLock), resuspended in 150 μL WB, and incubated with 5 μL α-FLAG antibody solution (Sigma-Aldrich) under agitation for 10 min at room temperature. The beads were washed once more with WB and resuspended in 150 μL WB. The suspension of α-FLAG-coated Dynabeads was added to the remaining supernatant of the seedling samples and incubated for 2 h while shaking gently. The beads were separated from the supernatant using a magnet and washed with 5 mL polysome extraction buffer followed by three washes with WB. Finally, the tagged ribosomes were eluted with 400 μL WB containing 200 ng/μL FLAG peptide (Sigma-Aldrich) for 30 min while shaking. The elution fraction was split into 300 and 100 μL for RNA and protein isolation, respectively. The RNA and protein samples were further processed as described for the subcellular fractionation.

RNA Isolation, Reverse Transcription, and PCR

RNA was isolated with the Universal RNA Purification Kit (EURx) in combination with an on-column DNase digest according to the manufacturer's instructions and eluted in 40 μL RNase-free water. RevertAid Premium (Thermo Fisher Scientific) or AMV Reverse Transcriptase Native (EURx) was used for reverse transcription, mostly following the manufacturers' specifications but using the maximum volume of RNA possible in the reaction. Unless stated otherwise, dT_{20} primer was used.

Coamplification PCRs were performed using a homemade Taq polymerase and following standard protocols. Resulting RT-PCR products were separated on agarose gels and stained with ethidium bromide solution. Gel pictures were taken under UV light and, if needed, modified using Adobe Photoshop auto-contrast function. Quantification of coamplified PCR products was performed using the Agilent DNA1000 kit and 2100 Bioanalyzer. The CFX384 real-time PCR system (Bio-Rad) and MESA BLUE qPCR MasterMix Plus (Eurogentec) were used for relative quantification of individual cDNAs. *PROTEIN PHOSPHATASE 2A* (*PP2A*, *AT1G13320*) was used as a reference transcript, except for the half-life assay, for which *ACTIN7* (*At5G09810*) was used as reference. A detailed quantitative PCR protocol is described by Stauffer et al. (2010).

Cloning Procedures

SR30 overexpression constructs for immunoblots were based on the vector pBinAR (Höfgen and Willmitzer, 1992). All primers used for cloning are listed in Supplemental Table S2. For cds constructs, inserts were amplified from cDNA using LH163/211 (SR30.1) or LH163/212 (SR30.2) omitting the STOP codon and cloned into a pBinAR containing HA3-STOP via *Bam*HI/*Xba*I. The inserts of the cDNA constructs were amplified each in two parts inserting an HA-tag at the C-terminus and removing the STOP codon with LH186/187 and LH188/189 (SR30.1) or LH186/190 and LH191/189 (SR30.2). The respective parts were combined using the corresponding outer primers. Cloning into *Bam*HI/*Sal*I digested pBinAR was done via *Bam*HI/*Xho*I. To generate HA3-tagged versions, the inserts both were amplified in two parts and HA3 added using LH186/312 and LH311/189. Insertion into pBinAR was done as described above for the untagged cDNA constructs. For constructs used for confocal microscopy, splice variants of *SR30* were amplified with primers LH159/160 or LH159/161, respectively, omitting the STOP codon, and recombined into pDONR201, then pB7CWG2 or pB7YWG2 (Karimi et al., 2002) using the Gateway system (Invitrogen). The genomic reporter used in the splice assay (Fig. 5) was amplified using primers LH163/169 inserting the C-terminal HA-tag and cloned into *Bam*HI/*Sal*I digested pBinAR via *Bam*HI/*Xho*I. The splice form-specific Flag-tagged cds constructs were cloned similarly using primers LH163/164 and LH163/165, respectively. The amiRNA was designed using the web tool WMD3 (http://wmd3.weigelworld.org; Ossowski et al., 2008) and cloned following the available protocol (http://wmd3.weigelworld.org/downloads/Cloning_of_artificial_microRNAs.pdf) using primers LH192-195. After extension of the partial attachment sites with primers ES32/33, the precursor was recombined into pDONR201, then pB7WG2 (Karimi et al., 2002) using the Gateway system (Invitrogen). For expression of recombinant SR30 for immunization, *SR30.2* cds was amplified using LH163/182 and cloned into pQE30 (Qiagen) via *Bam*HI/*Xho*I. Sequencing *SR30*, we discovered an insertion relative to the TAIR10 reference sequence. One G nucleotide was inserted between positions 2926 and 2927 of the annotated gene in the 11th intron. We found this insertion both in our wild-type line and the *lba1* mutant.

Plant Transformation

Heterotrophic cell culture protoplasts were transformed according to a previously published protocol (Schütze et al., 2009) with 2 μg of each plasmid and kept in darkness for 2 d before microscopy. *Nicotiana benthamiana* leaves were transiently transformed by leaf infiltration as previously described (Wachter et al., 2007) using transformed agrobacteria of an optical density 0.8 at 600 nm in water. Cotransformation of luciferase or one of the splicing variants with the reporter was achieved by mixing the respective bacterial suspensions 1:1 before infiltration. Cotransformation of the reporter with the luciferase control or with one of the splicing variants was always done on corresponding leaf halves for normalization purposes. Infiltrated plants were grown for additional 2 d before sampling. Arabidopsis plants were stably transformed by the floral dip method (Clough and Bent, 1998).

Antibody Generation

Escherichia coli M15 expressing *SR30.2* in the vector pQE30 were grown in 3 L Terrific Broth medium to an optical density >1 at 37°C. Protein expression was induced with 1 mM isopropyl β-D-thiogalactopyranoside and the culture further incubated at 37°C overnight. All following steps were done at 4°C or on ice unless specified otherwise. The cells were spun down and resuspended in cold lysis-equilibration-wash buffer (LEW; 300 mM NaCl and 50 mM NaH_2PO_4, pH 8.0), then lysed using a cooled French pressure cell (Aminco; 3× 1,000 psi). The lysate was treated with 50 μg/mL DNase for 20 min at room temperature under agitation and then centrifuged (10,000*g*, 30 min). The pellet was washed once with cold LEW, then resuspended in 25 mL denaturing solubilization buffer (DSB; 300 mM NaCl, 50 mM NaH_2PO_4, pH 8.0, and 8 M urea), incubated on a wheel shaker for 1 h, and spun at room temperature for 40 min at 10,000*g* or until supernatant was clear. The supernatant was added to Protino Ni-TED resin (Macherey-Nagel) prepared according to the manufacturer's instructions and incubated on a wheel shaker for 1 h at room temperature. The column was drained by gravity at room temperature and the flow-through was collected. At room temperature, the resin was washed with 200 mL DSB, and protein was eluted three times with 3 mL 150 mM and three times with 3 mL 200 mM imidazole-containing DSB. Elution fractions were combined, diluted with 5 mL LEW per mL elution fraction, and incubated on a wheel shaker overnight. Precipitated protein was spun down, resuspended in 2× SDS sample buffer, and denatured at 95°C for 10 min. Protein concentration was estimated by comparing band intensities on a gel to marker bands. Approximately 200 μg protein per lane was loaded on a 12% polyacrylamide gel. After Coomassie staining, the prominent band was excised excluding a slightly smaller band, and the gel pieces were washed in water until the pH was neutral. Rabbits were immunized six times with the gel-bound protein (BioGenes). The antibody was affinity purified from raw sera using membrane-bound antigen as described before (Rühl et al., 2012), but partly using a 1:1 dilution of 7 mL serum in one purification.

Protein Extraction, Immunoprecipitation, and Immunoblot Analyses

Starting material from infiltrated *N. benthamiana* leaves was ~100 mg, and 200 to 300 mg Arabidopsis seedlings was used per extraction. For immunoblot analyses, proteins were extracted as described previously (Rühl et al., 2012), using an extraction buffer containing 65 mM KCl, 15 mM NaCl, 10 mM HEPES

(pH 7.6), 10 mM Na_2EDTA, 5 mM DTT, 4 mM ATP, 1× phosphatase inhibitor mix (Serva), and 1× Complete (Roche; after Zahler et al., 1992). All extracts were cleared by centrifugation at 4°C for ~20 min at ~15,000*g*.

Using Protein G-coupled Dynabeads (Life Technologies), α-SR30 was coupled to the beads in PBS-T by incubation under agitation for 10 min at room temperature. The beads were washed once with PBS-T. Protein extract was added to the beads and protein was allowed to bind to the beads for 1 h at room temperature on a wheel shaker. The beads were washed three times using the extraction buffer and transferred to a fresh tube in a fourth washing step. Protein bound to Dynabeads was eluted at 95°C in 5× SDS sample buffer for 10 min while mixing.

SDS-PAGE and semidry immunoblotting were performed according to standard protocols. For detection, the following commercial antibodies were used: rabbit α-histone H3 (Agrisera), rabbit α-UGPase (Agrisera), rabbit α-FLAG (Sigma-Aldrich), mouse α-HA (Sigma-Aldrich), α-mouse-peroxidase (Sigma-Aldrich), and α-rabbit-peroxidase (Sigma-Aldrich). Chemiluminescence detection used Super or Ultra Signal West Dura (Pierce).

Confocal Microscopy

Microscopy was conducted with a TCS SP2 AOBS (Leica). The excitation (ex.) and emission (em.) settings were as follows: YFP 514 nm (ex.), 524 to 575 nm (em.) and DsRED 561 nm (ex.), 575 to 641 nm (em.) in Figure 4A; CFP 405 nm (ex.), 453 to 511 nm (em.) and YFP 514 nm (ex), 566 to 617 nm (em.) in Figure 4B; CFP 405 nm (ex.), 457 to 540 nm (em.) and YFP as for Figure 4A in Figure 4, C and D. The protoplasts were scanned in sequential mode, with the exception of the one shown in Figure 4B.

Accession Numbers

The following mutants have been used in different experiments: *sr30* (GK325-E11, N322146), *lba1* (Yoine et al., 2006), *upf3-1* (Hori and Watanabe, 2005), 35S:HF-RPL18 (N66056; Zanetti et al., 2005), *sop2-1* (Hématy et al., 2016), *mtr3* (also referred to as *rrp41l*; Yang et al., 2013), *hen2-4* and *mtr4-1* (Lange et al., 2011), *ski2-6* (Zhao and Kunst, 2016), *xrn4-5* (Souret et al., 2004), and *xrn2-1 xrn4-6*, *xrn3-3 xrn4-6*, and *fry1-6* (Gy et al., 2007). The following genes have been analyzed: *AT1G09140* (*SR30*), *AT2G37340* (*RS2Z33*), *AT5G37055* (*SEF*), *AT1G13320* (*PP2A*), and *At5G09810* (*ACTIN7*).

Supplemental Data

The following supplemental materials are available.

Supplemental Figure S1. Sequences of *SR30* Splicing Variants Analyzed in this Work.

Supplemental Figure S2. Levels of *SR30* Splicing Variants in RNA Degradation Mutants.

Supplemental Figure S3. SR30 Expression in T-DNA Mutants and in Response to Light.

Supplemental Figure S4. Detection of SR30 Fused to Fluorescent Proteins.

Supplemental Figure S5. Sequences of Splicing Variants from Light-Regulated AS Events in *SR30*.

Supplemental Figure S6. *SR30* Splicing Variant Patterns in Response to Light, Sugar, and *SR30* Overexpression.

Supplemental Figure S7. Examples of *SR* Genes with Long Introns Containing NMD-Triggering Cassette Exons.

Supplemental Table S1. *SR30* Transcript Levels and Segregation of Lines upon Splicing Variant-Specific Misexpression of *SR30*.

Supplemental Table S2. Sequences of DNA Oligos Used in This Study.

ACKNOWLEDGMENTS

We thank the Nottingham Arabidopsis Stock Centre for providing seeds of the *sr30*, *lba1*, and *upf3-1* mutants and of the 35S:HF-RPL18 line. Seeds of the *xrn* mutants were kindly provided by Hervé Vaucheret. We acknowledge Dominique Gagliardi and Heike Lange for providing seeds of the other RNA decay mutants and for discussion of the corresponding data. Furthermore, we thank Hsin-Chieh Lee for providing samples for the RNA stability assay, and Marcella Amorim and Sascha Laubinger for sharing an unpublished protocol for the subcellular fractionation experiment. We also thank Eva Stauffer and Gabriele Drechsel for help with the confocal microscope, and Gabriele Wagner and Natalie Faiss for laboratory assistance. We thank Xaq Pitkow for input on the graphical design of Figure 7. Technical support by the central facilities of the Center for Plant Molecular Biology (University of Tübingen) is acknowledged.

Received September 5, 2017; accepted February 16, 2018; published March 1, 2018.

LITERATURE CITED

Ali GS, Golovkin M, Reddy AS (2003) Nuclear localization and in vivo dynamics of a plant-specific serine/arginine-rich protein. Plant J **36:** 883–893

Ali GS, Palusa SG, Golovkin M, Prasad J, Manley JL, Reddy AS (2007) Regulation of plant developmental processes by a novel splicing factor. PLoS One **2:** e471

Bardou F, Ariel F, Simpson CG, Romero-Barrios N, Laporte P, Balzergue S, Brown JW, Crespi M (2014) Long noncoding RNA modulates alternative splicing regulators in Arabidopsis. Dev Cell **30:** 166–176

Boothby TC, Zipper RS, van der Weele CM, Wolniak SM (2013) Removal of retained introns regulates translation in the rapidly developing gametophyte of Marsilea vestita. Dev Cell **24:** 517–529

Braunschweig U, Gueroussov S, Plocik AM, Graveley BR, Blencowe BJ (2013) Dynamic integration of splicing within gene regulatory pathways. Cell **152:** 1252–1269

Carvalho RF, Szakonyi D, Simpson CG, Barbosa IC, Brown JW, Baena-González E, Duque P (2016) The Arabidopsis SR45 splicing factor, a negative regulator of sugar signaling, modulates SNF1-Related Protein Kinase 1 stability. Plant Cell **28:** 1910–1925

Chen M, Manley JL (2009) Mechanisms of alternative splicing regulation: insights from molecular and genomics approaches. Nat Rev Mol Cell Biol **10:** 741–754

Chin A, Lécuyer E (2017) RNA localization: Making its way to the center stage. Biochim Biophys Acta **1861:** 2956–2970

Clough SJ, Bent AF (1998) Floral dip: a simplified method for Agrobacterium-mediated transformation of Arabidopsis thaliana. Plant J **16:** 735–743

Cook-Andersen H, Wilkinson MF (2015) Molecular biology: Splicing does the two-step. Nature **521:** 300–301

Day IS, Golovkin M, Palusa SG, Link A, Ali GS, Thomas J, Richardson DN, Reddy AS (2012) Interactions of SR45, an SR-like protein, with spliceosomal proteins and an intronic sequence: insights into regulated splicing. Plant J **71:** 936–947

de Francisco Amorim M, Willing E-M, Droste-Borel I, Macek B, Schneeberger K, Laubinger S (2017) Arabidopsis U1 snRNP subunit LUC7 functions in alternative splicing and preferential removal of terminal introns. bioRxiv doi.org/10.1101/150805

Dolata J, Guo Y, Kołowerzo A, Smoliński D, Brzyżek G, Jarmołowski A, Świeżewski S (2015) NTR1 is required for transcription elongation checkpoints at alternative exons in Arabidopsis. EMBO J **34:** 544–558

Dominguez D, Tsai YH, Weatheritt R, Wang Y, Blencowe BJ, Wang Z (2016) An extensive program of periodic alternative splicing linked to cell cycle progression. eLife **5:** e10288

Drechsel G, Kahles A, Kesarwani AK, Stauffer E, Behr J, Drewe P, Rätsch G, Wachter A (2013) Nonsense-mediated decay of alternative precursor mRNA splicing variants is a major determinant of the Arabidopsis steady state transcriptome. Plant Cell **25:** 3726–3742

Duff MO, Olson S, Wei X, Garrett SC, Osman A, Bolisetty M, Plocik A, Celniker SE, Graveley BR (2015) Genome-wide identification of zero nucleotide recursive splicing in Drosophila. Nature **521:** 376–379

Fang Y, Hearn S, Spector DL (2004) Tissue-specific expression and dynamic organization of SR splicing factors in Arabidopsis. Mol Biol Cell **15:** 2664–2673

Filichkin SA, Priest HD, Givan SA, Shen R, Bryant DW, Fox SE, Wong WK, Mockler TC (2010) Genome-wide mapping of alternative splicing in *Arabidopsis thaliana*. Genome Res **20:** 45–58

Filichkin SA, Cumbie JS, Dharmawardhana P, Jaiswal P, Chang JH, Palusa SG, Reddy AS, Megraw M, Mockler TC (2015) Environmental stresses modulate abundance and timing of alternatively spliced circadian transcripts in Arabidopsis. Mol Plant **8:** 207–227

Ghosh S, Marchand V, Gáspár I, Ephrussi A (2012) Control of RNP motility and localization by a splicing-dependent structure in oskar mRNA. Nat Struct Mol Biol **19:** 441–449

Göhring J, Jacak J, Barta A (2014) Imaging of endogenous messenger RNA splice variants in living cells reveals nuclear retention of transcripts inaccessible to nonsense-mediated decay in Arabidopsis. Plant Cell **26:** 754–764

Golovkin M, Reddy AS (1998) The plant U1 small nuclear ribonucleoprotein particle 70K protein interacts with two novel serine/arginine-rich proteins. Plant Cell **10:** 1637–1648

Gueroussov S, Gonatopoulos-Pournatzis T, Irimia M, Raj B, Lin ZY, Gingras AC, Blencowe BJ (2015) An alternative splicing event amplifies evolutionary differences between vertebrates. Science **349:** 868–873

Gy I, Gasciolli V, Lauressergues D, Morel JB, Gombert J, Proux F, Proux C, Vaucheret H, Mallory AC (2007) Arabidopsis FIERY1, XRN2, and XRN3 are endogenous RNA silencing suppressors. Plant Cell **19:** 3451–3461

Hachet O, Ephrussi A (2004) Splicing of oskar RNA in the nucleus is coupled to its cytoplasmic localization. Nature **428:** 959–963

Hartmann L, Drewe-Boß P, Wießner T, Wagner G, Geue S, Lee HC, Obermüller DM, Kahles A, Behr J, Sinz FH, Rätsch G, Wachter A (2016) Alternative splicing substantially diversifies the transcriptome during early photomorphogenesis and correlates with the energy availability in Arabidopsis. Plant Cell **28:** 2715–2734

Hatton AR, Subramaniam V, Lopez AJ (1998) Generation of alternative Ultrabithorax isoforms and stepwise removal of a large intron by resplicing at exon-exon junctions. Mol Cell **2:** 787–796

Hématy K, Bellec Y, Podicheti R, Bouteiller N, Anne P, Morineau C, Haslam RP, Beaudoin F, Napier JA, Mockaitis K, et al (2016) The zinc-finger protein SOP1 is required for a subset of the nuclear exosome functions in Arabidopsis. PLoS Genet **12:** e1005817

Höfgen R, Willmitzer L (1992) Transgenic potato plants depleted for the major tuber protein patatin via expression of antisense RNA. Plant Sci **87:** 45–54

Hori K, Watanabe Y (2005) UPF3 suppresses aberrant spliced mRNA in Arabidopsis. Plant J **43:** 530–540

James AB, Syed NH, Bordage S, Marshall J, Nimmo GA, Jenkins GI, Herzyk P, Brown JW, Nimmo HG (2012) Alternative splicing mediates responses of the Arabidopsis circadian clock to temperature changes. Plant Cell **24:** 961–981

Kalyna M, Lopato S, Barta A (2003) Ectopic expression of atRSZ33 reveals its function in splicing and causes pleiotropic changes in development. Mol Biol Cell **14:** 3565–3577

Kalyna M, Lopato S, Voronin V, Barta A (2006) Evolutionary conservation and regulation of particular alternative splicing events in plant SR proteins. Nucleic Acids Res **34:** 4395–4405

Kalyna M, Simpson CG, Syed NH, Lewandowska D, Marquez Y, Kusenda B, Marshall J, Fuller J, Cardle L, McNicol J, et al (2012) Alternative splicing and nonsense-mediated decay modulate expression of important regulatory genes in Arabidopsis. Nucleic Acids Res **40:** 2454–2469

Karimi M, Inze D, Depicker A (2002) GATEWAY vectors for Agrobacterium-mediated plant transformation. Trends Plant Sci **7:** 193–195

Kerényi Z, Mérai Z, Hiripi L, Benkovics A, Gyula P, Lacomme C, Barta E, Nagy F, Silhavy D (2008) Inter-kingdom conservation of mechanism of nonsense-mediated mRNA decay. EMBO J **27:** 1585–1595

Kim SH, Koroleva OA, Lewandowska D, Pendle AF, Clark GP, Simpson CG, Shaw PJ, Brown JW (2009) Aberrant mRNA transcripts and the nonsense-mediated decay proteins UPF2 and UPF3 are enriched in the Arabidopsis nucleolus. Plant Cell **21:** 2045–2057

Kriechbaumer V, Wang P, Hawes C, Abell BM (2012) Alternative splicing of the auxin biosynthesis gene YUCCA4 determines its subcellular compartmentation. Plant J **70:** 292–302

Lamesch P, Berardini TZ, Li D, Swarbreck D, Wilks C, Sasidharan R, Muller R, Dreher K, Alexander DL, Garcia-Hernandez M, et al (2012) The Arabidopsis Information Resource (TAIR): improved gene annotation and new tools. Nucleic Acids Res **40:** D1202–D1210

Lange H, Sement FM, Gagliardi D (2011) MTR4, a putative RNA helicase and exosome co-factor, is required for proper rRNA biogenesis and development in *Arabidopsis thaliana*. Plant J **68:** 51–63

Li Q, Zheng S, Han A, Lin CH, Stoilov P, Fu XD, Black DL (2014) The splicing regulator PTBP2 controls a program of embryonic splicing required for neuronal maturation. eLife **3:** e01201

Li S, Yamada M, Han X, Ohler U, Benfey PN (2016) High-resolution expression map of the Arabidopsis root reveals alternative splicing and lincRNA regulation. Dev Cell **39:** 508–522

Liu N, Dai Q, Zheng G, He C, Parisien M, Pan T (2015) N(6)-methyladenosine-dependent RNA structural switches regulate RNA-protein interactions. Nature **518:** 560–564

Lopato S, Kalyna M, Dorner S, Kobayashi R, Krainer AR, Barta A (1999) atSRp30, one of two SF2/ASF-like proteins from *Arabidopsis thaliana*, regulates splicing of specific plant genes. Genes Dev **13:** 987–1001

Lorković ZJ, Hilscher J, Barta A (2004) Use of fluorescent protein tags to study nuclear organization of the spliceosomal machinery in transiently transformed living plant cells. Mol Biol Cell **15:** 3233–3243

Mandadi KK, Scholthof KB (2015) Genome-wide analysis of alternative splicing landscapes modulated during plant-virus interactions in *Brachypodium distachyon*. Plant Cell **27:** 71–85

Marquez Y, Brown JW, Simpson C, Barta A, Kalyna M (2012) Transcriptome survey reveals increased complexity of the alternative splicing landscape in Arabidopsis. Genome Res **22:** 1184–1195

Meyer K, Köster T, Nolte C, Weinholdt C, Lewinski M, Grosse I, Staiger D (2017) Adaptation of iCLIP to plants determines the binding landscape of the clock-regulated RNA-binding protein AtGRP7. Genome Biol **18:** 204

Mohr SE, Dillon ST, Boswell RE (2001) The RNA-binding protein Tsunagi interacts with Mago Nashi to establish polarity and localize oskar mRNA during Drosophila oogenesis. Genes Dev **15:** 2886–2899

Mori T, Yoshimura K, Nosaka R, Sakuyama H, Koike Y, Tanabe N, Maruta T, Tamoi M, Shigeoka S (2012) Subcellular and subnuclear distribution of high-light responsive serine/arginine-rich proteins, atSR45a and atSR30, in *Arabidopsis thaliana*. Biosci Biotechnol Biochem **76:** 2075–2081

Mustroph A, Zanetti ME, Girke T, Bailey-Serres J (2013) Isolation and analysis of mRNAs from specific cell types of plants by ribosome immunopurification. Methods Mol Biol **959:** 277–302

Newmark PA, Boswell RE (1994) The mago nashi locus encodes an essential product required for germ plasm assembly in Drosophila. Development **120:** 1303–1313

Ossowski S, Schwab R, Weigel D (2008) Gene silencing in plants using artificial microRNAs and other small RNAs. Plant J **53:** 674–690

Palacios IM, Gatfield D, St Johnston D, Izaurralde E (2004) An eIF4AIII-containing complex required for mRNA localization and nonsense-mediated mRNA decay. Nature **427:** 753–757

Palusa SG, Ali GS, Reddy AS (2007) Alternative splicing of pre-mRNAs of Arabidopsis serine/arginine-rich proteins: regulation by hormones and stresses. Plant J **49:** 1091–1107

Palusa SG, Reddy AS (2010) Extensive coupling of alternative splicing of pre-mRNAs of serine/arginine (SR) genes with nonsense-mediated decay. New Phytol **185:** 83–89

Palusa SG, Reddy AS (2015) Differential recruitment of splice variants from SR pre-mRNAs to polysomes during development and in response to stresses. Plant Cell Physiol **56:** 421–427

Pan Q, Shai O, Lee LJ, Frey BJ, Blencowe BJ (2008) Deep surveying of alternative splicing complexity in the human transcriptome by high-throughput sequencing. Nat Genet **40:** 1413–1415

Penfield S, Josse EM, Halliday KJ (2010) A role for an alternative splice variant of PIF6 in the control of Arabidopsis primary seed dormancy. Plant Mol Biol **73:** 89–95

Reddy AS, Marquez Y, Kalyna M, Barta A (2013) Complexity of the alternative splicing landscape in plants. Plant Cell **25:** 3657–3683

Remy E, Cabrito TR, Baster P, Batista RA, Teixeira MC, Friml J, Sá-Correia I, Duque P (2013) A major facilitator superfamily transporter plays a dual role in polar auxin transport and drought stress tolerance in Arabidopsis. Plant Cell **25:** 901–926

Rühl C, Stauffer E, Kahles A, Wagner G, Drechsel G, Rätsch G, Wachter A (2012) Polypyrimidine tract binding protein homologs from Arabidopsis are key regulators of alternative splicing with implications in fundamental developmental processes. Plant Cell **24:** 4360–4375

Sanchez SE, Petrillo E, Beckwith EJ, Zhang X, Rugnone ML, Hernando CE, Cuevas JC, Godoy Herz MA, Depetris-Chauvin A, Simpson CG, et al (2010) A methyl transferase links the circadian clock to the regulation of alternative splicing. Nature **468:** 112–116

Schöning JC, Streitner C, Meyer IM, Gao Y, Staiger D (2008) Reciprocal regulation of glycine-rich RNA-binding proteins via an interlocked

feedback loop coupling alternative splicing to nonsense-mediated decay in Arabidopsis. Nucleic Acids Res **36:** 6977–6987

Schütze K, Harter K, Chaban C (2009) Bimolecular fluorescence complementation (BiFC) to study protein-protein interactions in living plant cells. Methods Mol Biol **479:** 189–202

Shikata H, Hanada K, Ushijima T, Nakashima M, Suzuki Y, Matsushita T (2014) Phytochrome controls alternative splicing to mediate light responses in Arabidopsis. Proc Natl Acad Sci USA **111:** 18781–18786

Shikata H, Shibata M, Ushijima T, Nakashima M, Kong S-G, Matsuoka K, Lin C, Matsushita T (2012) The RS domain of Arabidopsis splicing factor RRC1 is required for phytochrome B signal transduction. Plant J **70:** 727–738

Sibley CR, Emmett W, Blazquez L, Faro A, Haberman N, Briese M, Trabzuni D, Ryten M, Weale ME, Hardy J, et al (2015) Recursive splicing in long vertebrate genes. Nature **521:** 371–375

Souret FF, Kastenmayer JP, Green PJ (2004) AtXRN4 degrades mRNA in Arabidopsis and its substrates include selected miRNA targets. Mol Cell **15:** 173–183

Staiger D, Brown JW (2013) Alternative splicing at the intersection of biological timing, development, and stress responses. Plant Cell **25:** 3640–3656

Staiger D, Green R (2011) RNA-based regulation in the plant circadian clock. Trends Plant Sci **16:** 517–523

Staiger D, Zecca L, Wieczorek Kirk DA, Apel K, Eckstein L (2003) The circadian clock regulated RNA-binding protein AtGRP7 autoregulates its expression by influencing alternative splicing of its own pre-mRNA. Plant J **33:** 361–371

Stauffer E, Westermann A, Wagner G, Wachter A (2010) Polypyrimidine tract-binding protein homologues from Arabidopsis underlie regulatory circuits based on alternative splicing and downstream control. Plant J **64:** 243–255

Streitner C, Köster T, Simpson CG, Shaw P, Danisman S, Brown JW, Staiger D (2012) An hnRNP-like RNA-binding protein affects alternative splicing by in vivo interaction with transcripts in Arabidopsis thaliana. Nucleic Acids Res **40:** 11240–11255

Sureshkumar S, Dent C, Seleznev A, Tasset C, Balasubramanian S (2016) Nonsense-mediated mRNA decay modulates FLM-dependent thermosensory flowering response in Arabidopsis. Nat Plants **2:** 16055

Tanabe N, Yoshimura K, Kimura A, Yabuta Y, Shigeoka S (2007) Differential expression of alternatively spliced mRNAs of Arabidopsis SR protein homologs, atSR30 and atSR45a, in response to environmental stress. Plant Cell Physiol **48:** 1036–1049

Thomas J, Palusa SG, Prasad KV, Ali GS, Surabhi GK, Ben-Hur A, Abdel-Ghany SE, Reddy AS (2012) Identification of an intronic splicing regulatory element involved in auto-regulation of alternative splicing of SCL33 pre-mRNA. Plant J **72:** 935–946

Tillemans V, Dispa L, Remacle C, Collinge M, Motte P (2005) Functional distribution and dynamics of Arabidopsis SR splicing factors in living plant cells. Plant J **41:** 567–582

Tillemans V, Leponce I, Rausin G, Dispa L, Motte P (2006) Insights into nuclear organization in plants as revealed by the dynamic distribution of Arabidopsis SR splicing factors. Plant Cell **18:** 3218–3234

Traunmüller L, Gomez AM, Nguyen TM, Scheiffele P (2016) Control of neuronal synapse specification by a highly dedicated alternative splicing program. Science **352:** 982–986

van Eeden FJ, Palacios IM, Petronczki M, Weston MJ, St Johnston D (2001) Barentsz is essential for the posterior localization of oskar mRNA and colocalizes with it to the posterior pole. J Cell Biol **154:** 511–523

Wachter A (2010) Riboswitch-mediated control of gene expression in eukaryotes. RNA Biol **7:** 67–76

Wachter A (2014) Gene regulation by structured mRNA elements. Trends Genet **30:** 172–181

Wachter A, Rühl C, Stauffer E (2012) The role of polypyrimidine tract-binding proteins and other hnRNP proteins in plant splicing regulation. Front Plant Sci **3:** 81

Wachter A, Tunc-Ozdemir M, Grove BC, Green PJ, Shintani DK, Breaker RR (2007) Riboswitch control of gene expression in plants by splicing and alternative 3′ end processing of mRNAs. Plant Cell **19:** 3437–3450

Wang B, Tseng E, Regulski M, Clark TA, Hon T, Jiao Y, Lu Z, Olson A, Stein JC, Ware D (2016) Unveiling the complexity of the maize transcriptome by single-molecule long-read sequencing. Nat Commun **7:** 11708

Wang X, Wu F, Xie Q, Wang H, Wang Y, Yue Y, Gahura O, Ma S, Liu L, Cao Y, et al (2012) SKIP is a component of the spliceosome linking alternative splicing and the circadian clock in Arabidopsis. Plant Cell **24:** 3278–3295

Wu Z, Zhu D, Lin X, Miao J, Gu L, Deng X, Yang Q, Sun K, Zhu D, Cao X, et al (2016) RNA binding proteins RZ-1B and RZ-1C play critical roles in regulating pre-mRNA splicing and gene expression during development in Arabidopsis. Plant Cell **28:** 55–73

Xing D, Wang Y, Hamilton M, Ben-Hur A, Reddy AS (2015) Transcriptome-wide identification of RNA targets of Arabidopsis SERINE/ARGININE-RICH45 uncovers the unexpected roles of this RNA binding protein in RNA processing. Plant Cell **27:** 3294–3308

Yan Q, Xia X, Sun Z, Fang Y (2017) Depletion of Arabidopsis SC35 and SC35-like serine/arginine-rich proteins affects the transcription and splicing of a subset of genes. PLoS Genet **13:** e1006663

Yang M, Zhang B, Jia J, Yan C, Habaike A, Han Y (2013) RRP41L, a putative core subunit of the exosome, plays an important role in seed germination and early seedling growth in Arabidopsis. Plant Physiol **161:** 165–178

Yoine M, Ohto MA, Onai K, Mita S, Nakamura K (2006) The lba1 mutation of UPF1 RNA helicase involved in nonsense-mediated mRNA decay causes pleiotropic phenotypic changes and altered sugar signalling in Arabidopsis. Plant J **47:** 49–62

Zahler AM, Lane WS, Stolk JA, Roth MB (1992) SR proteins: a conserved family of pre-mRNA splicing factors. Genes Dev **6:** 837–847

Zanetti ME, Chang IF, Gong F, Galbraith DW, Bailey-Serres J (2005) Immunopurification of polyribosomal complexes of Arabidopsis for global analysis of gene expression. Plant Physiol **138:** 624–635

Zhang XN, Mount SM (2009) Two alternatively spliced isoforms of the Arabidopsis SR45 protein have distinct roles during normal plant development. Plant Physiol **150:** 1450–1458

Zhang Y, Gu L, Hou Y, Wang L, Deng X, Hang R, Chen D, Zhang X, Zhang Y, Liu C, Cao X (2015) Integrative genome-wide analysis reveals HLP1, a novel RNA-binding protein, regulates plant flowering by targeting alternative polyadenylation. Cell Res **25:** 864–876

Zhao L, Kunst L (2016) SUPERKILLER complex components are required for the RNA exosome-mediated control of cuticular wax biosynthesis in Arabidopsis inflorescence stems. Plant Physiol **171:** 960–973

IV.1.3. Unpublished manuscript

"Energy Sensor Signalling Affects Early Seedling Development and Correlates with Alternative Splicing"

- Authors:
  Saile J.[*], Wießner-Kroh T.[*] and Wachter A.

- aspired Journal: Nature Plants

- aspired submission in 2021

SnRK1-TOR manuscript

Title

Energy sensor signalling affects early seedling development and correlates with alternative splicing

Authors

Jennifer Saile, Theresa Wießner-Kroh, Andreas Wachter

Introduction

One of the most crucial factors during the plant life cycle is light, an important energy source and a key regulator of development[1], e.g. during photomorphogenesis. Accordingly, changes in ambient light conditions substantially reprogram gene expression including adjustments of alternative precursor mRNA splicing (AS)[2,3]. AS is a powerful means to increase transcriptome complexity that support the developmental plasticity displayed by plants under changing environmental conditions[4] as previously demonstrated for light-driven expression of reduced red light responses in *cry1 cry2* background 1 (RRC1) with consequences on hypocotyl growth[2]. However, the upstream signalling of light-mediated AS is not well understood. Recently, metabolic and kinase signalling were correlated to light-regulated AS[2]. Metabolic signals including sucrose can function as signalling molecules or as energy source[5]. Due to their photoautotrophic life style, it is of utmost importance for plants to sense energy levels to adjust growth and metabolism based on the available resources. Here we provide evidence that the signalling of the central energy sensors SNF1-related protein kinase 1 (SnRK1) and target of rapamycin (TOR) correlate with several AS events in response to altered energy availability. In fact, SnRK1 repression resulted in a comparable AS shift for RRC1 and other AS events upon illumination. Moreover, reduced kinase signalling were paralleled with strongly inhibited hypocotyl elongation in etiolated seedlings, reminiscent to light-grown seedlings. Surprisingly, inhibition of TOR signalling resulted in similar phenotypes and AS pattern changes for analysed AS evens, despite its reported antagonistic function compared to SnRK1. Based on our data, we propose that SnRK1 and TOR might act as upstream regulators for light-mediated AS and control seedling development during the early photomorphogenesis.

Results & Discussion

Based on our earlier findings that transcript levels of SnRK1 targets paralleled the responses on the AS levels[2], we raised the question whether the energy sensor SnRK1 is involved in controlling AS during photomorphogenesis. The SnRK1 kinase complex is

activated under energy deprivation, e.g. in darkness[6]. To test for a direct link between SnRK1 signalling and light-/sugar-regulated AS, we first generated two independent artificial microRNA (*amiR*) lines for simultaneous, constitutive downregulation of *SnRK1.1* and *SnRK1.2* referred to as *c-amiR-SnRK1-I* and *c-amiR-SnRK1-II* (Supplementary Fig. 1a,b). We were not able to obtain homozygous lines during our selection process, however some plant showed serve developmental phenotypes and a higher mortality (see Supplementary information and Supplementary Fig. 2). These observations suggested that constitutive SnRK1 repression leads to non-viable plants, which is in line with previous studies [6-8].

To avoid the drastic long-term effects on plant development, we successfully generated transgenic lines expressing estradiol-inducible *amiRs* targeting both *SnRK1.1* and *SnRK1.2*, referred to as *i-amiR-SnRK1-I* and *i-amiR-SnKR1-II,* to get viable plant (Fig.1a, Supplementary Fig.1a,c). The new approach enabled us to repress SnRK1 signalling at specific developmental stages. In the absence of estradiol, *i-ami-SnRK1* plants were not affected in growth and development (Supplementary Fig. 3). During our characterization of the mutant lines, we could correlate a reduced hypocotyl length of etiolated seedlings with effective SnRK1 repression upon *amiR* induction (Supplementary Fig. 4a, b). We used the hypocotyl length as screening parameter and select the most efficient *i-amiR-SnRK1-I_2* and *i-amiR-SnRK1-II_9* lines (Supplementary Fig. 4c). To confirm the phenotype in the following generation, wild type and homozygous *i-amiR* lines were grown in darkness. We included the T-DNA insertion line *snrk1.1-3* as a control since this mutant does not show any growth defects[9], probably due to remaining activity of the mutant allele or functional redundancy of the two close homologs SnRK1.1 and SnRK1.2. In the absence of estradiol, wild type, *snrk1.1-3,* and both *i-amiR-SnRK1* lines showed a typical skotomorphogenic phenotype with an elongated hypocotyl, formation of an apical hook, and pale, closed cotyledons (Fig. 1b). Exposure to estradiol resulted in shortened hypocotyls of *i-amiR-SnRK1-I_2* and *i-amiR-SnRK1-II_9* lines, whereas wild type and *snrk1.1-3* remained unaffected in their skotomorphogenic development. Moreover, plant development of *i-amiR-SnRK1* mutants were strongly impaired when grown under long-day conditions for two weeks. Compared to the control plants*, i-amiR-SnRK1-I_2* and *i-amiR-SnRK1-II_9* were delayed in their growth and showed chlorosis in their cotyledons (Fig. 1c), a similar effect we observed in *c-amiR-SnRK1* rosette leaves (Supplementary Fig. 2b). To test whether the phenotypes are dependent on light intensities, wild type and mutant lines were cultivated under 10, 140 or 300 µmol min^{-1} s^{-1}, respectively. We observed that the decrease in chlorophyll levels was most pronounced under low light conditions in the *SnRK1* knockdown lines suggesting that the mutants may be more susceptible to energy deficiency upon SnRK1 repression (Fig. 1c, d; Supplementary Fig. 5). Recently, the senescence-promoting transcription factor ETHYLENE INSENSITIVE 3 (EIN3) was demonstrated to be directly phosphorylated by SnRK1, resulting in EIN3 destabilization and decelerated plant leaf

senescence[10]. Moreover, SnRK1 acts as a positive regulator of the cellular recycling mechanism autophagy, inter alia, by targeting AUTOPHAGY RELATED 1. Accordingly, up- or downregulation of SnRK1 expression result in delayed or enhanced senescence, respectively[11,12]. Intriguingly, ethylene recognition initiates hypocotyl elongation under light conditions. This process connects photosynthesis with ethylene and SnRK1 signalling. Loss of ethylene responsiveness in *etr1* mutant causes low energy syndrome via inhibition of photosystem II resulting in SnRK1 activation and finally the suppression of hypocotyl growth[13]. EIN3 is also known to be a key regulator of leaf senescence and chlorophyll degradation[14,15] linking both observed phenotypes. Finally, the application of exogenous glucose also inhibits hypocotyl elongation and proper cotyledon development in wild type[16-18] strengthening the involvement of energy signalling during early seedling development. Therefore, we hypothesize that SnRK1 may integrate the light input with other signalling pathways to adjust the plant development program.

To correlate the aforementioned phenotypes with *SnRK1* repression, we analysed *SnRK1* transcript levels in the selected mutants upon different periods of estradiol treatment. Both mutant lines exhibited maximal repression of *SnRK1.1* and *SnRK1.2* after 24 h induction of *amiR* expression. Longer incubation times up to 6 d did not further enhance this effect (Fig. 2a, Supplementary Fig. 6a). Additionally, we confirmed that the downstream target *DIN1* was responsive to *SnRK1* repression. Accordingly, a clear reduction of SnRK1 signalling could be seen after 3 d of *amiR* induction, which was used for further experiments to avoid side effects resulting from extended SnRK1 repression (Fig. 2b, Supplementary Fig. 6a). Next, we analysed the abundance of SnRK1 proteins upon inducible knockdown. Both kinases showed only slightly reduced total protein levels in 6-d-old seedlings (Fig. 2c, upper panel), which may be explained by high protein stability of SnRK1. However, SnRK1 kinase activity is defined by the phosphorylation status of Thr175, situated in the T-loop of the catalytic subunit. Therefore, active SnRK1 protein was determined using the mammalian anti-p-AMPK antibody which detects the phosphorylated versions of both SnRK1 homologs *in planta*, as two discrete bands due to their size difference. Interestingly, a substantial decrease of active SnRK1 protein was observed after 3 d estradiol treatment, while all control samples did not differ in the corresponding protein levels (Fig. 2c, middle panel). These data suggest, that SnRK1 activation via T-loop phosphorylation might also trigger the destabilization of the kinase at the same time, whereas unphosphorylated SnRK1 shows a higher stability under these conditions and might function as a storage pool to quickly reactivate SnRK1 signalling upon environmental variation. However, the complex regulation of SnRK1 is not fully understood so far. SnRK1 signalling is dependent on several aspects including post-transcriptional modification of the kinase subunits, stability and localization[19]. In fact, SnRK1 activation is

mediated by the upstream kinases SnRK1-activating kinase 1 (SnAK1) and SnAK2, which are in turn phosphorylated and inhibited by SnRK1 in a negative feedback loop[20]. Due to their specific spatial expression in developing and virus-infected tissues, we can assume that also other kinases are important for SnRK1 activity regulation during plant development and under different environmental conditions[21]. Proteasomal degradation of SnRK1 total protein were shown in response to glucose[22], however, the phosphorylated and dephosphorylated forms of SnRK1 protein were not separately analysed. Remarkably, a recent paper demonstrated stress-induced nuclear translocation of the catalytic α-subunit (SnRK1.1, SnRK1.2) to induce target gene expression such as DIN6[19]. Plants expressing SnRK1 α-subunit tagged with nuclear localisation signal appeared more resistant to extended darkness and displayed significant changes in its rosette leaf and root morphology[19].
Note that the induction of *SnRK1* repression for 3 d was sufficient to reduce hypocotyl elongation in etiolated *i-amiR-SnRK1* seedlings, but there was also a mild but significant estradiol effect for wild type seedlings (Supplementary Fig. 4d). Already previous studies reported a negative effect of high estradiol concentrations on plant growth which is in line with our observations[23]. In contrast, the seedlings in the experiments for the hypocotyl screen were grown on solid agar plates, which probably resulted in less estradiol uptake and therefore identical hypocotyl lengths of mock- and estradiol-treated wild type seedlings (Fig. 1b).

The phenotypical adaptation to altered light regimes needs to be well-orchestrated on the molecular level. Next to comprehensive light-dependent changes in total transcript levels, several hundred AS events responding to changes in illumination were recently identified[2,3]. Furthermore, SnRK1 was proposed as a negative regulator of light- and sugar-mediated AS during photomorphogenesis[2]. Very recently, the mammalian homologue of SnRK1, AMPK was shown to regulate the AS of a gene encoding an immune system-related receptor in human cell culture[24]. Nevertheless, little is known about the extent of AMPK-mediated AS control in animals, and moreover, it is a completely open question if SnRK1 has related functions in AS regulation in plants. We therefore raised the question whether downregulating SnRK1 is sufficient to induce the same AS changes as observed upon light and sugar treatment. 3-d-old etiolated seedlings were subjected to estradiol or mock treatment and then kept for additional 3 d in darkness before harvesting and AS pattern analysis. Indeed, repression of *SnRK1* signalling significantly changed the AS ratio of the pre-mRNAs encoding RRC1 and the serine/arginine-rich protein splicing factor 30 (SR30) towards the generation of the productive splice variant in 6-day-old etiolated seedlings (Fig. 3a,b; Supplementary Fig. 6b). Promotion of RRC1 protein expression via a light-induced AS shift was previously demonstrated to contribute to photomorphogenic growth under red light[2]. Interestingly, the *RRC1* AS response to SnRK1 repression was as effective as for light or sugar treatment, whereas *SR30* showed

a less pronounced AS shift when comparing SnRK1 repression and light treatment[2]. AS is a complex and highly dynamic mechanism, involving many splicing regulators e.g. SR proteins[4]. These regulators need to be tightly controlled such as SR30 and SR-like protein 45 (SR45), which were shown to be differentially spliced in response to different light regimes, intensities or temperatures[25,26]. To identify upstream regulators, studies using photoreceptor mutants revealed that PHY signalling participates in controlling light-regulated AS[3,27]. Accordingly, splicing factor for phytochrome signalling (SFPS) and RRC1 were shown to control a subset of AS events upon illumination[28,29]. Interestingly, light-regulated AS can also occur independent of photoreceptors and is responsive to energy and retrograde signalling[2,30,31]. Despite the knowledge that different signalling pathways are involved, little is known about the mechanism of how these pathways control splicing and at which level they might be integrated. Here in this study, we provide initial indications that SnRK1 signalling controls some light- and sugar-triggered AS events *in planta*. Probably more than the tested AS events related to altered energy availability undergo SnRK1-mediated splicing control. To delight this aspect, a quantitative transcriptome analysis would be required. Moreover, SnRK1 might be considered as positive regulator of hypocotyl elongation during the early seedling development. Since darkness boosts SnRK1 kinase signalling[6], SnRK1 could function as growth promoter in the etiolated seedling in order to enhance hypocotyl growth to more quickly reach the sun light and establish a photoautotrophic life style. Accordingly, light and sucrose exposure for 6 h significantly reduced *SnRK1.1* and *SnRK1.2* transcript level in etiolated wild type seedlings (Supplementary Fig. 8a), however protein levels were just slightly diminished (Supplementary Fig. 8b,c). Nevertheless, the expression of the downstream targets *DIN1* and *DIN6* was strongly reduced after exposure to light or external sucrose underlining an effective repression of SnRK1 signalling[2]. SnRK1 has been connected to ABA-insensitive 4 (ABI4)[32], a negative regulator of elongated hypocotyl 5 (HY5). It was shown that under stress conditions such as submergence, SnRK1 phosphorylates MPK6[33] and thus triggers the activation of ABI4 through phosphorylation[34]. Promotion of ABI4 leads to competitive displacement of HY5 from G-boxes[35] and thereby inhibits light-dependent seed development.

We also observed AS shifts in other light-regulated AS events including *peapod 2* (*PPD2*), *MYB-like domain transcription factor* (*MYBD*) and *PSBP-like protein 1* (*PPL1*), however, most were not statistically significant and far less pronounced than upon light exposure[2] (Fig. 3c, Supplementary Fig. 7a,b). The less pronounced AS responses for some AS events upon estradiol treatments compared to light-/ sugar-triggered AS shifts might be explained by the involvement of alternative upstream regulators. The energy sensor TOR is activated under favourable energy conditions and was described to act antagonistically to SnRK1[36]. TOR has already been connected to light signalling by promoting light-enhanced protein synthesis, and cotyledon opening in de-etiolating Arabidopsis seedlings[37]. Furthermore, stem cell activation

is positively regulated by TOR in response to light and metabolic signals[38]. Therefore, we were interested whether the antagonistic functions of SnRK1 and TOR are also reflected on the AS level during early seedling development. To study the role of TOR in light-/sugar-regulated AS, we analysed an estradiol-inducible *amiR-TOR* mutant (*i-amiR-TOR*), since *tor* knockout plants show embryo lethality[39,40]. The effective TOR repression revealed a significantly reduced hypocotyl elongation upon 6 d growth in darkness compared to wild type seedlings (Supplementary Fig. 9a,b), whereas etiolated *i-amiR-TOR* seedlings displayed normal development in the absence of estradiol (Supplementary Fig. 9a). This phenotype was unexpected considering the findings upon *SnRK1* knockdown and the proposed opposite functions of both energy sensors. TOR was previously described as positive regulator of hypocotyl elongation in etiolated seedlings[37,41]. Moreover, TOR seems to be crucial for the transition from skoto- to photomorphogenesis since TOR downregulation in light-grown seedlings causes pale, less expanded cotyledons and diminished hypocotyl growth[42,43]. Chemical inhibition of TOR classified several small auxin upregulated RNA (SAUR) genes, which are highly engaged during deetiolation, as putative downstream targets[44]. Accordingly, TOR signalling leads to phosphorylation of brassinosteriod insensitive 2 (BIN2), a major component of brassinosteriod and auxin signalling[43]. An EMS-mutant screen identified the TOR inhibitor AZD8055-insensitive mutant 1 (*trin1*). This mutant displays green and well-developed cotyledons in the presence of AZD8055[45]. *TRIN1* encodes ABI4. Since TRIN1/ABI4 protein accumulated upon TOR repression, the authors postulated that the developmental transition at the early seedling stage is mediated by TOR-dependent degradation of TRIN1/ABI4[45]. These studies support a crucial function of TOR signalling during early plant development by promoting photoautotrophic growth via several phytohormone pathways. Interestingly, in contrast to the proposed opposite roles of SnRK1 and TOR, both regulate ABI4 and are required for hypocotyl elongation in etiolated seedlings[32-35,45]. Since repression of SnRK1 and TOR during early seedling stage resulted in similar phenotypes, we were interested if TOR knock-down also affects AS pattern. Splicing patterns of *SR30*, *RRC1* and *PPD2* were significantly shifted to the protein-coding mRNA isoform upon TOR repression whereas *MYBD* did not respond on the AS level (Supplementary Fig. 9c). The extent of AS pattern shifts of *SR30* and *RRC1* were also comparable to those upon light exposure[2] and SnRK1 downregulation. Interestingly, chemical TOR repression was recently reported to abolish light-/sugar-dependent AS for *SR30* and *RS31* in root tissue of 2-week-old light-grown plants which were kept in extended darkness before re-illumination[46]. Contrary, the AS responses in leaves were TOR-independent according to this study. The authors proposed that sucrose serves as signalling molecule to transmit the information of changed light conditions from the shoot to the root. Altered sucrose levels are recognized by TOR and translated into an AS response in roots[46]. Similar phenotypical and AS responses upon

impaired SnRK1 and TOR signalling further adds to the accumulating evidence for cross-regulation between these two energy sensors. Therefore, we tested the *DIN*1 expression in *amiR-TOR* mutants, however, the *amiR-TOR* mutant did not show a significant difference in *DIN1* expression (Supplementary Fig. 9d). Nevertheless, SnRK1-TOR cross-regulation has already been described. In fact, recent phosphoproteomics revealed altered phosphorylation of the TOR downstream target ribosomal protein S6 (RPS6) upon SnRK1 misexpression[47,48]. Additionally, SnRK1.1 directly interacts and phosphorylates with regulatory-associated protein of TOR (RAPTOR)[48]. A crosstalk of both energy sensor is also supported by similar senescence phenotype upon SnRK1 or TOR repression, respectively. As shown for SnRK1, reduction of TOR expression resulted in early senescence accompanied with chlorophyll degradation in light-grown plants[42,49,50]. A possible explanation of this similar phenotype could be deregulated autophagy[12,51]. However, it remains unclear if both kinases are acting independently or could function as a SnRK1-TOR-relay.

We could demonstrate that SnRK1 and TOR signalling correlate with AS shifts for several AS events which were previously shown to respond to light and sugar exposure in etiolated seedlings. The transcriptional reprogramming is paralleled by phenotypical adaptations such as a reduction of hypocotyl elongation. However, whether the central energy sensors are direct upstream regulators of the splicing-relevant components and the exact regulatory mechanism e.g. if SnRK1 and TOR act synergistically remains elusive. AMPK directly phosphorylates the mammalian homologue of SR30, SRSF1, at the RNA-binding domain[24]. Hence, splicing factor binding to its RNA targets is prevented with consequences on the AS decision for SRSF1 targets. A recent phosphoproteome study in Arabidopsis plants compared protein phosphorylation status of wild type plants with *snrk1.1 snrk1.2* knock-down mutant and identified many phosphopeptides derived from proteins related to RNA metabolism were enriched in a *snrk1.1 snrk1.2* knock-down mutant upon extended darkness, whereas the wild type showed an upregulated set of phosphopeptides fitting to chloroplast and light reaction-associated proteins[48]. These findings suggest that SnRK1 acts as a negative regulator of light signalling in plants[48]. Additionally, the splicing factor SR45 impairs the AS outcome of the SnRK1-interacting phosphatase 5PTase13, which was suggested to promote proteasomal degradation of SnRK1 under glucose-fed conditions[22] and thus could act as negative feedback loop. Moreover, mammalian TOR regulates the expression of U2AF1 protein isoforms, which is involved in 3’ splice site selection, thus the mutually spliced exon is selected depending on the U2AF1 protein isoform[52]. This TOR-mediated U2AF1 expression can affect the translation of the target transcript if the splice event happens within the 5’ UTR. TOR was recently shown to regulate the light-dependent AS pattern of splicing-related proteins including U2AF65A, SR30 and RS31 in light-grown plants. Accordingly, an *in silico* motif analysis revealed that

many *SR* transcripts contain translation-promoting motives regulated by light and TOR signalling[46].

We postulate that both kinases can work together in light-mediated AS control by sensing the energy status of the plant. Upon light exposure, the energy is used to assimilate carbohydrates via photosynthesis. The level of freely available sugars modulates the kinase activity, which in turn may alter the phosphorylation status or translation of downstream targets such as splicing regulators. Finally, the splicing patterns for development-related components such as RRC1 shift, thereby contributing to growth adaptations in response to altered light conditions. Our work presents interesting insights into the complex AS regulation coordinated by the plant energy status and suggests a SnRK1- and TOR-dependent developmental transition during photomorphogenesis.

Methods

Plant material, growth conditions, and phenotyping. All mutants and wild type used in this study were in Col-0 background. The T-DNA insertion line *snrk1.1-3* (GABI_579E09) was previously described[9]. Seeds were surface sterilized in 3.75% NaOCl and 0.01% Triton X-100 and plated on ½ strength Murashige and Skoog (MS) medium (Duchefa) containing 0.8% phytoagar (Duchefa). Depending on the experiment, MS media was lacking or containing 1% or 2% sucrose, as well as 5 µM β-Estradiol (Sigma-Aldrich, St Louis, MO, US) or DMSO (mock).

For segregation analyses of constitutive *c-amiR* lines, seeds were plated singly on ½ MS plates containing 1% sucrose, 5 mg/L Basta (Bayer, Leverkusen, Germany), and 0.8% phytoagar. After stratification (2 days at 4 °C), plates were transferred to regular light (~100 µmol m^{-2} s^{-1}) and seedlings were grown for 2 weeks at 22 °C, and 60% relative humidity under long day (16-h light/8-h dark) conditions. Plates without sucrose and Basta for wild type growth served as controls. F1 lines with 75% survival rates (number of alive plants/total plant number) and more on selection medium (*cI-amiR_4, cI-amiR_5, cI-amiR_22, cII-amiR_5*) were selected for further analysis. After 2 weeks, resistant seedlings were transferred to soil for further characterization. Transferred plants were grown under a long day regime (16-h light/8-h dark) with a regular light intensity (~100 µmol m^{-2} s^{-1}) at 22 °C. For phenotypical analysis, plants were rated daily regarding their developmental stage and pictures were taken weekly with a Nikon D3200 camera.

Hypocotyl assay. To measure hypocotyl length, seedlings were grown on either 5 µM β-Estradiol- or mock-containing solid ½ MS plates without sucrose. Alternatively, seedlings were grown in liquid ½ MS media, and β-Estradiol and mock was added after 3 d of growth, respectively. After stratification (2 days at 4 °C), germination was induced by a 2 h light

treatment (~100 µmol m^{-2} s^{-1}) and plates were placed in darkness. 6 d-old etiolated seedlings were transferred to ½ MS plates containing 1.5% agar. Plates were scanned and hypocotyl length was measured using ImageJ.

Plasmid constructions and generation of transgenic plants. Two independent amiR sequences for targeting both *SnRK1.1* and *SnRK1.2* (Supplementary Fig. 1a) were identified and corresponding cloning primers (Supplementary Table 2) designed using the Web MicroRNA Designer (WMD3, http://wmd3.weigelworld.org)[53,54]. A detailed description of the cloning procedures is provided in the supplement. In short, site-directed PCR mutagenesis was performed on plasmid pRS300 to introduce DNA sequences corresponding to the amiRs. Constructs for constitutive amiR-SnRK1 expression were generated using Gateway cloning technology from Invitrogen (Carlsbad, CA, US)[53]. To this end, amiR sequences were cloned into pDONR201, followed by recombination into the vector pB7WG2 that enables driving expression under control of the 35S promoter[55]. Constructs for inducible amiR expression were created by using the modular GreenGate cloning system[56]. First, amiR sequences were cloned into the entry vector pGGC000. Individual expression cassettes for XVE and each amiR sequence were then assembled into an intermediate vector. Finally, the XVE module was coupled with either the amiR-I or amiR-II cassette via an adapter sequence and cloned into the destination vector pGGZ003 to create two independent β-Estradiol-inducible amiR constructs. A summary of all plasmids is provided in Supplementary Table 3. For generating the respective *A. thaliana* (Col-0) mutants, the final Gateway and GreenGate constructs were transformed into *Agrobacterium tumefaciens* strain C58C1 or ASE, respectively, followed by the floral dip method[57] .

Chlorophyll content measurements. For chlorophyll content analyses, seeds were plated on ½ MS medium supplemented with either 5 µM β-Estradiol or mock and stratified for 2 days at 4 °C. Plates were transferred to low (10 µmol m^{-2} s^{-1}), regular (140 µmol m^{-2} s^{-1}) or high (300 µmol m^{-2} s^{-1}) intensities of white light, followed by plant growth under long day conditions (16-h light/8-h dark). After 14 d, seedlings were transferred to ½ MS plates containing 1.5% agar and photographed using Fusion Fx (Vilber, Collégien, France). Furthermore, seedlings were harvested for chlorophyll content measurements, 22 to 250 mg fresh weight were resuspended in 200 µl phosphate buffer [25 mM KH_2PO_4, 25 mM K_2HPO_4 pH 7.0 and 2 mM EDTA (pH 8.0)] and chlorophyll was extracted with 800 µl 100% acetone. Mixtures were incubated for 1 h at room temperature under constant shaking. Subsequently, samples were centrifuged for 2 min at 10.000*g* and 4°C and supernatants were used for spectrophotometric analysis at 646 nm, 663 nm and 750 nm, respectively. Total chlorophyll was calculated using the previously

described formula 17.76 * OD_{646} + 7.34 * OD_{663}/1000 *V/FW, where V indicates the volume (ml) and FW the fresh weight (g)[58] .

Light and sucrose treatments. For light and sucrose treatments, wild type seedlings were grown in liquid ½ MS media in darkness. After 6 d, 1.06% mannitol or 2% sucrose was added to the media. Subsequently, seedlings were either kept in darkness or transferred to white light (~100 µmol m^{-2} s^{-1}) and incubated for 6 h.

RNA extraction, RT-qPCR, and PCR product analyses. RNA isolation was performed using the Universal RNA purification kit (EURx). Possible DNA contaminations were eliminated with an on-column DNaseI digest. cDNAs were generated with Superscript II Reverse Transcriptase (Invitrogen, Carlsbad, CA, US) following the manufacturer´s instructions. RT-qPCR was performed using the MESA GREEN qPCR Mastermix and a CFX384 real-time PCR cycler (Bio-Rad, Hercules, CA, US). *PP2A* (*AT1G13320)* served as reference transcript for normalisation. A detailed protocol for the RT-qPCR and the analysis was previously described[59]. For some events, splice variants were co-amplified via RT-PCR and isoform concentrations were determined using the 2100 Bioanalyzer with the DNA1000 kit (Agilent Technologies, Santa Clara, CA, US). The oligonucleotides used for RT-qPCR and RT-PCR are listed in Supplementary Table 4 and 5, respectively.

Protein extraction and immunoblot analyses. Immunoblot analyses were carried out as previously described[2]. In brief, 0.2 g of 6-d-old etiolated seedlings were freeze grounded to powder and homogenized in 0.2 mL extraction buffer [50 mM Tris-HCl (pH 7.5), 150 mM NaCl, 0.1% (v/v) Tween 20, 0.1% (v/v) β-mercaptoethanol and 1x protease inhibitor cocktail[56]]. Lysates were clarified by centrifugation at 15.000*g* and 4°C for 15 min and proteins were denatured by boiling in SDS sample buffer. Samples were separated by SDS-PAGE and transferred to a nitrocellulose membrane using semi-dry transfer. Membranes were probed with commercial antibodies: rabbit α-AKIN10 (Agrisera, Vännäs, Sweden), rabbit α-pAMPK (T172) (Cell Signalling Technology, Danvers, MA, US), rabbit α-tubulin (Agrisera, Vännäs, Sweden). Chemiluminescence was imaged using the Fusion Fx system (Vilber, Collégien, France). The relative band intensities were quantified using the quantification tool BioID.

Statistical Analysis. Statistical analyses were performed with GraphPad Prism 8.0.2 (GraphPad Software, Inc., CA, US). Statistical details of each experiment including biological replicates (*n*), types of error bars and used test are defined in the results and figure legend sections. The significance level was set to 0.05 in all cases.

Supplementary Information to *c-amiR-SnRK1*

During the mutant screening for the constitutive knockdown mutants, more than 25% of the F1 progeny of heterozygous, independent *c-amiR-SnRK1-I* lines died compared to the control plants two weeks after growth on selection media indicating plants homozygous for the transgene are not able to survive (Supplementary Table 1). Studies trying to repress SnRK1

signalling reported similar limitations including male sterility in barley[8] or seed maturation defects in pea[7] and supported our conclusion that even a knock-down of *SnRK1.1* and *SnRK1* results in nonviable plants. The progeny of heterozygous *c-amiR-SnRK1-I* plants could survive longer when plants were cultivated on soil in absence of Basta. However, severe phenotypes appeared at different developmental stages during the propagation. In fact, the *c-amiR-SnRK1-I* plants flowered earlier on average than the controls, while overall growth was retarded (Supplementary Fig. 2a,c). Some *c-amiR-SnRK1-I* plants showed symptoms of early senescence and died before bolting, whereas others bolted but failed to produce inflorescences (Supplementary Fig. 2b). Interestingly, *c-amiR-SnRK1-I* plants showed an increased mortality at different developmental stages (Supplementary Fig. 2c,d). The fraction of plants dying before seed set suggests that plants being homozygous in the *amiR* expression construct are infertile due to premature death. A previous study using a transient knockdown of both *SnRK1.1* and *SnRK1.*2 reported retarded growth and early senescence as well consistent with our observations[6]. While characterizing the progeny of heterozygous mutant lines, we also looked at the hypocotyl length of etiolated seedlings. Interestingly, a proportion of the *c-amiR* mutants, probably corresponding to the homozygous mutant seedlings, exhibited strongly shortened hypocotyls in darkness compared to the controls (Supplementary Fig. 2e). The hypocotyl phenotype was reminiscent of the light response during photomorphogenesis, however a defect in cell elongation cannot be excluded.

Supplementary Method

The constructs 35S::amiR-SnRK1-I and 35S::amiR-SnRK1-II for constitutive amiR expression were generated via Gateway cloning (Invitrogen, Carlsbad, CA, US). Site-directed mutagenesis on pRS300 was performed in three single PCR reactions using Herculase II Fusion DNA Polymerase (Agilent Technologies, Santa Clara, CA, US) and the following primer combinations: For amiR-I, SL11/TW026, TW024/TW025, and SL12/TW023. For amiR-II, SL11/TW030, TW028/TW029, and SL12/TW027. The purified PCR products were mixed with the primer pair SL11/SL12 to perform an overlap PCR for each construct generating the corresponding amiR precursor sequence flanked by *att*B sites. Performing the BP reaction, the DNA insert was introduced into the entry vector pDONR201[37]. Subsequently, the amiR-containing sequences were transferred into the expression vector pB7WG2 via the LR reaction[55].

The constructs Est::amiR-SnRK1-I and Est::amiR-SnRK1-II for inducible amiR expression were cloned using the GreenGate system[56]. The DNA fragments corresponding to the amiR sequences were generated by overlap PCR, as described before for the constitutive constructs, but using TW080/TW081 as outer primers. The amiR precursor sequences were integrated into the entry vector pGGC000 by restriction with *BsaI* HF (NEB, Ipswich, MA, US)

and subsequent ligation using T4 DNA ligase (Thermo Fisher Scientific, Waltham, MA, US), resulting in pGGCTW01 and pGGCTW02. The expression cassettes for XVE and the amiR-containing sequences were assembled and ligated to intermediate vectors following the procedure described in[56]. The combination of modules for generating intermediate vectors pGGMTW01, pGGNTW01, and pGGNTW02 are displayed in Supplemental Table 3. Finally, the expression cassettes were combined using the FH and HA adapter sequences. To this end, the XVE-encoding vector pGGMTW01 was mixed with the destination vector pGGZ003 and either pGGNTW01 or pGGNTW02, resulting in the final constructs pGGZTW01 and pGGZTW02, respectively.

Supplementary Tables

Supplementary Table 1. Number of surviving seedlings after 2 weeks of growth on Basta-containing MS plates.

Lines	Alive [%]	Dead [%]	n[1]
wild type	0	100	148
pGPTV	100	0	138
cI-amiR_4	71	29	133
cI-amiR_5	60	40	90
cI-amiR_22	73	27	121

[1]Total number of plants analysed.

Supplementary Table 2. Primers for cloning *amiR-SnRK1* constructs.

Target	Primer	Sequence	Details
amiR-SnRK1-I	TW023	gaTACTGAAGTCCAAGAGCGCATctctcttttgtattcca	I miR-s[1]
	TW024	agATGCGCTCTTGGACTTCAGTAtcaaagagaatcaatg a	II miR-a[1]
	TW025	agATACGCTCTTGGAGTTCAGTTtcacaggtcgtgatatg	III miR*s[1]
	TW026	gaAACTGAACTCCAAGAGCGTATctacatatatattccta	IV miR*a[1]
amiR-SnRK1.1-II	TW027	gaTTCGATGGCAGTATTCCACTGctctcttttgtattcca	I miR-s[1]
	TW028	agCAGTGGAATACTGCCATCGAAtcaaagagaatcaatg a	II miR-a[1]
	TW029	agCAATGGAATACTGGCATCGATtcacaggtcgtgatatg	III miR*s[1]
	TW030	gaATCGATGCCAGTATTCCATTGctacatatatattccta	IV miR*a[1]
	SL11	aaaaagcaggctCTGCAAGGCGATTAAGTTGGGTAAC	Primer A with *att*B site[1]
	SL12	agaaagctgggtGCGGATAACAATTTCACACAGGAAA CAG	Primer B with *att*B site[1]
	TW080	aaca*ggtctc*aggctCTGCAAGGCGATTAAGTTGGGTA AC	Primer A with *Bsa*I site[1]
	TW081	aaca*ggtctc*actgaGCGGATAACAATTTCACACAGGA AACAG	Primer B with *Bsa*I site[1]

[1]primer name in details refers to naming from[53] .

Supplementary Table 3. GreenGate cloning modules and destination constructs.

Name	Type	Reference
Intermediate vectors		
pGGMTW01		
pGGA006	UBQ10 promoter	[56]
pGGB003	B-dummy	[56]
pGGC124	CDS of chimeric TF XVE	Provided by RG Lohmann
pGGD002	D-dummy	[56]
pGGE009	UBQ10 terminator	[56]
pGGG004	FH adapter to combine two expression cassettes in the destination vector	Provided by RG Lohmann
pGGM000	Assembly of expression cassette #1 (intermediate vector)	[56]
pGGNTW01		
pGGA044	Olex TATA, activated by XVE – EST system	Provided by RG Lohmann
pGGB003	B-dummy	[56]
pGGCTW01	CDS of amiR-SnRK1.1/1.2	Generated in this study
pGGD002	D-dummy	[56]
pGGE001	RBCS terminator	[56]
pGGF005	*pUBQ10:HygrR:tOCS*	[56]
pGGG005	250 bp HA adapter	Provided by RG Lohmann
pGGN000	Assembly of expression cassette #2 (intermediate vector)	[56]
pGGNTW02		
pGGA044	Olex TATA, activated by XVE – EST systen	Provided by RG Lohmann
pGGB003	B-dummy	**[56]**
pGGCTW02	CDS of amiR-SnRK1.1/1.2	Generated in this study
pGGD002	D-dummy	**[56]**
pGGE001	*RBCS* terminator	**[56]**
pGGF005	*pUBQ10:HygrR:tOCS*	**[56]**
pGGG005	250 bp HA adapter	Provided by RG Lohmann
pGGN000	Assembly of expression cassette #2 (intermediate vector)	**[56]**
Destination vectors		
pGGZTW01	pGGMTW01 pGGNTW01	Generated in this study

	pGGZ003	
pGGZTW02	pGGMTW01 pGGNTW02 pGGZ003	Generated in this study
pGGZ003	Plant resistance at LB (destination vector)	[56]

Supplementary Table 4. qPCR primers.

Primer	Gene ID	Gene	Fw/ Rev	Sequence	Details
TW052	*AT3G01090*	*SnRK1.1*	Fwd	TGAGTTTCAAGAGACCATGGAAG	
TW053	*AT3G01090*	*SnRK1.1*	Rev	CCAACTCCTTGATATTCCATCAG	
TW067	*AT3G29160*	*SnRK1.2*	Fwd	ACGCAACAGAACACAAAACG	
TW068	*AT3G29160*	*SnRK1.2*	Rev	TGTCTCCTGAAACTCGGATTCT	
TW013	*At4g35770*	*DIN1*	Fwd	GAATGAGCTGCCGGTAGAAG	
TW014	*At4g35770*	*DIN1*	Rev	TGATGATTGATACTTGCGTTGAG	
TW170	*AT1G50030*	*TOR*	Fwd	GATGGCGAGTGCAGTGGTA	
TW171	*AT1G50030*	*TOR*	Rev	CCCCCACGGCAAGTAAAGA	
DNA28	*AT1G69960*	*PP2A*	Fwd	GGTAATAACTGCATCTAAAGACAGAGTTCC	
DNA29	*AT1G69960*	*PP2A*	Rev	CCACAACCGCTTGGTCG	
LH50	*AT1G09140*	*SR30*	Fwd	GCAAGAGCAGGAGTGTGTCA	
LH51	*AT1G09140*	*SR30*	Rev	TTGATCTTGATTGGGACCTTG	specific for *.1*
LH52	*AT1G09140*	*SR30*	Fwd	TCACCTGCTAGATCCATTTCC	
LH53	*AT1G09140*	*SR30*	Rev	CCCAGCTCGTAGCAGTGAG	specific for *.2*
LH302	*AT5G25060*	*RRC1*	Fwd	CCTAAGGTTGATTCTGAAGGTGA	
LH303	*AT5G25060*	*RRC1*	Rev	GTGGTGGTGGAAGGAAAGAG	specific for *.1*
LH304	*AT5G25060*	*RRC1*	Fwd	CCTAAGGTTGATTCTGAAGGTATG	
LH305	*AT5G25060*	*RRC1*	Rev	CTTTCCCTAGGCCTCTCCTC	specific for *.2*
JS152	*AT3G55330*	*PPL1*	Fwd	GTAGAGCTCCATTATCATTTGC	specific for *.1*
JS153	*AT3G55330*	*PPL1*	Rev	CTGCCAACCAAATGGATAGAG	
JS154	*AT3G55330*	*PPL1*	Fwd	AGTAGAGCTCCATTATCATAAAG	specific for *.2*
JS148	*AT1G70000*	*MYBD*	Fwd	CGTGAACGCAAACGAGGAAC	
JS149	*AT1G70000*	*MYBD*	Rev	TTCTAGAGATTCCTCTCCAATC	specific for *.1*
JS150	*AT1G70000*	*MYBD*	Fwd	CCAAATCTCATCTCTGTTTTTG	
JS151	*AT1G70000*	*MYBD*	Rev	CAGTAAGAAACAATCTATGTTCT	specific for *.2*
LH527	*AT4G14720*	*PPD2*	Fwd	AGTAAAGAGAAGATGGTGGAGCT	

LH528	*AT4G14720*	*PPD2*	Rev	TTTCTGTTCGCCTGACCCTC	specific for *.1*
LH529	*AT4G14720*	*PPD2*	Fwd	TGTCCAATTTTGAAAGGAGGCA	
LH530	*AT4G14720*	*PPD2*	Rev	CACGAGGCATCTGTAGACACA	specific for *.2*

Supplementary Table 5. Co-amplification primers.

Primer	Gene ID	Gene	Fwd/Rev	Sequence	Product lengths
LH4	*AT1G09140*	*SR30*	Fwd	GTCACCTGCTAGATCCATTTCC	*.1*: 200 bp
LH5	*AT1G09140*	*SR30*	Rev	AGCCTGAGAAGCTTGAGACG	*.2:* 550 bp
LH321	*AT3G55330*	*PPL1*	Fwd	GTGTTGTTGCTCCTTGGAT	*.1*: 175 bp
LH322	*AT3G55330*	*PPL1*	Rev	AGGCTCAATCACATCTTTG	*.2:* 185 bp
LH336	*AT1G70000*	*MYBD 1*	Fwd	TCAAACTCCTGATCCCAACC	*.1*: 120 bp *.2:* 200 bp
LH363	*AT1G70000*	*MYBD1*	Rev	CTATGTTCTTCCTCTGTCCA	

References

1 Kami, C., Lorrain, S., Hornitschek, P. & Fankhauser, C. Light-Regulated Plant Growth and Development. *Curr Top Dev Biol* **91**, 29-66, doi:10.1016/S0070-2153(10)91002-8 (2010).

2 Hartmann, L. *et al.* Alternative Splicing Substantially Diversifies the Transcriptome during Early Photomorphogenesis and Correlates with the Energy Availability in Arabidopsis. *Plant Cell* **28**, 2715-2734, doi:10.1105/tpc.16.00508 (2016).

3 Shikata, H. *et al.* Phytochrome controls alternative splicing to mediate light responses in Arabidopsis. *Proc Natl Acad Sci U S A* **111**, 18781-18786, doi:10.1073/pnas.1407147112 (2014).

4 Reddy, A. S., Marquez, Y., Kalyna, M. & Barta, A. Complexity of the alternative splicing landscape in plants. *Plant Cell* **25**, 3657-3683, doi:10.1105/tpc.113.117523 (2013).

5 Sakr, S. *et al.* The Sugar-Signaling Hub: Overview of Regulators and Interaction with the Hormonal and Metabolic Network. *Int J Mol Sci* **19**, doi:10.3390/ijms19092506 (2018).

6 Baena-Gonzalez, E., Rolland, F., Thevelein, J. M. & Sheen, J. A central integrator of transcription networks in plant stress and energy signalling. *Nature* **448**, 938-942, doi:10.1038/nature06069 (2007).

7 Radchuk, R., Radchuk, V., Weschke, W., Borisjuk, L. & Weber, H. Repressing the expression of the SUCROSE NONFERMENTING-1-RELATED PROTEIN KINASE gene in pea embryo causes pleiotropic defects of maturation similar to an abscisic acid-insensitive phenotype. *Plant Physiol* **140**, 263-278, doi:10.1104/pp.105.071167 (2006).

8 Zhang, Y. *et al.* Expression of antisense SnRK1 protein kinase sequence causes abnormal pollen development and male sterility in transgenic barley. *Plant J* **28**, 431-441 (2001).

9 Mair, A. *et al.* SnRK1-triggered switch of bZIP63 dimerization mediates the low-energy response in plants. *Elife* **4**, doi:10.7554/eLife.05828 (2015).

10 Kim, G. D., Cho, Y. H. & Yoo, S. D. Regulatory Functions of Cellular Energy Sensor SNF1-Related Kinase1 for Leaf Senescence Delay through ETHYLENE- INSENSITIVE3 Repression. *Sci Rep* **7**, 3193, doi:10.1038/s41598-017-03506-1 (2017).
11 Chen, L. *et al.* The AMP-Activated Protein Kinase KIN10 Is Involved in the Regulation of Autophagy in Arabidopsis. *Frontiers in Plant Science* **8**, doi:ARTN 120110.3389/fpls.2017.01201 (2017).
12 Soto-Burgos, J. & Bassham, D. C. SnRK1 activates autophagy via the TOR signaling pathway in Arabidopsis thaliana. *PLoS One* **12**, e0182591, doi:10.1371/journal.pone.0182591 (2017).
13 Kim, G. D., Cho, Y. H. & Yoo, S. D. Phytohormone ethylene-responsive Arabidopsis organ growth under light is in the fine regulation of Photosystem II deficiency-inducible AKIN10 expression. *Sci Rep* **7**, 2767, doi:10.1038/s41598-017-02897-5 (2017).
14 Li, Z. H., Peng, J. Y., Wen, X. & Guo, H. W. ETHYLENE-INSENSITIVE3 Is a Senescence-Associated Gene That Accelerates Age-Dependent Leaf Senescence by Directly Repressing miR164 Transcription in Arabidopsis. *Plant Cell* **25**, 3311-3328, doi:10.1105/tpc.113.113340 (2013).
15 Qiu, K. *et al.* EIN3 and ORE1 Accelerate Degreening during Ethylene-Mediated Leaf Senescence by Directly Activating Chlorophyll Catabolic Genes in Arabidopsis. *Plos Genetics* **11**, doi:ARTN e100539910.1371/journal.pgen.1005399 (2015).
16 Moore, B. *et al.* Role of the Arabidopsis Glucose Sensor HXK1 in Nutrient, Light, and Hormonal Signaling. *Science* **300**, 332, doi:10.1126/science.1080585 (2003).
17 Morita-Yamamuro, C., Tsutsui, T., Tanaka, A. & Yamaguchi, J. Knock-out of the plastid ribosomal protein S21 causes impaired photosynthesis and sugar-response during germination and seedling development in Arabidopsis thaliana. *Plant Cell Physiol* **45**, 781-788, doi:10.1093/pcp/pch093 (2004).
18 Singh, M., Gupta, A., Singh, D., Khurana, J. P. & Laxmi, A. Arabidopsis RSS1 Mediates Cross-Talk Between Glucose and Light Signaling During Hypocotyl Elongation Growth. *Scientific Reports* **7**, 16101, doi:10.1038/s41598-017-16239-y (2017).
19 Ramon, M. *et al.* Default activation and nuclear translocation of the plant cellular energy sensor SnRK1 regulate metabolic stress responses and development. *Plant Cell*, doi:10.1105/tpc.18.00500 (2019).
20 Crozet, P. *et al.* Mechanisms of regulation of SNF1/AMPK/SnRK1 protein kinases. *Front Plant Sci* **5**, 190, doi:10.3389/fpls.2014.00190 (2014).
21 Shen, W. & Hanley-Bowdoin, L. Geminivirus infection up-regulates the expression of two Arabidopsis protein kinases related to yeast SNF1- and mammalian AMPK-activating kinases. *Plant Physiol* **142**, 1642-1655, doi:10.1104/pp.106.088476 (2006).
22 Carvalho, R. F. *et al.* The Arabidopsis SR45 Splicing Factor, a Negative Regulator of Sugar Signaling, Modulates SNF1-Related Protein Kinase 1 Stability. *Plant Cell* **28**, 1910-1925, doi:10.1105/tpc.16.00301 (2016).
23 Siligato, R. *et al.* MultiSite Gateway-Compatible Cell Type-Specific Gene-Inducible System for Plants. *Plant Physiol* **170**, 627-641, doi:10.1104/pp.15.01246 (2016).
24 Matsumoto, E. *et al.* AMP-activated protein kinase regulates alternative pre-mRNA splicing by phosphorylation of SRSF1. *Biochemical Journal* **477**, 2237-2248, doi:10.1042/BCJ20190894 (2020).
25 Tanabe, N., Yoshimura, K., Kimura, A., Yabuta, Y. & Shigeoka, S. Differential expression of alternatively spliced mRNAs of Arabidopsis SR protein homologs, atSR30 and atSR45a, in response to environmental stress. *Plant Cell Physiol* **48**, 1036-1049, doi:10.1093/pcp/pcm069 (2007).
26 Hartmann, L., Wießner, T. & Wachter, A. Subcellular Compartmentation of Alternatively-Spliced Transcripts Defines SERINE/ARGININE-RICH PROTEIN 30 Expression. *Plant Physiology*, pp.01260.02017, doi:10.1104/pp.17.01260 (2018).
27 Wu, H. P. *et al.* Genome-wide analysis of light-regulated alternative splicing mediated by photoreceptors in Physcomitrella patens. *Genome Biol* **15**, R10, doi:10.1186/gb-2014-15-1-r10 (2014).

28 Xin, R., Kathare, P. K. & Huq, E. Coordinated Regulation of Pre-mRNA Splicing by the SFPS-RRC1 Complex to Promote Photomorphogenesis. *Plant Cell* **31**, 2052-2069, doi:10.1105/tpc.18.00786 (2019).
29 Xin, R. *et al.* SPF45-related splicing factor for phytochrome signaling promotes photomorphogenesis by regulating pre-mRNA splicing in Arabidopsis. *Proc Natl Acad Sci U S A* **114**, E7018-E7027, doi:10.1073/pnas.1706379114 (2017).
30 Mancini, E. *et al.* Acute Effects of Light on Alternative Splicing in Light-Grown Plants. *Photochem Photobiol* **92**, 126-133, doi:10.1111/php.12550 (2016).
31 Petrillo, E. *et al.* A chloroplast retrograde signal regulates nuclear alternative splicing. *Science* **344**, 427-430, doi:10.1126/science.1250322 (2014).
32 Wurzinger, B. *et al.* Redox state-dependent modulation of plant SnRK1 kinase activity differs from AMPK regulation in animals. *FEBS Lett* **591**, 3625-3636, doi:10.1002/1873-3468.12852 (2017).
33 Cho, H. Y., Wen, T. N., Wang, Y. T. & Shih, M. C. Quantitative phosphoproteomics of protein kinase SnRK1 regulated protein phosphorylation in Arabidopsis under submergence. *J Exp Bot* **67**, 2745-2760, doi:10.1093/jxb/erw107 (2016).
34 Guo, H. *et al.* Plastid-nucleus communication involves calcium-modulated MAPK signalling. *Nat Commun* **7**, 12173, doi:10.1038/ncomms12173 (2016).
35 Jarvis, P. & López-Juez, E. Biogenesis and homeostasis of chloroplasts and other plastids. *Nat Rev Mol Cell Biol* **14**, 787-802, doi:10.1038/nrm3702 (2013).
36 Dobrenel, T. *et al.* The Arabidopsis TOR Kinase Specifically Regulates the Expression of Nuclear Genes Coding for Plastidic Ribosomal Proteins and the Phosphorylation of the Cytosolic Ribosomal Protein S6. *Front Plant Sci* **7**, 1611, doi:10.3389/fpls.2016.01611 (2016).
37 Chen, G. H., Liu, M. J., Xiong, Y., Sheen, J. & Wu, S. H. TOR and RPS6 transmit light signals to enhance protein translation in deetiolating Arabidopsis seedlings. *P Natl Acad Sci USA* **115**, 12823-12828, doi:10.1073/pnas.1809526115 (2018).
38 Pfeiffer, A. *et al.* Integration of light and metabolic signals for stem cell activation at the shoot apical meristem. *Elife* **5**, doi:10.7554/eLife.17023 (2016).
39 Menand, B. *et al.* Expression and disruption of the Arabidopsis TOR (target of rapamycin) gene. *Proc Natl Acad Sci U S A* **99**, 6422-6427, doi:10.1073/pnas.092141899 (2002).
40 Ren, M. *et al.* Target of rapamycin regulates development and ribosomal RNA expression through kinase domain in Arabidopsis. *Plant Physiol* **155**, 1367-1382, doi:10.1104/pp.110.169045 (2011).
41 Ren, M. *et al.* Target of rapamycin signaling regulates metabolism, growth, and life span in Arabidopsis. *Plant Cell* **24**, 4850-4874, doi:10.1105/tpc.112.107144 (2012).
42 Deprost, D. *et al.* The Arabidopsis TOR kinase links plant growth, yield, stress resistance and mRNA translation. *EMBO Rep* **8**, 864-870, doi:10.1038/sj.embor.7401043 (2007).
43 Xiong, F. *et al.* Brassinosteriod Insensitive 2 (BIN2) acts as a downstream effector of the Target of Rapamycin (TOR) signaling pathway to regulate photoautotrophic growth in Arabidopsis. *New Phytol* **213**, 233-249, doi:10.1111/nph.14118 (2017).
44 Dong, P. *et al.* Expression profiling and functional analysis reveals that TOR is a key player in regulating photosynthesis and phytohormone signaling pathways in Arabidopsis. *Front Plant Sci* **6**, 677, doi:10.3389/fpls.2015.00677 (2015).
45 Li, L. *et al.* TOR-inhibitor insensitive-1 (TRIN1) regulates cotyledons greening in Arabidopsis. *Front Plant Sci* **6**, 861, doi:10.3389/fpls.2015.00861 (2015).
46 Petrillo, E. *et al.* Remote control of alternative splicing in roots through TOR kinase. *bioRxiv*, 472126, doi:10.1101/472126 (2018).
47 Li, L. & Sheen, J. Dynamic and diverse sugar signaling. *Curr Opin Plant Biol* **33**, 116-125, doi:10.1016/j.pbi.2016.06.018 (2016).
48 Nukarinen, E. *et al.* Quantitative phosphoproteomics reveals the role of the AMPK plant ortholog SnRK1 as a metabolic master regulator under energy deprivation. *Sci Rep* **6**, 31697, doi:10.1038/srep31697 (2016).

49 Cho, Y. H., Hong, J. W., Kim, E. C. & Yoo, S. D. Regulatory functions of SnRK1 in stress-responsive gene expression and in plant growth and development. *Plant Physiol* **158**, 1955-1964, doi:10.1104/pp.111.189829 (2012).

50 Caldana, C. *et al.* Systemic analysis of inducible target of rapamycin mutants reveal a general metabolic switch controlling growth in Arabidopsis thaliana. *Plant J* **73**, 897-909, doi:10.1111/tpj.12080 (2013).

51 Hanaoka, H. *et al.* Leaf senescence and starvation-induced chlorosis are accelerated by the disruption of an Arabidopsis autophagy gene. *Plant Physiol* **129**, 1181-1193, doi:10.1104/pp.011024 (2002).

52 Chang, J.-W. *et al.* mTOR-regulated U2af1 tandem exon splicing specifies transcriptome features for translational control. *Nucleic Acids Research* **47**, 10373-10387, doi:10.1093/nar/gkz761 (2019).

53 Ossowski, S., Schwab, R. & Weigel, D. Gene silencing in plants using artificial microRNAs and other small RNAs. *Plant J* **53**, 674-690, doi:10.1111/j.1365-313X.2007.03328.x (2008).

54 Schwab, R., Ossowski, S., Riester, M., Warthmann, N. & Weigel, D. Highly specific gene silencing by artificial microRNAs in Arabidopsis. *Plant Cell* **18**, 1121-1133, doi:10.1105/tpc.105.039834 (2006).

55 Karimi, M., Inze, D. & Depicker, A. GATEWAY vectors for Agrobacterium-mediated plant transformation. *Trends Plant Sci* **7**, 193-195 (2002).

56 Lampropoulos, A. *et al.* GreenGate---a novel, versatile, and efficient cloning system for plant transgenesis. *PLoS One* **8**, e83043, doi:10.1371/journal.pone.0083043 (2013).

57 Clough, S. J. & Bent, A. F. Floral dip: a simplified method for Agrobacterium-mediated transformation of Arabidopsis thaliana. *Plant J* **16**, 735-743, doi:10.1046/j.1365-313x.1998.00343.x (1998).

58 Porra, R. J., Thompson, W. A. & Kriedemann, P. E. Determination of accurate extinction coefficients and simultaneous equations for assaying chlorophylls a and b extracted with four different solvents: verification of the concentration of chlorophyll standards by atomic absorption spectroscopy. *Biochimica et Biophysica Acta (BBA) - Bioenergetics* **975**, 384-394, doi:https://doi.org/10.1016/S0005-2728(89)80347-0 (1989).

59 Stauffer, E., Westermann, A., Wagner, G. & Wachter, A. Polypyrimidine tract-binding protein homologues from Arabidopsis underlie regulatory circuits based on alternative splicing and downstream control. *Plant J* **64**, 243-255, doi:10.1111/j.1365-313X.2010.04321.x (2010).

Figures

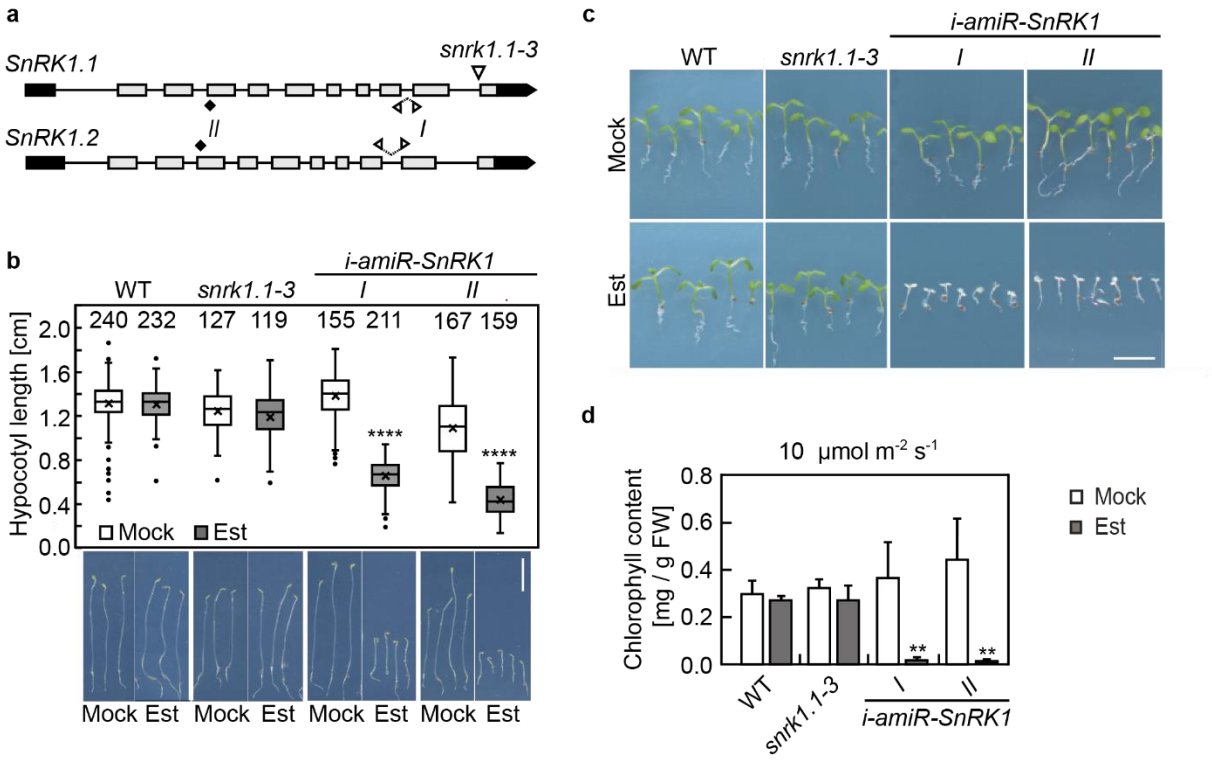

Figure 1| *SnRK1* knockdown causes impaired development in dark and low light conditions. a, Transcript models of *SnRK1.1* and *SnRK1.2* based on representative gene models and *amiR* target sites. *amiR-SnRK1-I* (*I*, unfilled separated square) binds to exon4 whereas *amiR-SnRK1-II* (*II,* filled square) targets the exon9-exon10 junction. T-DNA insertion site in *snrk1.1-3* is indicated by a triangle. Lines correspond to introns, black and grey shapes depict UTRs and coding exons, respectively. **b**, The quantitation of hypocotyl lengths (upper panel) and representative pictures (lower panel) of 6-d-old wildtype (WT), *snrk1.1-3,* and *i-amiR-SnRK1* mutant seedlings. The seedlings were grown on mock or β-estradiol (Est)-containing plates. White scale bar indicates 1 cm. The plot depicts interquartile range, maximum as well as minimum of the data set as box and whiskers, respectively. The middle line, the cross and single dots represent the median, mean value and outliers, respectively. Asterisks indicate significant difference compared to corresponding mock control based on one-way ANOVA with post hoc Tukey test (P value: ****P < 0.0001). n is indicated above each line. **c**, Representative photographs of 14-d-old seedlings that were either grown on mock or Est-containing plates under low light conditions (10 µmol m^{-2} s^{-1}). Scale bar represents 0.5 cm. **d**, Total chlorophyll content of 14-d-old seedlings. Growth conditions and treatments as described in **c**. Mean values (n = 3 - 4) +SD are shown. Asterisks indicate significant difference compared to corresponding mock control based on independent t test (P value: *P < 0.05, **P < 0.01, ***P < 0.001).

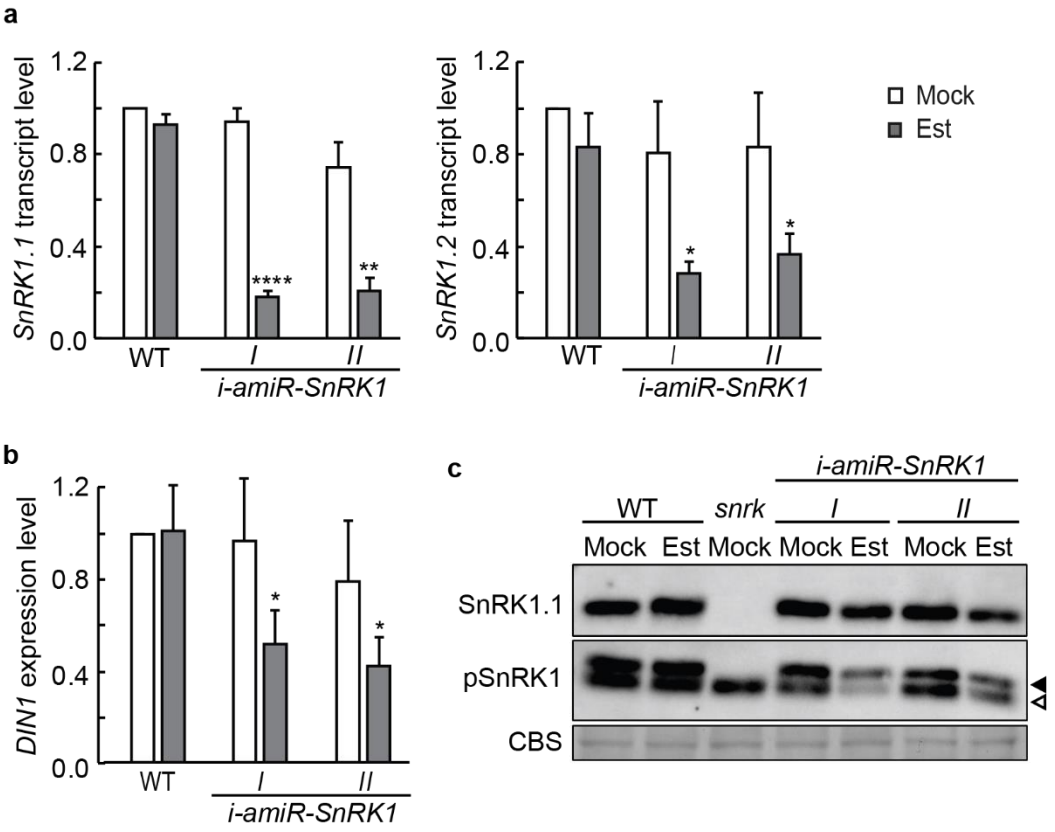

Figure 2| Inducible repression of *SnRK1* diminishes the mRNA level of its transcriptional target *DIN1*. a, Relative transcript levels of *SnRK1.1* and *SnRK1.2* in 6-d-old etiolated wild type (WT) and *i-amiR-SnRK1* mutant seedlings, treated with either mock or β-estradiol (Est) for 3 d. Data are mean values (n = 3) +SD, normalised to WT mock samples. Statistical comparison of the mock and Est-treated *i-amiR-SnRK1* mutants was performed using an independent *t* test. In case of the WT, a one-sample *t* test was used (P values: *P < 0.05, **P < 0.01, ***P < 0.001, ****P < 0.0001). **b,** Relative transcript level of the SnRK1 target *DIN1* in WT and *i-amiR-SnRK1* mutant seedlings. Sample description, and data normalisation as described in **a**. Statistical comparison was performed using a one-sample *t* test (P value: *P < 0.05). **c,** Immunoblot detection of total SnRK1.1 protein (upper panel) as well as phosphorylated SnRK1.1 and SnRK1.2 proteins (middle panel) in WT and different *snrk1* mutant seedlings. The upper band corresponds to phosphorylated SnRK1.1, whereas the lower band can be assigned to the active SnRK1.2 protein. This assumption was supported by the absence of the upper band in *snrk1.1-3*. Coomassie blue staining (CBS) is shown as loading control (lower panel). Black and white triangle indicate p-SnRK1.1 and pSnRK1.2 protein, respectively. Other details of plant growth and treatments are as described in **a**.

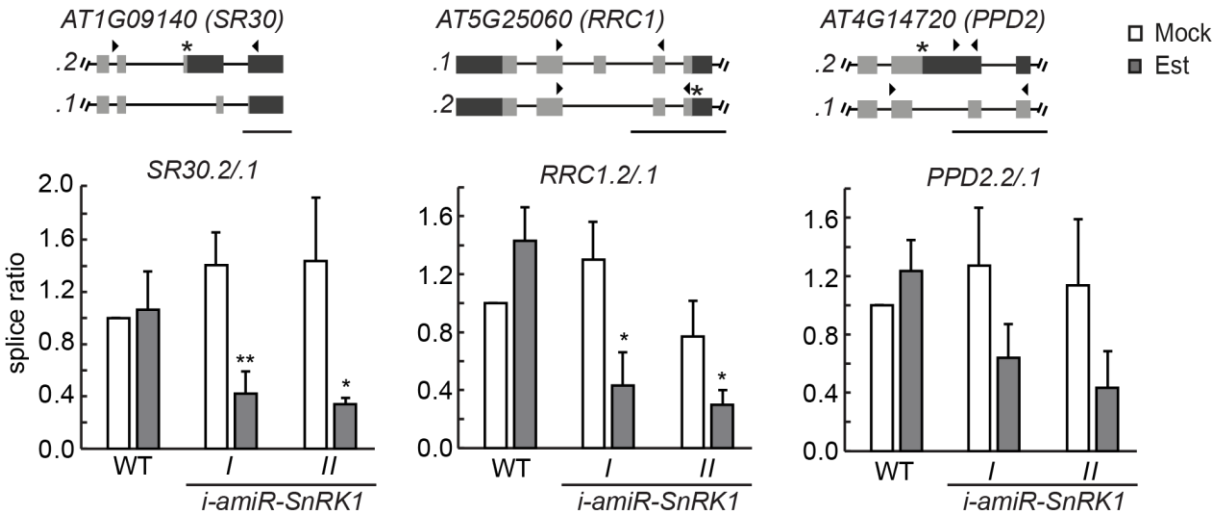

Figure 3| *SnRK1* knockdown can trigger shifts of light-regulated AS events. Splicing ratios of *SR30*, *RRC1* and *PPD2* were determined in 6-d-old etiolated wild type (WT) and *i-amiR-SnRK1* seedlings that were either incubated in mock or β-estradiol (Est) for 3 d. Corresponding gene models are shown above each graph. Introns are represented by lines and exons by boxes. Regions coloured in dark grey are UTRs, and asterisks mark the introduction of a premature termination codon. Primer binding sites are shown as arrowheads. Scale bars beneath the models represent 500 bp. Data were quantified via Bioanalyzer (*SR30*) or RT-qPCR of the single mRNA isoforms (*RRC1, PPD2*). Displayed are mean values +SD (n = 3) and data was normalised to the WT mock control. An independent *t* test was performed when not tested against 1, and one-sample *t* test for WT (P values: *P < 0.05, **P < 0.01).

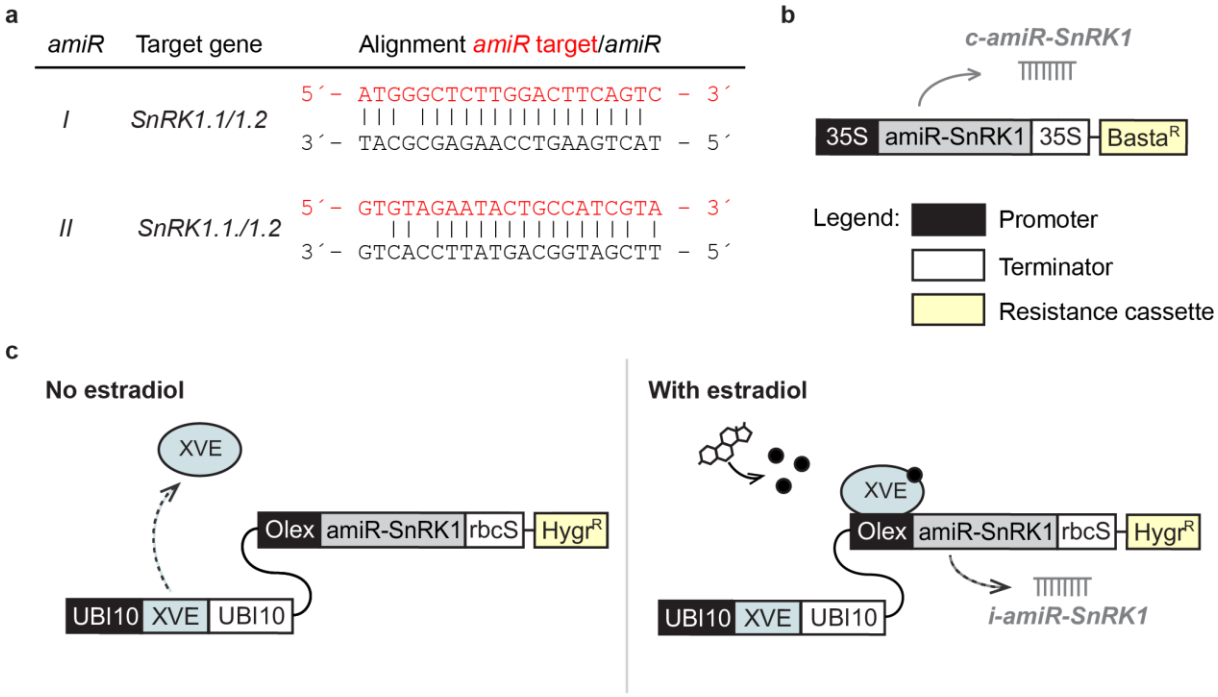

Supplemental Figure 1| Schematic overview of *amiR-SnRK1* constructs. a, Sequences of *amiR-SnRK1s* (black aligned to their target sites (red). **b**, Cartoon of the constitutive *amiR-SnRK1* construct under control of the CaMV 35S promoter and terminator, and containing a Basta resistance cassette for selection. **c**, Cartoon of the inducible *amiR-SnRK1* construct. Two expression cassettes were modularly fused together. The synthetic transcription factor XVE is under the control of the ubiquitously active UBI10 promoter and the UBI10 terminator. Upon treatment with β-estradiol, XVE gets activated and binds to the Olex promoter, thus activating the expression of the i-*amiR-SnRK1-I* or *i-amiR-SnRK1-II*. The construct also includes a RuBisCO terminator (rbcs) and a Hygromycin resistance cassette.

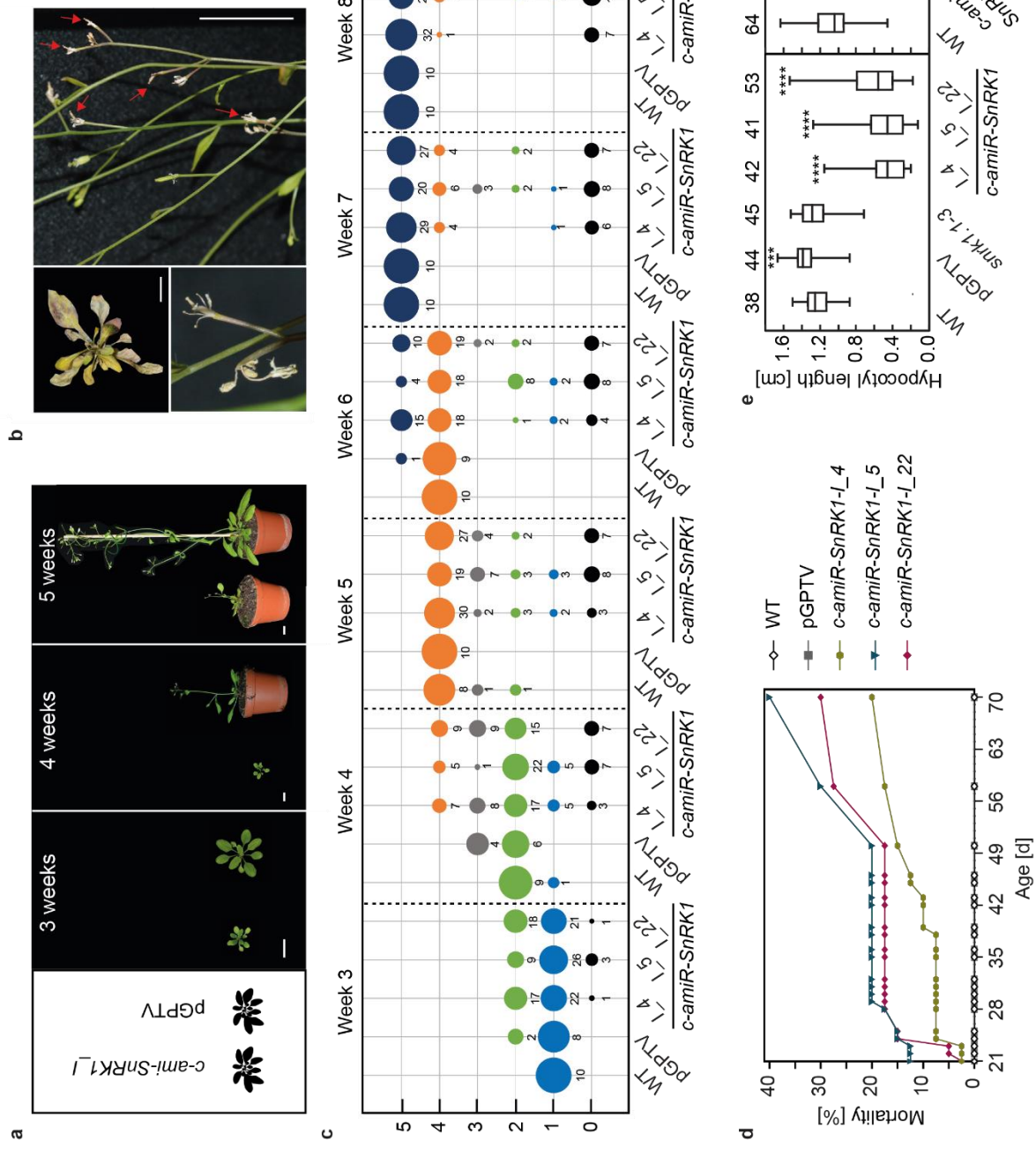
a
3 weeks
4 weeks
5 weeks
c-amiR-SnRK1_l
pGPTV
b
c
Week 3
Week 4
Week 5
Week 6
Week 7
Week 8
Week 10
WT
pGPTV
c-amiR-SnRK1
d
Mortality [%]
Age [d]
WT
pGPTV
c-amiR-SnRK1-l_4
c-amiR-SnRK1-l_5
c-amiR-SnRK1-l_22
e
Hypocotyl length [cm]
snrk1.1-3
c-amiR-SnRK1-l_5

Supplemental Figure 2| Constitutive knockdown of *SnRK1* causes growth defects and probably lethality upon homozygosity of the knockdown construct. a, Representative pictures of 3-, 4-, and 5-week-old *c-amiR-SnRK1-I* and pGPTV control plants grown under long day conditions. Scale bar = 1 cm. **b**, Likely homozygous *snrk1* mutants are dying at different developmental stages. Senescent 7-week-old rosette (upper left panel). Representative picture of a 7-week-old plant displaying dried siliques, while rosette leaves and main stem were still green. Red arrows indicate dried siliques (right). Close-up photograph from a 6-week-old plant showing dried flowers and siliques (lower left panel). Scale bar is set to 1 cm. **c**, Bubble plot of c-*amiR-SnRK1-I* and controls showing developmental stages over time. Developmental stages are defined as followed: 0 - dead, 1 - rosette, 2 - bolting, 3 - flowering, 4 – containing siliques, and 5 – siliques ripened. The size of each bubble is proportional to the percentage of analysed plants per genotype at the corresponding developmental stage during the appropriate time. Note that *c-amiR-SnRK1-I* and pGPTV plants were transferred from Basta and sugar-containing MS plates to soil, whereas wild type (WT) plants were grown on MS plates lacking Basta and sucrose. Corresponding n is displayed below each bubble. Total n for WT and pGPTV: 10, total n for each *c-amiR-SnRK1-I* line: 40. **d**, Mortality curve of c-*amiR-SnRK1-I* lines and control plants. Plants were grown under long day conditions and mortality was determined in a time period of 3 to 10 weeks. Before, plants were grown for 14 d on selection or control plates under long day conditions. **e**, Progeny of heterozygous *c-amiR-SnRK1-I* lines were cultivated for hypocotyl length determination in comparison to WT, pGPTV, and the T-DNA insertion line *snrk1.1-3*. All lines grown for 6 d under dark conditions. *c-amiR-SnRK1-I* lines show a tendency of shorter hypocotyls relative to the controls, which is reflected by the downwards skewed boxplot. The rectangle spans the interquartile, minimum, and maximum values are shown as whiskers and middle line represents the median. Numbers on top indicate seedlings analysed per genotype. Asterisks indicate significant difference of c-*amiR-SnRK1-I* lines and controls (pGPTV, *snrk1.1-3*) compared to WT based on independent *t* test with unequal variance and equal variance, respectively (P value: ***P < 0.001, ****P < 0.0001).

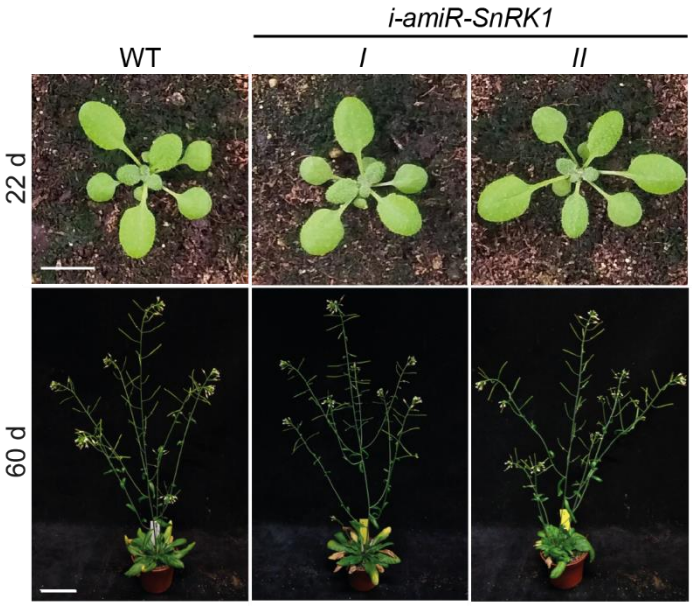

Supplemental Figure 3| Uninduced *i-amiR-SnRK1* plants show a wild type (WT)-like development. Comparable development of WT and inducible *amiR-SnRK1* lines under long day conditions and in the absence of β-estradiol. Representative pictures for each line at the age of 22 days (scale bar = 1 cm) and 60 days (scale bar = 5 cm) after sowing.

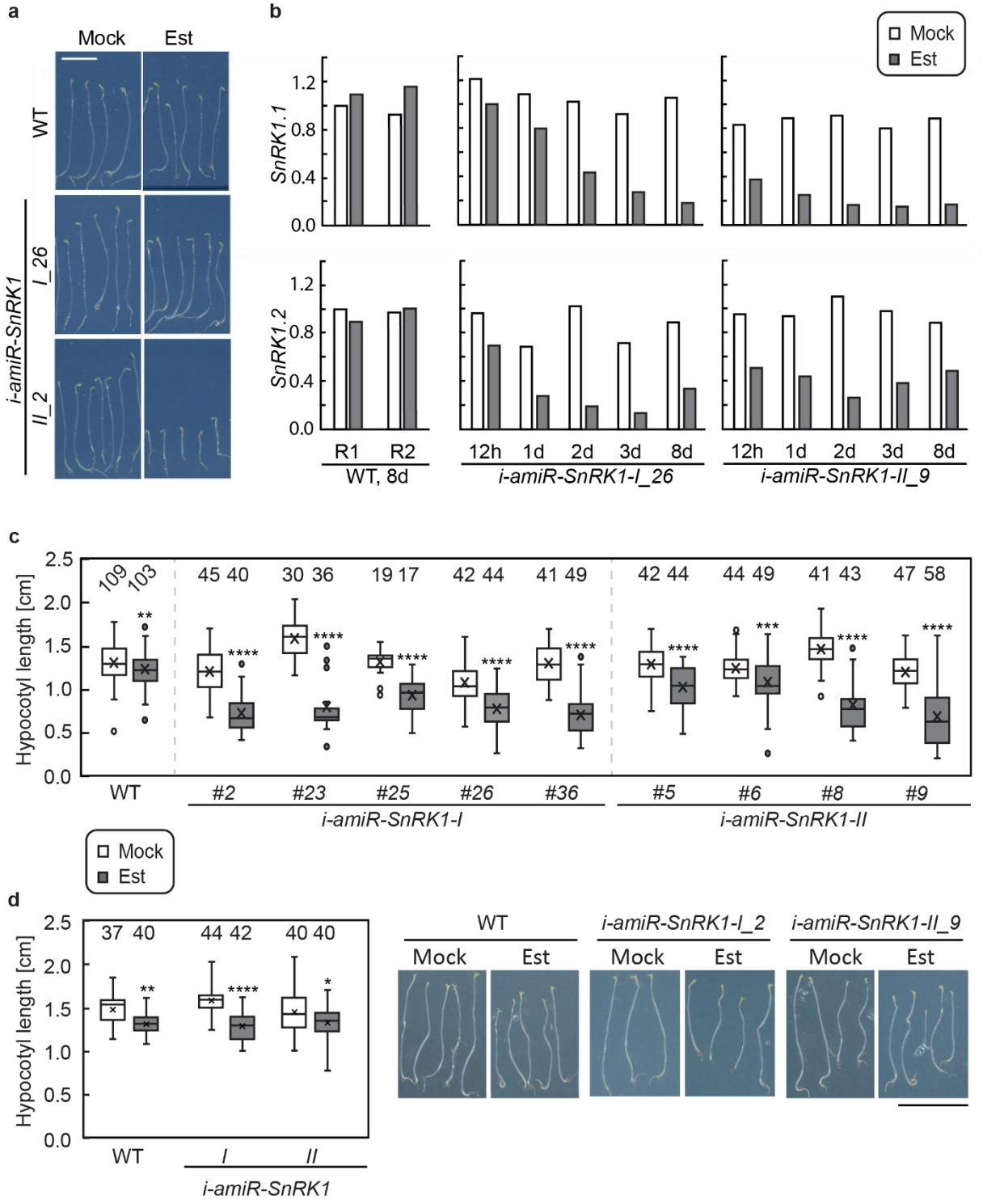
a
Mock
Est
WT
i-amiR-SnRK1
I_26
II_2
b
Mock
Est
SnRK1.1
SnRK1.2
1.2
0.8
0.4
0.0
R1
R2
WT, 8d
12h
1d
2d
3d
8d
i-amiR-SnRK1-I_26
i-amiR-SnRK1-II_9
c
Hypocotyl length [cm]
2.5
2.0
1.5
1.0
0.5
0.0
109 103
45 40
30 36
19 17
42 44
41 49
42 44
44 49
41 43
47 58
WT
#2
#23
#25
#26
#36
#5
#6
#8
#9
i-amiR-SnRK1-I
i-amiR-SnRK1-II
Mock
Est
d
Hypocotyl length [cm]
37 40
44 42
40 40
WT
I
II
i-amiR-SnRK1
WT
i-amiR-SnRK1-I_2
i-amiR-SnRK1-II_9
Mock
Est

Supplemental Figure 4| Hypocotyl length screen of independent *i-amiR-SnRK1* lines. **a**, Representative pictures of 6-d-old etiolated wild type (WT), *i-amiR-SnRK1-I_26* and *i-amiR-SnRK1-II_9* grown on MS plates supplemented with or without β-estradiol (Est). Scale is set to 0.5 cm. **b**, SnRK1.1 and SnRK1.2 transcript levels in WT, *i-amiR-SnRK1-I_26* and *i-amiR-SnRK1-II_9* upon different Est incubation times. Display are two or one biological replicate for WT or amiR-SnRK1 lines, respectively. **c**, Hypocotyl lengths of progeny derived from a heterozygous F1 generation of independent *i-amiR-SnRK1* lines. All lines were grown on either mock or Est-containing plates for 6 d and subsequently transferred to agar plates for scanning. Number of measured seedlings per line and treatment is indicated above each box plot. Interquartile range, maximum and minimum, median, and mean values are depicted as box, whiskers, middle line and cross, respectively. Dots display outliers. An independent *t* test with unequal variance was performed for i-*amiR-SnRK1* mutants, and an independent *t* test with equal variance for WT (P values: **P < 0.01, ***P < 0.001, ****P < 0.0001). **d**, Hypocotyl lengths (left) and representative pictures (right) of WT and *i-amiR-SnRK1* lines derived from a homozygous F2 generation. Seedlings were grown either in mock or Est-containing liquid media for 6 d and then transferred to agar plates for scanning. Scale bar = 1 cm. Asterisks indicate significant difference compared to corresponding mock control based on one-way ANOVA with post hoc Tukey test (P values: *P < 0.05, **P < 0.01, ***P < 0.001, ****P < 0.0001).

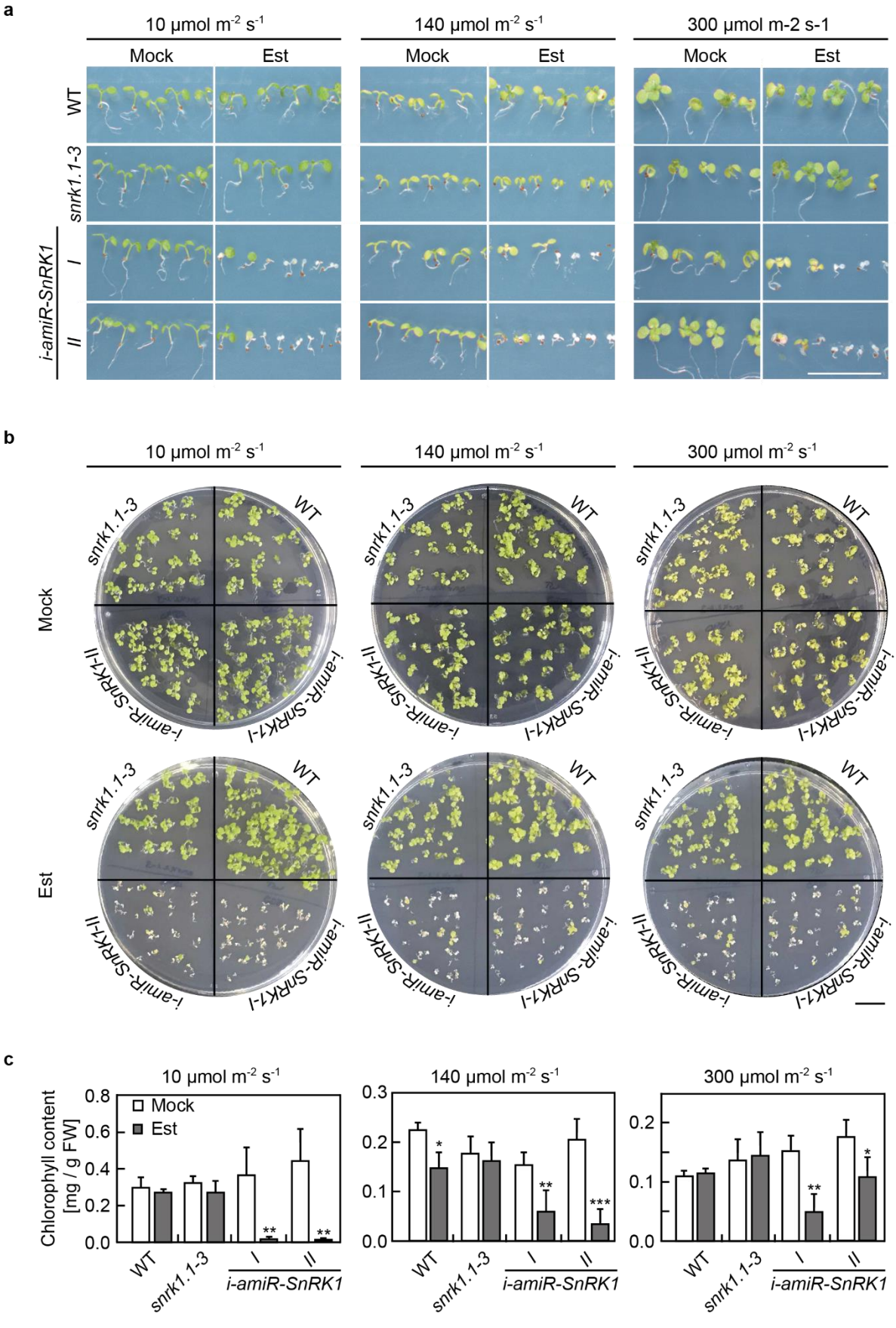
a
10 µmol m-2 s-1
140 µmol m-2 s-1
300 µmol m-2 s-1
Mock
Est
WT
snrk1.1-3
i-amiR-SnRK1
I
II
b
10 µmol m-2 s-1
140 µmol m-2 s-1
300 µmol m-2 s-1
Mock
Est
snrk1.1-3
WT
i-amiR-SnRK1-II
i-amiR-SnRK1-I
c
10 µmol m-2 s-1
140 µmol m-2 s-1
300 µmol m-2 s-1
Chlorophyll content [mg / g FW]
Mock
Est
WT
snrk1.1-3
I
II
i-amiR-SnRK1

Supplemental Figure 5| Knockdown of SnRK1 causes light-dependent cotyledon bleaching. a, b, Representative photographs of 14-d-old seedlings that were either grown on mock or β-estradiol (Est)-containing plates under low (left panel, 10 µmol m^{-2} s^{-1}, similar set up as in Fig. 1c, independent experiment), regular (middle panel, 140 µmol m^{-2} s^{-1}) and high light (right panel, 300 µmol m^{-2} s^{-1}) conditions, respectively. Pictures are either close ups of several plans (a) or overview of the whole agar plates (b) for each growing condition. Scale bar represents 1 cm. **c,** Total chlorophyll content of 14-d-old seedlings. Left graph is also shown in Fig. 1d. Details of plant growth and treatments as described in a. Displayed are mean values +SD (n = 3 - 4) and asterisks indicate significant difference compared to corresponding mock control based on independent t test (P value: *P < 0.05, **P < 0.01, ***P < 0.001).

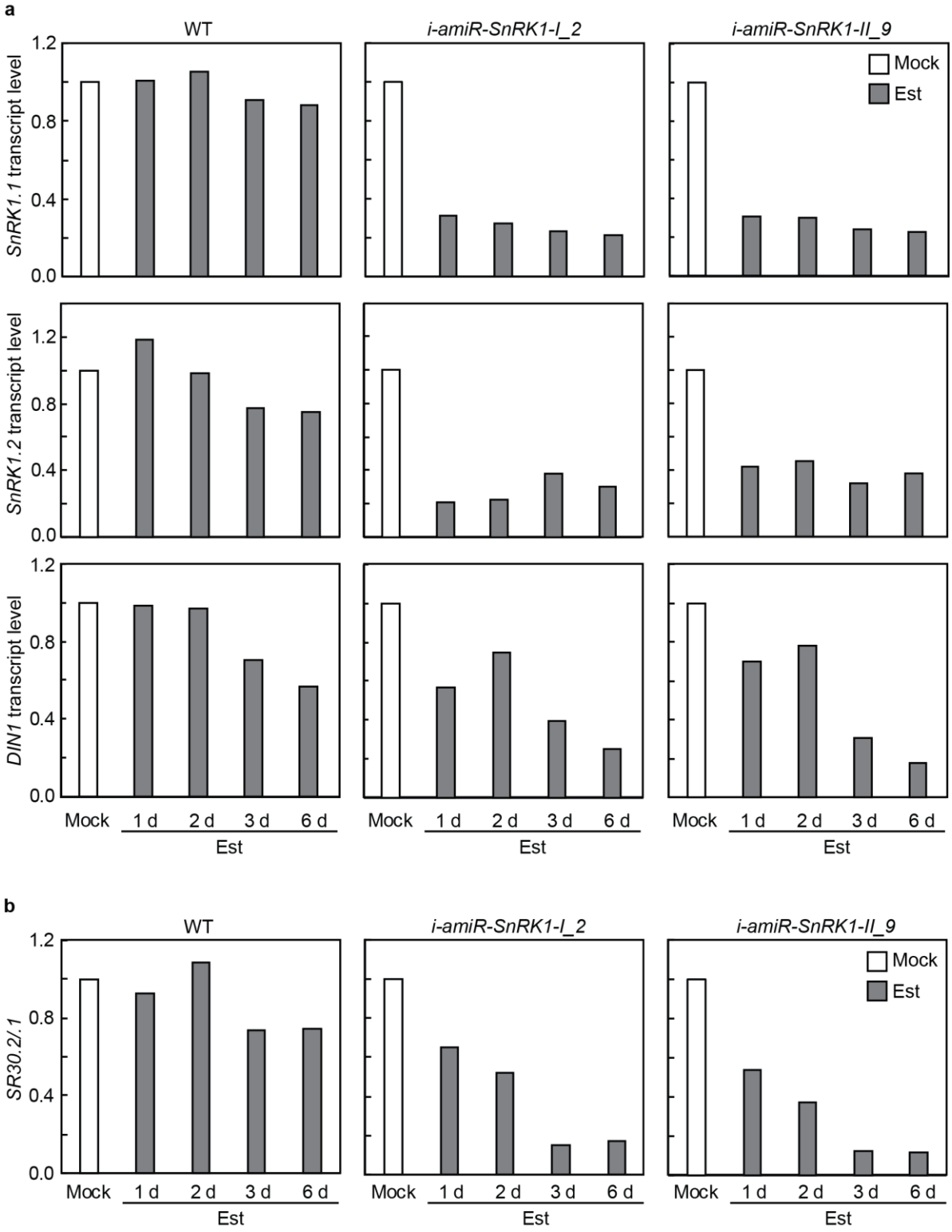

Supplemental Figure 6| *SR30* splice shift increases with duration of *SnRK1* knockdown. a, b, 6-d-old etiolated seedlings were treated with mock solution or β-estradiol (Est) for 1, 2, 3 and 6 d before harvest. *SnRK1.1*, *SnRK1.2*, and *DIN1* transcript levels (**a**) were measured using RT-qPCR, *SR30* splicing ratios (**b**) were determined via Bioanalyzer-based quantification. All data are normalised to the corresponding mock controls and represent single replicates.

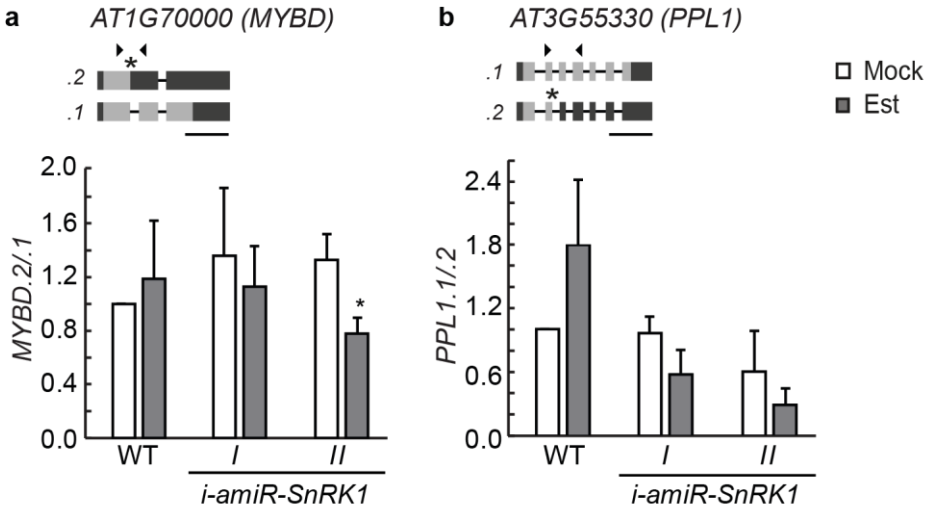

Supplemental Figure 7| AS pattern in *snrk1* mutants. a, b, Splicing ratios were determined in 6-d-old etiolated WT and *amiR* seedlings that were either incubated in mock or β-estradiol (Est) for 3 d. Corresponding gene models are shown above each graph. Introns are represented by lines and exons by boxes. Regions coloured in dark grey are UTRs, and asterisks mark the introduction of a premature termination codon. Primer binding sites are shown as arrowheads. Scale bars beneath the models represent 500 bp. Splicing variants were co-amplified and quantified on a Bioanalyzer. Displayed are mean values +SD (n = 3) and data was normalised to the WT mock control. Independent *t* test was performed when not tested against 1, and one-sample *t* test when tested against 1 (P value: *P < 0.05).

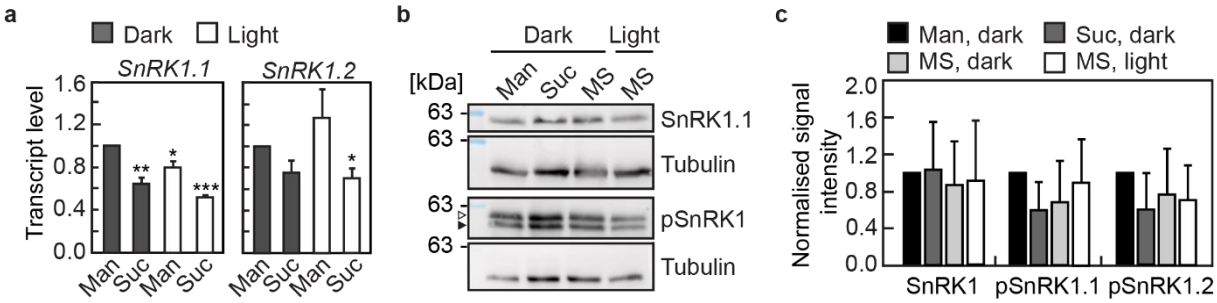

Supplemental Figure 8| Effect of light and sucrose on *SnRK1* expression in WT. a, Transcript levels of *SnRK1.1* and *SnRK1.2*. in 6-d-old etiolated WT seedlings that were exposed to continuous white light (~130 µmol m^{-2} s^{-1}) and/or 2 % sucrose (Suc) or kept in darkness for 6 h. Treatment with equimolar levels of mannitol (Man) served as osmotic control for the sucrose exposure. All data are normalised to the sample that was treated with Man in darkness. Shown are mean values (n = 3) +SD; asterisks indicate significant difference compared to the Man dark control based on one-sample *t* test (P values: *P < 0.05, **P < 0.01, ***P < 0.001). **b,** Immunoblot detection of SnRK1.1 (upper panel) and phosphorylated SnRK1.1 and SnRK1.2 in etiolated WT seedlings, cultivated under the same conditions as described in a. Tubulin served as loading control. **c,** Chemiluminescence detection of immunoblots in b. The band intensity of SnRK1.1, pSnRK1.1 and pSnRK1.2 were normalized to tubulin and shown as signal intensity relative to corresponding Dark Man sample. Displayed are mean values (n=4) +SD.

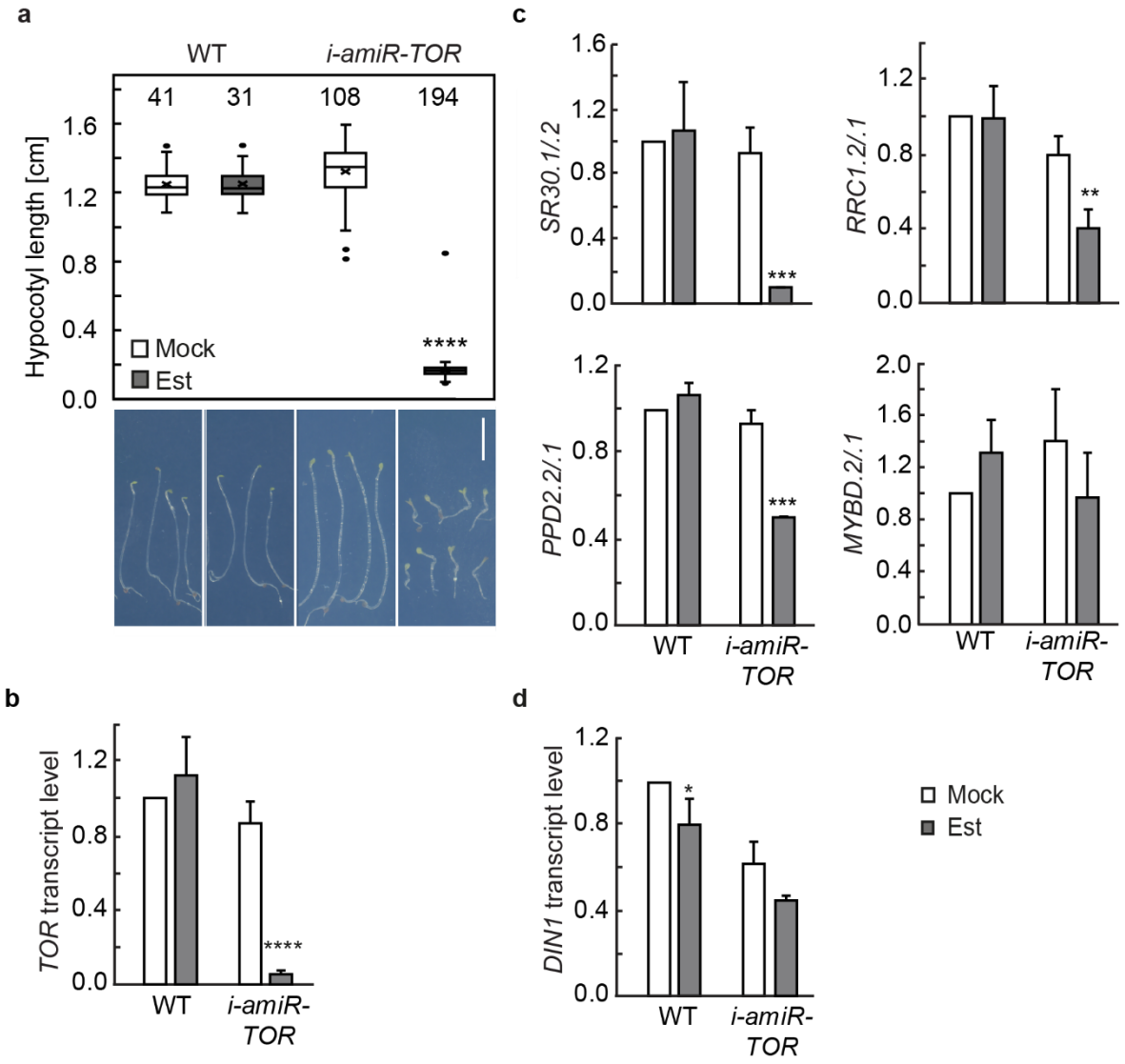

Supplemental Fig. 9| TOR signalling repression results in similar phenotypes and AS shifts as SnRK1 inhibition. a, Hypocotyl length boxplot (top) and representative pictures (bottom) of 6-d-old wildtype (WT), and *i-amiR-TOR* mutant seedlings. The seedlings were grown on mock or β-estradiol (Est)-containing plates. White scale bar indicates 1 cm. The plot depicts interquartile range, maximum as well as minimum of the data set as box and whiskers, respectively. The middle line and the cross represent the median and mean value, respectively, dots show outliers. Asterisks indicate significant difference compared to corresponding mock control based on one-way ANOVA with post hoc Tukey test. n is indicated above each line (P value: ****P < 0.0001). **b,** Relative transcript level of *TOR* in 6-d-old etiolated WT and *i-amiR-TOR* mutant seedlings, treated with either mock or Est for 3 d. Data are mean values (n = 3 from 2 independent experiments) + SD, normalised to WT mock samples. Statistical comparison of the mock and Est-treated *i-amiR-TOR* mutant was performed using an independent *t* test. In case of the WT, a one-sample *t* test was used (P value: ****P < 0.0001).

c, Splicing ratios of *SR30*, *RRC1*, *PPD2* and *MYBD* were determined in 6-d-old etiolated WT and *i-amiR-TOR* seedlings either incubated in mock or Est for 3 d. Data were quantified using RT-qPCR of the single mRNA isoforms and normalised to the WT mock control. Displayed are mean values +SD (n = 3 from 2 independent experiments). An independent *t* test was performed when not tested against 1, and one-sample *t* test for WT (P values: **P < 0.01, ***P <0.001). **d,** Relative transcript level of *DIN1* in 6-d-old etiolated WT and *i-amiR-TOR* mutant seedlings. Displayed are mean values +SD (n = 3 from 2 independent experiments) and statistical comparison of the mock and Est-treated *i-amiR-TOR* mutant was performed using an independent *t* test. In case of the WT, a one-sample *t* test was used (P values: *P < 0.05).

V. Danksagung

An dieser Stelle möchte ich mich noch ganz herzlich bei allen Menschen bedanken, die mich während meiner Promotion immer wieder bestärkt und unterstützt haben.

Lieber Andreas, du hast mich immer wieder gefordert und gefördert während der Zeit, die wir zusammen gearbeitet haben. Dabei könnte ich über mich hinauswachsen und sehr viel dazu lernen. Z. B. Hätte mir jemand ganz am Anfang meiner Promotion gesagt, dass ich einmal einen Vortrag vor über 100 Leuten auf einer internationalen Konferenz halten werde, hätte ich es nicht geglaubt. Dennoch es ist so passiert und es war ein richtig gutes Gefühl. Du hast es mir ermöglicht, an einem spannenden wissenschaftlichen Forschungsprojekt mitzuwirken. Ich konnte immer mit meinen Ideen und Problemen zu dir kommen. Für all die Möglichkeiten, möchte ich dir danken. Es war eine sehr schöne Zeit für mich in deiner Arbeitsgruppe.

Lieber Herr Harter, lieber Herr Laubinger, ich danke Ihnen, dass sie sich vor 6 Jahren bereiterklärt haben, mein Projekt mitzugestalten und mein Zweitgutachter bzw. Mitglied meines TAC Komitees zu wurden. Ich empfand unsere Treffen immer als konstruktiv und ich habe ihre Hinweise zu meinem Projekt wertgeschätzt.

Liebe Jenny, wir hatten zusammen eine sehr schöne Zeit am ZMBP und ich bin sehr froh, dass du an meinem Projekt mitgearbeitet und es schließlich übernommen hast. Du hattest immer gute Laune und hast mich damit meistens angesteckt. Vielen Dank für deine Freundschaft, unsere gute Zusammenarbeit, deine Hilfsbereitschaft und konstruktive Kritik. Ich konnte von dir viel lernen.

Liebe Jorinde, als du in unsere Truppe gekommen bist, hatte ich mich sehr gefreut, dass endlich jemand da war mit dem ich meine Kaffeeleidenschaft teilen konnte. Vielen Dank für dein offenes Ohr, deine Ratschläge und deine witzigen Geschichten.

Liebe Gabi, liebe Natalie, liebe Claudia. Ein großes Dankeschön an euch. Ihr hattet mich sehr herzlich in die Arbeitsgruppe aufgenommen, wart super liebe Kolleginnen, habt mir im Labor immer mit Rat und Tat zur Seite gestanden und es hat mir viel Freude bereitet mit euch zusammen zu arbeiten.

Und ein außerordentlich herzliches Dankeschön geht an meinen Mann, meine Eltern und meine Schwiegereltern, die mir ständig (und vor allem letztes Jahr) den Rücken freigehalten, mich ermutigt und mir auch das ein oder andere Mal in den Allerwertesten getreten haben. Danke, dass ich gleichzeitig Wissenschaftlerin und Mama sein kann.

VI. Eidesstattliche Erklärung

Ich erkläre hiermit, dass ich die zur Promotion eingereichte Arbeit selbständig verfasst, nur die angegebenen Quellen und Hilfsmittel benutzt und wörtlich oder inhaltlich übernommene Stellen als solche gekennzeichnet habe.

_____ , _____

Ort, Datum Unterschrift